2011

Analysis, design, and strengthening of communication towers

Cindy Dostatni
University of Windsor

ANALYSIS, DESIGN, AND STRENGTHENING OF COMMUNICATION TOWERS

by
Cindy Dostatni

A Dissertation
Submitted to the Faculty of Graduate Studies
through Civil and Environmental Engineering
in Partial Fulfillment of the Requirements for
the Degree of Doctor of Philosophy at the
University of Windsor

Windsor, Ontario, Canada
2011

Your file Votre référence
ISBN: 978-0-494-80243-4
Our file Notre référence
ISBN: 978-0-494-80243-4

Declaration of Co-Authorship / Previous Publication

I. Co-Authorship Declaration

I hereby declare that this dissertation incorporates material that is result of joint research, as follows:

This dissertation also incorporates the outcome of a joint research undertaken in collaboration with Ms. Lihong Shen under the supervision of Professor Murty K.S. Madugula and Professor Faouzi Ghrib. The collaboration is covered in Chapter 4 of the dissertation. In all cases, the key ideas, primary contributions, data analysis and interpretation, were performed by the author, and the contribution of co-author was primarily through the provision of conducting the experimental investigation.

This dissertation also incorporates the outcome of a joint research undertaken in collaboration with Mr. Yongcong Ding under the supervision of Professor Murty K.S. Madugula. The collaboration is covered in Chapter 5 of the dissertation. In all cases, the key ideas, primary contributions, experimental designs, data analysis and interpretation, were performed by the author, and the contribution of co-author was primarily through the provision of conducting the experimental investigation together with the author.

I am aware of the University of Windsor Senate Policy on Authorship and I certify that I have properly acknowledged the contribution of other researchers to my dissertation, and have obtained written permission from each of the co-authors to include the above materials in my dissertation.

I certify that, with the above qualification, this dissertation, and the research to which it refers, is the product of my own work.

II. Declaration of Previous Publication

This dissertation includes two original papers that have been previously published for publication in peer reviewed journals, as follows:

Dissertation Chapter	Publication title	Publication status
Chapter 4	*Tensile Strength of Bolted Ring-type Splices of Solid Round Leg Members of Guyed Communication Towers*	*Published*
Chapter 5	*Prying Action in Bolted Steel Circular Flange Connections*	*Published*

I certify that I have obtained a written permission from the copyright owner to include the above published materials in my dissertation. I certify that the above material described work completed during my registration as graduate student at the University of Windsor.

I declare that, to the best of my knowledge, my dissertation does not infringe upon anyone's copyright nor violate any proprietary rights and that any ideas, techniques, quotations, or any other material from the work of other people included in my dissertation, published or otherwise, are fully acknowledged in accordance with the standard referencing practices. Furthermore, to the extent that I have included copyrighted material that surpasses the bounds of fair dealing within the meaning of the Canada Copyright Act, I certify that I have obtained a written permission from the copyright owner to include such materials in my dissertation.

I declare that this is a true copy of my dissertation, including any final revisions, as approved by my dissertation committee and the Graduate Studies office, and that this dissertation has not been submitted for a higher degree to any other University or Institution.

ABSTRACT

This dissertation discusses several topics relating to the analysis, design, and strengthening of self-supporting and guyed communication towers, some of which are not covered by Canadian Standard CSA S37-01 and American Standard ANSI/TIA/EIA-222-G. The effect of sudden guy rupture and guy slippage on guyed towers, effect of eccentricity on the tensile strength of bolted ring-type splice connections, calculation of prying action on bolted circular splice connections, and strengthening of solid round leg members with split pipes were studied.

Experimental investigation was conducted on small-scale guyed tower test specimens, bolted ring-type and circular splice connections, and solid round steel members strengthened with split pipes. Finite element analysis models of small-scale guyed towers and solid round test specimens were built to simulate the experimental investigation.

Based on experimental investigation, it was found that the maximum load amplification factors due to sudden guy wire rupture with an initial tension of 10% of the guy wire breaking strength ranged from 1.45 to 2.21, and those with doubled initial tension decreased to a range of 1.43 to 1.96. For guy slippage, it was found that those factors ranged from 1.10 to 1.56. The maximum load amplification factors are highest when rupture or slippage happened at top level guy wires. The finite element models can be used to determine the maximum load amplification factors due to sudden guy rupture and guy slippage on tower test specimens.

On the basis of the research, it was concluded that bolted ring-type splices should be designed for combined stresses due to axial tension and bending moment. The equations for prying action given in the Canadian Institute of Steel Construction Handbook and American Institute of Steel Construction Manual can be used in circular flange connections, with the bolt pitch taken as the distance between the centres of bolts measured along the bolt circle.

It is recommended that split pipes be used along the entire solid round steel member and be connected with end welds in addition to U-bolts/tabs. For stocky members, stitch welds are preferable since there is a minimal strength increase by using U-bolts/tabs only. The finite element models can be used to determine the failure loads of un-strengthened and strengthened solid round steel test specimens.

To my late father, Djatilaksono Limantara

"Nobody can take education from you"

1946 - 1994

ACKNOWLEDGEMENTS

The author would like to thank God for His blessings throughout her study and the development of this research.

The author would like to express her thanks and gratitude to:

1. Her principal advisor, Dr. Faouzi Ghrib, Associate Professor and Acting Head of Department of Civil and Environmental Engineering, for his help in the finite element analysis part of this research and support in the writing of scholarly publications;
2. Her co-advisor, Dr. John B. Kennedy, Professor Emeritus, Department of Civil and Environmental Engineering, for his encouragement given to the author in the writing of scholarly publications;
3. Her co-advisor, Dr. Murty K.S. Madugula, Professor Emeritus, Department of Civil and Environmental Engineering, for his patience, inspiration, informative guidance, and encouragement given during her studies and especially during the development of this dissertation;
4. Dr. Sreekanta Das, Associate Professor, Department of Civil and Environmental Engineering, for his informative guidance in experimental works and assistance throughout her studies;
5. Mr. Ernest R. Jones, Vice President of Engineering, and Mr. John Robinson, Principal Engineer, Electronics Research, Inc., Chandler, IN, USA, who donated the test specimens used in the investigation and gave information about real problems in the field;
6. Mr. Peter D. Jeffrey, President, and Mr. Calvin Payne, CEO and Chief Engineer, of Westower Communications Ltd., who provided support for the author to complete her study;
7. Civil and Environmental Engineering technicians, Messrs. Pat Seguin, Lucien Pop, Matthew St. Louis, and Louis Beaudry, for their assistance in the experimental setups and tests; and
8. The last but not least, Mr. Grzegorz Dostatni, her husband, who provides continuous support and encouragement to the author.

The author also acknowledges the financial support provided by:

1. The University of Windsor in the form of Tuition Scholarship and Graduate Assistantship;
2. Natural Sciences and Engineering Research Council of Canada in the form of Research Assistantship and Canada Graduate Scholarship; and
3. Westower Communications Ltd.;

All of which make it possible for the author to achieve her degree.

TABLE OF CONTENTS

LIST OF TABLES

LIST OF FIGURES

LIST OF APPENDICES

NOMENCLATURE

a	Distance from bolt line to edge of flange (not more than 1.25 b), page 106
a	Length of the strengthening member, page 113
A	Gross area of cross-section
a'	Distance from bolt inside edge to edge of flange
A_{nng}	Area of ring flange
$A_{nng+bolt}$	Area of ring flange and splice bolt
b	Distance from bolt line to face of fillet welds, page 106
b	Ring thickness, page 165
b'	Distance from bolt inside edge to face of fillet welds
C_r	Compressive resistance
d	Bolt diameter
d'	Nominal hole diameter
d_b	Bolt diameter
D_i	Inside diameter of ring flange
d_l	Leg diameter
D_o	Outside diameter of ring flange
e	Eccentricity of ring flange connection and tower leg
E	Young's modulus of elasticity
$\bar{E}$	Variable modulus lying between Young's modulus and tangent modulus
EI	Bending stiffness
F_{cr}	Critical stress
F_u	Tensile stress
F_y	Specified minimum yield stress, or yield strength of material
h	Height of ring flange, page 90
h	Distance from centroidal axis to neutral axis measured toward centre of curvature, page 159
I	Moment of inertia
I_1	Moments of inertia of un-strengthened cross-section
I_2	Moments of inertia of strengthened cross-sections
ID	Ring inside diameter
k	Axial stiffness
K	Parameter defined in Equation [5.3], page 106
K	Effective length factor, page 115
KL	Effective length of column
L	Unbraced length of column

m	Numerical factor depending on the ratios of $\frac{a}{L}$ and $\frac{I_1}{I_2}$
M	Moment due to load eccentricity
M_A	Maximum positive moment (at point A) on ring
M_B	Maximum negative moment (at point B) on ring
n	Parameter for compressive resistance (1.34 for angles and hot-rolled solid rounds up to 51 mm in diameter)
OD	Ring outside diameter
p	Length of flange tributary of each bolt, or bolt pitch
P	Force
P_{cr}	Critical load, also known as Euler load
P_E	Euler column load, also known as critical load
P_f	Applied tensile load per bolt
P_{total}	Axial force with additional force due to bending moment
Q	Prying force per bolt
r	Minimum radius of gyration
R	Average radius of ring
r_n	Tensile strength of the bolt
S_{bolt}	Section modulus of splice bolt
$S_{ring+bolt}$	Section modulus of ring flange and splice bolt
t	Time step, page 49
t	Thickness of flange, page 106
t	Ring wall thickness, page 165
t_c	Flange thickness required to develop design tensile strength of bolts with no prying action
u_x	Translational degree of freedom in x-direction
u_y	Translational degree of freedom in y-direction
u_z	Translational degree of freedom in z-direction
W	Load applied to ring
y	Perpendicular distance to the centroidal *x*-axis, equals to half the ring thickness
α	Numerical damping parameter, page 51
α	Parameter defined in Equation [5.5], page 106
α	Ratio of distance from centroidal axis to neutral axis measured toward centre of curvature over average radius of ring, page 165
δ	Parameter defined in Equation [5.4]
Δt	Time increment

ε	Strain
λ	Non-dimensional slenderness parameter
σ	Maximum stress on ring
ϕ	Resistance factor

CHAPTER 1
INTRODUCTION

1.1 INTRODUCTION

Telecommunication and broadcasting systems require antennas to be located at certain heights above ground due to the radiation pattern of some antenna types. Those antennas are most economically supported on structures known as telecommunication towers. Owing to the recent advances in wireless industry due to internet and cell phone use, demand for wireless networks is increasing, which subsequently increases the demand for new telecommunication towers or strengthening of existing towers.

This dissertation discusses selected issues relating to the analysis, design, and strengthening of communication towers that are commonly faced by tower design engineers but not covered by Canadian standard CSA S37-01 "Antennas, Towers, and Antenna-supporting Structures" [CSA 2001] and American standard ANSI/TIA/EIA-222-G.5 "Structural Standard for Antenna Supporting Structures and Antennas" [TIA 2005], as follows:

1. Load amplification factors for intact guy wires due to sudden guy wire rupture on a guyed tower;
2. Load amplification factors for intact guy wires due to guy wire slippage on a guyed tower;
3. Effect of eccentricity on the tensile strength of bolted ring-type splice connections;
4. Calculation of prying action on bolted circular splice connections; and
5. Strengthening of solid round steel legs and diagonal members with split pipes.

These topics are significant for the overall safety of both new and existing communication towers. Guy wire rupture and guy wire slippage can cause a major failure of tower structural members and sometimes re-building a new tower is necessary. When a bolt does not have enough required capacity, the bolt often needs to be replaced with a larger size bolt or the connection needs to be strengthened. Both require field drilling or welding at high elevation which will be not economical. Compared with building a new tower, strengthening of tower members is an option that definitely can save time and money for wireless providers.

The most common telecommunication tower structures are monopoles, self-supporting, and guyed lattice towers as shown in Figure 1.1. Of these three structures, the monopole is generally the shortest and requires least land area, and guyed tower is the tallest but requires a vast area since the guy radius is typically about 75% of the tower height. Since failure of taller structures is

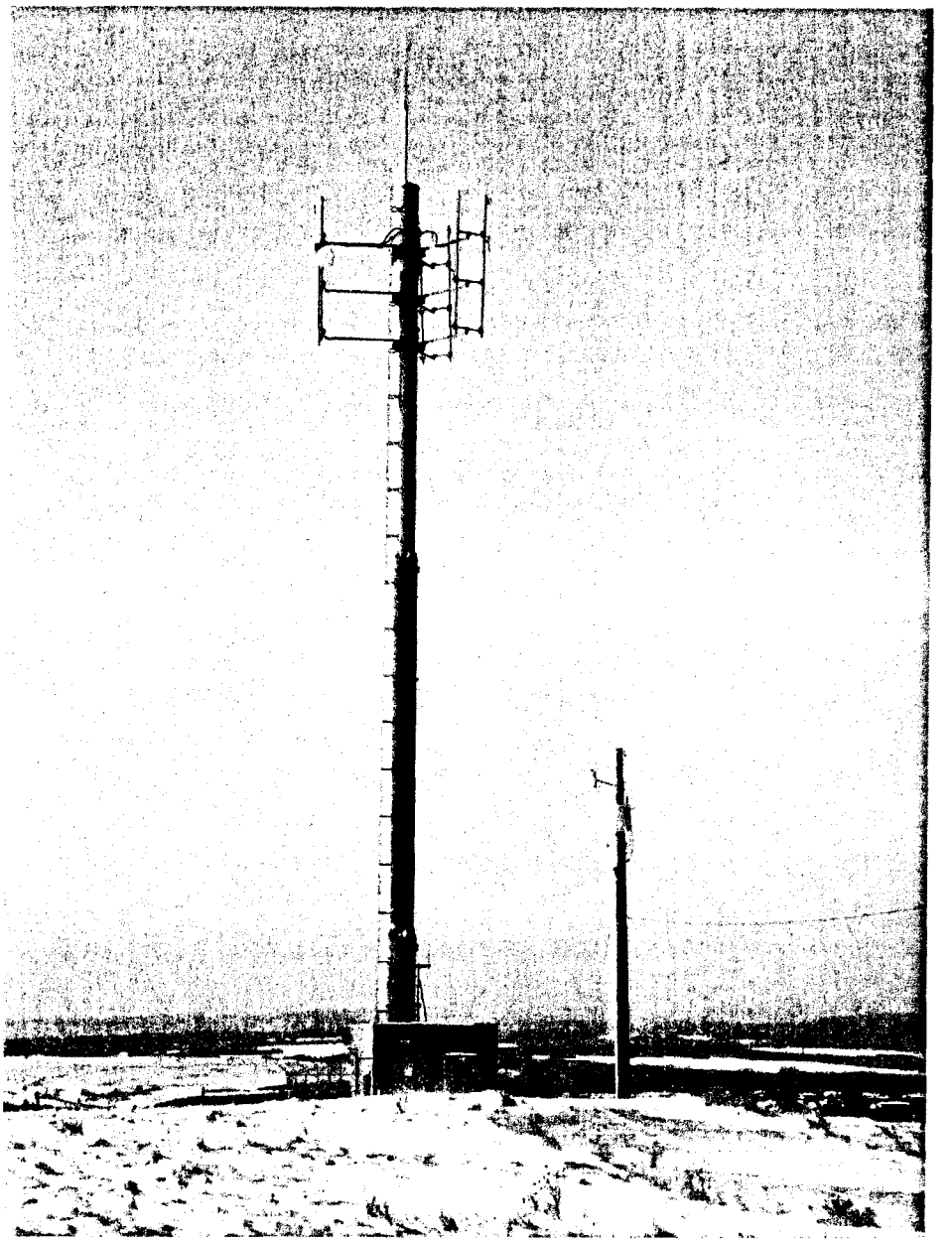

(a) A monopole in Calgary, Alberta
(courtesy of Westower Communications Ltd.)

Figure 1.1. Photographs of Communication Towers

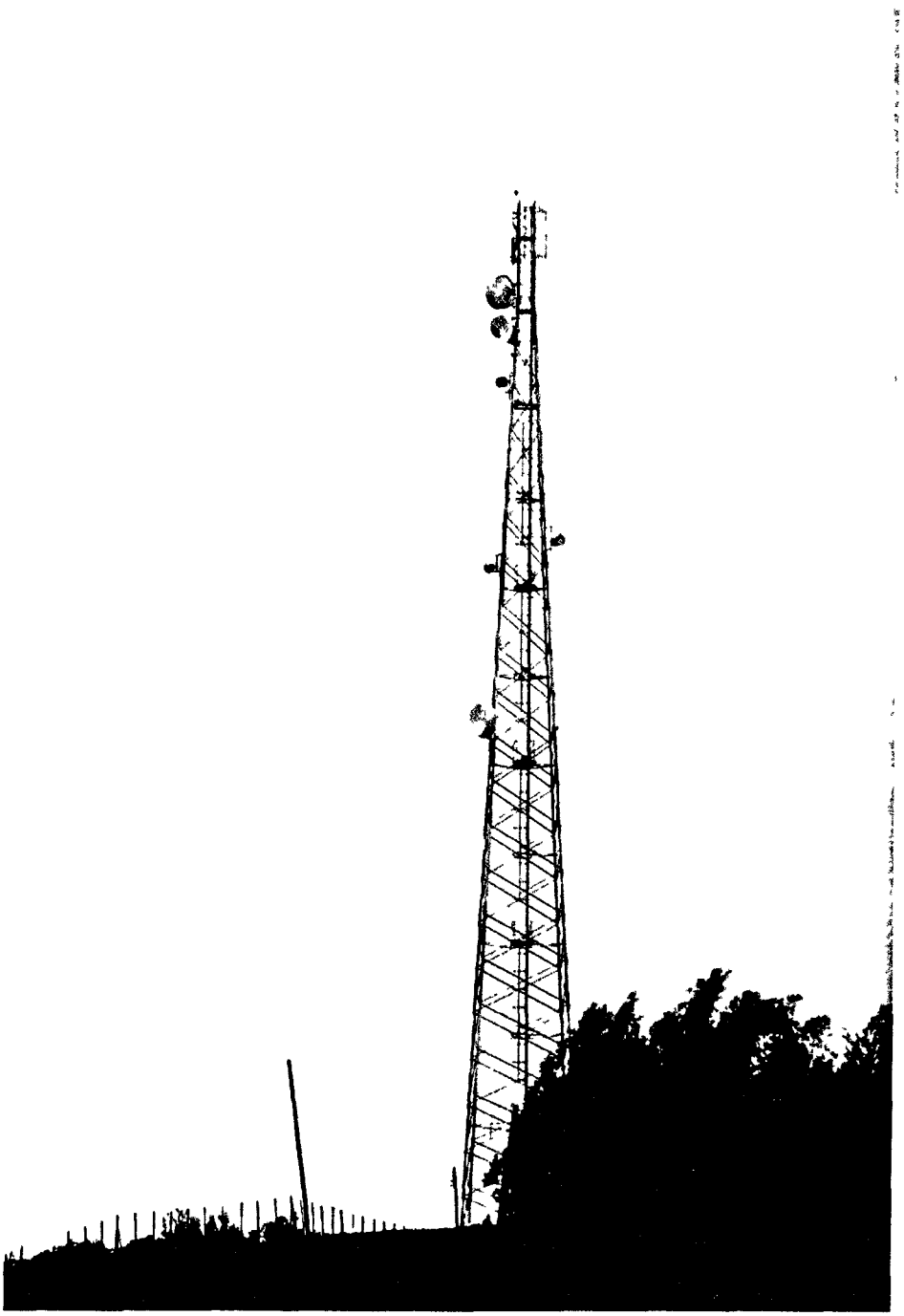

(b) A self-supporting tower in Africa
(courtesy of Mr. Grzegorz Dostatni)

Figure 1.1. Photographs of Communication Towers (continued)

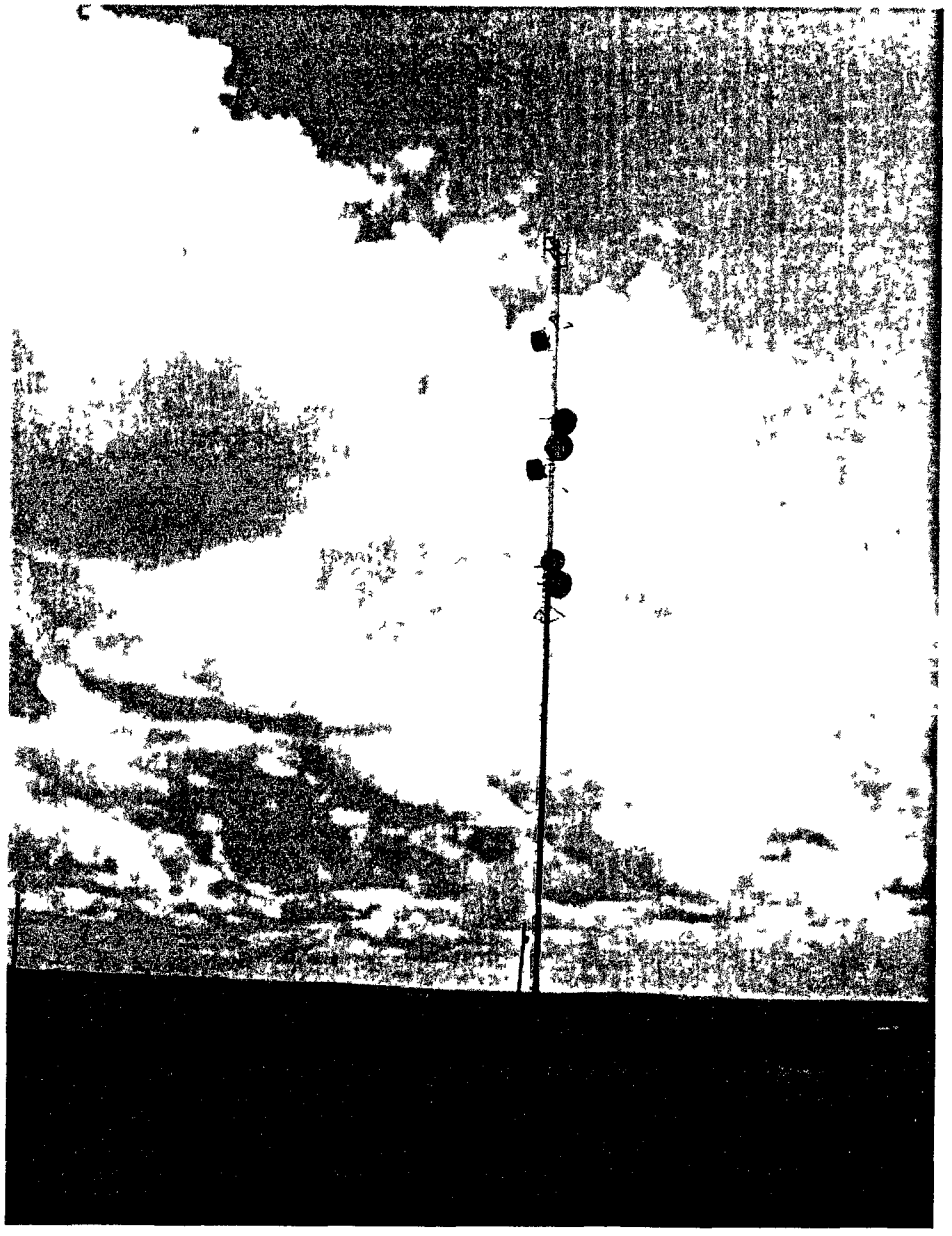

(c) A guyed tower in Valleyview, Alberta
(courtesy of Westower Communications Ltd)

Figure 1.1. Photographs of Communication Towers (concluded)

more catastrophic and also more expensive to rectify than those of shorter structures, this dissertation focuses on self-supporting towers and guyed towers only.

1.2 NEED FOR THE INVESTIGATION

A guyed tower is a slender mast supported by guy wires at intervals. Guy wire tension has a significant impact on the integrity of a guyed tower. Adjustment of guy wire tension can cause additional tensile/compressive loading on tower mast due to bending of the mast, and changes in the tension of other guy wires. Guy wire rupture and/or guy wire slippage will remove/reduce the guy wire tension required to maintain the stability of the tower and major structural failure can occur. A guyed tower needs to be designed with reserve capacity in tower legs and guy wires in order to prevent major failure to happen.

To the best of author's knowledge, there is no previous experimental investigation conducted on the effect of sudden guy rupture and guy slippage on guyed towers. Previous research discussed in Chapter 2 was conducted by simulation and analytical calculation, and it was found that the Eurocode simplified method [CEN 2008] commonly used by tower design engineers is a simple but conservative method. Thus, to confirm previous findings, experimental investigation on small-scale guyed tower test specimens was conducted.

Guyed towers and self-supporting towers are built by stacking tower sections and connecting those sections with sleeves, splice plates, or bolted connection splices. There are two types of bolted connection splice: (i) symmetrical bolted connection, where the line of load of the tower legs is aligned with the line of load of the overall connection (as shown in Figure 1.2), and (ii) unsymmetrical bolted connection, e.g., bolted ring-type connection as shown in Figure 1.3. The latter, due to its shape, makes the transport and arrangement of those tower sections relatively easier than the former. However, there is eccentricity between the centre of tower leg and the centre of the bolt, and there is no guidance in North American standards and specifications to calculate the tensile capacity of such connections. The splice bolts should be designed by taking into account load eccentricity which causes bending of the bolt prior to failure, as shown in Figure 1.4.

Although load eccentricity does not exist on symmetrical bolted connection, such as flange-type connection shown in Figure 1.5, prying action can occur on relatively flexible flange plates. This prying action induces additional tensile force on splice bolts, and bolt failure can occur if the bolts were not properly designed. Prying action is discussed on the Canadian Institute of Steel Construction Handbook of Steel Construction [CISC 2010] and American Institute of Steel

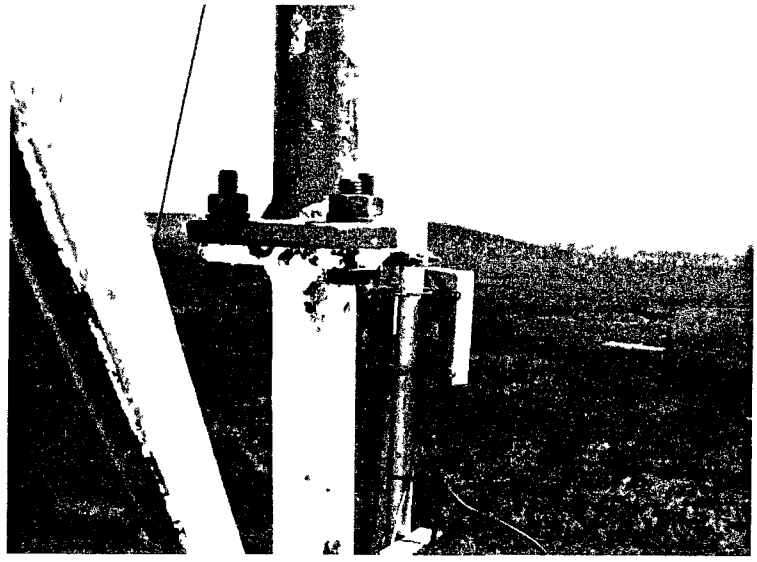

(a) Elevation view

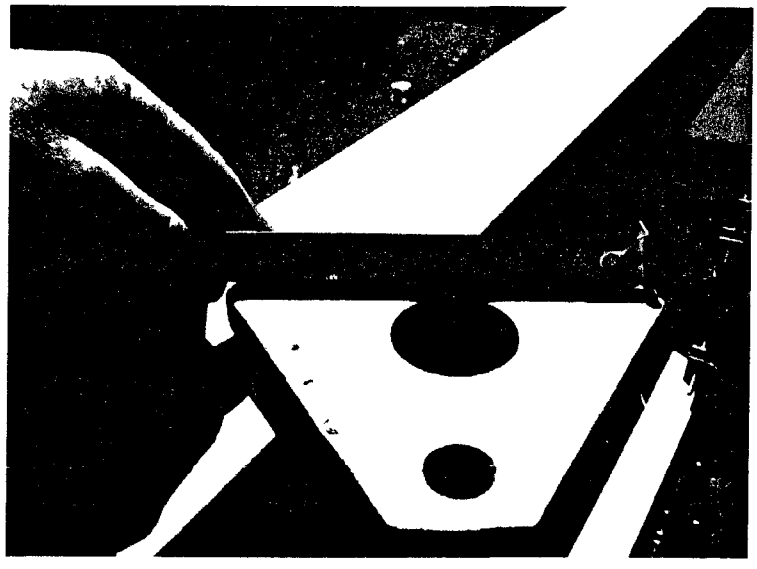

(b) Plan view

Figure 1.2. Symmetrical Bolted Splice Connection
(courtesy of Westower Communications Ltd)

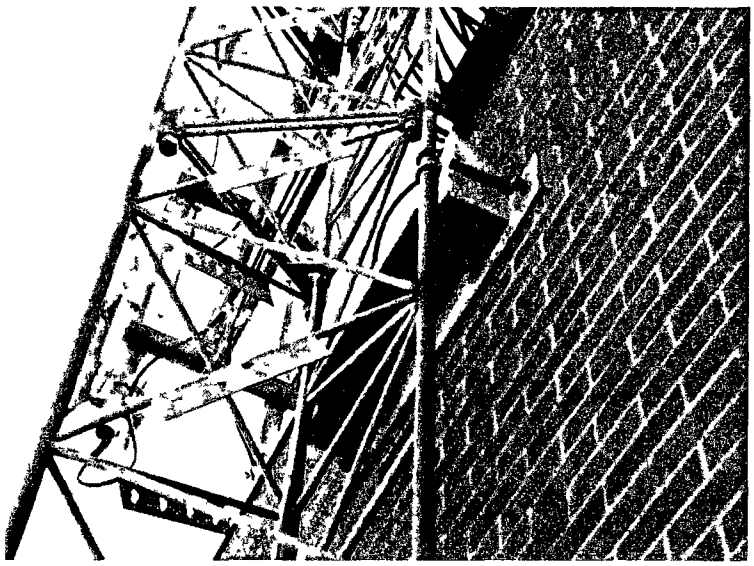

(a) Bolted ring-type connection - 1

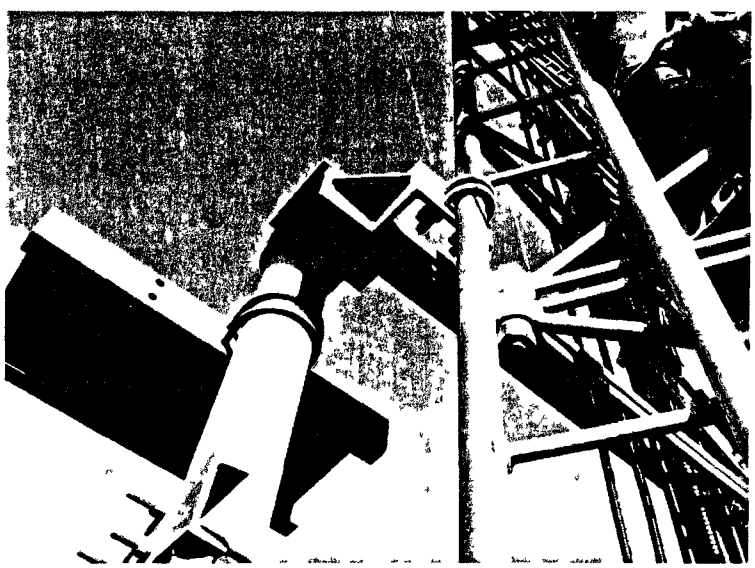

(b) Bolted ring-type connection - 2

Figure 1.3. Unsymmetrical Bolted Splice Connection
(courtesy of Westower Communications Ltd)

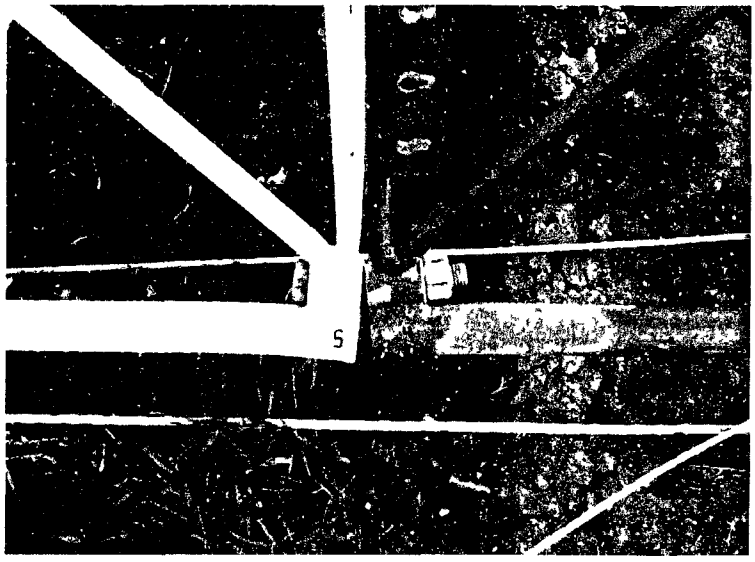

Figure 1.4. Failure of Bolted Ring-type Splice Connection
(courtesy of Westower Communications Ltd)

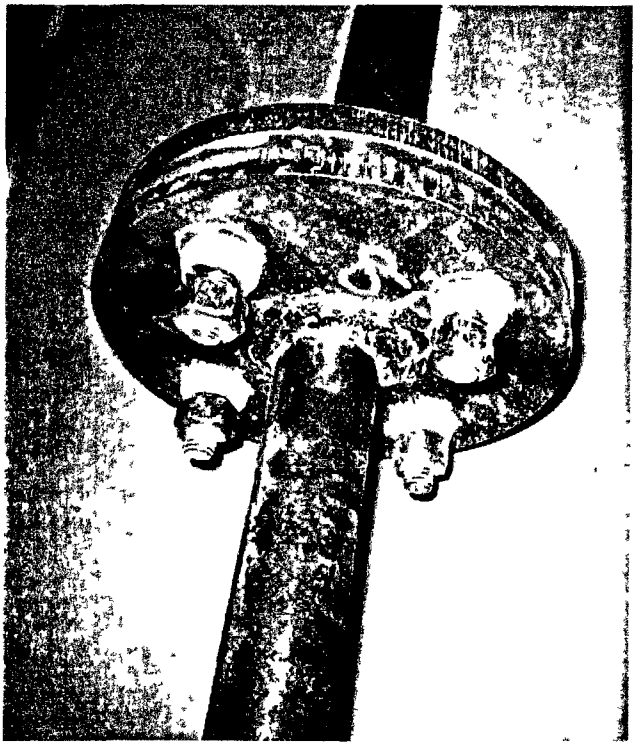

Figure 1.5. Bolted Circular Flange Connection

Construction Steel Construction Manual [AISC 2005], but only on tee-type connections where the line of the bolt pitch is straight. To the best of author's knowledge, there is no guidance provided for bolted circular connections as shown in Figure 1.5 which is very common in self-supporting and guyed towers.

Ignoring the eccentricity and prying action of the connection during the design stage is unsafe and can be very difficult to fix later during service. Therefore, there is a need to study the tensile strength of bolted ring-type connections and the prying action of bolted circular splice connections.

While a tower may already be designed by considering reserve capacity due to guy wire rupture or slippage as well as additional loading on the tower section connections, a tower often needs to be strengthened to carry additional antenna and transmission line loading. This commonly is encountered when building a new tower is not feasible due to building permit, cost, and land restriction, and wireless providers have to share existing towers. The common strengthening methods are (i) adding sub-bracing to reduce the effective length of leg and diagonal members, and (ii) attaching additional members to the main members. The calculation of compressive strength in the first method is straightforward. However, for the second method, there is ambiguity among tower design engineers on the calculation of the compressive strength of strengthened member since this topic has not been covered by any North American standards and specifications. The author has been conducting research on strengthening of tower leg and diagonal members since 2003 and the dissertation covers the continuation of this research.

1.3 OBJECTIVES OF PRESENT RESEARCH

The main objective of this research is to increase overall safety of communication towers by providing guidance for tower design engineers on selected issues related to the analysis, design, and strengthening, which include:

1. The study of the dynamic load amplification factor of intact guy wires due to sudden rupture of one guy wire by carrying out an experimental investigation on small-scale guyed tower test specimens and comparing the results with those obtained from the Eurocode simplified method [CEN 2008] and finite element analyses;
2. The study of the effect of guy wire slippage on the load amplification factor of intact guy wires by conducting an experimental investigation on small-scale guyed tower test specimens and finite element analyses;
3. The study of the effect of eccentricity on the tensile strength of bolted ring-type splice connections;

4. The study of the prying action on bolted circular splice connections; and
5. Study the compressive strength of solid round steel members strengthened using split pipes with various types of connections by carrying out experimental investigation on test specimens and modelling the experiment with finite element analysis.

1.4 ORGANIZATION OF THE DISSERTATION

This dissertation consists of seven chapters. In Chapter 1, the need for the study and the objectives of the research are presented. In Chapter 2, the dynamic load amplification factor of intact guy wires due to sudden guy wire rupture on small-scale test specimens and finite element modelling are discussed. Chapter 3 presents the finite element analysis and experimental investigation on the effect of guy slippage on load amplification factor of intact guy wires. The effect of eccentricity on bolted ring-type connections and a proposed calculation method are discussed in Chapter 4. In Chapter 5, the prying action on bolted circular splice connections is determined by comparing experimental results with a proposed method to determine bolt pitch. Comparison of experimental investigation and finite element analysis results on the compressive strength of solid round steel leg and bracing members strengthened with split pipes is presented in Chapter 6. Finally, contributions and recommendations for future research are given in Chapter 7.

REFERENCES

AISC. 2005. Steel Construction Manual. 13th ed. American Institute of Steel Construction, Chicago, IL.

CEN. 2008. Design of Steel Structures - Part 3-1: Towers, masts and chimneys - Towers and masts. Eurocode EN 1993-3-1:2006/AC:2009. European Committee for Standardization, Brussels, Belgium.

CISC. 2010. Handbook of Steel Construction. 10th ed. Canadian Institute of Steel Construction, Markham, ON.

CSA. 2001. Antennas, towers, and antenna-supporting structures. S37-01. Canadian Standards Association, Toronto, ON.

TIA. 2005. Structural standard for antenna supporting structures and antennas. ANSI/TIA/EIA-222-G. Telecommunications Industry Association, Arlington, VA.

CHAPTER 2
DYNAMIC LOAD AMPLIFICATION FACTORS OF GUY WIRES IN A COMMUNICATION TOWER DUE TO SUDDEN RUPTURE OF ONE GUY WIRE

2.1 INTRODUCTION

Telecommunication systems, such as radio and television broadcasting, require elevated antennas which are most economically supported on monopole, self-supporting, and guyed lattice towers as shown in Figure 1.1. Unfortunately, failures of communication structures due to dynamic effects are high compared with other structures of equal economic and social importance. One of most significant incidents is the failure of the former world's tallest guyed tower (646 m tall), Warsaw radio mast, at Konstantynów, Gąbin, Poland, in 1991 during guy wire replacement [Wikipedia 2010], as shown in Figure 2.1.

The complex non-linear behaviour of the guyed towers as shown in Figures 1.1(c) and 2.1 presents a more difficult problem than that of typical building frame. Some adverse conditions likely to introduce significant dynamic response of guyed towers are sudden guy wire ruptures, windstorms, ice storms, and earthquakes. In order to use existing and future towers more effectively, a better understanding of the dynamic response of guyed towers is required. This chapter discusses the dynamic load amplification factors of guy wire tensions due to sudden rupture of one of the guy wires in guyed communication towers.

2.2 LITERATURE REVIEW

Sudden guy wire ruptures could happen either accidentally, e.g., by collision of a plane or farming equipment with the guy wire, or intentionally, e.g., by sabotage or vandalism. Research has been conducted to determine the effect of sudden guy wire ruptures. El-Ghazaly and Al-Khaiat [1995] carried out dynamic analysis and found that the consequences could be catastrophic if guy wire rupture occurs on the top level of guy wires while the wind speed is at its maximum. Non-linear dynamic response of a guyed tower to a sudden guy wire rupture was investigated by Kahla [1997, 2000] on a 150 m (500 ft) tall guyed tower with three levels of guy wires using a computer program called NSDAGT. The dynamic amplification factors for guy wire tensions were found to range from 1.22 to 2.27 under no wind conditions, and from 1.16 to 2.84 under 120 km/h wind speed (720 Pa wind pressure).

Due to uncertainty of several factors influencing the behaviour of guyed towers, e.g., vibration, damping of guy wires and masts, and character of the rupture, a dynamic analysis is typically not

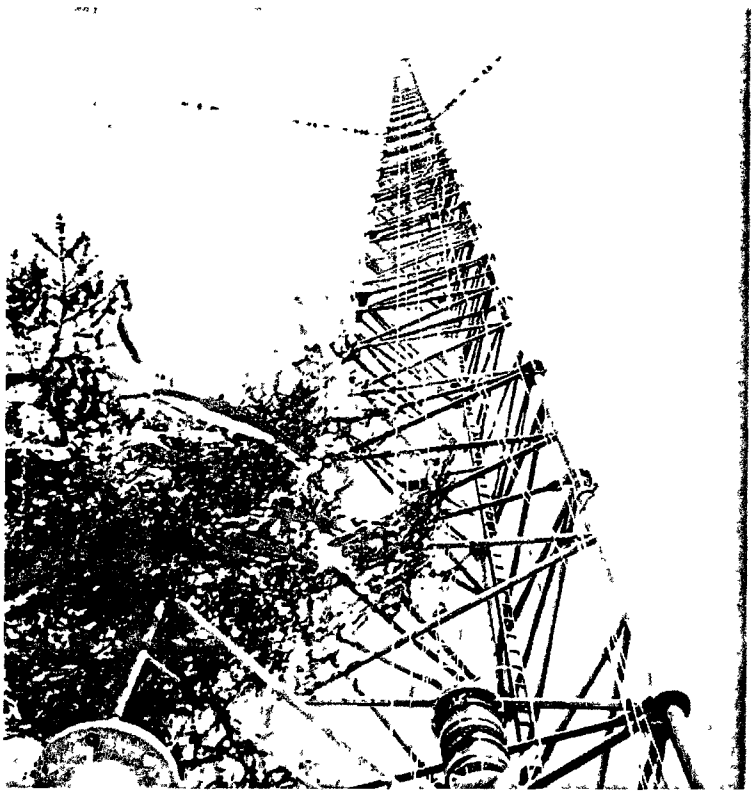

(a) In service (prior to failure)

(b) After failure

Figure 2.1. Photographs of Warsaw Radio Mast [Wikipedia 2010]

feasible for tower design engineers [Madugula 2002]. Conventional static analysis methods for guyed towers are known to underestimate critical load effects by wind turbulence, but more rigorous dynamic analyses are not routinely employed due to greater difficulty [Davenport and Sparling 1998].

Instead of carrying out complicated analyses, Eurocode 3 [CEN 2008] suggests two approaches, i.e. (i) the conservative static method (where the horizontal component of the force in a guy wire before rupture is applied as additional load acting on the mast at the ruptured guy level), and (ii) the simplified analytical method (also known as simplified energy method). Nielsen [1999, 2006] carried out dynamic analyses of top-level guy wire rupture on a 244 m guyed mast in Pyhätunturi, Finland and a 300 m guyed mast in Kisielice, Poland, and compared the results with those two approaches suggested by Eurocode. Nielsen reached a conclusion that the static approach is a fast approach that leads to conservative values while the simplified energy method, although more complicated than the former, gives the most precise estimation of the dynamic effects without doing a full dynamic analysis. The simplified analytical method summarized in Section 5 of this chapter is now mostly used by tower design engineers.

To the best of the author's knowledge, there is no experimental research previously conducted to determine the dynamic load amplification factor of guy wires due to guy wire rupture. In the present work, a total of 348 guy wire rupture tests were carried out and the results were compared with the results from dynamic analysis and Eurocode simplified analytical method.

Since there is ambiguity about the effect of guy wire initial tension on the dynamic load amplification factor, the effect of initial tension was also studied. The usual practice in the field is to apply guy wire initial tensions in the range of 8% to 15% of the breaking strength of the guy wires. Therefore, tests were conducted with two different guy wire initial tensions, i.e. 10% and 20% of the guy wire breaking strength. In addition, 25 tower configurations were built to find correlations between the distance of guy wires (distance between ruptured guy wire and remaining guys) and dynamic load amplification factor.

2.3 EXPERIMENTAL INVESTIGATION

A total of 348 guy wire rupture tests were conducted at the Structural Laboratory of University of Windsor, Windsor, Ontario, Canada during September 2005 to December 2005, which consisted of 228 guy wire rupture tests with a guy wire initial tension of 222 N (50 lb; approximately 10% of guy wire breaking strength) and 120 guy wire rupture tests with a guy wire initial tension of 445 N (100 lb; approximately 20% of guy wire breaking strength). There were three replicate tests for each level and configuration.

2.3.1 Details of Tower Specimens

The purpose of this experiment was to determine the dynamic load amplification factors of guy wire tensions for a small-scale guyed tower test specimen after the sudden rupture of a guy wire. The tower was 2.2 m high, with three guy wire levels (designated as G3, G2, and G1) and a guy wire anchor radius of 1.2 m as shown in Figure 2.2. There were seven levels of guy lugs (guy attachment points at tower mast) on the tower mast at elevations 0.3 m, 0.6 m, 0.9 m, 1.2 m, 1.5 m, 1.8 m, and 2.1 m, as shown in Figure 2.2 and Table 2.1. The mast of the tower was a steel pipe with an outside diameter of 21.3 mm and wall thickness of 2.77 mm. The guy wires were made from 1.59 mm ($^1/_{16}$ in.) diameter galvanized steel strand with a breaking strength of 2140 N (480 lb).

The choice of the steel pipe and guy wires were based on the ratio of bending stiffness EI over axial stiffness k (AE/L) of the tower mast and guy wires, where E is the Young's modulus of elasticity, I is the moment of inertia, A is the cross-sectional area, and L is the length of the member (in this case, is taken as guy wires interval). Of the six typical 115 m guyed tower produced by Westower Communications Ltd. with typical guy wires interval at 20 m and guy radius of 78.8 m, the EI/k of the tower mast are ranging from 2.70×10^9 to 8.11×10^9, and those of the most common guy wires used ($^5/_8$" diameter, 1 x 7 Guy Strand) are ranging from 1.01×10^{11} to 2.71×10^{11}. The EI/k of the mast of the tower test specimens was 1.32×10^4 and those of the guy wires were ranging from 2.41×10^5 to 9.21×10^5. This makes the ratio of the EI/k of tower mast of actual guyed towers versus the test specimens are ranging from 1.62×10^{-6} to 4.87×10^{-6}, and those of the guy wires are ranging from 2.38×10^{-6} to 3.40×10^{-6}. Since the ratio of the EI/k of the mast and guy wires between the actual guyed tower and test specimens are comparable, the steel pipe and guy strand with properties described in the previous paragraph were selected.

The test setup is shown in Figure 2.3. The details of tapered mast base, guy lugs, and guy wire anchor points of typical guyed tower in the field and those of test specimens are shown in Figures 2.4, 2.5, and 2.6, respectively. There were two linear variable displacement transducers and two accelerometers in mutually perpendicular directions as shown in Figure 2.7 to measure the displacement and acceleration of the mast at the ruptured guy level. The guy wire tensions, mast displacement at the ruptured guy level, and mast accelerations were recorded by a MEGADAC Data Acquisition System at a rate of 1200 Hz.

During experimental investigation, three levels of guy wires were attached at different guy lugs to make 25 tower configurations and the guy wire tensions were adjusted using turnbuckles.

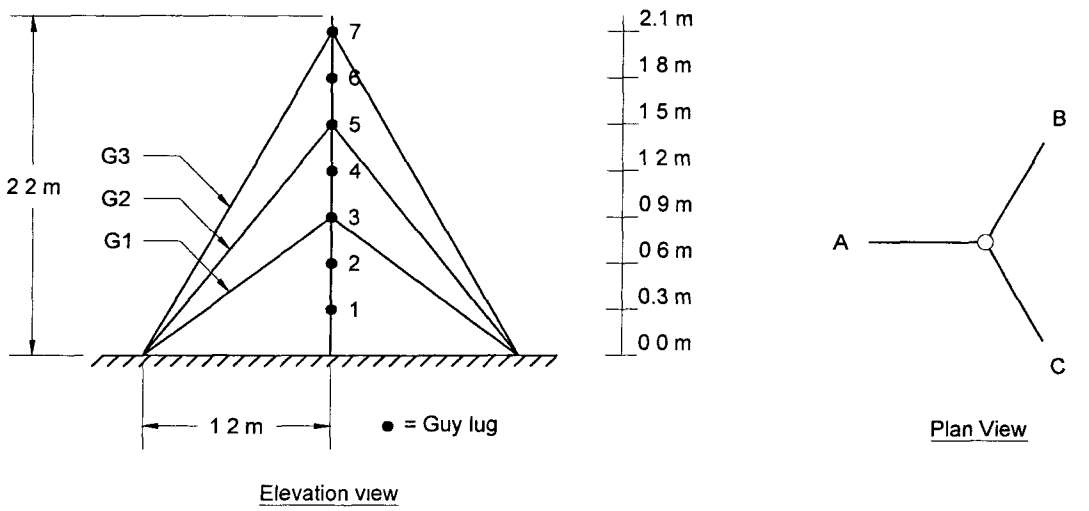

Figure 2.2. Designation of Guy Wire Levels, Guy Lugs, and Guy Wire Orientations of Tower Specimen

Table 2.1. Location of Guy Lugs

Guy lug #	Elevation (m)
1	0.3
2	0 6
3	0 9
4	1 2
5	1 5
6	1.8
7	2.1

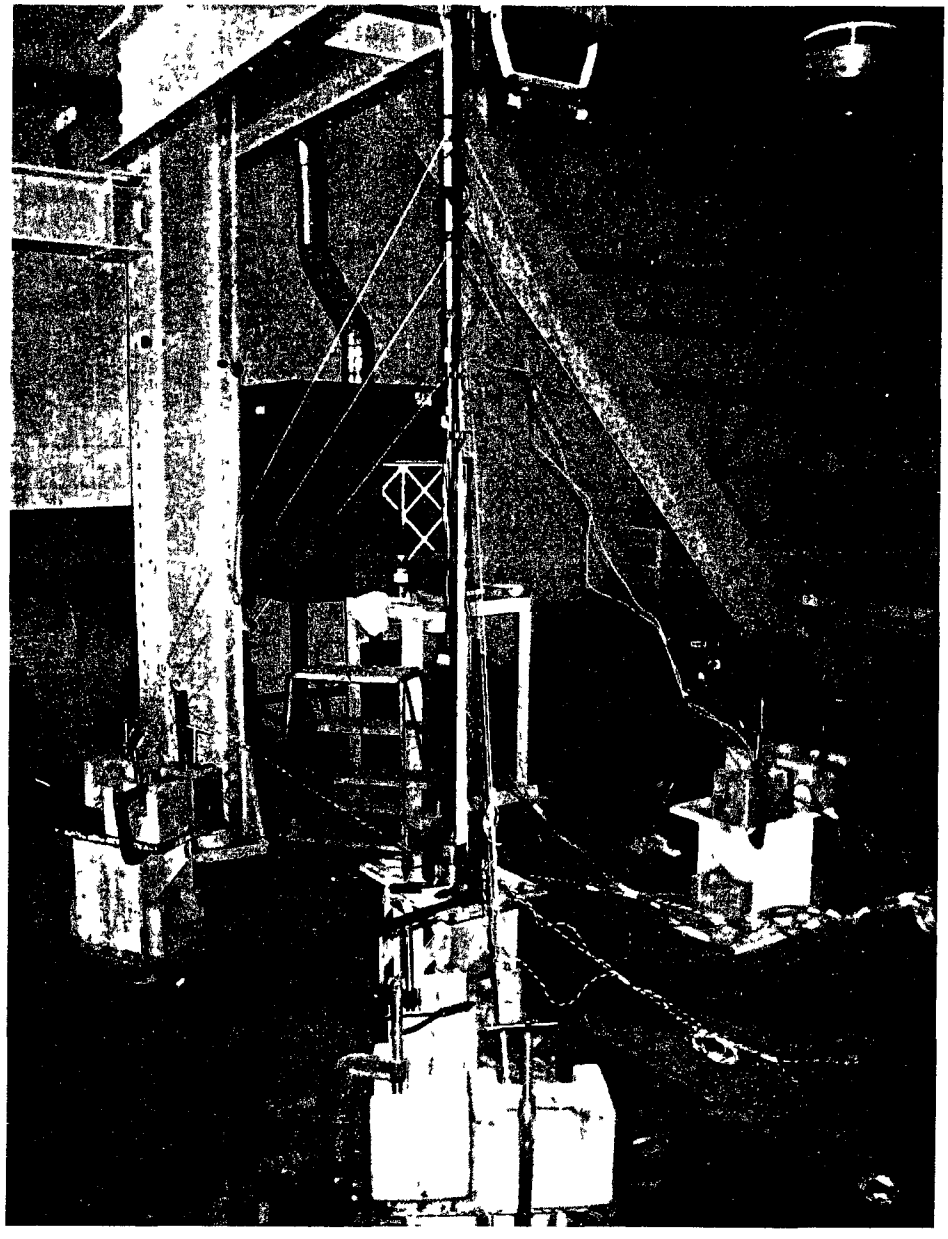

Figure 2.3. Photograph of Tower Test Specimen Anchored in Three Directions

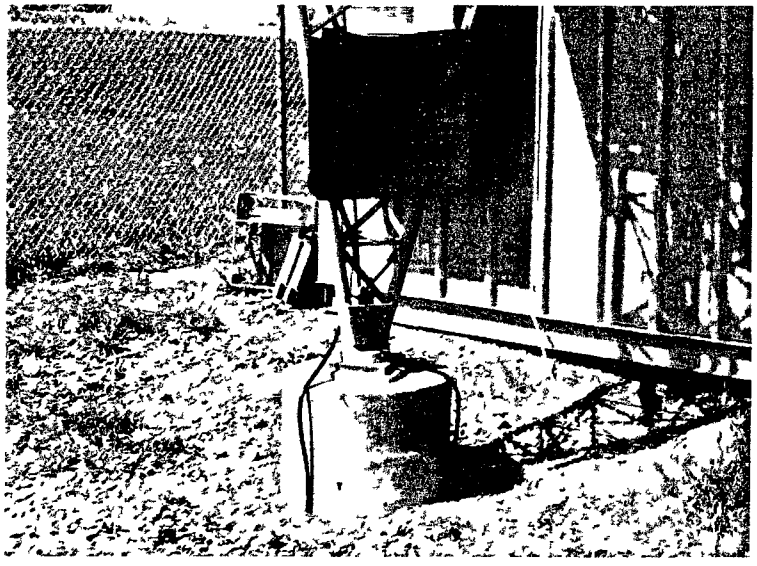

(a) Base of typical guyed tower
(courtesy of Westower Communications Ltd)

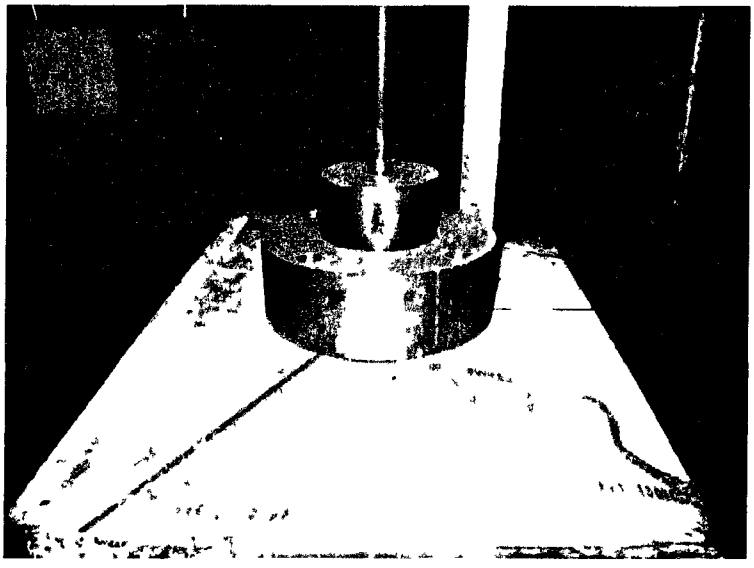

(b) Base of tower specimen

Figure 2.4. Mast Base of Typical Guyed Tower and Tower Specimen

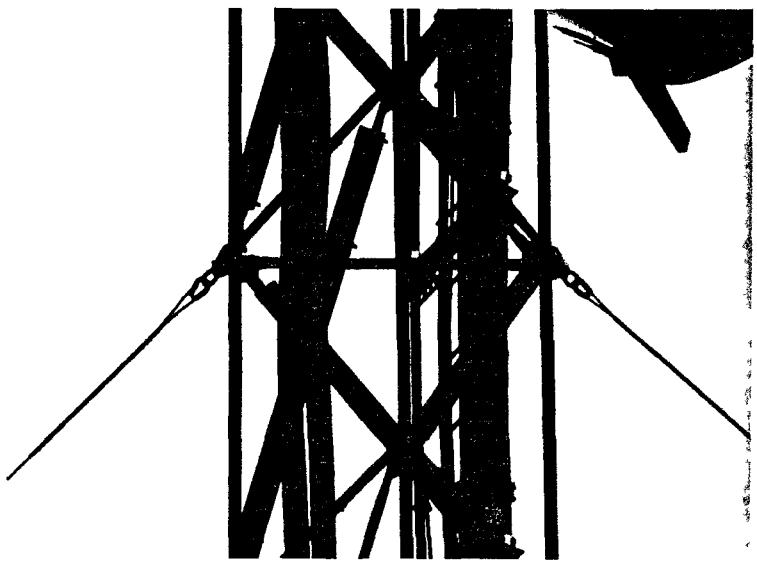

(a) Guy lugs of typical guyed tower
(courtesy of Westower Communications Ltd)

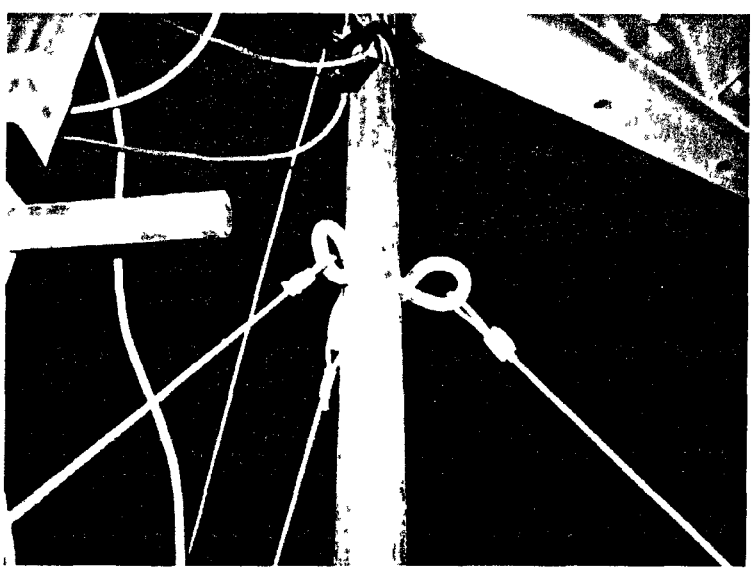

(b) Guy lugs of tower specimen

Figure 2.5. Guy Lugs of Typical Guyed Tower and Tower Specimen

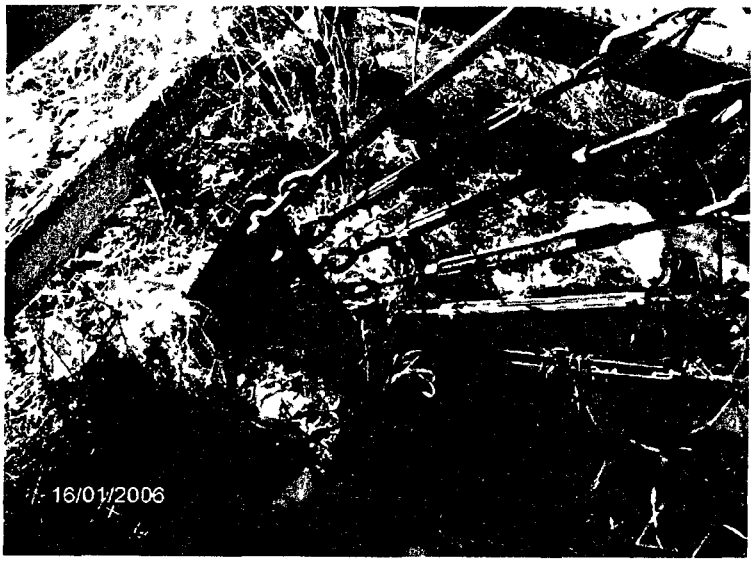

(a) Anchor of typical guyed tower
(courtesy of Westower Communications Ltd)

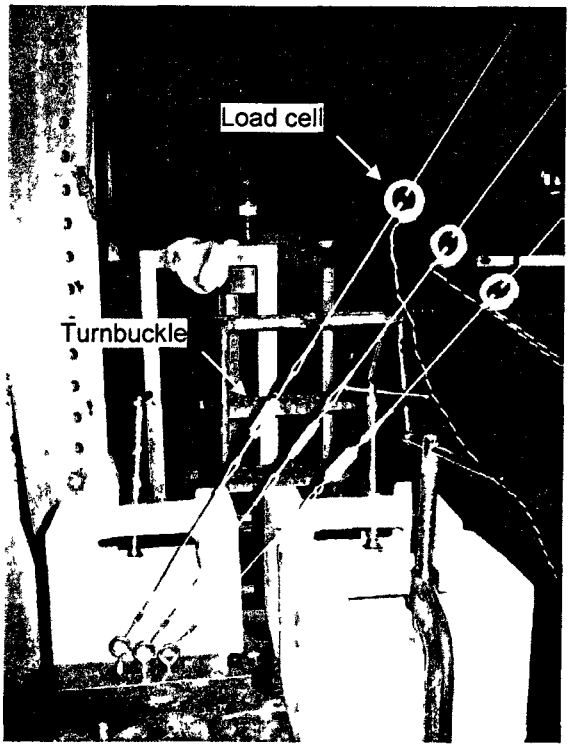

(b) Anchor of test specimen

Figure 2.6. Anchor of Typical Guyed Tower and Tower Specimen

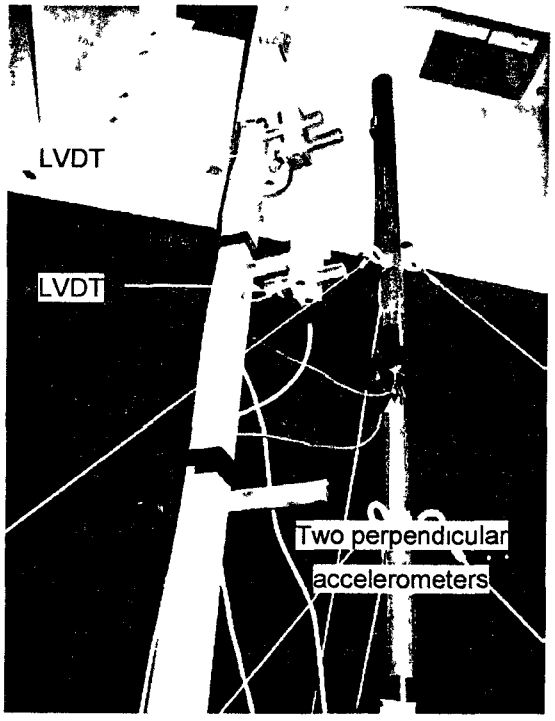

Figure 2.7. Details of Test Specimen

The 25 tower configurations are listed in Table 2.2 In order to measure the tensions in the guy wires, an aluminum half bridge load cell was attached near the guy wire anchor point of each guy wire (for a total nine load cells). Each load cell was made from a ring with a 37.5 mm outside diameter and a 6.25 mm wall thickness, which remained in the elastic range during the testing (see details in Appendix A). The calibration of these load cells is shown in Appendix B. Two holes in guy wire axial direction were made in the ring to accommodate the crimped end guy wires. Two 350-ohm strain gages (with a gauge factor of 2.13) were attached, one to the inside and the other to the outside of the ring. The turnbuckles were adjusted iteratively to make the initial guy wire tensions as close as possible to the desired initial tensions and as equal as possible to initial tension of other two guy wires.

2.3.2 Details of Experiments

There were two series of tests. The initial tensions of all guy wires were approximately 222 N (50 lb) for the first series of tests (Series 1) on 12 tower configurations as listed in Table 2.3. For second series of tests (Series 2), there were two initial tensions applied to the 13 tower configurations to study the effect of initial tension on the dynamic load amplification factor. For Series 2(a), the initial tension of the guy wires was approximately 222 N (50 lb). After the guy wire rupture tests had been done for three levels of guy wires of a tower, the same tower configuration was re-built and a guy wire initial tension of 445 N (100 lb) was given (Series 2(b)).

Guy wire was ruptured by cutting it suddenly with shears near its guy lug. The test started with the cutting of the top level guy wire. After the tower came to a rest position, the ruptured guy wire was replaced with a new one. The test was continued by cutting the mid level guy wire, and finally by cutting the bottom level guy wire. For a given test, a peak tension value was selected for each individual guy wire, independently of each other.

2.3.3 Experimental Results

The detailed experimental results were reported by Madugula and Kumalasari [2006], and example of the results is shown in Table 2.4. In Table 2.4, experiments # 1 to 3 were identical tests done with rupture at G3, experiments # 4 - 6 were for rupture at G2, and the rest were for rupture at G1, all of which were done on tower configuration # 1 (refer to Table 2.2). The load amplification factor was obtained as the ratio of peak guy wire tension after rupture over guy wire tension before rupture (or the initial tension of the guy wire). Each identical experiments were averaged and summarized in Tables 2.5 and 2.6 for test specimens with guy wire initial tension of 222 N and 445 N, respectively. Figure 2.8 shows the load amplification factors versus the level of

Table 2.2. Tower Configurations

Tower #	Guy lug location*			Tower #	Guy lug location*		
	G3	G2	G1		G3	G2	G1
1	7	6	5	16	6	4	2
2	7	6	4	17	6	4	1
3	7	6	3	18	6	3	2
4	7	5	4	19	6	3	1
5	7	5	3	20	5	4	3
6	7	5	2	21	5	4	2
7	7	5	1	22	5	4	1
8	7	4	3	23	5	3	2
9	7	4	2	24	5	3	1
10	7	4	1	25	5	2	1
11	7	3	1				
12	6	5	4				
13	6	5	3				
14	6	5	2				
15	6	4	3				

* Refer to Figure 2 2 for guy lug location

Table 2.3. Tower Configurations for Guy Wire Rupture Tests

	Series 1	Series 2(a)	Series 2(b)
	222 N initial tension	222 N initial tension	445 N initial tension
Tower configuration #	1-5, 7, 10, 11, 13-15, 22	6, 8, 9, 12, 16-21, 23-25	6, 8, 9, 12, 16-21, 23-25

Table 2.4. Example Load Amplification Factor due to Sudden Guy Wire Rupture – Tower # 1

(Guy Wire Initial Tension of 222 N)

Experiment #	Rupture at	Guy level	Initial tension (N)			Final tension (N)			Load amplification factor			Displacement at ruptured guy level (mm)
		Direction	A	B	C	A	B	C	A	B	C	
1	G3	G3	227	222	226	-	185	185	-	0.835	0.819	9.32
		G2	232	231	225	461	229	216	1.99	0.992	0.959	
		G1	226	241	229	270	345	305	1.19	1.43	1.33	
2	G3	G3	226	222	221	-	187	182	-	0.844	0.825	8.99
		G2	226	234	230	456	233	221	2.02	0.994	0.962	
		G1	222	236	227	263	320	306	1.18	1.35	1.35	
3	G3	G3	226	229	220	-	198	183	-	0.865	0.833	8.82
		G2	231	227	232	458	225	226	1.98	0.991	0.974	
		G1	220	237	225	262	320	308	1.19	1.35	1.37	
4	G2	G3	227	227	222	348	221	214	1.54	0.974	0.963	2.97
		G2	227	226	224	-	207	207	-	0.917	0.925	
		G1	223	238	227	313	224	216	1.40	0.941	0.950	
5	G2	G3	226	225	224	361	224	218	1.60	0.996	0.974	3.18
		G2	223	224	223	-	210	207	-	0.940	0.928	
		G1	223	236	223	325	217	209	1.46	0.922	0.935	
6	G2	G3	232	231	229	372	230	226	1.61	0.995	0.986	3.21
		G2	228	223	226	-	210	213	-	0.939	0.940	
		G1	225	232	223	330	216	208	1.47	0.931	0.933	
7	G1	G3	231	230	224	264	251	256	1.14	1.09	1.14	7.65
		G2	225	225	226	385	208	209	1.71	0.926	0.926	
		G1	229	235	232	-	197	196	-	0.839	0.845	
8	G1	G3	227	233	227	261	260	252	1.15	1.11	1.11	6.84
		G2	226	221	223	389	206	206	1.73	0.932	0.921	
		G1	227	231	222	-	198	181	-	0.855	0.818	
9	G1	G3	228	233	227	260	260	252	1.14	1.12	1.11	6.88
		G2	228	224	222	394	210	207	1.73	0.936	0.930	
		G1	228	230	229	-	200	197	-	0.871	0.862	

Table 2.5. Average Load Amplification Factors and Deflections – 222 N Initial Tension

Tower	Rupture at	Guy level Direction	Load amplification factor A	B	C	Deflection at ruptured guy level (mm)
1	G3	G3	-	0 848	0 825	9 04
		G2	2 00	0 992	0 965	
		G1	1 19	1 38	1 35	
	G2	G3	1 58	0 988	0 974	3 12
		G2	-	0 932	0 931	
		G1	1 44	0 931	0 939	
	G1	G3	1 14	1 11	1 12	7 13
		G2	1 72	0 931	0 926	
		G1	-	0 855	0 842	
2	G3	G3	-	0 870	0 825	8 24
		G2	2 04	0 967	0 932	
		G1	1 25	1 18	1 24	
	G2	G3	1 68	0 976	0 955	4 19
		G2	-	0 956	0 930	
		G1	1 41	1 01	1 00	
	G1	G3	1 02	1 11	1 13	10 8
		G2	1 61	0 977	0 976	
		G1	-	0 782	0 763	
3	G3	G3	-	0 796	0 815	8 37
		G2	2 01	0 957	0 938	
		G1	1 39	1 31	1 29	
	G2	G3	1 64	0 969	0 952	4 98
		G2	-	0 936	0 920	
		G1	1 48	1 10	1 10	
	G1	G3	1 01	1 10	1 12	11 6
		G2	1 67	1 02	1 02	
		G1	-	0 683	0 733	
4	G3	G3	-	0 783	0 806	19 4
		G2	2 02	1 00	1 01	
		G1	1 18	1 24	1 24	
	G2	G3	1 55	1 02	1 03	2 82
		G2	-	0 932	0 945	
		G1	1 60	0 960	0 988	
	G1	G3	1 07	1 15	1 15	5 38
		G2	1 64	0 897	0 900	
		G1	-	0 780	0 773	
5	G3	G3	-	0 809	0 856	17 4
		G2	2 21	1 02	1 08	
		G1	1 04	1 22	1 25	
	G2	G3	1 70	1 03	1 04	4 54
		G2	-	0 905	0 930	
		G1	1 56	0 977	1 00	
	G1	G3	0 978	1 10	1 10	6 74
		G2	1 65	0 979	1 00	
		G1	-	0 701	0 766	

Table 2.5. Average Load Amplification Factors and Deflections ... (continued)

Tower	Rupture at	Guy level Direction	Load amplification factor A	B	C	Deflection at ruptured guy level (mm)
		G3	-	0 830	0 855	
	G3	G2	2 17	1 07	1 06	-
		G1	1 05	1 24	1 21	
		G3	1 61	1 02	1 03	
6	G2	G2	-	0 908	0 920	7 24
		G1	1 61	1 04	1 04	
		G3	1 02	1 18	1 14	
	G1	G2	1 79	1 13	1 11	7 03
		G1	-	0 686	0 635	
		G3	-	0 804	0 858	
	G3	G2	1 88	1 02	1 07	17 3
		G1	1 07	1 21	1 23	
		G3	1 47	1 02	1 03	
7	G2	G2	-	0 854	0 897	8 97
		G1	1 72	1 05	1 08	
		G3	1 05	1 12	1 13	
	G1	G2	1 48	1 08	1 13	3 56
		G1	-	0 596	0 687	
		G3	-	0 786	0 800	
	G3	G2	2 13	1 09	1 07	-
		G1	0 969	1 20	1 25	
		G3	1 57	1 07	1 11	
8	G2	G2	-	0 885	0 893	2 97
		G1	1 76	0 944	0 949	
		G3	1 00	1 08	1 07	
	G1	G2	1 74	0 940	0 965	4 01
		G1	-	0 867	0 902	
		G3	-	0 786	0 855	
	G3	G2	1 99	1 11	1 07	-
		G1	1 13	1 28	1 27	
		G3	1 76	1 13	1 14	
9	G2	G2	-	0 879	0 905	5 45
		G1	1 62	1 01	1 01	
		G3	1 14	1 19	1 11	
	G1	G2	1 84	1 04	1 06	5 37
		G1	-	0 841	0 711	
		G3	-	0 781	0 808	
	G3	G2	1 95	1 09	1 09	28 0
		G1	1 11	1 31	1 29	
		G3	1 61	1 06	1 07	
10	G2	G2	-	0 823	0 838	8 31
		G1	1 65	1 03	1 01	
		G3	1 12	1 11	1 12	
	G1	G2	1 50	1 04	1 07	2 43
		G1	-	0 738	0 793	

Table 2.5. Average Load Amplification Factors and Deflections ... (continued)

Tower	Rupture at	Guy level Direction	Load amplification factor A	B	C	Deflection at ruptured guy level (mm)
11	G3	G3	-	0 762	0 795	-
		G2	2 08	1 15	1 16	
		G1	1 05	1 25	1 19	
	G2	G3	1 70	1 11	1 10	5 41
		G2	-	0 795	0 836	
		G1	1 66	0 971	0 980	
	G1	G3	1 17	1 10	1 12	1 98
		G2	1 50	1 03	1 04	
		G1	-	0 781	0 813	
12	G3	G3	-	0 900	0 902	7 53
		G2	1 77	0 930	0 933	
		G1	1 18	1 16	1 14	
	G2	G3	1 47	0 961	0 968	2 20
		G2	-	0 936	0 945	
		G1	1 59	0 977	0 994	
	G1	G3	1 20	1 13	1 18	7 43
		G2	1 83	0 914	0 906	
		G1	-	0 837	0 921	
13	G3	G3	-	0 947	0 904	9 06
		G2	2 05	0 955	0 922	
		G1	1 08	1 16	1 16	
	G2	G3	1 62	0 963	0 978	3 25
		G2	-	0 877	0 933	
		G1	1 56	1 07	1 09	
	G1	G3	1 31	1 20	1 25	7 32
		G2	1 58	1 02	0 988	
		G1	-	0 668	0 790	
14	G3	G3	-	0 974	0 923	8 84
		G2	1 94	0 981	0 943	
		G1	1 05	1 18	1 14	
	G2	G3	1 70	0 977	0 974	4 44
		G2	-	0 898	0 923	
		G1	1 58	1 08	1 08	
	G1	G3	1 21	1 16	1 30	7 54
		G2	1 72	1 04	1 10	
		G1	-	0 586	0 698	
15	G3	G3	-	0 875	0 893	16 2
		G2	1 89	0 986	0 983	
		G1	1 07	1 18	1 18	
	G2	G3	1 36	0 996	1 02	2 79
		G2	-	0 922	0 929	
		G1	1 79	0 991	1 04	
	G1	G3	1 17	1 19	1 16	4 43
		G2	1 81	0 923	0 948	
		G1	-	0 837	0 853	

Table 2.5. Average Load Amplification Factors and Deflections ... (continued)

Tower	Rupture at	Guy level Direction	Load amplification factor A	B	C	Deflection at ruptured guy level (mm)
		G3	-	0 865	0 876	
	G3	G2	2 00	1 05	0 980	16 8
		G1	1 09	1 23	1 26	
		G3	1 41	0 997	1 01	
16	G2	G2	-	0 902	0 928	4 52
		G1	1 69	1 02	1 03	
		G3	1 12	1 15	1 17	
	G1	G2	1 78	1 08	1 11	4 40
		G1	-	0 719	0 770	
		G3	-	0 876	0 941	
	G3	G2	1 87	0 990	1 01	16 4
		G1	1 12	1 25	1 27	
		G3	1 54	1 06	1 09	
17	G2	G2	-	0 865	0 931	7 03
		G1	1 76	1 05	1 09	
		G3	1 14	1 18	1 18	
	G1	G2	1 61	1 08	1 15	2 60
		G1	-	0 726	0 757	
		G3	-	0 878	0 878	
	G3	G2	1 81	1 02	1 01	-
		G1	1 05	1 22	1 25	
		G3	1 31	1 07	1 06	
18	G2	G2	-	0 887	0 920	2 77
		G1	1 75	0 952	0 980	
		G3	1 04	1 10	1 10	
	G1	G2	1 68	0 959	0 981	2 73
		G1	-	0 838	0 878	
		G3	-	0 988	0 883	
	G3	G2	1 74	1 05	1 01	16 1
		G1	1 06	1 28	1 22	
		G3	1 53	1 12	1 13	
19	G2	G2	-	0 786	0 823	5 70
		G1	1 80	1 01	1 01	
		G3	1 05	1 12	1 11	
	G1	G2	1 51	1 04	1 04	2 01
		G1	-	0 819	0 830	
		G3	-	0 830	0 846	
	G3	G2	1 86	0 925	0 936	6 96
		G1	1 18	1 15	1 18	
		G3	1 49	0 947	0 942	
20	G2	G2	-	0 926	0 927	1 94
		G1	1 53	0 977	0 977	
		G3	1 15	1 16	1 17	
	G1	G2	1 65	0 926	0 960	4 04
		G1	-	0 762	0 823	

Table 2.5. Average Load Amplification Factors and Deflections ... (concluded)

Tower	Rupture at	Guy level Direction	Load amplification factor A	B	C	Deflection at ruptured guy level (mm)
21	G3	G3	-	0 877	0 928	7 07
		G2	2 00	0 958	0 956	
		G1	1 21	1 24	1 26	
	G2	G3	1 73	0 991	0 995	4 34
		G2	-	0 950	0 935	
		G1	1 57	1 06	1 05	
	G1	G3	1 19	1 22	1 21	4 37
		G2	1 69	1 03	1 06	
		G1	-	0 715	0 791	
22	G3	G3	-	0 914	0 924	7 75
		G2	1 92	0 948	0 964	
		G1	1 21	1 24	1 23	
	G2	G3	1 60	1 01	0 998	4 11
		G2	-	0 917	0 935	
		G1	1 67	1 03	1 04	
	G1	G3	1 18	1 20	1 22	2 84
		G2	1 54	1 04	1 10	
		G1	-	0 703	0 723	
23	G3	G3	-	0 866	0 874	13 8
		G2	1 83	1 00	1 02	
		G1	1 10	1 21	1 21	
	G2	G3	1 44	1 08	1 04	2 29
		G2	-	0 910	0 875	
		G1	1 68	0 983	0 953	
	G1	G3	1 21	1 16	1 16	3 00
		G2	1 75	0 920	0 933	
		G1	-	0 828	0 870	
24	G3	G3	-	0 859	0 855	14 4
		G2	1 90	1 04	1 03	
		G1	1 13	1 27	1 26	
	G2	G3	1 62	1 10	1 06	4 39
		G2	-	0 897	0 876	
		G1	1 62	1 04	1 00	
	G1	G3	1 12	1 15	1 14	1 88
		G2	1 50	1 02	1 01	
		G1	-	0 801	0 829	
25	G3	G3	-	0 843	0 836	-
		G2	1 87	1 04	1 06	
		G1	1 13	1 18	1 17	
	G2	G3	1 45	1 10	1 13	2 89
		G2	-	0 815	0 844	
		G1	1 76	0 914	0 904	
	G1	G3	1 08	1 07	1 08	1 11
		G2	1 45	0 963	0 953	
		G1	-	0 823	0 826	

Table 2.6. Average Load Amplification Factors and Deflections – 445 N Initial Tension

Tower	Rupture at	Guy level Direction	Load amplification factor A	B	C	Deflection at ruptured guy level (mm)
6	G3	G3	-	0 826	0 785	-
		G2	1 96	1 10	1 06	
		G1	1 06	1 24	1 23	
	G2	G3	1 50	1 04	1 03	12 8
		G2	-	0 894	0 911	
		G1	1 55	1 05	1 04	
	G1	G3	1 12	1 16	1 18	11 3
		G2	1 65	1 09	1 18	
		G1	-	0 612	0 645	
8	G3	G3	-	0 686	0 696	-
		G2	1 90	1 07	1 07	
		G1	1 01	1 21	1 21	
	G2	G3	1 53	1 08	1 07	5 09
		G2	-	0 874	0 886	
		G1	1 66	0 947	0 939	
	G1	G3	1 11	1 13	1 11	8 26
		G2	1 64	1 08	1 08	
		G1	-	0 785	0 680	
9	G3	G3	-	0 740	0 790	-
		G2	1 91	1 10	1 08	
		G1	1 12	1 27	1 29	
	G2	G3	1 65	1 14	1 15	9 67
		G2	-	0 847	0 873	
		G1	1 53	1 02	1 02	
	G1	G3	1 07	1 11	1 10	7 70
		G2	1 65	1 00	1 01	
		G1	-	0 804	0 769	
12	G3	G3	-	0 860	0 864	14 9
		G2	1 88	0 927	0 927	
		G1	1 20	1 21	1 22	
	G2	G3	1 47	0 968	0 980	4 18
		G2	-	0 925	0 947	
		G1	1 58	0 957	0 988	
	G1	G3	1 16	1 11	1 14	10 6
		G2	1 62	0 908	0 922	
		G1	-	0 746	0 743	
16	G3	G3	-	0 856	0 838	16 8
		G2	1 90	1 03	1 02	
		G1	1 07	1 25	1 24	
	G2	G3	1 38	1 01	1 01	8 52
		G2	-	0 898	0 914	
		G1	1 62	1 03	1 03	
	G1	G3	1 14	1 15	1 16	7 51
		G2	1 70	1 09	1 14	
		G1	-	0 652	0 739	

Table 2.6. Average Load Amplification Factors and Deflections ... (continued)

Tower	Rupture at	Guy level Direction	Load amplification factor A	B	C	Deflection at ruptured guy level (mm)
		G3	-	0 868	0 899	
	G3	G2	1 74	0 993	1 00	-
		G1	1 11	1 24	1 26	
		G3	1 41	1 01	1 04	
17	G2	G2	-	0 872	0 920	12 4
		G1	1 74	1 09	1 10	
		G3	1 14	1 18	1 20	
	G1	G2	1 57	1 10	1 12	4 80
		G1	-	0 635	0 657	
		G3	-	0 835	0 840	
	G3	G2	1 71	1 00	1 02	-
		G1	0 986	1 18	1 23	
		G3	1 23	1 03	1 04	
18	G2	G2	-	0 857	0 887	5 11
		G1	1 70	0 941	0 963	
		G3	1 03	1 06	1 07	
	G1	G2	1 61	0 934	0 941	4 76
		G1	-	0 810	0 847	
		G3	-	0 837	0 838	
	G3	G2	1 69	1 03	1 02	-
		G1	1 04	1 28	1 24	
		G3	1 46	1 11	1 13	
19	G2	G2	-	0 799	0 845	9 76
		G1	1 73	1 04	1 04	
		G3	1 04	1 09	1 09	
	G1	G2	1 47	1 02	1 03	3 45
		G1	-	0 787	0 808	
		G3	-	0 842	0 822	
	G3	G2	1 83	0 925	0 923	16 3
		G1	1 17	1 19	1 18	
		G3	1 49	0 965	0 964	
20	G2	G2	-	0 927	0 937	3 34
		G1	1 53	0 979	0 979	
		G3	1 12	1 16	1 16	
	G1	G2	1 58	0 926	0 946	6 91
		G1	-	0 750	0 777	
		G3	-	0 828	0 932	
	G3	G2	1 87	0 916	0 950	12 2
		G1	1 17	1 20	1 24	
		G3	1 60	0 988	0 975	
21	G2	G2	-	0 937	0 938	5 60
		G1	1 53	1 04	1 05	
		G3	1 16	1 21	1 21	
	G1	G2	1 59	1 04	1 07	7 49
		G1	-	0 623	0 692	

Table 2.6. Average Load Amplification Factors and Deflections ... (concluded)

Tower	Rupture at	Guy level	Load amplification factor			Deflection at ruptured guy level (mm)
		Direction	A	B	C	
23	G3	G3	-	0 825	0 801	23 5
		G2	1 82	1 01	0 973	
		G1	1 08	1 20	1 21	
	G2	G3	1 45	1 09	1 08	4 23
		G2	-	0 863	0 870	
		G1	1 64	0 941	0 937	
	G1	G3	1 13	1 13	1 13	4 59
		G2	1 61	0 926	0 938	
		G1	-	0 805	0 842	
24	G3	G3	-	0 788	0 780	22 2
		G2	1 78	1 03	1 12	
		G1	1 06	1 22	1 23	
	G2	G3	1 46	1 07	1 06	11 4
		G2	-	0 768	0 782	
		G1	1 79	1 02	1 02	
	G1	G3	1 08	1 11	1 12	3 38
		G2	1 47	0 962	0 971	
		G1	-	0 752	0 776	
25	G3	G3	-	0 799	0 797	-
		G2	1 66	1 09	1 11	
		G1	1 12	1 18	1 16	
	G1	G3	-	-	-	-
		G2	-	-	-	
		G1	-	-	-	

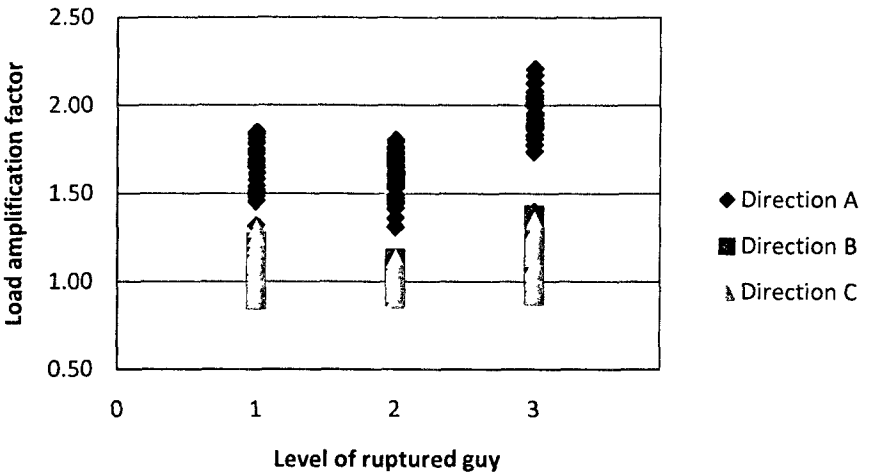

(a) Guy wire initial tension of 222 N

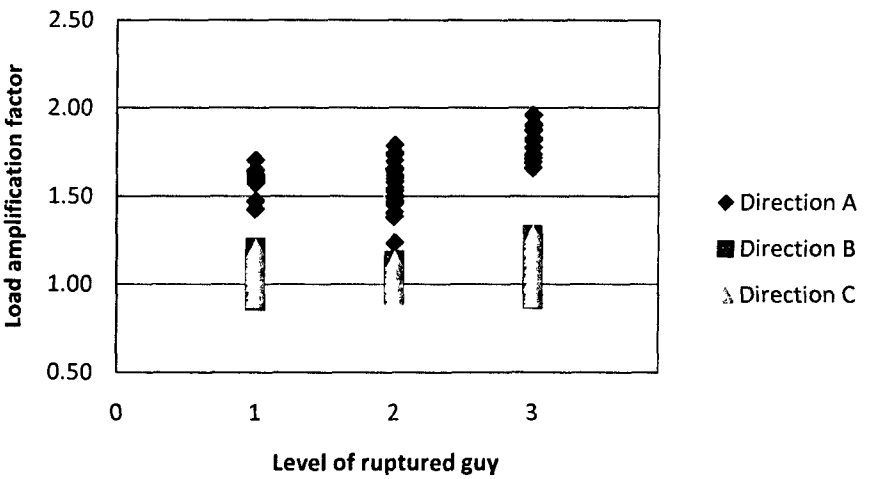

(b) Guy wire initial tension of 445 N

Figure 2.8. Load Amplification Factor versus Level of Ruptured Guy

ruptured guy for both 222 N initial tension and 445 N initial tension. It can be concluded from the graphs that load amplification factors are higher for the remaining guy wires in the same direction as the ruptured guy wire (direction A) and highest when guy wire rupture occurs on the top guy level due to deflection and bending of the tower mast.

The load amplification factors were plotted with the deflection on the ruptured guy level in Figures 2.9 to 2.14. The designation of "guy level-direction" is used to simplify the graphs, e.g. "G2-A" refers to second guy level (G2) in direction A. It can be seen from those graphs that guy wires in directions B and C have comparable load amplification factors, which are expected since those guy wires were arranged to be as symmetrical as possible.

From Figures 2.9 and 2.10 (load amplification factors due to ruptures at G1) and Figures 2.11 and 2.12 (load amplification factors due to ruptures at G2), the load amplification factors for guy wires in direction A are increasing with the increase in the deflection of tower mast at the ruptured guy level, while those for guy wires in directions B and C are almost constant. From Figures 2.13 and 2.14, the load amplification factors for intact guy wires in direction A due to rupture at "G3-A" are decreasing with the increase in the deflection of tower mast at ruptured guy level, and those in directions B and C are almost constant. This decrease can be explained as the result of bending of the tower mast cantilever during ruptures of G3.

To determine the effect of initial tension, Tables 2.7 and 2.8 show the summary of maximum load amplification factors and deflections of tower test specimens for Series 1 (222 N initial tension) and Series 2 (222 N and 445 N initial tensions), respectively. By increasing the initial tension from 222 N to 445 N, the load amplification factors were decreased by 0.08 while the deflections at ruptured guy level were increased by 3.66 mm, in average. The maximum load amplification factors for guy wires with initial tension of 222 N was found to be ranging from 1.45 to 2.21, and those for guy wires with initial tension of 445 N was found to be ranging from 1.43 to 1.96. The decrease of the load amplification factors with the increase of the initial tension was mostly due to the stiffness of intact guy wires with higher initial tension.

Figures 2.15 to 2.20 show the dynamic load amplification factors versus the ratio of elevation of ruptured guy wire over elevation of remaining guy wire. It can be seen from Figures 2.15 to 2.16 (G1 ruptured) and Figures 2.19 to 2.20 (G3 ruptured), that load amplification factors decrease when the distance between the ruptured guy wire and remaining guy wire increase. However, for ruptures at mid-level G2, Figures 2.17 and 2.18 show that load amplification factors increase with an increase of distance between the ruptured guy wire and remaining guy wire.

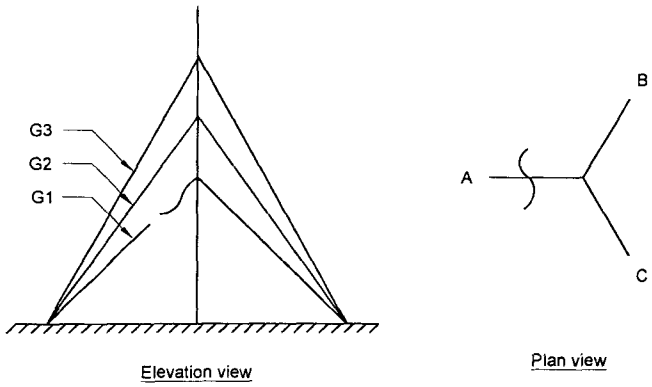

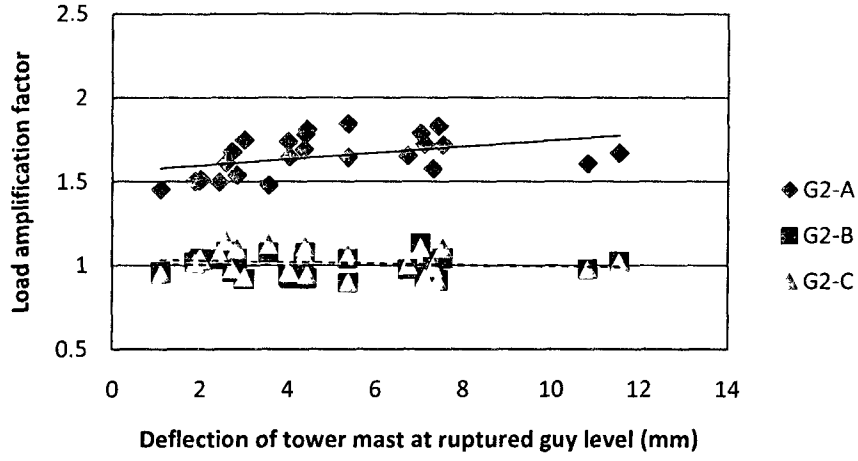

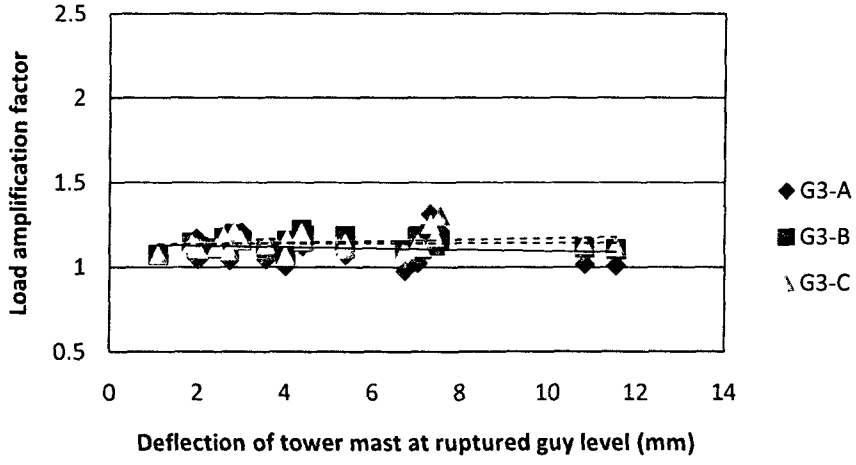

Figure 2.9. Load Amplification Factors of Guy Wires at 2nd and 3rd Level due to Guy Wire Rupture at 1st Level - 222 N Initial Tension

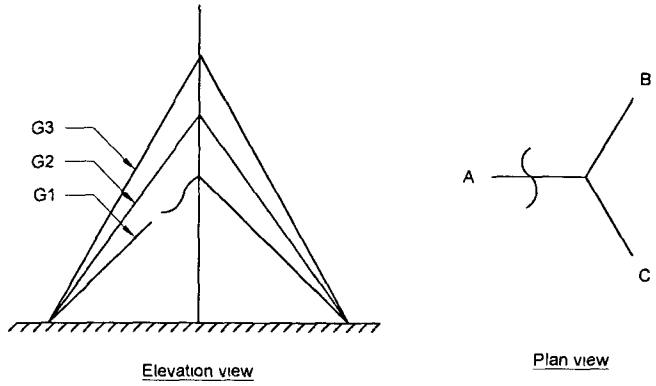

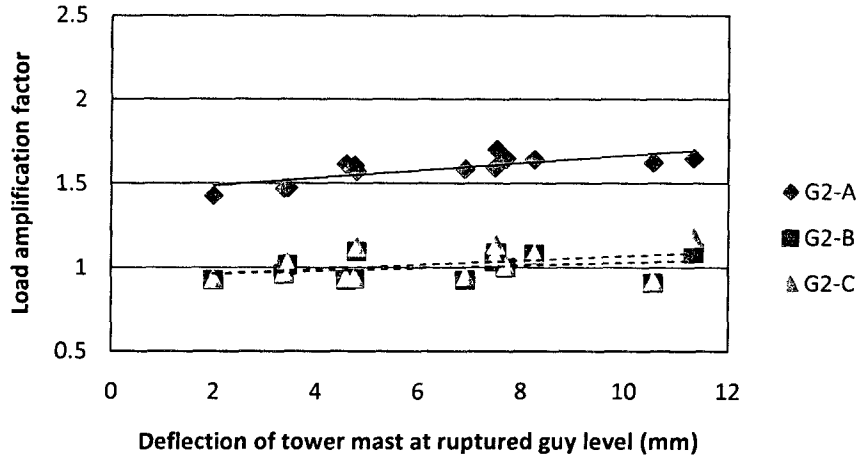

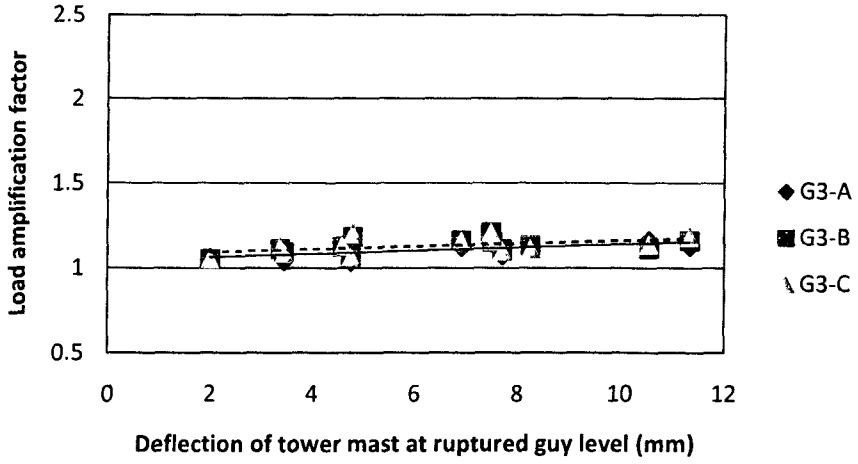

Figure 2.10. Load Amplification Factors of Guy Wires at 2nd and 3rd Level due to Guy Wire Rupture at 1st Level - 445 N Initial Tension

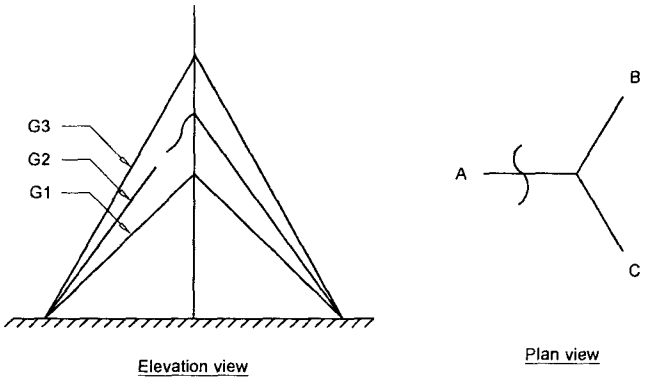

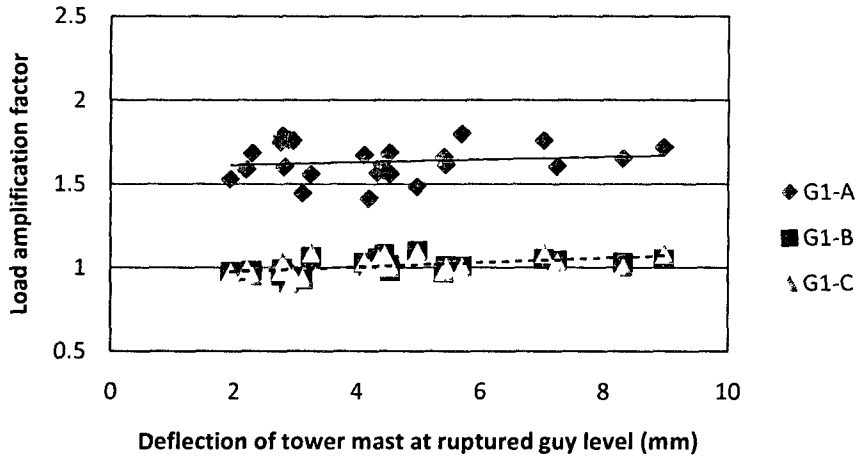

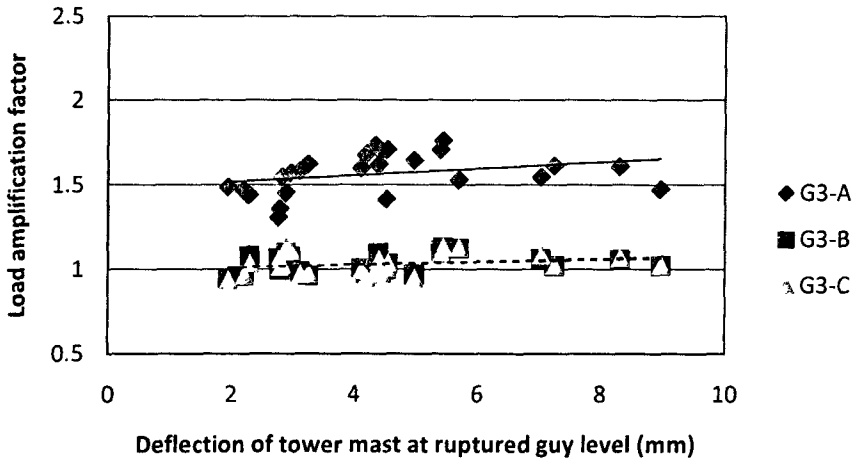

Figure 2.11. Load Amplification Factors of Guy Wires at 1st and 3rd Level due to Guy Wire Rupture at 2nd Level - 222 N Initial Tension

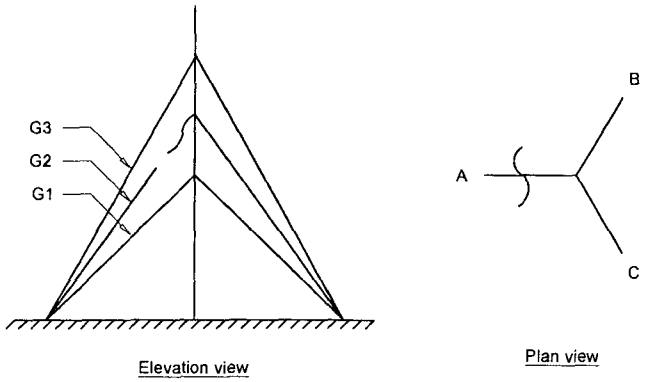

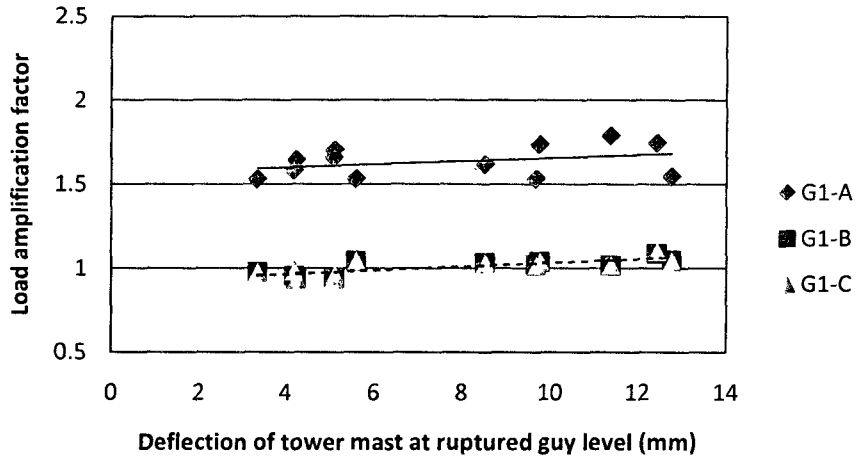

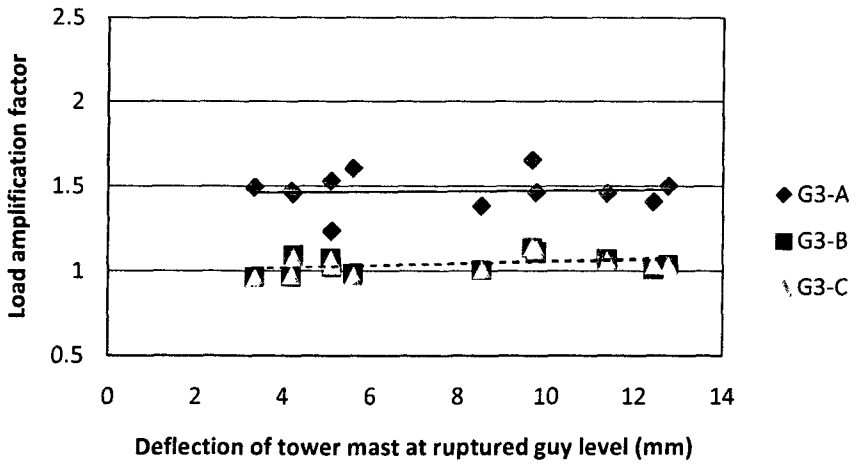

Figure 2.12. Load Amplification Factors of Guy Wires at 1st and 3rd Level due to Guy Wire Rupture at 2nd Level - 445 N Initial Tension

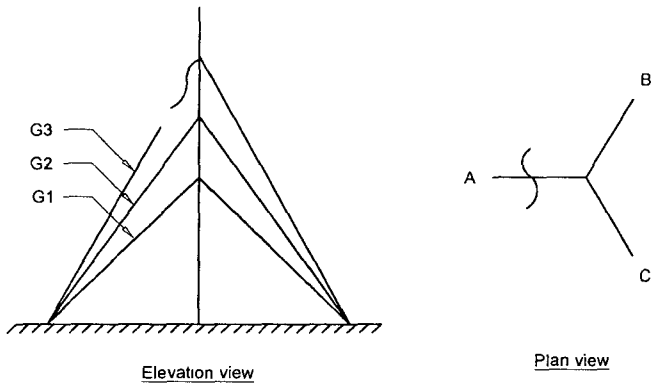

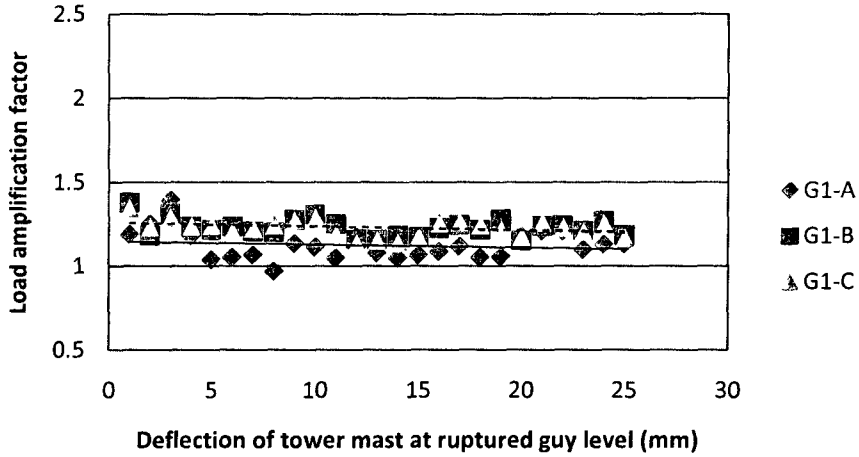

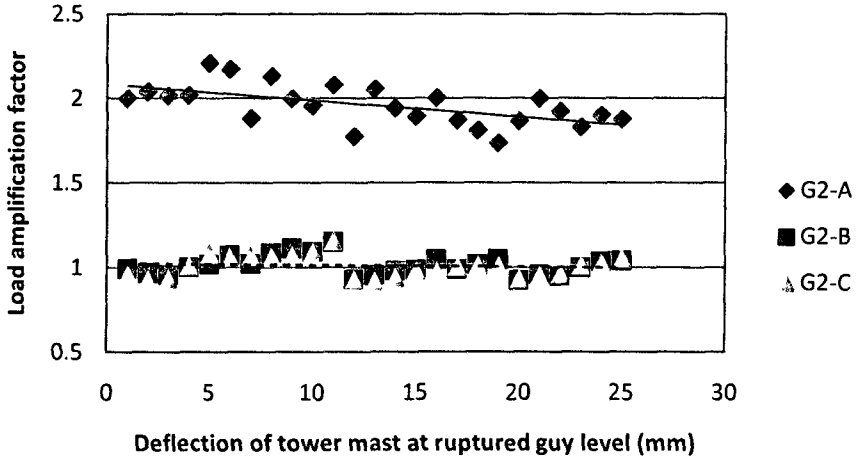

Figure 2.13. Load Amplification Factors of Guy Wires at 1st and 2nd Level due to Guy Wire Rupture at 3rd Level - 222 N Initial Tension

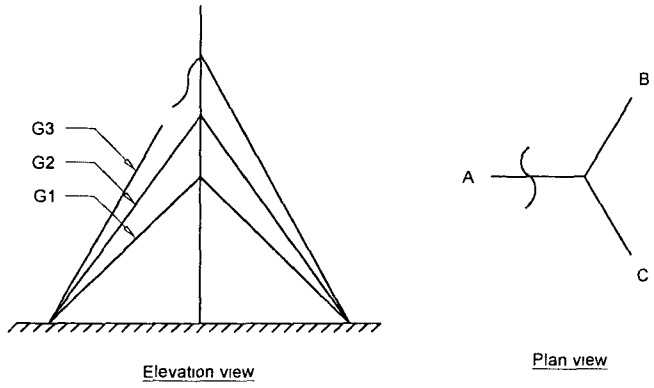

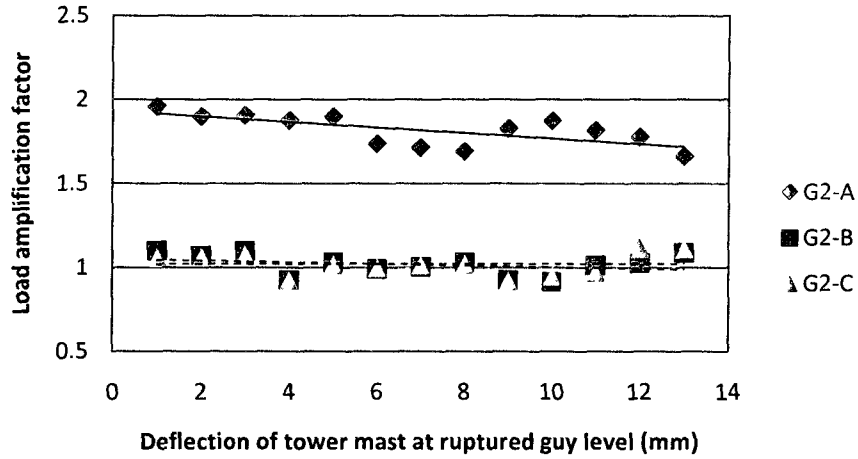

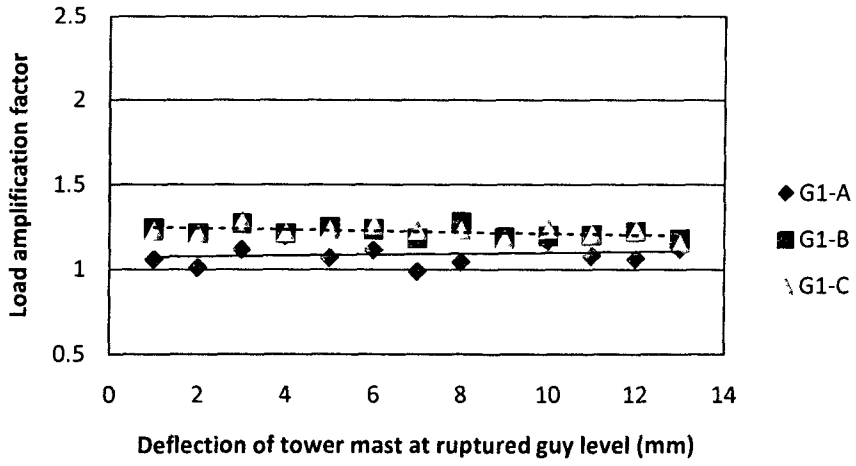

Figure 2.14. Load Amplification Factors of Guy Wires at 1st and 2nd Level due to Guy Wire Rupture at 3rd Level - 445 N Initial Tension

Table 2.7. Maximum Load Amplification Factors of Guy Wires and Mast Deflections of Series 1 Test (Initial Tension of 222 N)

Tower #	Rupture at	Load amplification factor	Deflection at ruptured guy level (mm)
1	G3	2 00	9 04
	G2	1 58	3 12
	G1	1 72	7 13
2	G3	2 04	8 24
	G2	1 68	4 19
	G1	1 61	10 84
3	G3	2 01	8 37
	G2	1 64	4 98
	G1	1 67	11 55
4	G3	2 02	19 42
	G2	1 60	2 82
	G1	1 64	5 38
5	G3	2 21	17 44
	G2	1 70	4 54
	G1	1 65	6 74
7	G3	1 88	17 32
	G2	1 72	8 97
	G1	1 48	3 56
10	G3	1 95	27 99
	G2	1 65	8 31
	G1	1 50	2 43
11	G3	2 08	-
	G2	1 70	5 41
	G1	1 50	1 98
13	G3	2 05	9 06
	G2	1 62	3 25
	G1	1 58	7 32
14	G3	1 94	8 84
	G2	1 70	4 44
	G1	1 72	7 54
15	G3	1 89	16 15
	G2	1 79	2 79
	G1	1 81	4 43
22	G3	1 92	7 75
	G2	1 67	4 11
	G1	1 54	2 84

Table 2.8. Maximum Load Amplification Factors of Guy Wires and Mast Deflections of Series 2 Test (Initial Tension of 222 N and 445 N)

Tower #	Rupture at	Dynamic amplification factor		Deflection at ruptured guy level (mm)	
		Initial tension of 222 N	Initial tension of 445 N	Initial tension of 222 N	Initial tension of 445 N
6	G3	2 17	1 96	-	-
	G2	1 61	1 55	7 24	12 8
	G1	1 79	1 65	7 03	11 3
8	G3	2 13	1 90	-	-
	G2	1 76	1 66	2 97	5 09
	G1	1 74	1 64	4 01	8 26
9	G3	1 99	1 91	-	-
	G2	1 76	1 65	5 45	9 67
	G1	1 84	1 65	5 37	7 70
12	G3	1 77	1 88	7 53	14 9
	G2	1 59	1 58	2 20	4 18
	G1	1 83	1 62	7 43	10 6
16	G3	2 00	1 90	16 8	16 8
	G2	1 69	1 62	4 52	8 52
	G1	1 78	1 70	4 40	7 51
17	G3	1 87	1 74	16 4	-
	G2	1 76	1 74	7 03	12 4
	G1	1 61	1 57	2 60	4 80
18	G3	1 81	1 71	-	-
	G2	1 75	1 70	2 77	5 11
	G1	1 68	1 61	2 73	4 76
19	G3	1 74	1 69	16 1	-
	G2	1 80	1 73	5 70	9 76
	G1	1 51	1 47	2 01	3 45
20	G3	1 86	1 83	6 96	16 3
	G2	1 53	1 53	1 94	3 34
	G1	1 65	1 58	4 04	6 91
21	G3	2 00	1 87	7 07	12 2
	G2	1 73	1 60	4 34	5 60
	G1	1 69	1 59	4 37	7 49
23	G3	1 83	1 82	13 8	23 5
	G2	1 68	1 64	2 29	4 23
	G1	1 75	1 61	3 00	4 59
24	G3	1 90	1 78	14 4	22 2
	G2	1 62	1 79	4 39	11 4
	G1	1 50	1 47	1 88	3 38
25	G3	1 87	1 66	-	-
	G2	1 76	-	2 89	-
	G1	1 45	1 43	1 11	2 00

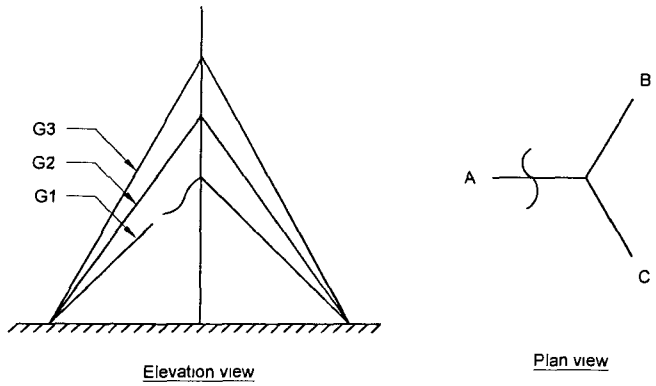

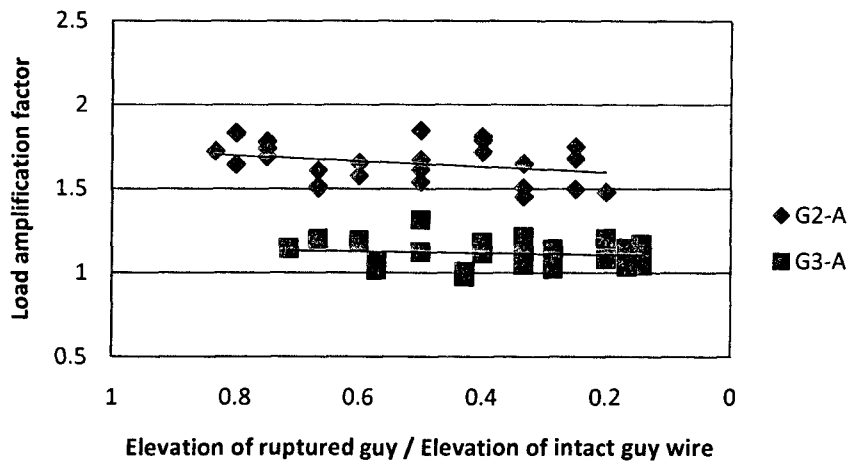

Figure 2.15. Load Amplification Factors of Guy Wires at 2nd and 3rd Level (Direction A) due to Guy Rupture at 1st Level versus the Ratio of Ruptured Guy Elevation over Intact Guy Wire Elevation (222 N Initial Tension)

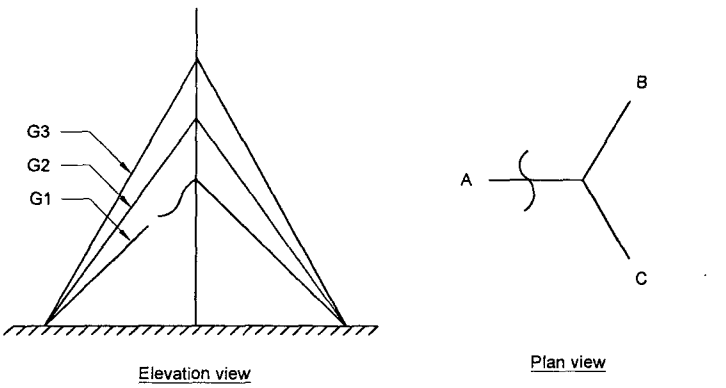

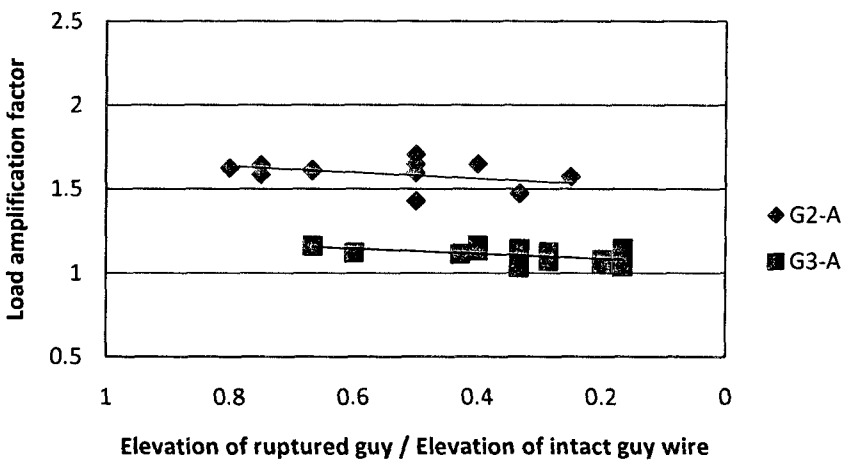

Figure 2.16. Load Amplification Factors of Guy Wires at 2nd and 3rd Level (Direction A) due to Guy Rupture at 1st Level versus the Ratio of Ruptured Guy Elevation over Intact Guy Wire Elevation (445 N Initial Tension)

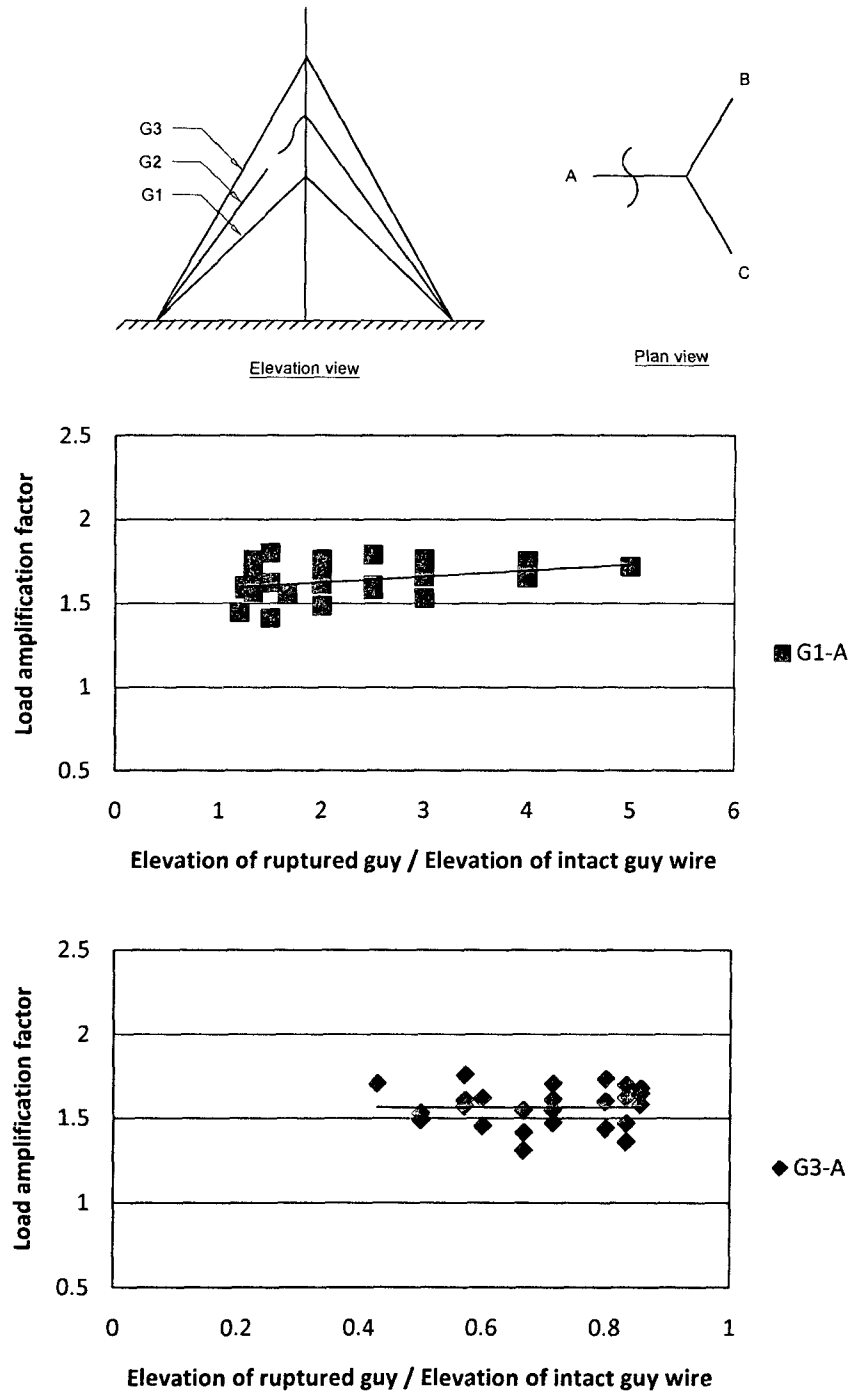

Figure 2.17. Load Amplification Factors of Guy Wires at 1st and 3rd Level (Direction A) due to Guy Rupture at 2nd Level versus the Ratio of Ruptured Guy Elevation over Intact Guy Wire Elevation (222 N Initial Tension)

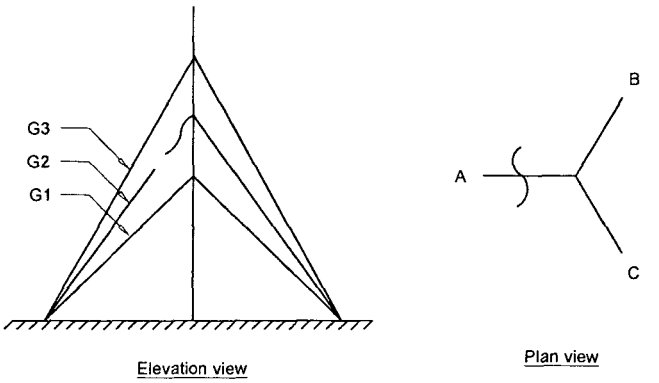

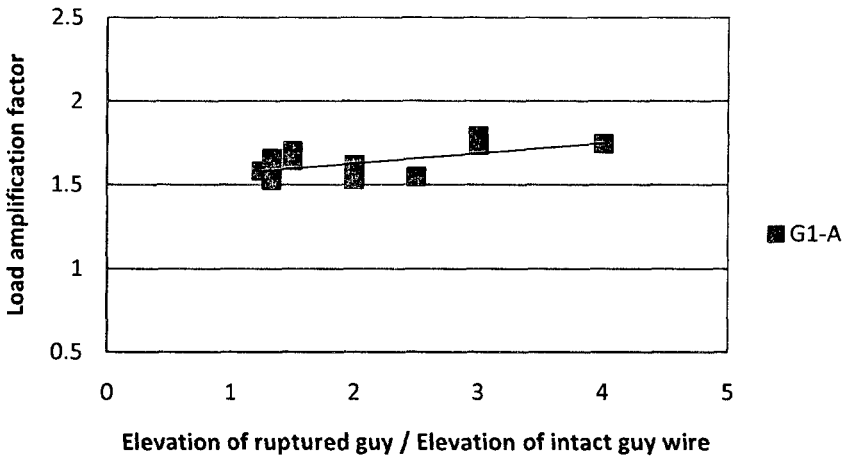

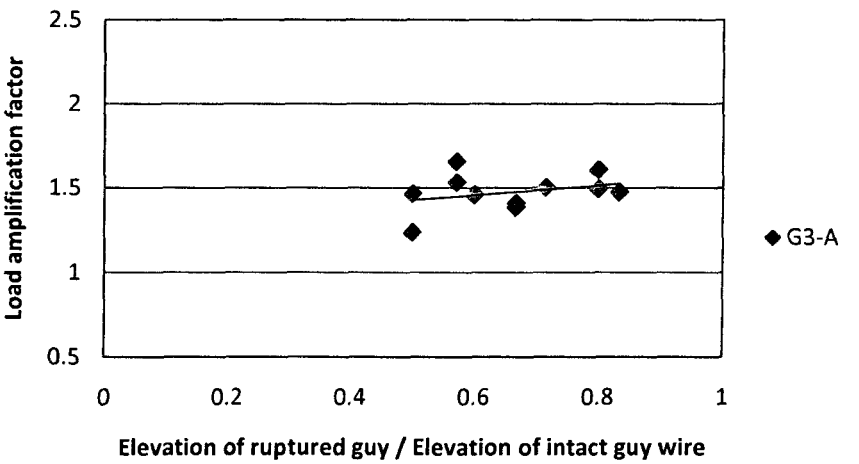

Figure 2.18. Load Amplification Factors of Guy Wires at 1st and 3rd Level (Direction A) due to Guy Rupture at 2nd Level versus the Ratio of Ruptured Guy Elevation over Intact Guy Wire Elevation (445 N Initial Tension)

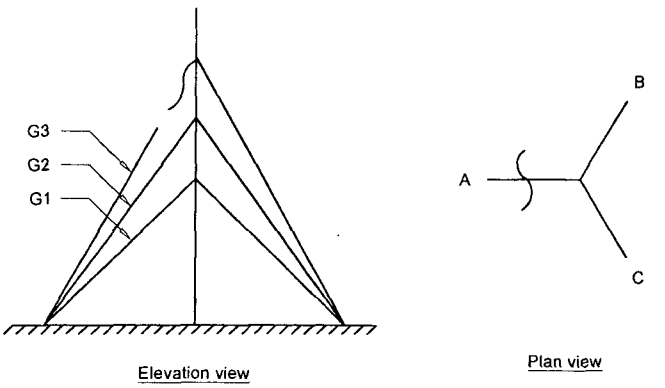

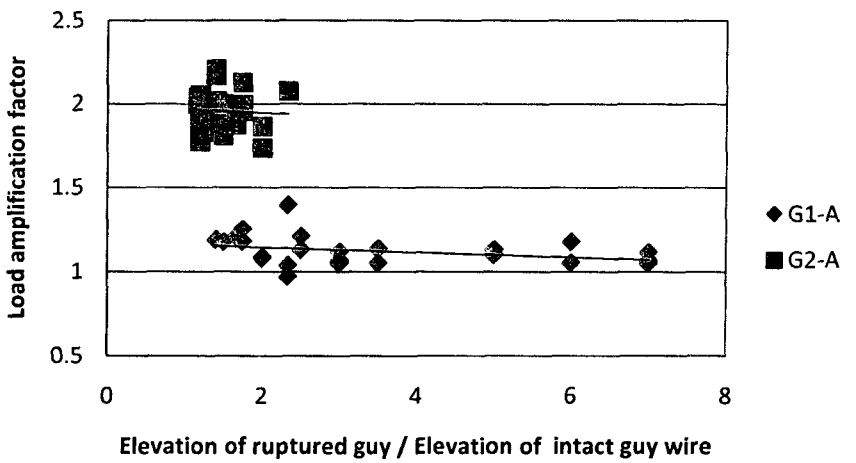

Figure 2.19. Load Amplification Factors of Guy Wires at 1st and 2nd Level (Direction A) due to Guy Rupture at 3rd Level versus the Ratio of Ruptured Guy Elevation over Intact Guy Wire Elevation (222 N Initial Tension)

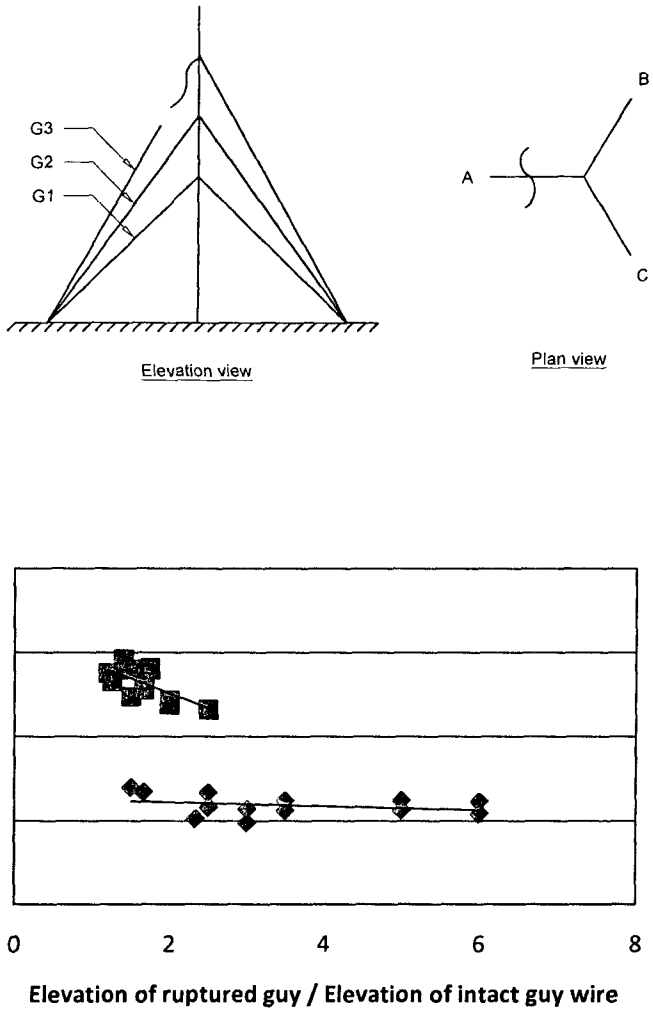

Figure 2.20. Load Amplification Factors of Guy Wires at 1st and 2nd Level (Direction A) due to Guy Rupture at 3rd Level versus the Ratio of Ruptured Guy Elevation over Intact Guy Wire Elevation (445 N Initial Tension)

2.4 FINITE ELEMENT ANALYSIS

In order to evaluate the dynamic load amplification factor due to sudden guy wire rupture, dynamic analysis was carried out using ABAQUS, a commercial finite element package by Simulia [2007]. To take into account the bending of the tower mast and the sagging of the guy wires, the mast and guy wires were modeled using a two-node cubic 3D beam elements with moment release applied to the guy wires. The mast was divided into 20 elements and each guy wire was divided into 6 elements as shown in Figure 2.21. Further refinement of tower mast and guy wires did not result in significant difference. The bottom of the mast was pinned, with torsional restraint, and the ends of the guy wires were pinned.

After gravity load was applied to the mast and guy wires, pretension loading or initial tension was applied to guy wires by using *PRE-TENSION SECTION. This command allows introduction of assembly loads in the model. To maintain the stability of the model, the ruptured guy wire was modelled as a load equivalent to its initial tension which was applied to tower mast at ruptured guy level. The load was then removed immediately to initiate dynamic response of the model. The direct integration method with numerical damping of 5% was used for the dynamic analysis. In ABAQUS, direct integration of the system must be used when nonlinear dynamic response is being studied, since modal superposition procedures are a cost-effective option for performing only linear or mildly nonlinear dynamic analyses.

The direct-integration dynamic procedure provided in Abaqus uses the implicit Hilber-Hughes-Taylor operator for integration of the equations of motion [Simulia 2007]. In an implicit dynamic analysis the integration operator matrix must be inverted and a set of nonlinear equilibrium equations must be solved at each time increment. This solution is done iteratively using Newton's method. Hilber-Hughes-Taylor operator is unconditionally stable and there is no limit on the size of the time increment that can be used for most analyses (accuracy governs the time increment).

The time step for implicit integration can be chosen automatically on the basis of the "half-step residual." By monitoring the values of equilibrium residuals at $t + \Delta t/2$, once the solution at $t + \Delta t$ has been obtained, the accuracy of the solution can be assessed and the time step adjusted appropriately.

HAFTOL is the parameter equal to the half-step residual tolerance to be used with the automatic time increment scheme. For automatic time increment, this value controls the accuracy of the solution. This parameter has dimensions of force and is usually chosen by comparison with typical actual force values, such as applied forces or expected reaction forces. For problems where considerable plasticity or other dissipation is expected to damp out the high frequency

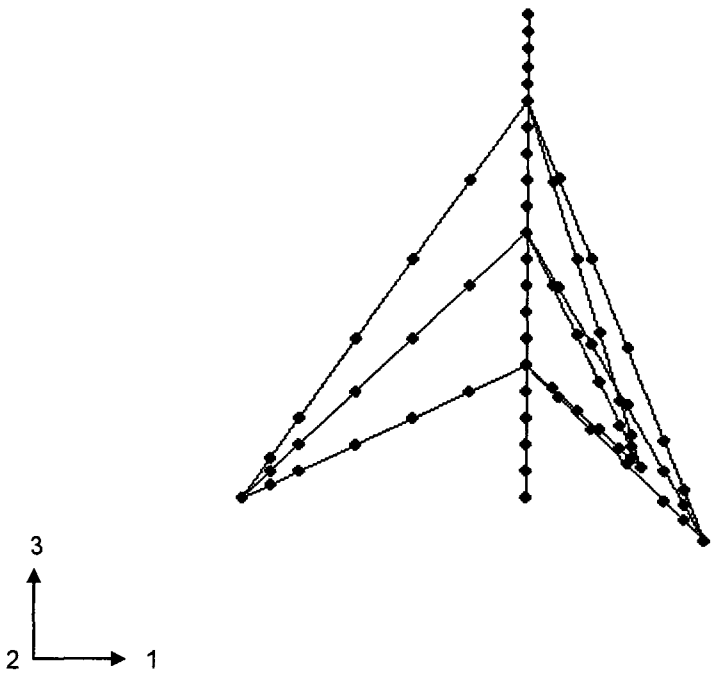

Figure 2.21. Finite Element Model of Tower Specimen

response, HAFTOL is chosen as 10 to 100 times typical actual force values for moderate accuracy and low cost, and as 1 to 10 times typical actual force values for higher accuracy. Since moderate accuracy and low cast is preferred than the later, this parameter was set into 20000, which is about 50 to 100 times the applied forces.

A numerical damping control parameter, α, of -0.05 (-5%) is introduced. This damping is purely numerical and introduces just enough artificial damping in the system to allow the automatic time stepping procedure to work smoothly. Nielsen in 1991 used structural damping of 0.025 for tower mast with pinned mast base [Smith 2006]. However, since the small-scale tower specimens were made from one steel pipe sections with no bolt and weld connections and the testing was done under no wind pressure, the structural damping was considered negligible on the finite element model. An example of ABAQUS input file for the tower test specimen # 25 with initial tension of 445 N, ruptured at G1, is shown in Appendix C.

The finite element analysis results of maximum load amplification factors and deflections at ruptured guy level are summarized in Table 2.9 for 12 towers tested with 222 N initial tension and Table 2.10 for 13 towers tested with both 222 N and 445 N initial tensions. From those tables, it can be concluded that the maximum load amplification factors with initial tension of 222 N ranged from 1.50 to 2.02, and those with initial tension of 445 N were within the range of 1.50 to 1.86.

The results also support the experimental investigation that most of the load amplification factors decreased with doubled initial tension of guy wires. With 445 N initial tension, the average load amplification factors were decreased by 0.04 while the deflections at ruptured guy level were increased by 2.89 mm, compared with those with 222 N initial tension.

The experimental displacement and acceleration of tower mast were compared with those obtained from finite element analysis. Figure 2.22 shows the horizontal deflection of mast at elevation 1.5 m and horizontal acceleration of mast of Tower # 6 with 222 N guy wire initial tension.

2.5 EUROCODE SIMPLIFIED ANALYTICAL METHOD [CEN 2008]

In the Eurocode simplified analytical method [CEN 2008], the rupture is assumed to be a simple cut through the guy wire. For calculating the equivalent static force, the elastic strain energy stored in the ruptured guy before the rupture, damping, and wind loading are neglected. The dynamic force is assumed to be equivalent to a static force $F_{h,dyn}$ acting on the mast at the ruptured guy level.

Table 2.9. Maximum Load Amplification Factors of Guy Wires and Mast Deflections from Finite Element Analysis (Initial Tension of 222 N)

Tower #	Rupture at	Load amplification factor	Deflection at ruptured guy level (mm)
1	G3	1 95	6 08
	G2	1 60	1 76
	G1	1 69	4 23
2	G3	2 02	5 83
	G2	1 69	2 65
	G1	1 55	5 15
3	G3	1 93	5 98
	G2	1 62	3 28
	G1	1 90	13 5
4	G3	1 84	9 31
	G2	1 66	1 96
	G1	1 68	2 95
5	G3	1 94	9 30
	G2	1 66	3 37
	G1	1 50	3 47
7	G3	1 72	9 58
	G2	1 64	4 72
	G1	1 59	2 03
10	G3	1 71	14 6
	G2	1 50	4 32
	G1	1 60	1 76
11	G3	2 01	16 2
	G2	1 61	3 23
	G1	1 60	1 35
13	G3	1 87	5 20
	G2	1 53	2 31
	G1	1 51	3 54
14	G3	1 76	5 07
	G2	1 59	2 77
	G1	1 69	2 68
15	G3	1 83	9 19
	G2	1 74	1 87
	G1	1 76	2 45
22	G3	1 73	4 30
	G2	1 69	2 50
	G1	1 59	1 70

Table 2.10. Maximum Load Amplification Factors of Guy Wires and Mast Deflections from Finite Element Analysis (Initial Tension of 445 N)

Tower #	Rupture at	Dynamic amplification factor		Deflection at ruptured guy level (mm)	
		Initial tension of 222 N	Initial tension of 445 N	Initial tension of 222 N	Initial tension of 445 N
6	G3	1 80	1 78	10 1	5 83
	G2	1 59	1 58	4 39	2 65
	G1	1 64	1 64	3 03	5 15
8	G3	1 90	1 84	14 0	5 98
	G2	1 66	1 57	2 31	3 28
	G1	1 68	1 69	2 21	13 5
9	G3	1 88	1 86	14 3	9 31
	G2	1 63	1 66	3 35	1 96
	G1	1 73	1 50	2 75	2 95
12	G3	1 82	1 83	5 25	9 30
	G2	1 62	1 62	1 52	3 37
	G1	1 65	1 70	3 03	3 47
16	G3	1 92	1 81	8 93	10 1
	G2	1 55	1 56	3 09	4 39
	G1	1 61	1 71	2 62	3 03
17	G3	1 74	1 66	9 21	9 58
	G2	1 52	1 72	3 93	4 72
	G1	1 67	1 57	1 63	2 03
18	G3	1 93	1 65	10 2	14 0
	G2	1 67	1 65	1 70	2 31
	G1	1 64	1 63	1 80	2 21
19	G3	1 91	1 68	12 5	14 3
	G2	1 72	1 60	3 27	3 35
	G1	1 60	1 58	1 37	2 75
20	G3	1 77	1 80	4 08	14 6
	G2	1 54	1 56	1 23	4 32
	G1	1 55	1 55	2 25	1 76
21	G3	1 88	1 83	4 39	16 2
	G2	1 69	1 70	2 04	3 23
	G1	1 58	1 66	2 55	1 35
23	G3	1 84	1 65	7 66	5 25
	G2	1 59	1 63	1 59	1 52
	G1	1 65	1 63	1 80	3 03
24	G3	1 84	1 66	7 14	5 20
	G2	1 59	1 68	2 50	2 31
	G1	1 59	1 57	1 38	3 54
25	G3	1 84	1 58	9 98	5 07
	G2	1 65	1 62	1 59	2 77
	G1	1 63	1 63	0 951	2 68

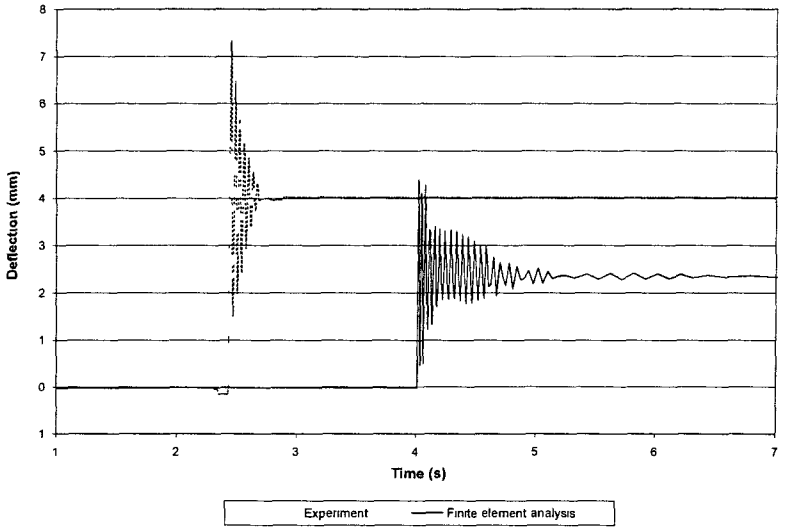

(a) Horizontal deflection of mast at 1.5 m

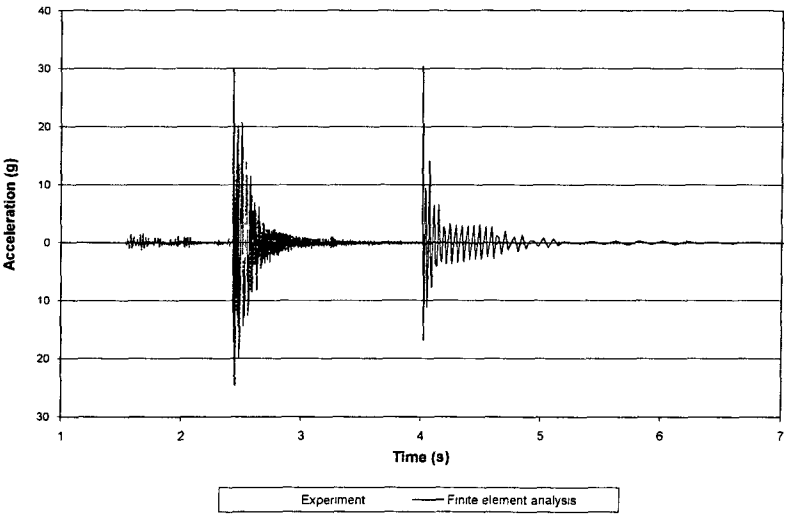

(b) Horizontal acceleration of mast at 1 35 m

Figure 2.22. Comparison of Tower Mast Horizontal Deflection and Acceleration of Tower # 6 with 222 N Guy Initial Tension (Ruptured at Second Guy Level)

For a mast guyed in three directions shown in Figure 2 23(a), the dynamic load amplification factor is calculated as follows

(a) Guy wires B and C act on the mast with a horizontal force F_h, which decreases with increasing deflection "U" due to the slackening of guy wires The force-deflection relationship is shown as curve 1 in Figure 2 23(b)

(b) For the mast without guy wires A, B, and C, the relationship between an external horizontal force "H" applied at the ruptured guy level and the deflection of the load application point is shown as curve 2 in Figure 2 23(b)

(c) Where curves 1 and 2 intersect, the two forces are equal and there is static equilibrium The force acting at the guy wire attachment point is $F_{h\,stat}$ with corresponding deflection of U_{stat}

(d) The dynamic force $F_{h\,dyn}$ and corresponding deflection U_{dyn} is determined by equating the two shaded areas under Curves 1 and 2

(e) The dynamic load amplification factor is the ratio of $F_{h\,dyn}$ to $F_{h\,stat}$

From the force-deflection diagrams obtained from the finite element model, the load amplification factors based on Eurocode method for the test specimens were determined An example of the ABAQUS input files used to determine the load amplification factors based on Eurocode method are shown in Appendix D The load amplification factors were calculated as the ratio of dynamic force to the static equilibrium force Example results from the Eurocode method for Tower # 6 with 222 N initial tension, with guy wire at G2 ruptured, is shown in force-deflection diagram in Figure 2 24 The dynamic load amplification factor was found to be 2 02 (a ratio of the 125 N dynamic force to the 61 6 N static force) with dynamic deflection of 4 75 mm

Load amplification factors based on the Eurocode simplified method are shown in Table 2 11 for the 12 towers with a 222 N initial tension and in Table 2 12 for the 13 towers with 222 N and 445 N initial tensions From those tables, it can be concluded that the maximum load amplification factors for 222 N initial tension ranged from 1 99 to 3 58, and those for 445 N initial tension from 2 00 to 3 41

2.6 COMPARISON OF RESULTS FROM THE THREE METHODS

The maximum load amplification factors and deflections at the ruptured guy level obtained from experimental investigation, finite element analysis, and Eurocode simplified analytical method are summarized in Table 2 13 for 12 towers tested with a 222 N initial tension (Series 1) and Table 2 14 for 13 towers tested with both 222 N and 445 N initial tensions (Series 2)

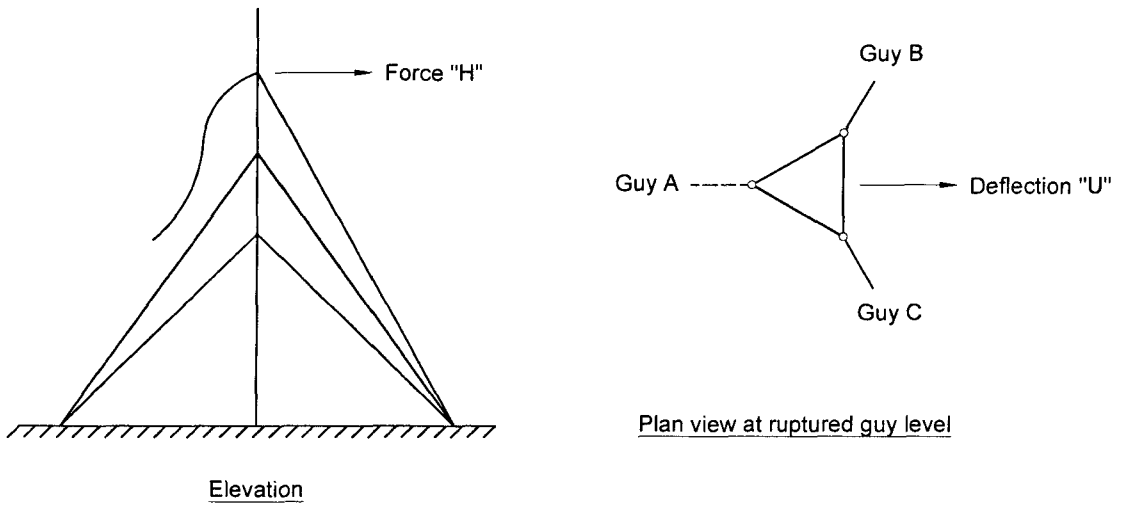

(a) Guy rupture

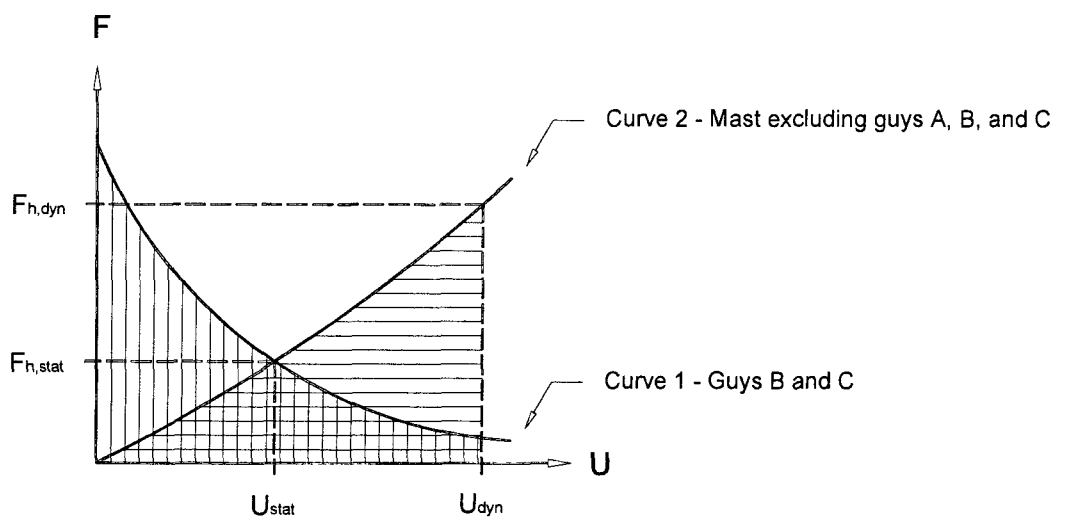

(b) Force-deflection diagram

Figure 2.23. Eurocode Simplified Analytical Method [CEN 2008]

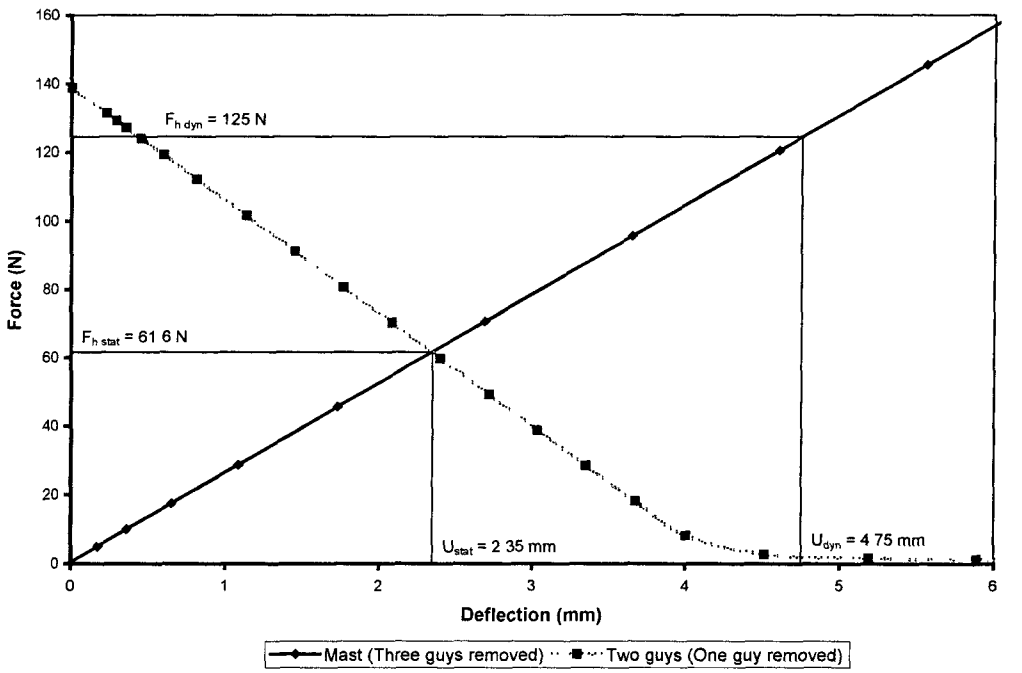

Figure 2.24. Force-deflection Diagram for Tower # 6 with 222 N Guy Initial Tension (Ruptured at Second Guy Level)

Table 2.11. Maximum Load Amplification Factors of Guy Wires and Mast Deflections from Finite Element Analysis (Initial Tension of 222 N)

Tower #	Rupture at	Load amplification factor	Deflection at ruptured guy level (mm)
1	G3	2 01	6 67
	G2	1 99	1 94
	G1	2 03	4 81
2	G3	2 00	6 20
	G2	2 00	2 82
	G1	2 47	6 35
3	G3	2 00	6 14
	G2	2 00	3 54
	G1	2 97	6 64
4	G3	2 29	11 2
	G2	2 00	2 37
	G1	2 01	3 45
5	G3	2 23	10 6
	G2	2 01	3 70
	G1	2 31	4 34
7	G3	2 28	11 2
	G2	2 10	5 71
	G1	2 20	2 70
10	G3	2 88	16 7
	G2	2 27	5 46
	G1	2 07	2 23
11	G3	3 58	22 5
	G2	2 26	4 20
	G1	2 01	1 74
13	G3	2 01	5 31
	G2	2 00	2 50
	G1	2 38	4 66
14	G3	2 01	5 34
	G2	2 00	3 13
	G1	2 62	4 40
15	G3	2 37	9 73
	G2	2 00	2 10
	G1	2 01	2 64
22	G3	2 02	4 68
	G2	2 01	2 82
	G1	2 10	2 29

Table 2.12. Maximum Load Amplification Factors of Guy Wires and Mast Deflections from Finite Element Analysis (Initial Tension of 445 N)

Tower #	Rupture at	Dynamic amplification factor		Deflection at ruptured guy level (mm)	
		Initial tension of 222 N	Initial tension of 445 N	Initial tension of 222 N	Initial tension of 445 N
6	G3	2 25	2 24	10 8	21 4
	G2	2 02	2 13	4 75	11 9
	G1	2 53	3 01	4 15	10 7
8	G3	2 84	2 85	16 3	32 5
	G2	2 00	2 00	2 55	6 50
	G1	2 01	2 08	2 62	6 63
9	G3	2 81	2 81	16 0	31 7
	G2	2 06	2 20	4 05	10 2
	G1	2 19	2 43	3 07	7 78
12	G3	2 01	2 01	5 65	11 3
	G2	2 00	2 00	1 71	4 71
	G1	2 03	2 16	3 72	9 62
16	G3	2 36	2 36	9 48	19 0
	G2	2 01	2 05	3 28	8 21
	G1	2 18	2 43	3 06	7 74
17	G3	2 38	2 36	9 81	19 2
	G2	2 08	2 25	4 29	10 7
	G1	2 08	2 25	2 22	5 65
18	G3	3 09	3 10	14 7	29 2
	G2	2 01	2 01	2 25	5 64
	G1	2 00	2 03	1 91	4 81
19	G3	3 10	3 11	14 8	29 4
	G2	2 15	2 36	3 67	9 18
	G1	2 01	2 05	1 73	4 32
20	G3	2 03	2 02	4 76	9 51
	G2	2 00	2 00	1 49	4 04
	G1	2 01	2 12	2 80	7 10
21	G3	2 01	2 01	4 56	9 14
	G2	2 00	2 00	2 21	5 73
	G1	2 18	2 49	2 79	8 11
23	G3	2 53	2 52	8 56	17 0
	G2	2 00	2 00	1 89	4 83
	G1	2 01	2 03	1 92	4 81
24	G3	2 53	2 54	8 58	17 0
	G2	2 04	2 14	2 99	7 42
	G1	2 00	2 05	1 72	4 29
25	G3	3 47	3 41	13 3	26 3
	G2	2 00	2 06	2 07	5 15
	G1	2 00	2 00	1 10	2 88

Table 2.13. Summary of Maximum Load Amplification Factors of Guy Wires and Mast Deflections (Initial Tension of 222 N)

Tower	Rupture at	Load amplification factor			Deflection at ruptured guy level (mm)		
		Experiment	FEA	Eurocode	Experiment	FEA	Eurocode
Col 1	*Col 2*	*Col 3*	*Col 4*	*Col 5*	*Col 6*	*Col 7*	*Col 8*
1	G3	2 00	1 95	2 01	9 04	6 08	6 67
	G2	1 58	1 60	1 99	3 12	1 76	1 94
	G1	1 72	1 69	2 03	7 13	4 23	4 81
2	G3	2 04	2 02	2 00	8 24	5 83	6 20
	G2	1 68	1 69	2 00	4 19	2 65	2 82
	G1	1 61	1 55	2 47	10 8	5 15	6 35
3	G3	2 01	1 93	2 00	8 37	5 98	6 14
	G2	1 64	1 62	2 00	4 98	3 28	3 54
	G1	1 67	1 90	2 97	11 6	13 5	6 64
4	G3	2 02	1 84	2 29	19 4	9 31	11 2
	G2	1 60	1 66	2 00	2 82	1 96	2 37
	G1	1 64	1 68	2 01	5 38	2 95	3 45
5	G3	2 21	1 94	2 23	17 4	9 30	10 6
	G2	1 70	1 66	2 01	4 54	3 37	3 70
	G1	1 65	1 50	2 31	6 74	3 47	4 34
7	G3	1 88	1 72	2 28	17 3	9 58	11 2
	G2	1 72	1 64	2 10	8 97	4 72	5 71
	G1	1 48	1 59	2 20	3 56	2 03	2 70
10	G3	1 95	1 71	2 88	28 0	14 6	16 7
	G2	1 65	1 50	2 27	8 31	4 32	5 46
	G1	1 50	1 60	2 07	2 43	1 76	2 23
11	G3	2 08	2 01	3 58	-	16 2	22 5
	G2	1 70	1 61	2 26	5 41	3 23	4 20
	G1	1 50	1 60	2 01	1 98	1 35	1 74
13	G3	2 05	1 87	2 01	9 06	5 20	5 31
	G2	1 62	1 53	2 00	3 25	2 31	2 50
	G1	1 58	1 51	2 38	7 32	3 54	4 66
14	G3	1 94	1 76	2 01	8 84	5 07	5 34
	G2	1 70	1 59	2 00	4 44	2 77	3 13
	G1	1 72	1 69	2 62	7 54	2 68	4 40
15	G3	1 89	1 83	2 37	16 2	9 19	9 73
	G2	1 79	1 74	2 00	2 79	1 87	2 10
	G1	1 81	1 76	2 01	4 43	2 45	2 64
22	G3	1 92	1 73	2 02	7 75	4 30	4 68
	G2	1 67	1 69	2 01	4 11	2 50	2 82
	G1	1 54	1 59	2 10	2 84	1 70	2 29

Table 2.14. Summary of Maximum Load Amplification Factors of Guy Wires and Mast Deflections (Initial Tension of 222 N and 445 N)

Tower #	Rupture of	Dynamic amplification factor						Deflection at ruptured guy (mm)					
		Initial tension 222 N			Initial tension 445 N			Initial tension 222 N			Initial tension 445 N		
		Exp	FEA	Eurocode	Exp	FEA	Eurocode	Exp	FEA	Eurocode	Exp	FEA	Eurocode
Col 1	*Col 2*	*Col 3*	*Col 4*	*Col 5*	*Col 6*	*Col 7*	*Col 8*	*Col 9*	*Col 10*	*Col 11*	*Col 12*	*Col 13*	*Col 14*
	G3	2 17	1 80	2 25	1 96	1 78	2 24	-	10 1	10 8	-	5 83	21 4
6	G2	1 61	1 59	2 02	1 55	1 58	2 13	7 24	4 39	4 75	12 8	2 65	11 9
	G1	1 79	1 64	2 53	1 65	1 64	3 01	7 03	3 03	4 15	11 3	5 15	10 7
	G3	2 13	1 90	2 84	1 90	1 84	2 85	-	14 0	16 3	-	5 98	32 5
8	G2	1 76	1 66	2 00	1 66	1 57	2 00	2 97	2 31	2 55	5 09	3 28	6 50
	G1	1 74	1 68	2 01	1 64	1 69	2 08	4 01	2 21	2 62	8 26	13 5	6 63
	G3	1 99	1 88	2 81	1 91	1 86	2 81	-	14 3	16 0	-	9 31	31 7
9	G2	1 76	1 63	2 06	1 65	1 66	2 20	5 45	3 35	4 05	9 67	1 96	10 2
	G1	1 84	1 73	2 19	1 65	1 50	2 43	5 37	2 75	3 07	7 70	2 95	7 78
	G3	1 77	1 82	2 01	1 88	1 83	2 01	7 53	5 25	5 65	14 9	9 30	11 3
12	G2	1 59	1 62	2 00	1 58	1 62	2 00	2 20	1 52	1 71	4 18	3 37	4 71
	G1	1 83	1 65	2 03	1 62	1 70	2 16	7 43	3 03	3 72	10 6	3 47	9 62
	G3	2 00	1 92	2 36	1 90	1 81	2 36	16 8	8 93	9 48	16 8	10 1	19 0
16	G2	1 69	1 55	2 01	1 62	1 56	2 05	4 52	3 09	3 28	8 52	4 39	8 21
	G1	1 78	1 61	2 18	1 70	1 71	2 43	4 40	2 62	3 06	7 51	3 03	7 74
	G3	1 87	1 74	2 38	1 74	1 66	2 36	16 4	9 21	9 81	-	9 58	19 2
17	G2	1 76	1 52	2 08	1 74	1 72	2 25	7 03	3 93	4 29	12 4	4 72	10 7
	G1	1 61	1 67	2 08	1 57	1 57	2 25	2 60	1 63	2 22	4 80	2 03	5 65
	G3	1 81	1 93	3 09	1 71	1 65	3 10	-	10 2	14 7	-	14 0	29 2
18	G2	1 75	1 67	2 01	1 70	1 65	2 01	2 77	1 70	2 25	5 11	2 31	5 64
	G1	1 68	1 64	2 00	1 61	1 63	2 03	2 73	1 80	1 91	4 76	2 21	4 81
	G3	1 74	1 91	3 10	1 69	1 68	3 11	16 1	12 5	14 8	-	14 3	29 4
19	G2	1 80	1 72	2 15	1 73	1 60	2 36	5 70	3 27	3 67	9 76	3 35	9 18
	G1	1 51	1 60	2 01	1 47	1 58	2 05	2 01	1 37	1 73	3 45	2 75	4 32
	G3	1 86	1 77	2 03	1 83	1 80	2 02	6 96	4 08	4 76	16 3	14 6	9 51
20	G2	1 53	1 54	2 00	1 53	1 56	2 00	1 94	1 23	1 49	3 34	4 32	4 04
	G1	1 65	1 55	2 01	1 58	1 55	2 12	4 04	2 25	2 80	6 91	1 76	7 10

Table 2.14. Summary of Maximum Load Amplification Factors of Guy Wires and Mast Deflections ... (concluded)

Tower #	Rupture of	Dynamic amplification factor						Deflection at ruptured guy (mm)					
		Initial tension 222 N			Initial tension 445 N			Initial tension 222 N			Initial tension 445 N		
		Exp	FEA	Eurocode	Exp	FEA	Eurocode	Exp	FEA	Eurocode	Exp	FEA	Eurocode
Col 1	*Col 2*	*Col 3*	*Col 4*	*Col 5*	*Col 6*	*Col 7*	*Col 8*	*Col 9*	*Col 10*	*Col 11*	*Col 12*	*Col 13*	*Col 14*
21	G3	2 00	1 88	2 01	1 87	1 83	2 01	7 07	4 39	4 56	12 2	16 2	9 14
	G2	1 73	1 69	2 00	1 60	1 70	2 00	4 34	2 04	2 21	5 60	3 23	5 73
	G1	1 69	1 58	2 18	1 59	1 66	2 49	4 37	2 55	2 79	7 49	1 35	8 11
23	G3	1 83	1 84	2 53	1 82	1 65	2 52	13 8	7 66	8 56	23 5	5 25	17 0
	G2	1 68	1 59	2 00	1 64	1 63	2 00	2 29	1 59	1 89	4 23	1 52	4 83
	G1	1 75	1 65	2 01	1 61	1 63	2 03	3 00	1 80	1 92	4 59	3 03	4 81
24	G3	1 90	1 84	2 53	1 78	1 66	2 54	14 4	7 14	8 58	22 2	5 20	17 0
	G2	1 62	1 59	2 04	1 79	1 68	2 14	4 39	2 50	2 99	11 4	2 31	7 42
	G1	1 50	1 59	2 00	1 47	1 57	2 05	1 88	1 38	1 72	3 38	3 54	4 29
25	G3	1 87	1 84	3 47	1 66	1 58	3 41	-	9 98	13 3	-	5 07	26 3
	G2	1 76	1 65	2 00	-	1 62	2 06	2 89	1 59	2 07	-	2 77	5 15
	G1	1 45	1 63	2 00	1 43	1 63	2 00	1 11	0 951	1 10	2 00	2 68	2 88

Comparing column 3 with column 4 of Tables 2.13 and 2.14, and column 6 with column 7 of Table 2.14, it can be seen that the load amplification factors based on experimental investigation are in a good agreement with those of finite element analysis in a majority of the cases (the average difference is 2.3%). Thus, it can be concluded that the finite element model can be used to simulate the dynamic analysis of the small-scale guyed tower test specimens due to sudden guy wire rupture.

In addition, by comparing column 5 with columns 3 and 4 of Tables 2.13 and 2.14, and column 8 with columns 6 and 7 of Table 2.14, it can be concluded that Eurocode simplified analytical method yields more conservative results than those of experimental investigation and finite element analysis. The dynamic load amplification factor based on the Eurocode simplified method is approximately 32% higher, on average, than those obtained by experimental investigation.

2.7 CONCLUSIONS

Based on Sections 2.1 to 2.6, the following conclusions were drawn:

(a) Based on experimental investigation, the maximum load amplification factors for the small-scale tower specimens due to sudden guy wire rupture for towers with 222 N (10% of guy wire breaking strength) initial tension ranged from 1.45 to 2.21, and those for 445 N (20% of guy wire breaking strength) initial tension from 1.43 to 1.96. The results are in good agreement with finite element analysis results with an average difference of 2.3%. Load amplification factors were higher for remaining guy wires in the same direction of the ruptured guy wire and highest when guy rupture occured at the top guy level, which agrees with a previous finding by El-Ghazaly and Al-Khaiat in 1995.

(b) Unlike for the top guy wire, the load amplification factors for guy wires in the same direction as the ruptured guy increased with an increase of the deflection of tower mast at the ruptured guy level. The load amplification factors for guy wires in other directions are not significantly affected by an increase in the deflection.

(c) The dynamic load amplification factor based on the Eurocode simplified method is approximately 32% higher, on average, than those obtained by experimental investigation, which support Nielsen's [2006] finding about conservativeness of Eurocode method.

(d) By increasing the initial tension from 222 N to 445 N, the load amplification factors obtained from experimental investigation were decreased by 0.08 while the deflections at ruptured guy level were increased by 3.66 mm, on average. From the finite element analysis, the load amplification factors were decreased by 0.04 and mast deflections were increased by 2.89

mm by doubling the initial tension. It can be concluded that even though the initial tension doubled, the load amplification factor decreased by a small amount.

(e) Unlike for rupture at mid-level guy, load amplification factors decreased with the increase of distance between the ruptured guy and remaining guy.

However, it should be noted that conclusions above may only apply to a guyed tower with similar characteristics as the tower test specimens in normal temperature as well as with no wind pressure.

REFERENCES

CEN 2008 Design of Steel Structures - Part 3-1 Towers, masts and chimneys - Towers and masts Eurocode EN 1993-3-1 2006/AC 2009 European Committee for Standardization, Brussels, Belgium

Davenport, A G , and Sparling, B F 1998 The evolution of dynamic gust response factors for guyed towers Structural Engineering International, **8**(1) 45-49

El-Ghazaly, H A , and Al-Khaiat, H A 1995 Analysis and design of guyed transmission towers – Case study in Kuwait Computers and Structures, **55** 413-431

Kahla, N B 2000 Response of guyed tower to a guy rupture under no wind pressure Engineering Structures, **22** 699-706

Kahla, N B 1997 Nonlinear dynamic response of a guyed tower to a sudden guy rupture Engineering Structures, **19** 879-890

Madugula, M K S (editor) 2002 Dynamic response of lattice towers and guyed masts Structural Engineering Institute, American Society of Civil Engineers, Reston, VA

Madugula, M K S , and Kumalasari, C 2006 Experimental investigation of load amplification factors due to sudden guy rupture and guy slippage University of Windsor, Windsor, ON Report submitted to Electronics Research, Inc , Chandler, IN

Nielsen, M G 1999 Analysis of guy failure Paper presented at International Association for Shell and Spatial Structures – Working Group 4, 19th Meeting, Krakow, Poland

Nielsen, M G 2006 Guyed masts exposed to guy failure *In* Proceedings of the Structures Congress 2006 Structural Engineering and Public Safety, St Louis, MO, 18-21 May 2006 American Society of Civil Engineers, Reston, VA, pp 181-181

Simulia 2007 ABAQUS Version 6 7-1 Program documentation Dassault Systèmes Simulia Corp , Providence, RI

Smith, B W 2006 Communication structures 1st ed Thomas Telford Publishing, London

Wikipedia 2010 Warsaw radio mast [Internet] [Updated 22 December 2009], [Cited 4 January 2010], available from World Wide Web
<http //en wikipedia org/w/index php?title=Warsaw_radio_mast&oldid=333202592>

Young, W.C., and Budynas, R.G. 2002. Roark's formulas for stress and strain. 7th ed. McGraw-Hill, New York, NY.

CHAPTER 3
LOAD AMPLIFICATION FACTORS OF GUY WIRES IN A COMMUNICATION TOWER DUE TO SLIPPAGE OF ONE GUY WIRE

3.1 INTRODUCTION

As discussed in Chapter 2, guyed towers can fail due to sudden guy wire rupture. Failure of guyed towers also can be caused by guy wire slippage, either during service by slipping of the guy wire due to failure of bolt clips (as shown in Figure 3.1) or during construction by slipping of the guy wire on the mechanical devices. The tower sections cannot continue to be stacked without being supported by guy wires at intervals. Although tower failure and/or guy wire slippage during construction is not widely publicized since the tower is not yet in service, it concerns design engineers and tower owners if the construction can be resumed without any permanent damage to the tower, especially on the installed guy wire anchor system. Therefore, this chapter discusses the load amplification factors of guy wire tensions due to slippage of one guy wire in a guyed communication tower.

To the best of authors' knowledge, there is no previous research previously conducted, either by experimental investigation or analytical calculation, to determine the load amplification factor of guy wires due to guy wire slippage.

3.2 EXPERIMENTAL INVESTIGATION

The experimental setup of guy wire slippage is similar to that of guy wire rupture experiment previously shown in Figures 2.2 to 2.7. The same materials, load cell rings, data acquisition system, and test specimen configuration of guy wire rupture experiments were used for guy wire slippage experiments. To make the slippage possible, one guy strand near the anchor point was rigged and clamped as shown in Figures 3.2(a) and 3.2(b). The initial tensions of all guy wires were approximately 222 N (50 lb) and a total of 228 tests were done on all 25 tower configurations as listed in Table 2.2.

Guy slippage was simulated by slowly loosening the clamps with extra care to minimize disturbance on the initial tension of guy wires. The clamps were relaxed until slippage between connected guy wires ceased and the guy wire carried only its own self-weight. The experimental investigation started with the loosening of the top level guy. After the tower response stopped, the slipped guy was retightened and experimental investigation was continued by loosening the mid level guy, and finally by loosening the bottom level guy. A sketch to clarify the slippage

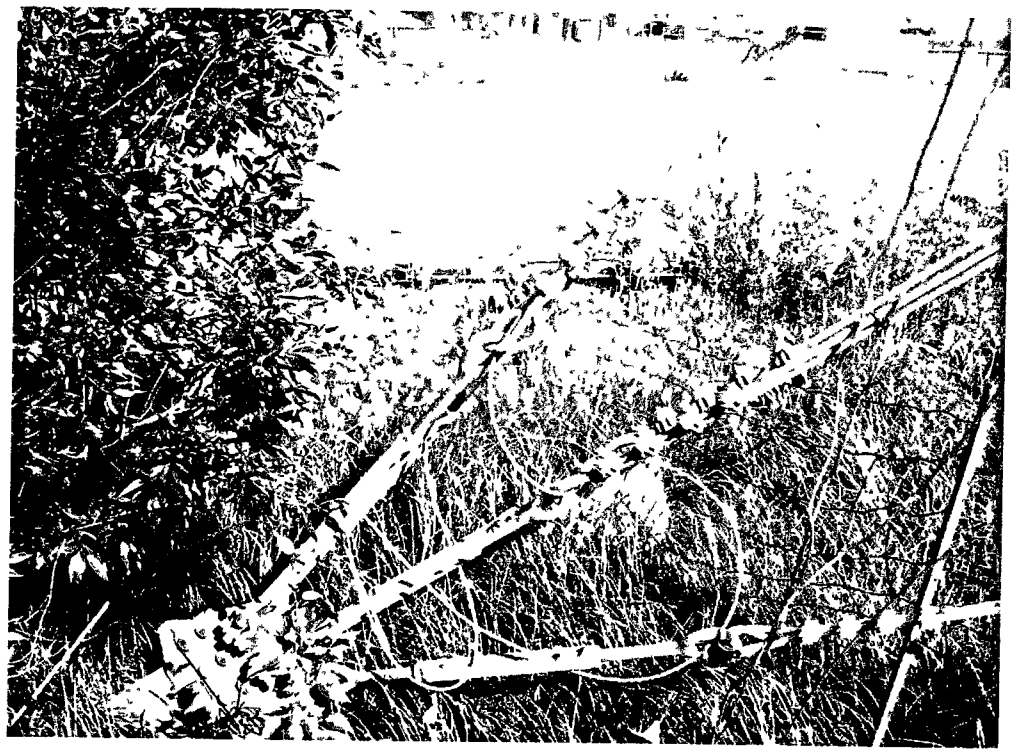

Figure 3.1. Guy Wires Secured with Bolt Clips
(courtesy of Westower Communications Ltd)

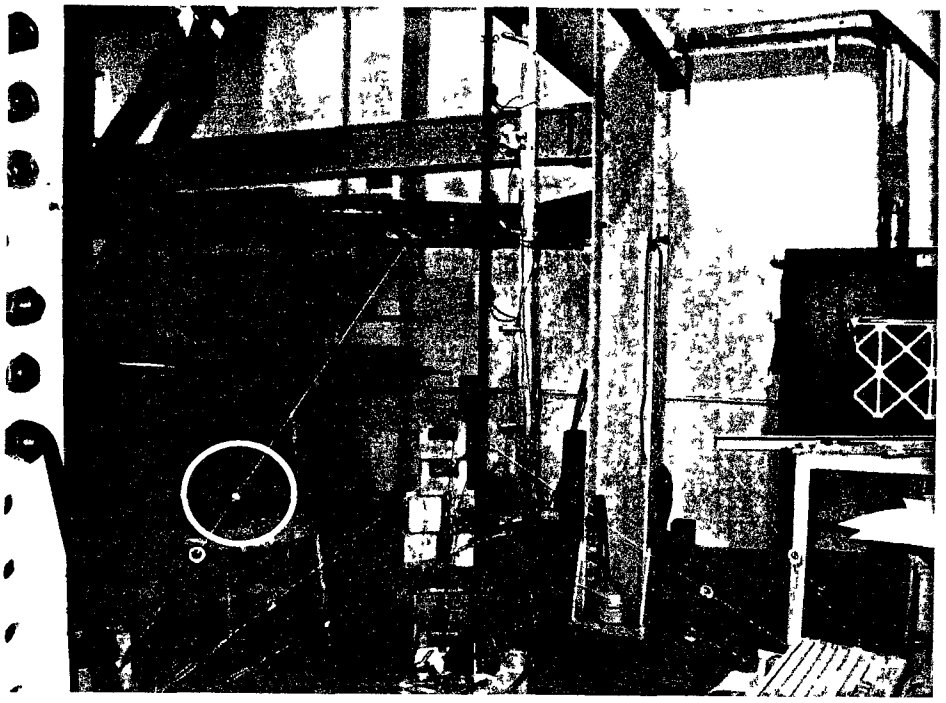

(a) Photograph of test specimen with rigged guy wires (circled)

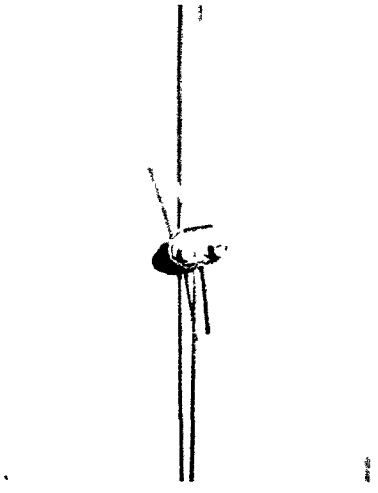

(b) Detail of rigged guy wires

Figure 3.2. Photographs of Test Specimen

experiment is shown in Figure 3 3 The guy wire tension, mast deflection at the level of the slipped guy wire, and mast acceleration were measured during the experiment There were three replicate tests for each configuration and rupture at each guy wire level

The detailed experimental results were reported by Madugula and Kumalasari [2006], and an example of the result is shown in Table 3 1 The load amplification factor is defined as the ratio of intact guy wire tension after slippage over guy wire initial tension The experimental results for each tower configuration and each level of slipped guy wire are averaged and are shown in Table 3 2 The maximum load amplification factor and mast deflection at the slipped guy level is summarized in Table 3 3 It can be seen from the table that maximum load amplification factor due to guy wire slippage ranged from 1 10 to 1 56

It can be concluded that the maximum load amplification factor is higher when the slippage happens at top level guy wire, as shown in Figure 3 4, which is more likely to happen on the field than at bottom or middle level guy wires since lower guy wires are already secured with guy grips before continuing the tower erection Load amplification factors were also higher for guy wires in the same direction with slipped guy wires

3.3 FINITE ELEMENT ANALYSIS

The same finite element model discussed in Chapter 2 was used to simulate guy wire slippage After the gravity load was applied to the mast and guy wires, pretension loading was applied to the guy wires The pretension section of one guy wire (initial tension of one guy wire) was then removed to initiate guy wire slippage An example of ABAQUS input file for the tower test specimen # 1, slipped at G3, is shown in Appendix E

The finite element analysis results of the maximum load amplification factors and deflections at slipped guy level are summarized in Table 3 4 It can be seen from the table that maximum load amplification factor due to guy wire slippage ranges from 1 06 to 1 48

3.4 COMPARISON OF RESULTS FROM EXPERIMENTAL INVESTIGATION AND FINITE ELEMENT ANALYSIS

The maximum load amplification factors and deflections at slipped guy level obtained from experimental investigation and finite element analysis are summarized in Table 3 5 Comparing Column 3 with Column 4 of that table, it can be seen that the load amplification factors based on experimental investigation are in a good agreement with those of finite element analysis in

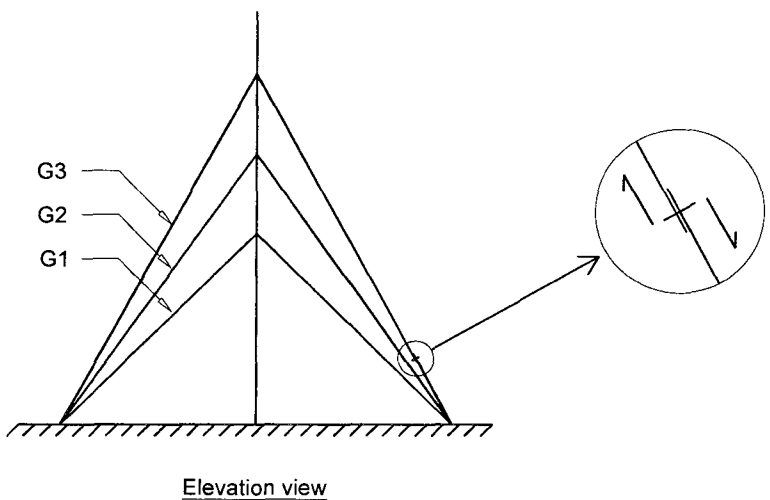

Figure 3.3. Sketch of Guy Wire Slippage Experiment

Table 3.1. Example Load Amplification Factor due to Guy Wire Slippage – Tower # 1

Experiment #	Slip at	Guy level	Initial tension (N)			Final tension (N)			Load amplification factor			Displacement at slipped guy level (mm)
		Direction	A	B	C	A	B	C	A	B	C	
1	G3	G3	227	236	222	-	161	140	-	0 685	0 630	4 45
		G2	227	249	226	322	208	185	1 42	0 838	0 819	
		G1	223	235	223	227	239	234	1 02	1 02	1 05	
2	G3	G3	230	234	226	24 0	169	151	-	0 723	0 669	3 70
		G2	232	249	226	322	215	191	1 39	0 866	0 844	
		G1	230	237	223	231	243	233	1 01	1 02	1 04	
3	G3	G3	230	236	226	-	165	148	-	0 698	0 652	4 08
		G2	229	249	226	327	211	188	1 43	0 849	0 832	
		G1	230	236	222	231	242	234	1 01	1 02	1 05	
4	G2	G3	240	237	224	301	216	200	1 25	0 913	0 893	0 375
		G2	230	249	226	-	220	194	-	0 885	0 859	
		G1	228	238	228	292	209	201	1 28	0 876	0 880	
5	G2	G3	240	236	224	299	218	201	1 25	0 923	0 894	-
		G2	227	250	226	-	221	195	-	0 887	0 866	
		G1	224	236	226	289	209	201	1 29	0 884	0 888	
6	G2	G3	239	236	224	294	219	202	1 23	0 929	0 903	-
		G2	224	249	226	24 0	223	197	-	0 895	0 874	
		G1	225	235	226	284	210	201	1 27	0 891	0 893	
7	G1	G3	225	246	228	219	252	235	0 975	1 02	1 03	3 34
		G2	251	245	231	331	215	199	1 32	0 879	0 862	
		G1	226	233	231	-	148	147	-	0 636	0 635	
8	G1	G3	225	247	230	220	251	235	0 977	1 02	1 02	3 12
		G2	250	245	231	326	217	201	1 30	0 883	0 867	
		G1	228	234	231	28 5	152	151	-	0 652	0 652	
9	G1	G3	225	246	230	220	251	237	0 976	1 02	1 03	3 35
		G2	250	245	232	330	215	200	1 32	0 878	0 862	
		G1	227	232	230	-	148	146	-	0 636	0 634	

Table 3.2. Average Load Amplification Factors and Deflections

Tower	Slip at	Guy level Direction	Load amplification factor A	B	C	Deflection at slipped guy level (mm)
1	G3	G3	-	0 702	0 650	4 08
		G2	1 41	0 851	0 831	
		G1	1 01	1 02	1 05	
	G2	G3	1 24	0 921	0 897	0 375
		G2	-	0 889	0 866	
		G1	1 28	0 884	0 887	
	G1	G3	0 976	1 02	1 03	3 27
		G2	1 31	0 880	0 864	
		G1	-	0 641	0 640	
2	G3	G3	-	0 699	0 647	-
		G2	1 46	0 833	0 798	
		G1	0 956	1 06	1 08	
	G2	G3	1 27	0 914	0 868	1 85
		G2	-	0 861	0 817	
		G1	1 20	0 928	0 940	
	G1	G3	0 966	1 02	1 04	3 61
		G2	1 25	0 912	0 903	
		G1	-	0 523	0 523	
3	G3	G3	-	0 716	0 683	4 07
		G2	1 48	0 828	0 818	
		G1	0 960	1 07	1 08	
	G2	G3	1 32	0 892	0 867	2 27
		G2	-	0 819	0 797	
		G1	1 15	0 959	0 965	
	G1	G3	0 941	1 04	1 06	4 21
		G2	1 22	0 936	0 931	
		G1	-	0 354	0 341	
4	G3	G3	-	0 512	0 478	7 94
		G2	1 39	0 827	0 943	
		G1	0 939	1 08	1 09	
	G2	G3	1 19	0 954	0 935	1 73
		G2	-	0 792	0 919	
		G1	1 40	0 855	0 861	
	G1	G3	0 965	1 03	1 04	2 60
		G2	1 41	0 825	0 934	
		G1	-	0 653	0 648	
5	G3	G3	-	0 536	0 510	7 38
		G2	1 43	0 823	0 944	
		G1	0 906	1 10	1 11	
	G2	G3	1 23	0 932	0 918	2 58
		G2	-	0 704	0 852	
		G1	1 29	0 901	0 912	
	G1	G3	0 943	1 04	1 06	3 15
		G2	1 32	0 883	0 957	
		G1	-	0 502	0 489	

Table 3.2. Average Load Amplification Factors and Deflections (continued)

Tower	Slip at	Guy level	Load amplification factor			Deflection at slipped guy level (mm)
		Direction	A	B	C	
		G3	-	0 502	0 485	
	G3	G2	1 43	0 826	0 937	8 02
		G1	0 912	1 11	1 11	
		G3	1 24	0 931	0 917	
6	G2	G2	-	0 617	0 737	3 48
		G1	1 26	0 930	0 941	
		G3	0 950	1 05	1 06	
	G1	G2	1 27	0 912	0 975	3 01
		G1	-	0 492	0 458	
		G3	-	0 492	0 443	
	G3	G2	1 38	0 846	0 919	8 43
		G1	0 910	1 13	1 12	
		G3	1 25	0 925	0 906	
7	G2	G2	-	0 531	0 697	4 51
		G1	1 29	0 926	0 932	
		G3	0 965	1 04	1 06	
	G1	G2	1 19	0 970	0 973	1 75
		G1	-	0 545	0 553	
		G3	-	0 378	0 366	
	G3	G2	1 35	0 880	0 920	11 7
		G1	0 936	1 11	1 11	
		G3	1 12	0 976	0 969	
8	G2	G2	-	0 744	0 761	1 88
		G1	1 41	0 827	0 835	
		G3	0 977	1 03	1 04	
	G1	G2	1 43	0 848	0 871	2 06
		G1	-	0 649	0 642	
		G3	0 211	0 421	0 382	
	G3	G2	1 31	0 902	0 941	10 0
		G1	0 925	1 12	1 11	
		G3	1 15	0 969	0 957	
9	G2	G2	-	0 586	0 620	3 11
		G1	1 36	0 886	0 887	
		G3	0 968	1 04	1 05	
	G1	G2	1 31	0 909	0 938	2 35
		G1	-	0 567	0 541	
		G3	-	0 409	0 394	
	G3	G2	1 28	0 911	0 950	10 9
		G1	0 938	1 13	1 12	
		G3	1 14	0 961	0 950	
10	G2	G2	-	0 465	0 492	4 15
		G1	1 35	0 923	0 911	
		G3	0 987	1 04	1 05	
	G1	G2	1 23	0 976	0 970	1 47
		G1	-	0 614	0 593	

Table 3.2. Average Load Amplification Factors and Deflections (continued)

Tower	Slip at	Guy level	Load amplification factor			Deflection at slipped guy level (mm)
		Direction	A	B	C	
11	G3	G3	-	0 214	0 208	18 3
		G2	1 33	0 900	0 941	
		G1	0 960	1 15	1 14	
	G2	G3	1 09	0 975	0 968	3 77
		G2	-	0 451	0 477	
		G1	1 31	0 810	0 806	
	G1	G3	0 999	1 03	1 04	2 53
		G2	1 26	0 962	0 958	
		G1	-	0 712	0 695	
12	G3	G3	-	0 604	0 598	4 94
		G2	1 56	0 805	0 804	
		G1	0 998	1 04	1 06	
	G2	G3	1 29	0 897	0 894	1 27
		G2	-	0 862	0 849	
		G1	1 32	0 929	0 891	
	G1	G3	0 983	1 02	1 03	2 93
		G2	1 42	0 858	0 832	
		G1	-	0 731	0 600	
13	G3	G3	-	0 650	0 609	4 06
		G2	1 51	0 798	0 804	
		G1	0 948	1 08	1 09	
	G2	G3	1 33	0 881	0 863	1 78
		G2	-	0 801	0 788	
		G1	1 23	0 930	0 931	
	G1	G3	0 946	1 05	1 07	3 39
		G2	1 30	0 898	0 896	
		G1	-	0 454	0 443	
14	G3	G3	-	0 627	0 602	4 54
		G2	1 56	0 795	0 797	
		G1	0 963	1 09	1 09	
	G2	G3	1 35	0 872	0 866	2 24
		G2	-	0 771	0 754	
		G1	1 20	0 950	0 947	
	G1	G3	0 944	1 07	1 09	3 20
		G2	1 27	0 954	0 927	
		G1	-	0 365	0 365	
15	G3	G3	-	0 428	0 368	7 02
		G2	1 43	0 841	0 866	
		G1	0 931	1 10	1 11	
	G2	G3	1 16	0 948	0 936	1 52
		G2	-	0 788	0 784	
		G1	1 37	0 861	0 851	
	G1	G3	0 970	1 04	1 05	2 07
		G2	1 45	0 841	0 840	
		G1	-	0 644	0 618	

Table 3.2. Average Load Amplification Factors and Deflections (continued)

Tower	Slip at	Guy level	Load amplification factor			Deflection at slipped guy level (mm)
		Direction	A	B	C	
		G3	-	0 520	0 478	
	G3	G2	1 33	0 870	0 871	5 90
		G1	0 950	1 10	1 10	
		G3	1 19	0 945	0 937	
16	G2	G2	-	0 704	0 690	2 07
		G1	1 27	0 911	0 906	
		G3	0 954	1 05	1 07	
	G1	G2	1 31	0 923	0 902	2 12
		G1	-	0 532	0 531	
		G3	-	0 504	0 444	
	G3	G2	1 28	0 885	0 881	6 20
		G1	0 954	1 10	1 11	
		G3	1 20	0 935	0 928	
17	G2	G2	-	0 583	0 569	2 99
		G1	1 29	0 930	0 926	
		G3	0 978	1 06	1 06	
	G1	G2	1 22	0 938	0 945	1 57
		G1	-	0 699	0 616	
		G3	-	0 474	0 424	
	G3	G2	1 25	0 941	0 946	6 97
		G1	0 972	1 09	1 08	
		G3	1 10	0 980	0 975	
18	G2	G2	-	0 743	0 724	1 36
		G1	1 39	0 859	0 868	
		G3	0 989	1 03	1 04	
	G1	G2	1 41	0 884	0 855	1 30
		G1	-	0 691	0 700	
		G3	-	0 458	0 410	
	G3	G2	1 23	0 947	0 947	7 41
		G1	0 979	1 08	1 09	
		G3	1 10	0 979	0 973	
19	G2	G2	-	0 622	0 600	2 08
		G1	1 32	0 916	0 896	
		G3	0 993	1 05	1 05	
	G1	G2	1 26	0 950	0 957	1 05
		G1	-	0 763	0 703	
		G3	-	0 606	0 586	
	G3	G2	1 47	0 811	0 798	3 83
		G1	1 01	1 04	1 07	
		G3	1 28	0 899	0 895	
20	G2	G2	-	0 837	0 831	1 07
		G1	1 31	0 874	0 883	
		G3	0 998	1 03	1 04	
	G1	G2	1 37	0 849	0 866	2 13
		G1	-	0 635	0 608	

Table 3.2. Average Load Amplification Factors and Deflections (concluded)

Tower	Slip at	Guy level Direction	Load amplification factor A	B	C	Deflection at slipped guy level (mm)
21	G3	G3	-	0 616	0 602	3 69
		G2	1 48	0 804	0 798	
		G1	0 962	1 09	1 10	
	G2	G3	1 34	0 871	0 862	1 72
		G2	-	0 754	0 751	
		G1	1 26	0 908	0 916	
	G1	G3	0 962	1 07	1 08	2 69
		G2	1 32	0 894	0 902	
		G1	-	0 520	0 486	
22	G3	G3	-	0 607	0 598	3 76
		G2	1 48	0 814	0 810	
		G1	0 972	1 10	1 10	
	G2	G3	1 36	0 861	0 863	2 23
		G2	-	0 690	0 692	
		G1	1 27	0 931	0 937	
	G1	G3	0 981	1 07	1 08	1 57
		G2	1 24	0 967	0 960	
		G1	-	0 560	0 525	
23	G3	G3	-	0 389	0 368	7 22
		G2	1 43	0 848	0 859	
		G1	0 958	1 09	1 10	
	G2	G3	1 16	0 947	0 937	1 50
		G2	-	0 740	0 730	
		G1	1 43	0 836	0 829	
	G1	G3	0 993	1 04	1 05	1 62
		G2	1 42	0 862	0 862	
		G1	-	0 704	0 678	
24	G3	G3	-	0 398	0 379	6 94
		G2	1 38	0 860	0 882	
		G1	0 964	1 11	1 12	
	G2	G3	1 21	0 935	0 935	2 53
		G2	-	0 569	0 583	
		G1	1 30	0 845	0 834	
	G1	G3	0 987	1 04	1 05	1 05
		G2	1 26	0 932	0 925	
		G1	-	0 705	0 683	
25	G3	G3	-	0 238	0 234	9 65
		G2	1 36	0 921	0 933	
		G1	1 03	1 11	1 10	
	G2	G3	1 10	0 979	0 972	1 62
		G2	-	0 673	0 657	
		G1	1 46	0 835	0 822	
	G1	G3	1 02	1 04	1 04	0 693
		G2	1 37	0 926	0 911	
		G1	-	0 792	0 780	

Table 3.3. Maximum Load Amplification Factors of Guy Wires and Mast Deflections from Experimental Investigation

Tower #	Slip at	Load amplification factor	Deflection at slipped guy level (mm)
1	G3	1 41	4 08
	G2	1 28	0 375
	G1	1 31	3 27
2	G3	1 46	-
	G2	1 27	1 85
	G1	1 25	3 61
3	G3	1 48	4 07
	G2	1 32	2 27
	G1	1 22	4 21
4	G3	1 39	7 94
	G2	1 40	1 73
	G1	1 41	2 60
5	G3	1 43	7 38
	G2	1 29	2 58
	G1	1 32	3 15
6	G3	1 43	8 02
	G2	1 26	3 48
	G1	1 27	3 01
7	G3	1 38	8 43
	G2	1 29	4 51
	G1	1 19	1 75
8	G3	1 35	11 7
	G2	1 41	1 88
	G1	1 43	2 06
9	G3	1 31	10 0
	G2	1 36	3 11
	G1	1 31	2 35
10	G3	1 28	10 9
	G2	1 35	4 15
	G1	1 23	1 47
11	G3	1 33	18 3
	G2	1 31	3 77
	G1	1 26	2 53
12	G3	1 56	4 94
	G2	1 32	1 27
	G1	1 42	2 93
13	G3	1 51	4 06
	G2	1 33	1 78
	G1	1 30	3 39
14	G3	1 56	4 54
	G2	1 35	2 24
	G1	1 27	3 20
15	G3	1 43	7 02
	G2	1 37	1 52
	G1	1 45	2 07

Table 3.3. Maximum Load Amplification Factors of Guy Wires and Mast Deflections from Experimental Investigation (concluded)

Tower #	Slip at	Load amplification factor	Deflection at slipped guy level (mm)
16	G3	1 33	5 90
	G2	1 27	2 07
	G1	1 31	2 12
17	G3	1 28	6 20
	G2	1 29	2 99
	G1	1 22	1 57
18	G3	1 25	6 97
	G2	1 39	1 36
	G1	1 41	1 30
19	G3	1 23	7 41
	G2	1 32	2 08
	G1	1 26	1 05
20	G3	1 47	3 83
	G2	1 31	1 07
	G1	1 37	2 13
21	G3	1 48	3 69
	G2	1 34	1 72
	G1	1 32	2 69
22	G3	1 48	3 76
	G2	1 36	2 23
	G1	1 24	1 57
23	G3	1 43	7 22
	G2	1 43	1 50
	G1	1 42	1 62
24	G3	1 38	6 94
	G2	1 30	2 53
	G1	1 26	1 05
25	G3	1 36	9 65
	G2	1 46	1 62
	G1	1 37	0 693

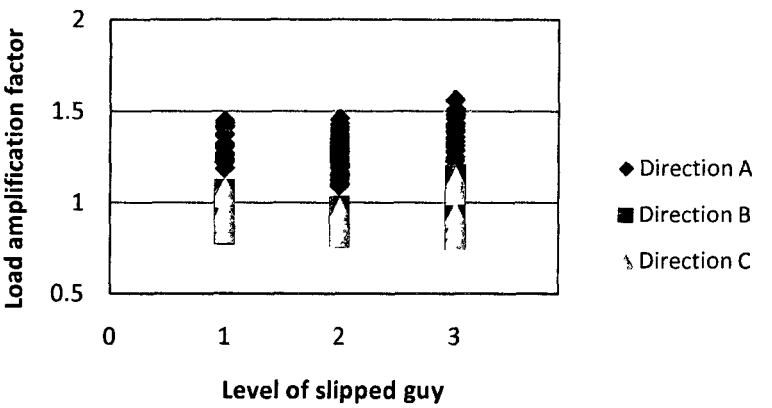

Figure 3.4. Load Amplification Factor versus Level of Ruptured Guy

Table 3.4. Maximum Load Amplification Factors of Guy Wires and Mast Deflections from Finite Element Analysis

Tower #	Slip at	Load amplification factor	Deflection at slipped guy level (mm)
1	G3	1 46	3 39
	G2	1 28	0 999
	G1	1 38	2 38
2	G3	1 48	3 13
	G2	1 33	1 41
	G1	1 24	2 58
3	G3	1 45	3 10
	G2	1 34	1 77
	G1	1 15	2 22
4	G3	1 34	4 90
	G2	1 34	1 18
	G1	1 39	1 71
5	G3	1 32	4 75
	G2	1 22	1 85
	G1	1 23	1 89
6	G3	1 28	4 82
	G2	1 18	2 35
	G1	1 15	1 64
7	G3	1 24	4 91
	G2	1 19	2 71
	G1	1 13	1 22
8	G3	1 23	5 73
	G2	1 35	1 27
	G1	1 35	1 31
9	G3	1 20	5 70
	G2	1 35	1 27
	G1	1 19	1 40
10	G3	1 16	5 77
	G2	1 21	2 40
	G1	1 14	1 08
11	G3	1 12	6 16
	G2	1 26	1 85
	G1	1 17	0 868
12	G3	1 45	2 83
	G2	1 28	0 853
	G1	1 37	1 84
13	G3	1 45	2 66
	G2	1 32	1 24
	G1	1 23	1 96
14	G3	1 42	2 68
	G2	1 32	1 57
	G1	1 16	1 67
15	G3	1 30	4 08
	G2	1 34	1 05
	G1	1 36	1 32

Table 3.4. Maximum Load Amplification Factors of Guy Wires and Mast Deflections from Finite Element Analysis (concluded)

Tower #	Slip at	Load amplification factor	Deflection at slipped guy level (mm)
16	G3	1 27	4 05
	G2	1 23	1 64
	G1	1 21	1 40
17	G3	1 23	4 09
	G2	1 22	2 06
	G1	1 16	1 07
18	G3	1 19	4 73
	G2	1 35	1 12
	G1	1 32	0 954
19	G3	1 16	4 73
	G2	1 27	1 71
	G1	1 19	0 860
20	G3	1 42	2 34
	G2	1 28	0 738
	G1	1 36	1 39
21	G3	1 41	2 26
	G2	1 29	1 10
	G1	1 22	1 44
22	G3	1 38	2 31
	G2	1 29	1 40
	G1	1 17	1 10
23	G3	1 26	3 36
	G2	1 34	0 940
	G1	1 34	0 955
24	G3	1 22	3 36
	G2	1 27	1 46
	G1	1 20	0 856
25	G3	1 15	3 81
	G2	1 39	1 03
	G1	1 29	0 549

Table 3.5. Summary of Maximum Load Amplification Factors of Guy Wires and Mast Deflections

Tower	Slip at	Load amplification factor		Deflection at ruptured guy level (mm)	
		Experiment	FEA	Experiment	FEA
Col 1	*Col 2*	*Col 3*	*Col 4*	*Col 6*	*Col 7*
	G3	1 41	1 46	4 08	3 39
1	G2	1 28	1 28	0 375	0 999
	G1	1 31	1 38	3 27	2 38
	G3	1 46	1 48	-	3 13
2	G2	1 27	1 33	1 85	1 41
	G1	1 25	1 24	3 61	2 58
	G3	1 48	1 45	4 07	3 10
3	G2	1 32	1 34	2 27	1 77
	G1	1 22	1 15	4 21	2 22
	G3	1 39	1 34	7 94	4 90
4	G2	1 40	1 34	1 73	1 18
	G1	1 41	1 39	2 60	1 71
	G3	1 43	1 32	7 38	4 75
5	G2	1 29	1 22	2 58	1 85
	G1	1 32	1 23	3 15	1 89
	G3	1 43	1 28	8 02	4 82
6	G2	1 26	1 18	3 48	2 35
	G1	1 27	1 15	3 01	1 64
	G3	1 38	1 24	8 43	4 91
7	G2	1 29	1 19	4 51	2 71
	G1	1 19	1 13	1 75	1 22
	G3	1 35	1 23	11 7	5 73
8	G2	1 41	1 35	1 88	1 27
	G1	1 43	1 35	2 06	1 31
	G3	1 31	1 20	10 0	5 70
9	G2	1 36	1 35	3 11	1 27
	G1	1 31	1 19	2 35	1 40
	G3	1 28	1 16	10 9	5 77
10	G2	1 35	1 21	4 15	2 40
	G1	1 23	1 14	1 47	1 08
	G3	1 33	1 12	18 3	6 16
11	G2	1 31	1 26	3 77	1 85
	G1	1 26	1 17	2 53	0 868
	G3	1 56	1 45	4 94	2 83
12	G2	1 32	1 28	1 27	0 853
	G1	1 42	1 37	2 93	1 84
	G3	1 51	1 45	4 06	2 66
13	G2	1 33	1 32	1 78	1 24
	G1	1 30	1 23	3 39	1 96
	G3	1 56	1 42	4 54	2 68
14	G2	1 35	1 32	2 24	1 57
	G1	1 27	1 16	3 20	1 67

Table 3.5. Summary of Maximum Load Amplification Factors of Guy Wires and Mast Deflections (concluded)

Tower	Slip at	Load amplification factor		Deflection at ruptured guy level (mm)	
		Experiment	FEA	Experiment	FEA
Col 1	*Col 2*	*Col 3*	*Col 4*	*Col 5*	*Col 6*
	G3	1 43	1 30	7 02	4 08
15	G2	1 37	1 34	1 52	1 05
	G1	1 45	1 36	2 07	1 32
	G3	1 33	1 27	5 90	4 05
16	G2	1 27	1 23	2 07	1 64
	G1	1 31	1 21	2 12	1 40
	G3	1 28	1 23	6 20	4 09
17	G2	1 29	1 22	2 99	2 06
	G1	1 22	1 16	1 57	1 07
	G3	1 25	1 19	6 97	4 73
18	G2	1 39	1 35	1 36	1 12
	G1	1 41	1 32	1 30	0 954
	G3	1 23	1 16	7 41	4 73
19	G2	1 32	1 27	2 08	1 71
	G1	1 26	1 19	1 05	0 860
	G3	1 47	1 42	3 83	2 34
20	G2	1 31	1 28	1 07	0 738
	G1	1 37	1 36	2 13	1 39
	G3	1 48	1 41	3 69	2 26
21	G2	1 34	1 29	1 72	1 10
	G1	1 32	1 22	2 69	1 44
	G3	1 48	1 38	3 76	2 31
22	G2	1 36	1 29	2 23	1 40
	G1	1 24	1 17	1 57	1 10
	G3	1 43	1 26	7 22	3 36
23	G2	1 43	1 34	1 50	0 940
	G1	1 42	1 34	1 62	0 955
	G3	1 38	1 22	6 94	3 36
24	G2	1 30	1 27	2 53	1 46
	G1	1 26	1 20	1 05	0 856
	G3	1 36	1 15	9 65	3 81
25	G2	1 46	1 39	1 62	1 03
	G1	1 37	1 29	0 693	0 549

majority of cases, with the average difference of 5 2% Thus, it can be concluded that the finite element model can be used to simulate the behaviour of the small-scale guyed tower test specimens due to guy wire slippage

3.5 CONCLUSIONS

Based on experimental investigation, the maximum load amplification factors for the small-scale tower specimens due to guy wire slippage is ranging from 1 10 to 1 56 The results are in good agreement with finite element analysis results with an average difference of 5 2% Since guy slippage happens during tower erection (which is carried out during low wind), the maximum load amplification factors due to guy wire slippage is lower than those due to sudden guy rupture discussed in Chapter 2 However, they still need to be considered as a precaution during tower erection It was also found that load amplification factor for intact guy wires is higher when the slippage happens at top level guy wire

REFERENCES

Madugula, M.K.S., and Kumalasari, C. 2006. Experimental investigation of load amplification factors due to sudden guy rupture and guy slippage. University of Windsor, Windsor, ON. Report submitted to Electronics Research, Inc., Chandler, IN.

CHAPTER 4
TENSILE STRENGTH OF BOLTED RING-TYPE SPLICES OF SOLID ROUND LEG MEMBERS OF GUYED COMMUNICATION TOWERS

4.1 INTRODUCTION

The primary application of guyed lattice towers using solid round legs is in the telecommunication industry. Such lattice tower sections are fabricated using welded splices, and these welded sections are bolted together in the field. Communication towers are subjected to dead load (self-weight of the structure plus the weight of all attachments), ice load (the weight of radial glaze ice on all exposed surfaces of the structure), guy tension, and wind load (or earthquake load). When these loads are applied to the antenna towers, the response of the whole tower is quite complex. The leg members of a steel tower, however, are subjected to compressive loads due to the dead load and guy tension and the tensile–compressive loads due to bending moments caused by wind or seismic loads.

Lattice towers made up of solid round legs, diagonals, and horizontal members are welded together as shown in Figure 4.1. These types of towers are referred to as "all-weld" towers. These all-weld tower sections are interconnected in the field using bolted leg splices. There are two types of bolted splices, namely bolted ring-type splices for leg diameters up to 65 mm ($2\text{-}^1/_2$ in.) as shown in Figure 4.2 and bolted flange-type splices for leg diameters greater than 65 mm ($2\text{-}^1/_2$ in.). This chapter deals with ring-type splices and this research has been published in Canadian Journal of Civil Engineering [Kumalasari et al. 2005].

4.2 EXPERIMENTAL INVESTIGATION

In this investigation, tensile tests were conducted by Lihong Shen in 2002 on 18 bolted ring-type splice specimens fabricated by Electronic Research Inc., Chandler, Indiana, USA. There were three groups of specimens in the investigation, each group with six specimens, as listed in Table 4.1. The first group was bolted ring-type splices with 25.4 mm (1 in.) diameter legs without horizontal tower members and 22.2 mm ($^7/_8$ in.) diameter ASTM A325 bolts pre-tensioned to a torque of 258 N-m (190 lb-ft) (except for specimen R2, which was snug-tight). The second group was bolted ring-type splices with 38.1 mm ($1\text{-}^1/_2$ in.) diameter legs with horizontal tower members and 22.2 mm ($^7/_8$ in.) diameter ASTM A325 bolts pre-tensioned to a torque of 258 N-m (190 lb-ft). The last group was bolted ring-type splices with 50.8 mm (2 in.) diameter legs with horizontal tower members and 31.8 mm ($1\text{-}^1/_4$ in.) diameter ASTM A325 bolts pre-tensioned to a torque of 339 N-m (250 lb-ft). The sketch of the specimens in the first group (without horizontal members)

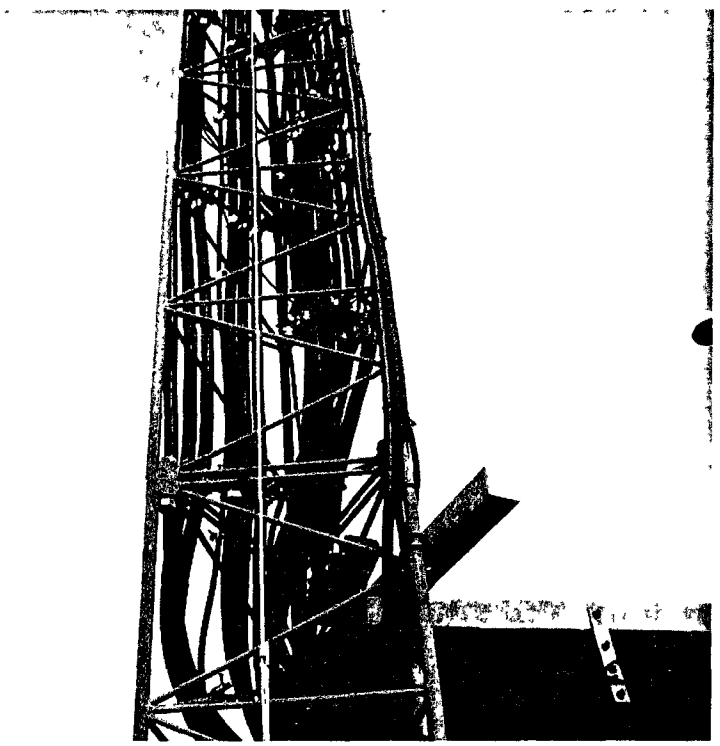

Figure 4.1. An All-weld Tower Section of a Guyed Communication Tower with Bolted Ring-type Splice

(courtesy of Westower Communications Ltd.)

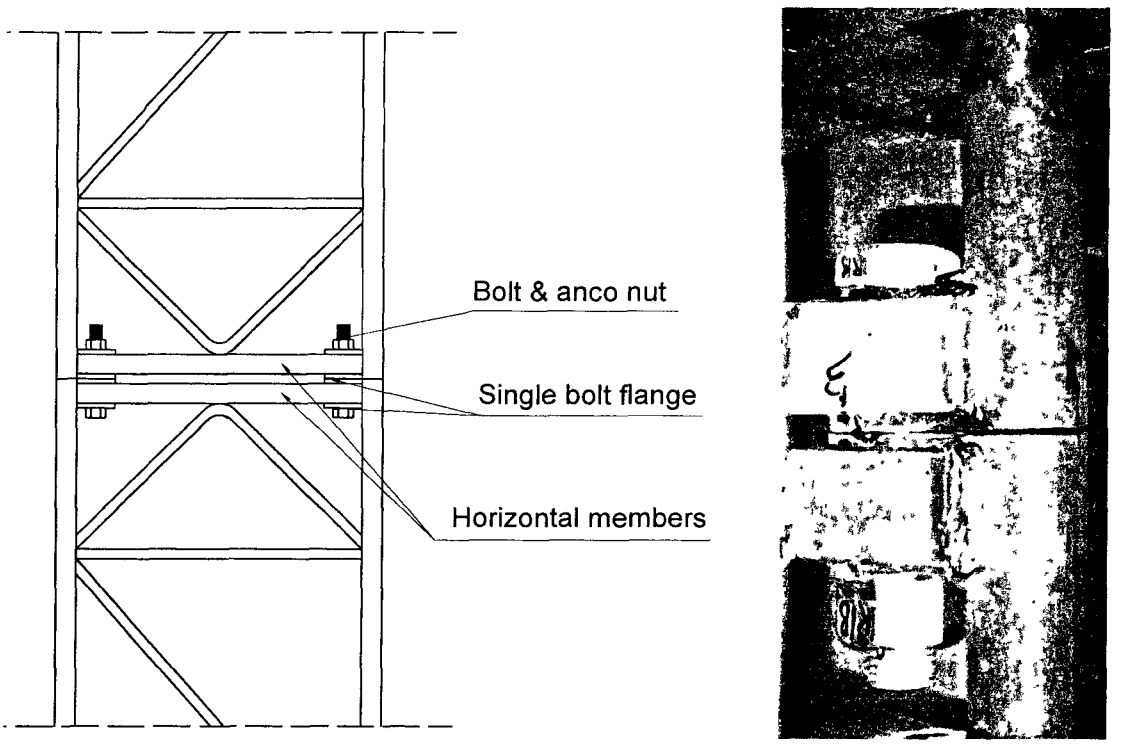

(a) Detail of splice section

(b) Photograph of splice section

Figure 4.2. Sketch and Photograph of Splice Section

Table 4.1. Details of Test Specimens and Failure Loads

Group #	Specimen #	Bolt diameter (d_b)	Leg dimension			Ring dimension			Failure load	Average failure load	Estimated load at first yield of the bolt	Load at first yield according to proposed method
			Length (L)	Thread length (t)	Size (d_l)	Internal diameter (D_i)	External diameter (D_o)	Height (h)				
		mm (in.)	mm (in.)	mm (in.)	mm (in.)	mm (in.)	mm (in.)	mm (in.)	kN (kip)	kN (kip)	kN (kip)	kN (kip)
1	R1	22.2 ($^7/_8$)	225 (8-$^3/_4$)	38.1 (1-$^1/_2$)	25.4 (1)	23.8 ($^{15}/_{16}$)	50.8 (2)	40 (1-$^9/_{16}$)	138 (31.0)	152 (34.1)	80.0 (18.0)	77.0 (17.3)
	R2								178 (40.1)			
	R3								137 (30.8)			
	R4								170 (38.2)			
	R5								147 (33.0)			
	R6								139 (31.2)			
2	R7	22.2 ($^7/_8$)	273 (10-$^3/_4$)	50.8 (2)	38.1 (1.5)	23.8 ($^{15}/_{16}$)	50.8 (2)	40 (1-$^9/_{16}$)	183 (41.1)	183 (41.1)	80.0 (18.0)	67.8 (15.2)
	R8								183 (41.1)			
	R9								185 (41.5)			
	R10								174 (39.1)			
	R11								181 (40.8)			
	R12								190 (42.8)			

Table 4.1. Details of Test Specimens and Failure Loads (concluded)

Group #	Specimen #	Bolt diameter (d_b)	Leg dimension			Ring dimension			Failure load	Average failure load	Estimated load at first yield of the bolt	Load at first yield according to proposed method
			Length (L)	Thread length (t)	Size (d_l)	Internal diameter (D_i)	External diameter (D_o)	Height (h)				
		mm (in.)	mm (in.)	mm (in.)	mm (in.)	mm (in.)	mm (in.)	mm (in.)	kN (kip)	kN (kip)	kN (kip)	kN (kip)
3	R13	31.8 ($1\text{-}^1/_4$)	400 ($15\text{-}^3/_4$)	152 (6)	50.8 (2)	33.3 ($1\text{-}^5/_{16}$)	69.9 (2.75)	63.5 (2.5)	271 (60.8)	271 (60.8)	140 (31.5)	126 (28.3)
	R14								268 (60.1)			
	R15								257 (57.8)			
	R16								276 (62.0)			
	R17								283 (63.5)			
	R18								271 (60.8)			

is shown in Figure 4 3(a), and those of the second and third groups (with horizontal members) is shown in Figure 4 3(b) The ring-type splices were fabricated by welding rings and horizontal tower members to legs and then connecting the sections by a pre-tensioned bolt Detailed measurements of the specimens are given in Shen [2002]

4.2.1 Test Setup

The tests were carried out in the Deformable Bodies Laboratory of the Civil and Environmental Engineering Department of the University of Windsor The specimens were placed in a vertical position on a 600 kN capacity Universal Testing Machine and a tensile load was applied to the specimens as shown in Figure 4 4 During testing, the maximum gap between the outside edges of the upper and lower leg members was measured using digital caliper, feeler gages, and divider

4.2.2 Testing Procedure and Results

Testing of each specimen was carried out in the following sequence

(a) The dimensions of specimens were measured and recorded

(b) Load was applied initially in approximately equal increments of 15 kN The maximum gap was measured at each load increment

(c) Load was applied in smaller increments towards the later stages of loading The recorded failure loads are shown in Table 4 1 From these results, it is evident that it is unsafe to ignore the eccentricity of the splices in the design because the failure loads of the splices are much smaller than the tensile strengths of the bolts, i e , 240 kN (54 0 kip) for 22 2 mm ($^{7}/_{8}$ in) diameter bolts and 431 kN (96 9 kip) for 31 8 mm (1-$^{1}/_{4}$ in) diameter bolts, with the resistance factor taken as unity

(d) From the load – maximum gap curves given in Shen [2002], average loads at first yield of the bolt were estimated as 80, 80, and 140 kN and are shown in Table 4 1 It can be readily observed that the failure loads are much greater than the loads at first yield, and the gaps are also very large The reason for this is the additional load after first yield was resisted not only by the bolt but also by the very high contact stresses on the compression side of the specimens

(e) It should be noted that the second and third groups of test specimens have horizontal members welded to the tower legs that would increase the tensile resistance of the leg splice in the actual tower, since horizontal members would resist rotation and offset the effect of load eccentricity As only one leg is tested in the experimental setup, however, a short length of horizontal member would not increase the tensile resistance of the leg splice

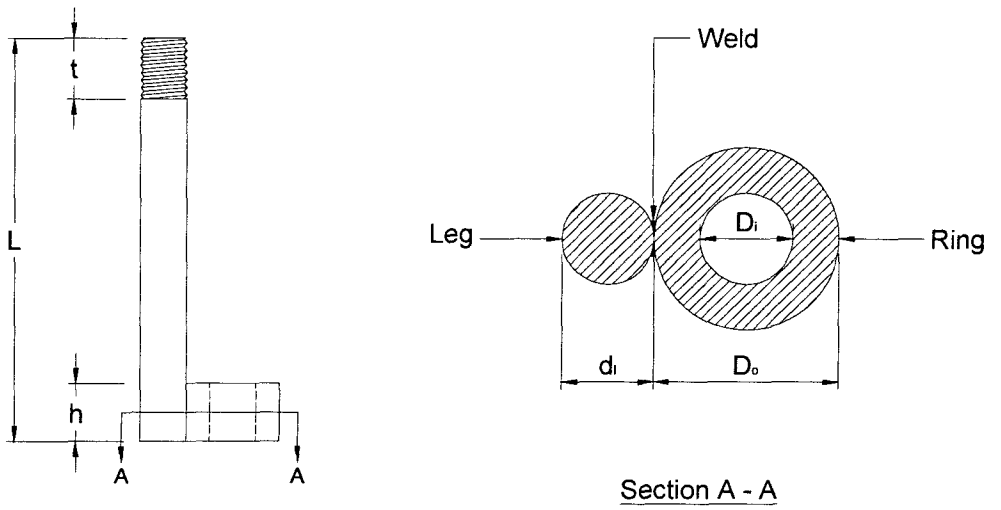

(a) Specimens without horizontals (1st group)

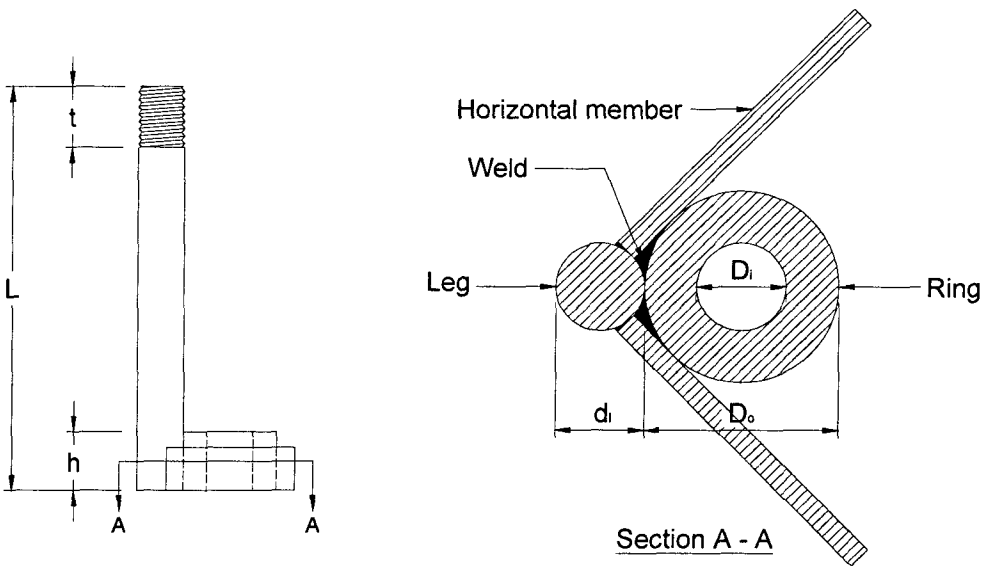

(b) Specimens with horizontals (2nd and 3rd groups)

Figure 4.3. Details of Test Specimens

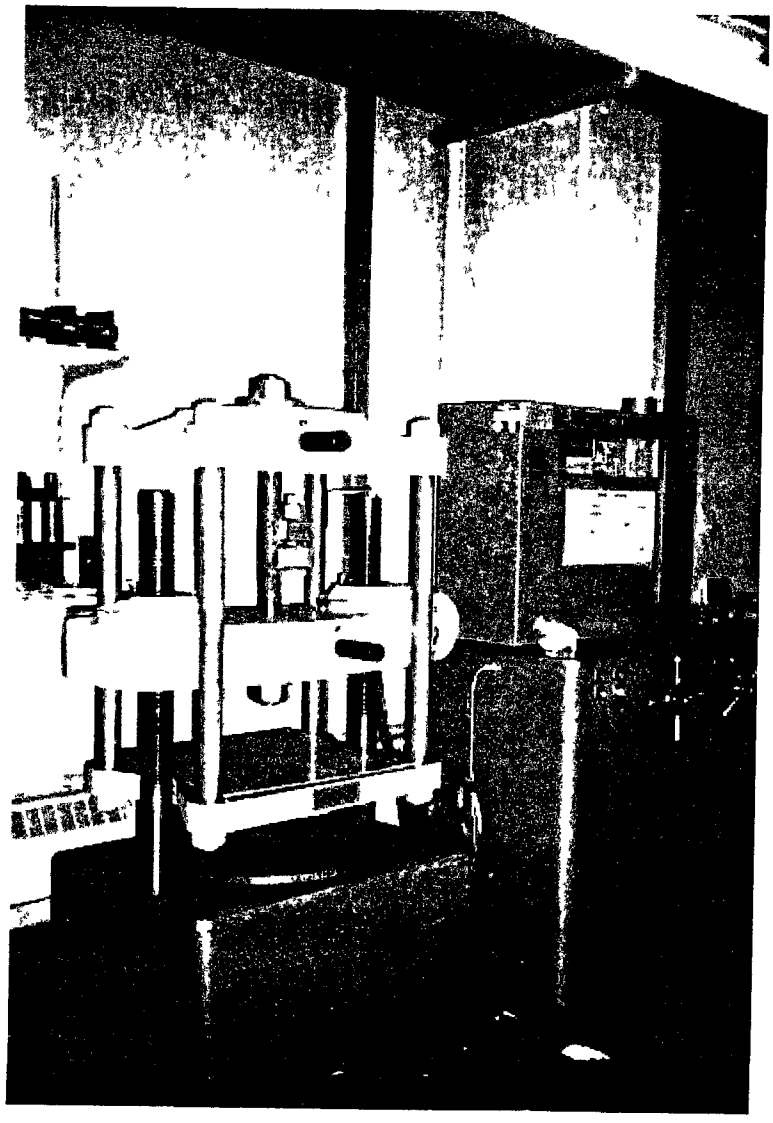

Figure 4.4. Test Setup

4.3 PROPOSED METHOD

The usual practice is to design the splice such that it behaves elastically. Therefore, the load at first yield can be taken as the maximum load that can be resisted by the splices. The following simplified method is proposed as a conservative design approach. The steps in this method are as follows:

(1) Assume that the bolt is tightened to the minimum initial tension (equal to 70% of the specified minimum tensile strength).

(2) Calculate the area of the ring and determine the initial bearing stress by dividing the initial bolt tension by the area of the ring.

(3) Calculate the section static modulus of the ring–bolt assembly, based on the external diameter of the ring.

(4) Determine the eccentricity of the load, defined as the distance between the centre of the leg to the centre of the bolt. Assume the effective eccentricity is half the actual eccentricity, resulting in a moment equal to $Pe/2$, where P is the load and e is the eccentricity. This assumption is justified because of fixity of the splice which is due to ring and horizontal members offsetting the effect of eccentricity. Calculate the load P that results in a tensile stress equal to the magnitude of the initial ring bearing (contact) stress. At this load, the contact stress is zero at the maximum gap location. The tensile stress in the bolt will still be the initial tensile stress (which is the initial tension divided by the nominal area of the bolt).

(5) Determine the additional stress required to initiate failure of the bolt. This is equal to the specified ultimate tensile stress of the bolt minus the stress due to the initial tension.

(6) Determine the additional moment required to induce this additional tensile stress in the bolt (this is assumed equal to the additional stress times the section modulus of the unthreaded portion of the bolt).

(7) Calculate the additional load corresponding to this additional moment (P additional = $M \times 2/e$, where M is the additional moment obtained in step 6).

(8) Compute the total force P required to initiate yielding in the bolt (P calculated in step 4 + P calculated in step 7).

The details of the calculations for the three groups of specimens are given in Table 4.2, and the results are given in Table 4.1. Comparing the values in the last two columns in Table 4.1, it can be readily seen that the loads according to the proposed method are in good agreement with the estimated yield loads obtained experimentally from load – maximum gap curves.

Table 4.2. Details of Calculations for the Proposed Design Method

Step	1	2(a)	2(b)	3	4(a)	4(b)	4(c)	5(a)	5(b)	6(a)	6(b)	7	8
Group #	Initial tension	A_{ring}	Bearing stress	$S_{ring+bolt}$	e	$A_{ring+bolt}$	P	Initial tensile stress in the bolt	Additional stress	S_{bolt}	Additional moment	Additional load	P_{total}
	kN (kip)	mm^2 (in^2)	MPa (ksi)	mm^3 (in^3)	mm (in.)	mm^2 (in^2)	kN (kip)	MPa (ksi)	MPa (ksi)	mm^3 (in^3)	N.m (in.lb)	kN (kip)	kN (kip)
Col. 1	*Col. 2*	*Col. 3*	*Col. 4*	*Col. 5*	*Col. 6*	*Col. 7*	*Col. 8*	*Col. 9*	*Col. 10*	*Col. 11*	*Col. 12*	*Col. 13*	*Col. 14*
1	174	1581	110	12870	38.1	2027	55.7	449	376	1078	406	21.3	77.0
	(39.1)	(2.45)	(16.0)	(0.79)	(1.50)	(3.14)	(12.5)	(65.1)	(54.6)	(0.07)	(3,592)	(4.79)	(17.3)
2	174	1581	110	12870	44.5	2027	49.6	449	376	1078	406	18.3	67.8
	(39.1)	(2.45)	(16.0)	(0.79)	(1.75)	(3.14)	(11.1)	(65.1)	(54.6)	(0.07)	(3,592)	(4.10)	(15.2)
3	316	2959	107	33458	60.3	3832	91.9	399	326	3142	1024	33.9	126
	(71.0)	(4.59)	(15.5)	(2.04)	(2.38)	(5.94)	(20.7)	(57.9)	(47.3)	(0.19)	(9,066)	(7.6)	(28.3)

Notes:

Column 2: From CSA S16-09 [CSA 2009]

Column 3: Area = $\frac{\pi}{4} \times \left(D_o^2 - D_i^2\right)$

Column 4: Bearing stress = Column (2) / Column (3)

Column 5: Section modulus = $\frac{\pi}{32} \times D_o^3$

Column 6: Eccentricity = 0.5 x (D_o + d_i)

Column 7: Area = $\frac{\pi}{4} \times D_o^2$

Column 8: Force = Bearing stress / (1 / $A_{ring+bolt}$ + e / (2 * $S_{ring+bolt}$))

Column 9: Initial tensile stress = Column (2) / ($\frac{\pi}{4} \times d_b^2$)

Column 10: Additional stress = F_u of bolt – Column (9)

Where F_u = 825 MPa (120 ksi) for $d_b \leq$ 25.4 mm (1 in.)

= 725 MPa (105 ksi) for $d_b >$ 25.4 mm (1 in.)

Column 11: Section modulus = $\frac{\pi}{32} \times d_b^3$

Column 12: Additional moment = Column (10) x Column (11)

Column 13: Additional load = Column (12) x 2 / e

Column 14: Total load = Column (8) + Column (13)

4.4 CONCLUSIONS

From this investigation, it can be concluded that it is unsafe to ignore the eccentricity of load in the design of ring-type bolted splices The splice should be designed for combined stresses due to axial tension and bending with a moment equal to the axial load times half the distance between the centre of the leg and the centre of the bolt (to take into account the fixity of the splice)

REFERENCES

CSA 2009 Design of steel structures S16-09 Canadian Standards Association, Mississauga, ON

Kumalasari, C , Shen, L , Madugula, M K S, and Ghrib, F 2005 Tensile strength of bolted ring-type connections of solid round leg members of guyed communication towers Canadian Journal of Civil Engineering, **32**(3) 595-600

Shen, L 2002 Strength of bolted ring-type connections of solid round leg members of guyed communication towers M A Sc thesis, Department of Civil and Environmental Engineering, University of Windsor, Windsor, ON

CHAPTER 5
PRYING ACTION IN BOLTED STEEL CIRCULAR FLANGE CONNECTIONS

5.1 INTRODUCTION

One common type of splice for solid round leg members of guyed lattice communication towers consists of circular flange plates welded to the members and bolted together. These splices will potentially be subjected to tension due to the applied lateral loads (wind or earthquake). Both CISC Handbook of Steel Construction [CISC 2010] and the AISC Steel Construction Manual [AISC 2005] discuss prying action only in tee-type and angle-type connections subjected to tensile force and no guidance is provided to determine the prying force in bolted steel circular flange connections. In order to use the formulas given in those publications discussed in Section 5.2, one must determine the value of *"p"*, i.e., the length of flange tributary to each bolt (bolt pitch).

In the case of tee-type connections and angle-type connections, this dimension *"p"* is simply the spacing between the bolts in the longitudinal direction. It is assumed that in the case of circular flange connections, the bolt pitch can be taken as the distance between the centres of bolts measured along the bolt circle (which is equal to the circumference of the bolt circle divided by the number of bolts). In order to test the validity of this assumption, tests were carried out on ten bolted steel circular flange connections. This research has been published in the Canadian Journal of Civil Engineering [Kumalasari et al. 2006].

5.2 LITERATURE REVIEW

Previous research on flanged joints for tubular legs were undertaken by British Steel at Cardiff University. Based on the research, it was recommended that the design strength of the bolts should be 20% higher than that of the tube, with the pitch circle diameter of the bolts should be as small as possible [Smith 2006].

5.3 EXPERIMENTAL INVESTIGATION

Two types of circular flange connections were included in the experimental investigation (Figures 5.1(a) and (b)). Figure 5.1(a) is a regular circular flange connection with constant flange thickness. Figure 5.1(b) is a special type of connection where the ends of the flanges were milled a short distance to reduce the contact area of the flanges (which is subsequently to reduce prying action) while still maintaining the required minimum edge distance for the bolts.

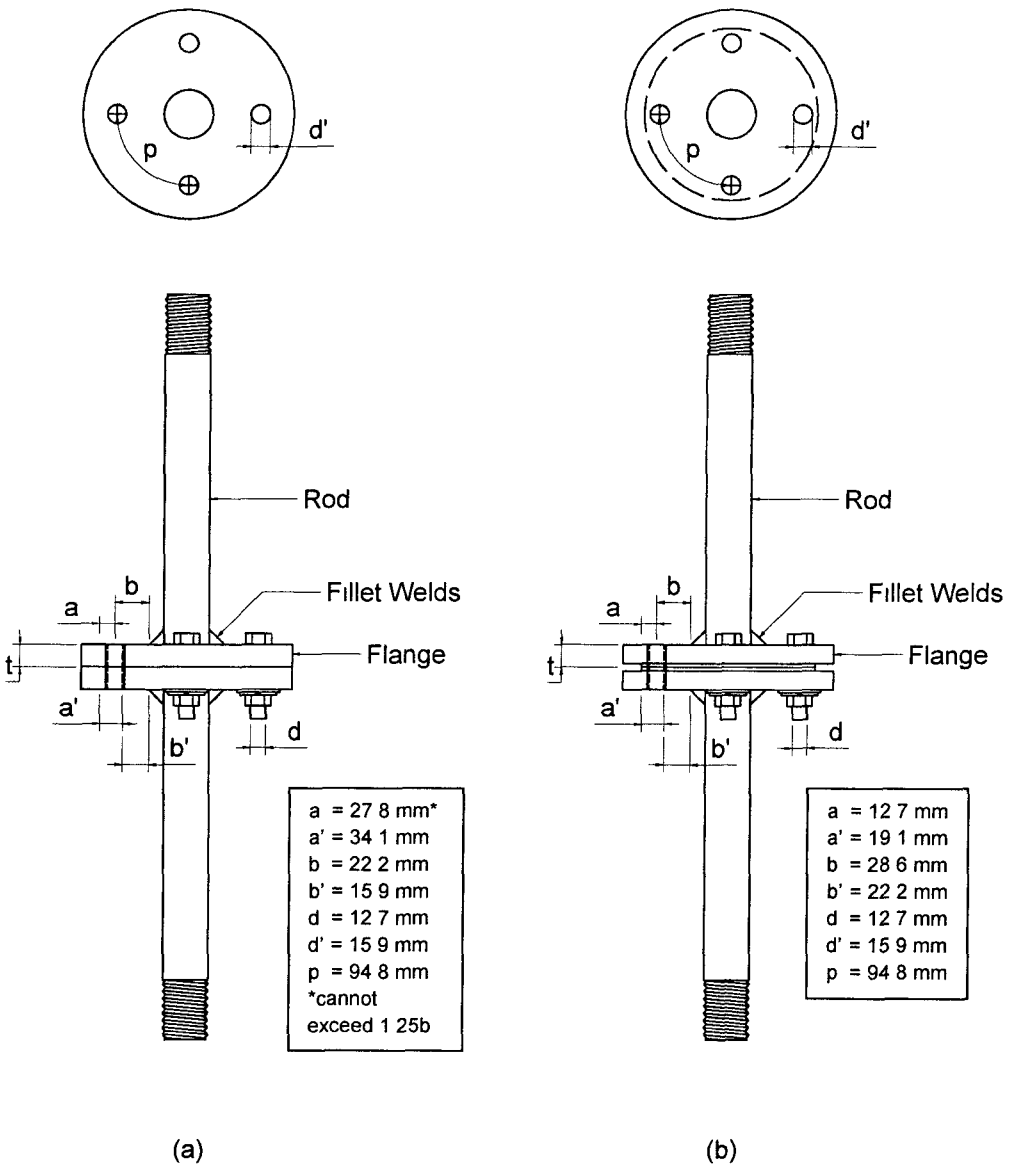

(a) Regular bolted steel circular flange connection (specimens # 1 and # 2)

(b) Special type of bolted steel circular flange connection (specimens # 3 to # 10)

Figure 5.1. Bolted Circular Flange Connection

All ten specimens of steel circular flange connections to splice tension members were made from 38.1 mm (1-$^1/_2$ in.) diameter rod and 178 mm (7 in.) diameter flange plate. The flanges are from ASTM A572-50 grade (yield strength 345 MPa (50 ksi)). The flange thickness for the regular connection was 7.94 mm ($^5/_{16}$ in.) with a weld size of 19.1 mm ($^3/_4$ in.). For the eight specimens of the special type of connection, the flange thicknesses varied from 9.53 mm ($^3/_8$ in.) to 19.1 mm ($^3/_4$ in.) (see column 2 of Table 5.1) with the end thickness reduced by 3.18 mm ($^1/_8$ in.) for a distance of 15.9 mm ($^5/_8$ in.) as shown in Figure 5.1(b). The weld size for this special type of connection was 12.7 mm ($^1/_2$ in.). All specimens were connected using four 12.7 mm ($^1/_2$ in.) diameter ASTM A325 bolts with a bolt torque of 149 N-m (110 lb-ft) on 121 mm (4-$^3/_4$ in.) bolt circle diameter. The bolt length was 57.2 mm (2-$^1/_4$ in.) for 7.94 mm ($^5/_{16}$ in.) thick flange specimens and 63.5 mm (2-$^1/_2$ in.) for other specimens.

To determine the tensile strength of the bolts, tests were carried out on 15 bolts. It was found that the average tensile strength of bolts is 90.3 kN (20.3 kip) with a range of 88.1 to 94.7 kN (19.8 to 21.3 kip). The circular flange connections were tested in a 600 kN (135 kip) Tinius Olsen Universal Testing Machine as shown in Figure 5.2 and the failure loads (peak loads) are given in column 3 of Table 5.1. For connections with flange plates with a thickness of 9.53 mm ($^3/_8$ in.) or less, the failure was by excessive bending of the flange plates with consequent elongation and bending of the bolts (Figure 5.3). For connections with thicker flange plates, the specimens failed through the fracturing of bolts, as shown in Figure 5.4, which is a close-up of failed specimen # 6. The load–elongation curve for this specimen is shown in Figure 5.5. Initially, the load–elongation curve was linear, as expected. Under increasing load the bolts elongated, and the load–elongation curve became flatter. Finally, failure occurred at 324 kN because two bolts fractured (Figure 5.4).

From the tensile strength of the bolts and the failure load of the connection, the prying force is calculated as follows:

[5.1] Total prying force = (Number of bolts x Tensile strength of one bolt) - Experimental failure load

[5.2] Prying force per bolt = Total prying force / Number of bolts

These experimentally determined prying forces are compared with the values calculated from the equations available in the CISC Handbook and AISC Manual as written in the following sub-sections.

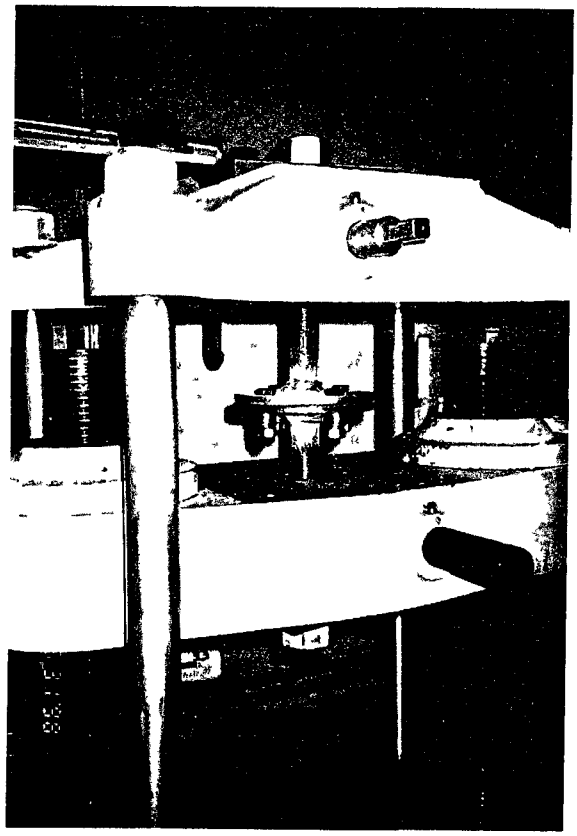

Figure 5.2. Test Setup

Table 5.1. Comparison of Experimental and Calculated Prying Forces

Specimen #	Flange thickness (t)	Experimental				Calculation	
		Failure load	Average failure load (4 P_f)	Total prying force (4 Q)	Prying force per bolt (Q)	Prying force per bolt (Q)	
						CISC	AISC
	mm (in)	kN (kip)	kN (kip)	kN (kip)	kN (kip)	kN (kip)	kN (kip)
Col 1	*Col 2*	*Col 3*	*Col 4*	*Col 5*	*Col 6*	*Col 7*	*Col 8*
1	7 94 ($^5/_{16}$)	297 (66 7)	292 (65 6)	69 4 (15 6)	17 4 (3 90)	18 9 (4 24)	18 9 (4 24)
2		287 (64 5)					
3	9 53 ($^3/_8$)	234 (52 7)	233 (52 4)	128 (28 8)	32 0 (7 20)	29 1 (6 55)	29 1 (6 54)
4		232 (52 2)					
5	12 7 ($^1/_2$)	265 (59 6)	294 (66 2)	66 8 (15 0)	16 7 (3 75)	16 8 (3 77)	16 7 (3 76)
6		324 (72 8)					
7	15 9 ($^5/_8$)	356 (80 0)	359 (80 6)	2 55 (0 573)	0 638 (0 143)	0 0 (0 0)	0 0 (0 0)
8		361 (81 2)					
9	19 1 ($^3/_4$)	356 (80 0)	352 (79 2)	8 95 (2 01)	2 24 (0 503)	0 0 (0 0)	0 0 (0 0)
10		349 (78 4)					

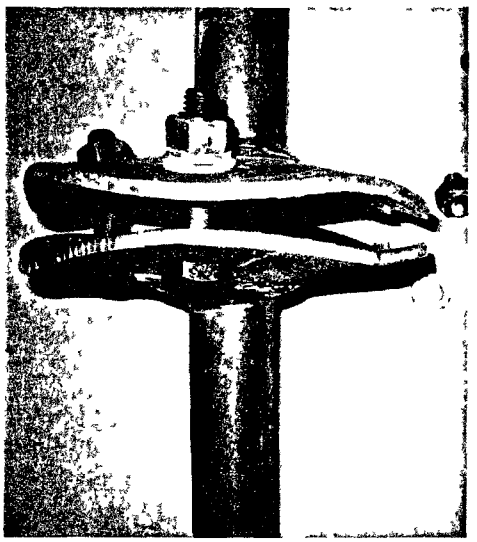

Figure 5.3. Excessive Bending of Flange Plates and Elongation of Bolts

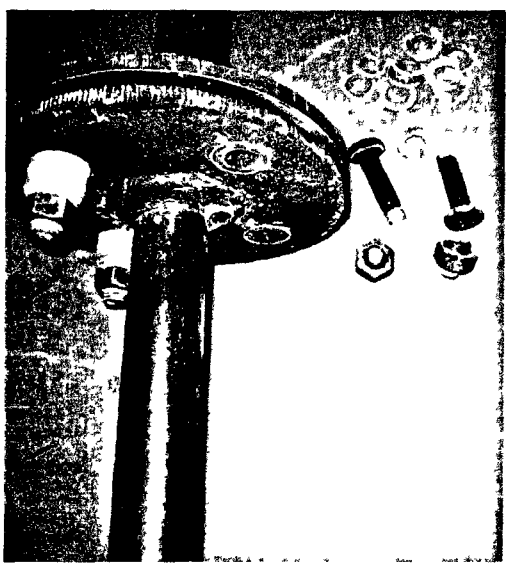

Figure 5.4. Test Specimen # 6 after Failure Showing Fracture of Bolts

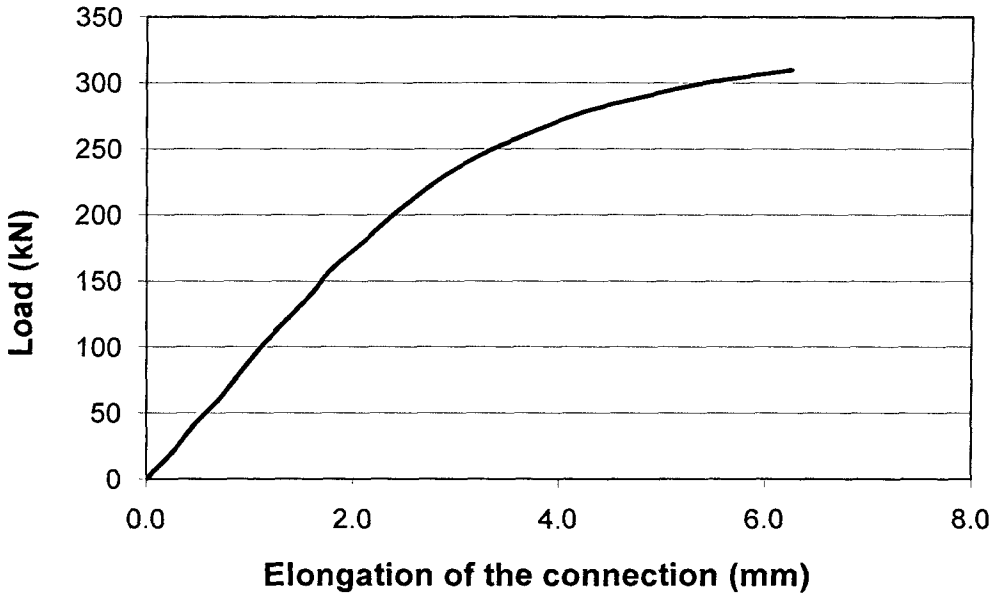

Figure 5.5. Load-elongation Curve for Specimen # 6

5.3.1 Calculation of Prying Force according to CISC Handbook of Steel Construction [CISC 2010]

Refer to Figures 5.1(a) and (b).

[5.3] $$K = \frac{4 \times b' \times 10^3}{\phi \times p \times F_y}$$

[5.4] $$\delta = 1 - \frac{d'}{p}$$

[5.5] $$\alpha = \left(\frac{K \times P_f}{t^2} - 1 \right) \times \frac{1}{\delta}$$

[5.6] $$Q = P_f \times \left(\frac{b'}{a'} \times \frac{\delta \times \alpha}{1 + \delta \times \alpha} \right)$$

where,

a = distance from bolt line to edge of flange (not more than 1.25 b), (mm)

a' = $a + \frac{d}{2}$, (mm)

b = distance from bolt line to face of fillet welds, (mm)

b' = $b - \frac{d}{2}$, (mm)

d = bolt diameter, (mm)

d' = nominal hole diameter, (mm)

K = parameter as defined in Equation [5.3]

p = length of flange tributary of each bolt, or bolt pitch, (mm)

P_f = applied tensile load per bolt, (kN)

Q = prying force per bolt, (kN)

t = thickness of flange, (mm)

F_y = yield strength of flange material, (MPa)

ϕ = resistance factor for the material, 0.9 (but taken as 1.0 for the investigation)

5.3.2 Calculation of Prying Force according to AISC Steel Construction Manual [AISC 2005]

Refer to Figures 5.1(a) and (b).

[5.7] $$t_c = \sqrt{\frac{4.44 \times \phi \times r_n \times b'}{p \times F_y}}$$

$$[5.8] \quad \alpha = \frac{1}{\delta}\left[\frac{P_f}{\phi \times r_n} \times \left(\frac{t_c}{t}\right)^2 - 1\right] \geq 0$$

$$[5.9] \quad Q = \phi \times r_n \left[\delta \times \alpha \times \frac{b'}{a'} \times \left(\frac{t}{t_c}\right)^2\right]$$

where,

a, a', b, b', d, d', p, t, as defined earlier (in units of inches)

P_f = applied tensile load per bolt, kip

F_y = yield strength of flange material, ksi

δ = as defined in Equation [5.4]

t_c = flange thickness required to develop design tensile strength of bolts with no prying action, (in.)

r_n = tensile strength of the bolt, kip

ϕ = resistance factor for the bolt, 0.9, but taken as 1.0 for the investigation, therefore the constant 4.44 in Equation [5.7] (which is derived from $4/\phi$) becomes 4 in the calculation.

5.4 COMPARISON OF PRYING FORCES OBTAINED FROM EXPERIMENTAL INVESTIGATION AND THOSE OBTAINED FROM CISC AND AISC

The nominal yield strength of the flange, i.e., 345 MPa (50 ksi), was used in these calculation. The bolt pitch is taken as the distance between the centres of bolts along the bolt circle (which is equal to the circumference of the bolt circle divided by the number of bolts), and the results are presented in columns 7 and 8 of Table 5.1.

It should be pointed out that in the calculations of the prying forces based on Equation [5.1], the average value is used for the tensile strength of the bolt. Variation in the tensile strength between individual bolts is not considered in the calculations since both tests of the individual bolts and the flanges were destructive and there were limited number of available test specimens. This explains the discrepancy between the experimentally determined prying force and the calculated prying force. This also makes it impossible to determine the error in the predicted prying force as a percentage of the failure load.

5.5 CONCLUSIONS

The following conclusions are applicable for the connection size and shapes used in the investigation. A comparison of columns 6, 7, and 8 of Table 5.1 clearly shows that the assumption regarding the bolt pitch *"p"* as the distance between the centres of bolts along the bolt

circle, is reasonable. Therefore, the equations given in the CISC Handbook and AISC Manual can be used to calculate the prying force in circular flange connections also in addition to tee-type and angle-type hangers. The prying forces calculated based on CISC Handbook yield the same values with the values obtained using AISC Manual.

REFERENCES

AISC. 2005. Steel Construction Manual. 13th ed. American Institute of Steel Construction, Chicago, IL.

CISC. 2010. Handbook of Steel Construction. 10th ed. Canadian Institute of Steel Construction, Markham, ON.

Kumalasari, C., Ding, Y., and Madugula, M.K.S. 2006. Prying action in bolted steel circular flange connections. Canadian Journal of Civil Engineering, Special Issue on Recent Advances in Steel Structures Research, **33**(4): 497-500.

Smith, B.W. 2006. Communication structures. 1st ed. Thomas Telford Publishing, London.

CHAPTER 6
COMPRESSIVE STRENGTH OF SOLID ROUND STEEL MEMBERS STRENGTHENED WITH SPLIT PIPES

6.1 INTRODUCTION

Communication towers are in high demand due to the ongoing increase of wireless activity. However, due to high cost, availability of land, and building permit restrictions, it is not always feasible to build a new communication tower to increase wireless coverage. Wireless providers have to share existing towers which causes additional loading and overstresses on tower legs and diagonals, especially for slender towers located in regions with high wind pressure and/or thick rime icing.

For lattice tower structures with leg and diagonal members of angle sections (which also known as knock-down towers), strengthening can be done by adding angle sub-bracings, or by replacing diagonal sections with back-to-back angle or bigger angle sections as shown in Figure 6.1. However, for all-weld sections made from solid rounds or for monopoles, strengthening is sometimes found to be challenging for tower engineers. Since lattice self-supporting and guyed towers are subjected to higher wind loads than monopoles due to the typical height of the structures, this chapter focuses on the strengthening of solid rounds for lattice tower structures only.

The common methods for strengthening solid rounds are by (i) reducing the effective buckling length of main members (either tower leg or diagonals) by using bolt-on secondary members (sub-bracings or Y-bracings), and (ii) attaching additional members parallel to the longitudinal axis of the main members as shown in Figure 6.2, commonly known as splints. The calculation of compressive strength of strengthened member using the first method is straightforward. However, for towers crowded with existing antennas and mounts, this is not always feasible due to intersection of antenna mounts and strengthening members. Coping the antenna mounts to accommodate the strengthening members is not desirable either.

The second method is commonly done by attaching angle splints for solid rounds with small diameter, and attaching channel splints for larger diameter solid rounds. However the intersection between the angle and channel sections with existing antenna mounts, as mentioned in the first method, is still a problem. Some tower designers proposed to strengthen solid round members with split pipes. A split pipe is made by dividing one single pipe into two sections of

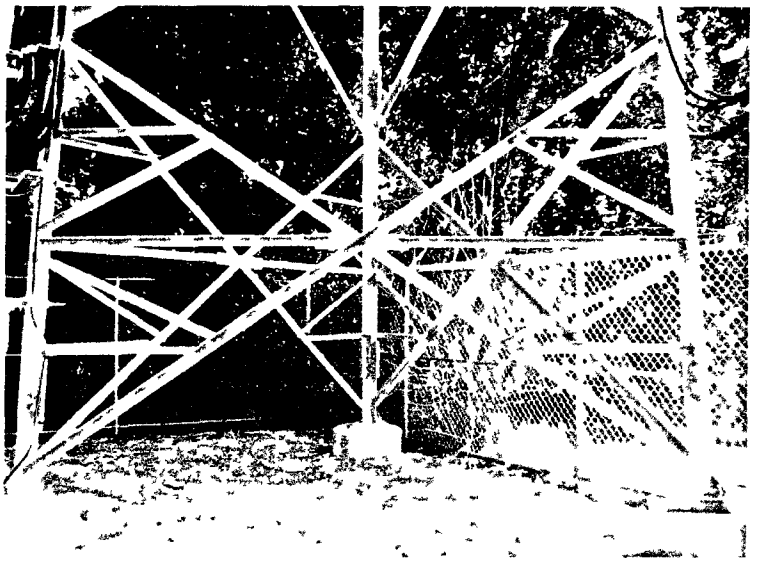

(courtesy of Westower Communications Ltd)

Figure 6.1. Strengthening with Sub-bracings

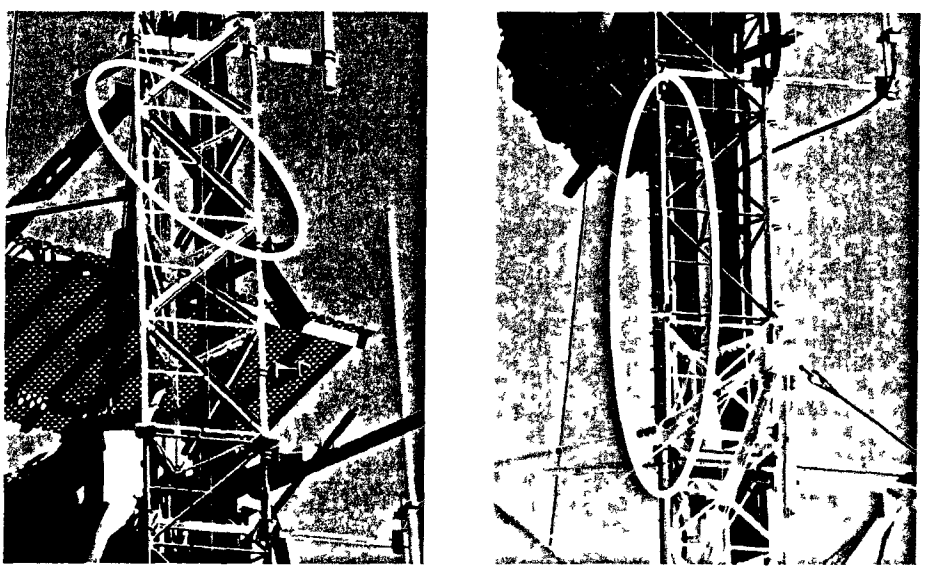

(a) Diagonal members strengthened with angle splints

(b) Leg members strengthened with channel splints

(courtesy of Westower Communications Ltd)

Figure 6.2. Strengthening with Splints

equal cross-sectional area. Those split pipes are attached longitudinally to the main member using U-bolts, tabs, or welds. Strengthening with split pipes can reduce the possible intersection with outstanding angle antenna mounts and also can reduce the exposed wind area of strengthening members, compared with angle or channel splints.

The common method used by tower design engineers to calculate the compressive strength of splint-strengthened members is by reducing the effective length by half. The choice of splint size is chosen based on the area of the splint/strengthening members to be the same or larger than the cross-section area of the main member. This method is an approximation and thus more precise calculation of compressive strength is needed. Previous research has been done on strengthening with angle splints and solid round splints [Kumalasari et al. 2006, 2005]. Therefore, this chapter discusses the compressive strength of solid round strengthened with split pipes.

6.2 LITERATURE REVIEW

6.2.1 Compressive Strength of Columns

The strength of a column is defined as the maximum compressive force that the column can resist without excessive lateral deformation or plastic deformation. For cold-formed steel columns which are perfectly straight with concentric loading, the strength of the column is given by the critical-load theory. For hot-rolled steel columns which are geometrically imperfect and/or slightly eccentrically loaded, the strength of the column is given by the theory of imperfect column. In general, the column strength must be determined by including imperfections, material non-linearity, and residual stress effects.

6.2.1.1 Critical-load theory

The strength of a perfectly straight, linearly elastic homogenous column with concentric loading was first given by Euler in 1744 [Bleich 1952]. The critical load (or Euler load) is defined as the axial load which is sufficient to maintain the bar in such a slightly bent form. If the load is less than the critical value, the bar remains straight and undergoes only axial compression. When the load is increased gradually, the straight form of equilibrium becomes unstable and a small lateral force produces an irreversible deflection that does not disappear when the lateral force is removed [Timoshenko and Gere 1961]. The Euler load, P_E (also known as P_{cr}), at which buckling first begins, is given by:

[6.1] $$P_E = \frac{\pi^2 EI}{(KL)^2}$$

where E is the modulus of elasticity, I is the moment of inertia of the column, and KL is the effective length of column Lamarle in 1845 had established the elastic limit as the limit of validity of Euler's formula If the compressive stress reaches the proportional or elastic limit before buckling can occur, Equation [6 1] cannot be used

Engesser presented the tangent-modulus theory in 1889 for inelastic buckling In 1891, Considère predicted that the column strength in the case of inelastic buckling may be determined by a generalized Euler formula,

[6 2] $$P = \frac{\pi^2 \bar{E} I}{(KL)^2}$$

where $\bar{E}$ is a variable modulus varying between Young's modulus and tangent modulus Engesser in 1895 acknowledged Considère's concept and gave an improved solution of the column problem by presenting his "double-modulus" theory also called "reduced-modulus" theory Engesser's theoretical studies were shown to be correct by a series of very careful tests performed by Kármán in 1908

Timoshenko and Gere [1961] discussed the buckling of bars with changes in cross-section, since bars with uniform cross-section are not the most economical to carry compressive loads The stability of columns can be increased by riveting or welding additional plates or angles along portions of its length If "a" is the length of the strengthening member, L is the length of the column, and I_1 and I_2 are the moments of inertia of un-strengthened and strengthened cross-sections, the Euler load for this type of column can be calculated from the following equation

[6 3] $$P_E = \frac{mEI_2}{L^2}$$

where m is the numerical factor depending on the ratios of $\frac{a}{L}$ and $\frac{I_1}{I_2}$

Dinnik [1932] calculated several values of m for both hinged-end and fixed-end columns

6.2.1.2 Imperfect column theory

Out-of-straightness of the column and/or eccentricity of the load which are unavoidable in practice, introduce bending from the start of loading Therefore, for real columns, there is no bifurcation of equilibrium, i e , no critical load, but only a buckling load

The principal imperfections that make an actual column different than an ideal column are [Timoshenko and Gere 1961]

1 Unavoidable load eccentricity,

2. Initial curvature of the column; and
3. Non-homogenous material of the column.

To apply Euler's formula in column design, various imperfections in a column are compensated for with safety factors determined from previous experimental investigation by several researchers [Timoshenko and Gere 1961].

6.2.2 Column Design based on Strength Theory

The present state of research is such that if the following information is known, accurate calculation of the maximum strength is possible [Ziemian 2010]:

1. Material properties (i.e., yield stress F_y and modulus of elasticity E);
2. Cross-sectional dimensions;
3. Distribution of the residual stresses;
4. The shape and magnitude of initial out-of-straightness; and
5. The moment-rotation relationship of the end restraint.

The design of structural steel columns is based on formulas proposed by Structural Stability Research Council (SSRC). The formulas were adopted by American Institute of Steel Construction (AISC), with safety factors applied to be used in design of steel columns [Craig 1996]. For long columns, the Euler formula, Equation [6.1], is used as long as proportional limit of the material is not exceeded.

Due to large residual stresses which occur during the rolling process, AISC limits the range of validity of Euler's formula to those values of effective slenderness ratio KL/r for which critical stress F_{cr} is less than 0.5 times yield stress F_y. This KL/r, which differentiates a long column from a short column, is called critical slenderness ratio [Young and Budynas 2002] and written as follows:

$$[6.4] \quad \left(\frac{KL}{r}\right)_c = \sqrt{\frac{\pi^2 E}{0.5F_y}}$$

For a short column, several formulas are used, e.g., secant formula with eccentric ratio of 0.25 (which was based on tests on structural steel columns), Rankine formula, polynomial, and exponential formulas [Young and Budynas 2002]. The Column Research Council proposed the use of parabolic curve, sometimes called Johnson column formula,

[6.5] $$\frac{F_{cr}}{F_y} = 1 - \frac{\left(\frac{KL}{r}\right)^2}{2\left(\frac{KL}{r}\right)_c^2}$$

In North America, calculation of compressive resistance is based on either Canadian Standard or American Specification discussed in the following section.

6.2.2.1 Compressive resistance of solid round steel members as per the Canadian Standard S16-09 [CISC 2010]

The Canadian Standard, CSA S16-09, specifies the compressive resistance as follows:

[6.6] $$C_r = \phi A F_y \left(1 + \lambda^{2n}\right)^{-\frac{1}{n}}$$

where the resistance factor ϕ = 0.9.

The non-dimensional slenderness parameter λ is given by:

[6.7] $$\lambda = \frac{KL}{r}\sqrt{\frac{F_y}{\pi^2 E}}$$

6.2.2.2 Compressive resistance of solid round steel members as per American Specification [AISC 2005]

Compressive resistance according to AISC-LRFD Specification is as follows:

[6.8] $$C_r = \phi A F_{cr}$$

where the resistance factor ϕ = 0.9.

[6.9] For $\lambda \leq 1.5$, $F_{cr} = 0.658^{\lambda^2} F_y$

[6.10] For $\lambda > 1.5$, $F_{cr} = \frac{0.877}{\lambda^2} F_y$

λ is as defined in Equation [6.4].

Where

A = gross area of cross-section

E = Young's modulus of elasticity

F_{cr} = critical stress

F_y = specified minimum yield stress

K = effective length factor

L = unbraced length of the member

n = parameter for compressive resistance (1.34 for angles and hot-rolled solid rounds up to 51 mm in diameter)

r = minimum radius of gyration

ϕ = resistance factor

λ = non-dimensional slenderness parameter

6.2.2.3 Compressive resistance of strengthened solid round steel members

Since 2003, the study of the compressive strength of solid round steel members strengthened with angle or solid round splints, with various types of connections between the main member and the strengthening member, has been conducted at the University of Windsor.

Results of experimental investigation conducted in the University of Windsor for solid round steel members strengthened with rods or angles were published by Kumalasari et al. [2005, 2006], Madugula et al. [2007], and Ziemian [2010]. Based on the experimental results, simple and conservative methods to calculate strengthened solid round steel members were proposed.

6.3 EXPERIMENTAL INVESTIGATION

Fifty-seven steel solid round members, 51 mm (2 in.) diameter, with 102 x 102 x 13 mm (4 x 4 x ½ in.) plates at top and bottom, were tested at the Structural Laboratory of the University of Windsor to determine the compressive strength of solid round members strengthened with 7.01 mm (0.276 in.) thick split pipes. Out of the 57 specimens, 18 were 1524 mm (60 in.) long and the others were 762 mm (30 in.) long. The average yield stress and tensile stress of the solid round are 414 MPa and 563 MPa, respectively. For the split pipe, the average yield stress and tensile stress are 550 MPa and 613 MPa, respectively. Those values were obtained from mill test certificates accompanying the test specimens.

In order to determine the effect of connection types on the compressive strength of strengthened member, there are four types of connections used to attach the strengthening member to the main member, i.e.:

1. U-bolts;
2. Tabs;
3. Stitch weld; and
4. U-bolts with welds at the end of the strengthening member.

The 18 test specimens, RF60 series, 1524 mm long, as summarized in Table 6.1, consisted of:

1. Three specimens un-strengthened, RF60, as shown in Figure 6.3(a);
2. Three specimens strengthened with two split pipes, RF60-B1, 73 mm (2-$^7/_8$ in.) diameter and 1372 mm (54 in.) long, connected with eight U-bolts, as shown in Figure 6.3(b);
3. Three specimens strengthened with two split pipes, RF60-B2, 73 mm diameter and 1372 mm long, connected with eight tabs, as shown in Figure 6.3(c);
4. Three specimens strengthened with two split pipes, RF60-B4, 73 mm diameter and 610 mm (24 in.) long, connected with four U-bolts, as shown in Figure 6.3(d);
5. Three specimens strengthened with two split pipes, RF60-W1, 73 mm diameter and 1372 mm long, connected with 3 mm ($^1/_8$ in.) stitch welds, as shown in Figure 6.3(e);
6. Three specimens strengthened with two split pipes, RF60-W2, 73 mm diameter and 1372 mm long, connected with six U-bolts and 3 mm ($^1/_8$ in.) end welds, as shown in Figure 6.3(f).

The 39 test specimens, RF30 series, 762 mm long, as summarized in Table 6.2, consisted of:

1. Twenty seven un-strengthened specimens, RF30, as shown in Figure 6.4(a);
2. Three specimens strengthened with two split pipes, RF30-B1, 73 mm (2-$^7/_8$ in.) diameter and 610 mm (24 in.) long, connected with four U-bolts, as shown in Figure 6.4(b);
3. Three specimens strengthened with two split pipes, RF30-B2, 73 mm diameter and 610 mm long, connected with four tabs, as shown in Figure 6.4(c);
4. Three specimens strengthened with two split pipes, RF30-W1, 73 mm and 610 mm long, connected with 3 mm ($^1/_8$ in.) stitch welds, as shown in Figure 6.4(d);
5. Three specimens strengthened with two split pipes, RF30-W2, 73 mm and 610 mm long, connected with two U-bolts and 3 mm ($^1/_8$ in.) end welds, as shown in Figure 6.4(e).

6.3.1 Test Details and Results for 1524 mm Long Test Specimens

6.3.1.1 Determination of suitable test setup

Tests were first conducted on un-strengthened specimens to determine a suitable test setup. The test setup is said to be acceptable if the failure load of an un-strengthened specimen is close to the analytical results of compressive strength with a fixed-end condition. Equations [6.6] and [6.8], with effective length factor K of 0.5, Young's modulus E of 206,700 MPa (30,000 ksi), yield strength F_y of 414 MPa (61.5 ksi), and resistance factor ϕ of 1.0, results in compressive strength of 584 kN (131 kip) and 628 kN (141 kip), respectively. It was expected that the test results should be very close to these results.

Table 6.1. Details and Specimens ID of 1524 mm (60 in.) Long Test Specimens

Specimen ID	Number of specimens	Split pipes strengthening member[a]				
		Length	U-bolts[b]	Tabs[b]	Stitch weld[c]	End weld[d]
RF60	3	-	-	-	-	-
RF60-B1	3	1372 (54")	8 - 178 (7")	-	-	-
RF60-B2	3	1372 (54")	-	8 - 178 (7")	-	-
RF60-B4	3	610 (24")	4 - 178 (7")	-	-	-
RF60-W1	3	1372 (54")	-	-	3 ($^1/_8$") 51 - 152 (2" - 6")	-
RF60-W2	3	1372 (54")	6 - 178 (7")	-	-	3 ($^1/_8$") - 76 (3")

[a] Unless specified, units of length and distance are in millimetres
[b] [Number of U-bolts or tabs] - [Distance to centre-to-centre (pitch) of U-bolts or tabs]
[c] [Size of Weld]
[Length of Weld] - [Pitch of Weld]
[d] [Size of Weld] - [Pitch of Weld]

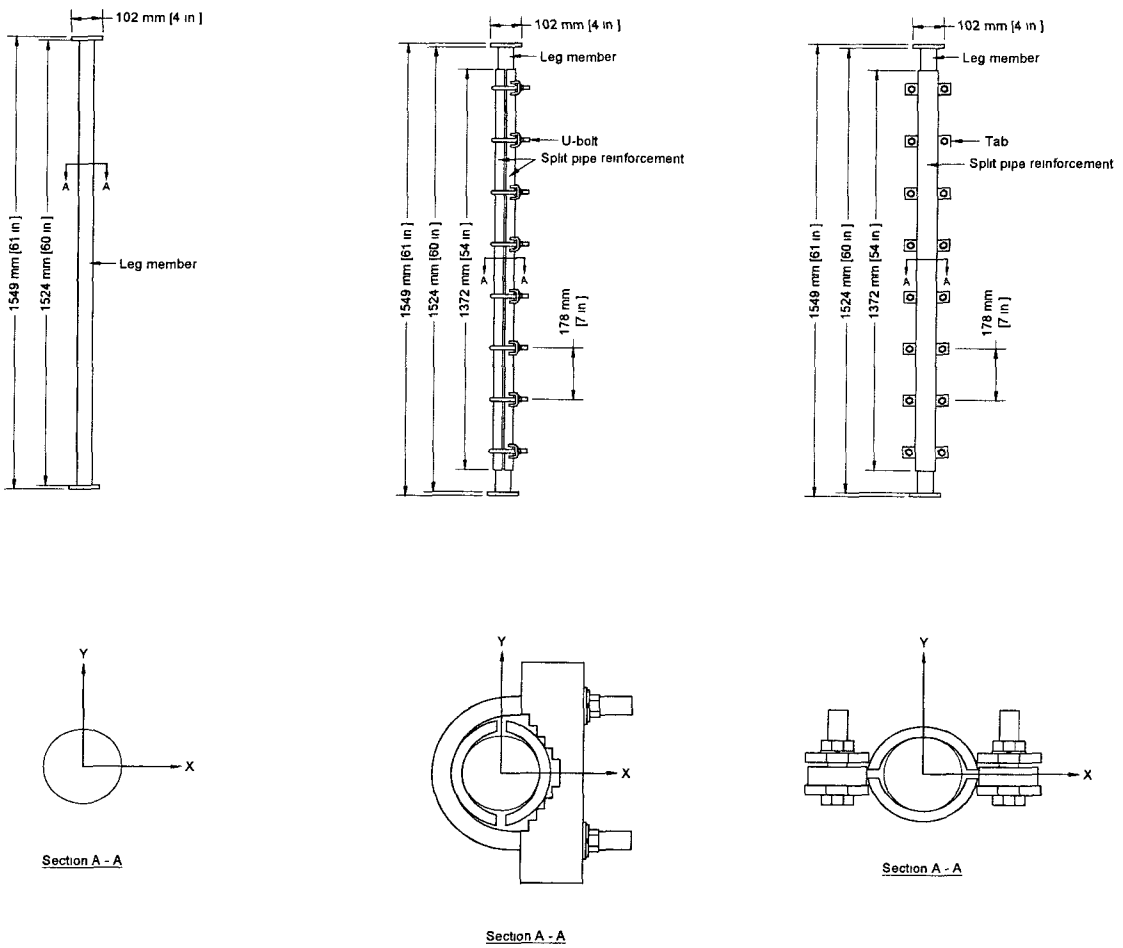

(a) RF60 (b) RF60-B1 (c) RF60-B2

Figure 6.3. Details of 1524 mm (60 in.) Long Test Specimens (RF60 Series)

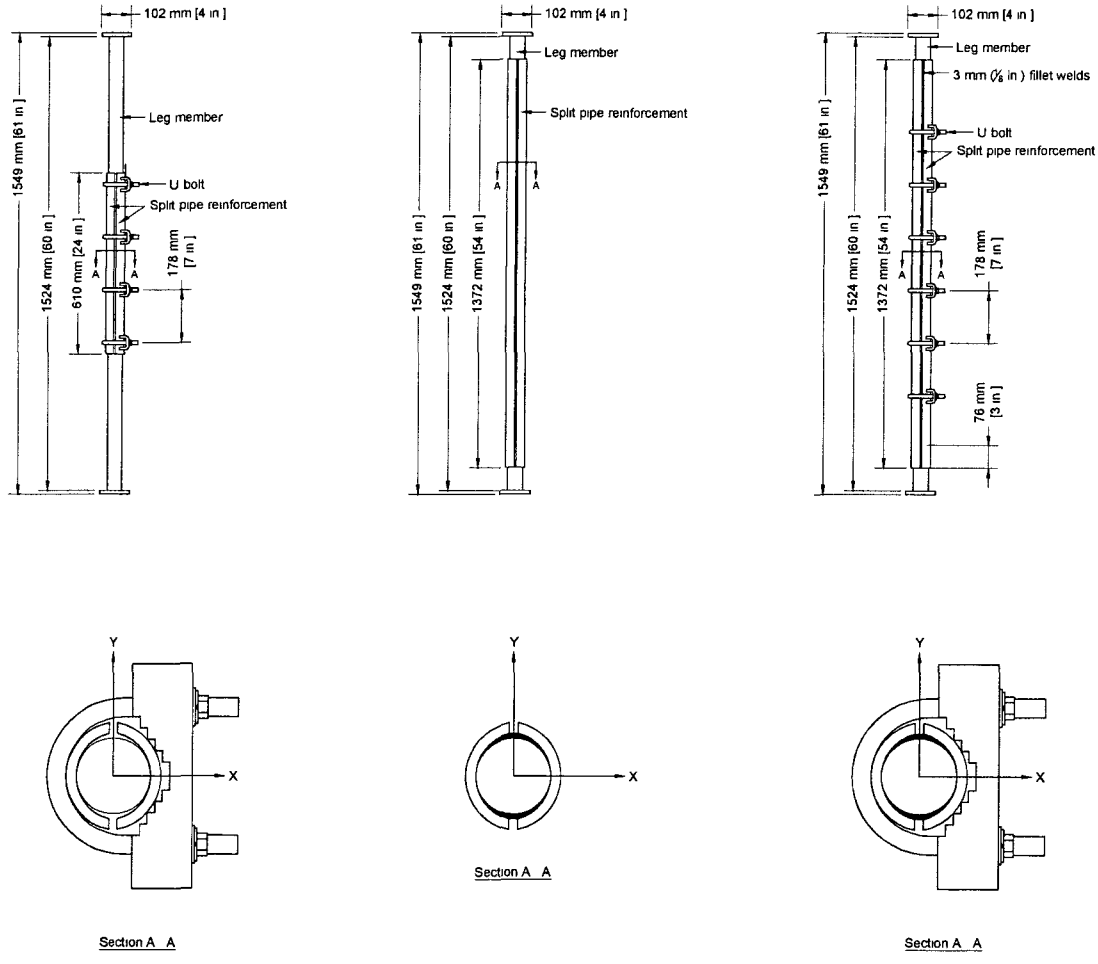

(d) RF60-B4 (e) RF60-W1 (f) RF60-W2

Figure 6.3. Details of 1524 mm (60 in.) Long Test Specimens (RF60 Series) (concluded)

Table 6.2. Details and Specimens ID of 762 mm (30 in.) Long Test Specimens

Specimen ID	Number of specimens	Split pipes strengthening member[a]				
		Length	U-bolts[b]	Tabs[b]	Stitch weld[c]	End weld[d]
RF30	27	-	-	-	-	-
RF30-B1	3	610 (24")	4 - 178 (7")	-	-	-
RF30-B2	3	610 (24")	-	4 - 178 (7")	-	-
RF30-W1	3	610 (24")	-	-	3 ($^1/_8$") 51 - 152 (2" - 6")	-
RF30-W2	3	610 (24")	2 - 178 (7")	-	-	3 ($^1/_8$") - 76 (3")

[a] Unless specified, units of length and distance are in millimetres
[b] [Number of U-bolts or tabs] - [Distance to centre-to-centre (pitch) of U-bolts or tabs]
[c] [Size of Weld]
[Length of Weld] - [Pitch of Weld]
[d] [Size of Weld] - [Pitch of Weld]

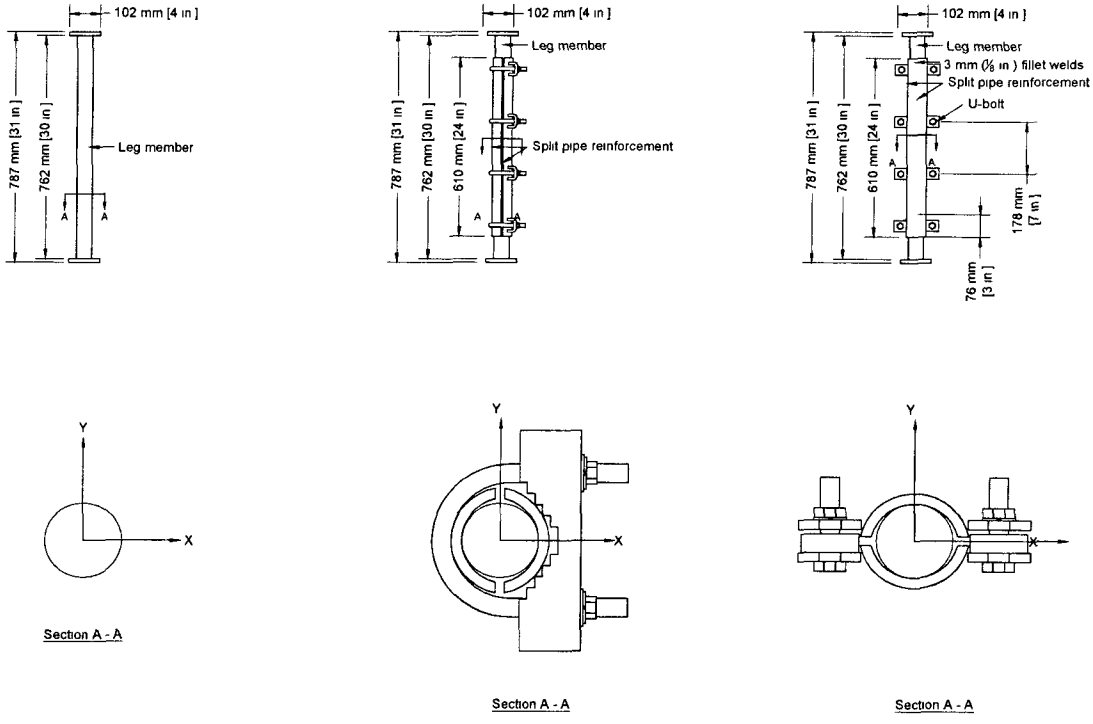

(a) RF30 (b) RF30-B1 (c) RF30-B2

Figure 6.4. Details of 762 mm (30 in.) Long Test Specimens (RF30 Series)

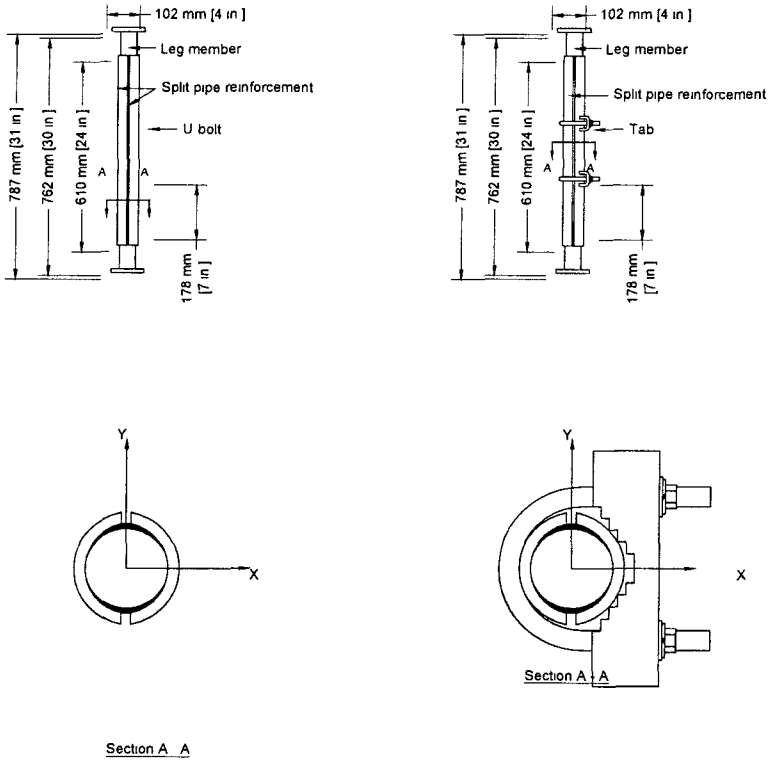

(d) RF30-W1 (e) RF30-W2

Figure 6.4. Details of 762 mm (30 in.) Long Test Specimens (RF30 Series) (concluded)

The first specimen, RF60 - 1, was placed in a bare foundation and tested directly under load cell as shown in Figure 6.5(a). The failure load was 455 kN (102 kip), 11% less than expected value. It was noticed that the load was not distributed uniformly to the specimen due to rotation at the top of the specimen. Therefore, this result was disregarded. To improve the test setup, 13 mm ($^1/_2$" in.) thick rubber pads were provided at the top and bottom of the second specimen (RF60 - 2) as shown in Figure 6.5(b). It was expected that the pads would distribute the load uniformly. However, the rubber pads allowed the specimen to slip from the original position. Due to the large eccentricity, the failure load was only 425 kN (96 kip) and this also was disregarded.

A better test setup was provided for the third specimen (RF60 - 3). At the bottom of the specimen, there were four bars with cross section of approximately 51 mm by 51 mm (2 in. by 2 in.) on four sides of the bottom plate, thus preventing the bottom plate from slipping (Figure 6.6(a)). There were also two clamps attached to the load cell to prevent slippage at the top (Figure 6.6(b)). The failure load of the third specimen was 636 kN (143 kip), as shown in Figure 6.7. This test setup yielded satisfactory result and was used for testing the other specimens.

6.3.1.2 Test details for strengthened specimens

For strengthened specimens, foil strain gages were attached to the solid round and split pipes to determine the load carried by the strengthening members. For specimen RF60-B2 - 1, the strain gage readings were done manually, thus the readings at failure could not be recorded. To record the strain gage readings at failure, a MEGADAC data acquisition system with frequency of 1 Hz was used for the remaining specimens.

Since the failure loads of welded specimens (RF60-W1 and RF60-W2) were first expected to exceed 890 kN (200 kip), another test setup with different load cell and hydraulic jack was used. The capacity of the load cell used for second test setup was 2670 kN (600 kip). At the bottom of the specimen, there were two plates bolted to the floor to prevent bottom plate from slipping.

The location of strain gages for specimens RF60-B1, RF60-B4, RF60-W1, and RF60-W2 are shown in Figure 6.8, and those for specimens RF60-B2 are shown in Figure 6.9(a) to 6.9(c). For simplicity, only imperial units are used on those figures. The strain readings versus the applied loads for every 1/10 increment of the failure load are shown in Tables 6.3 to 6.17. Photographs after failure for specimens RF60-B2 - 1, RF60-B4 - 1, and RF60-W1 - 1 are shown in Figure 6.10.

(a) RF60 - 1 (b) RF60 - 2

Figure 6.5. Specimens RF60 - 1 and RF60 - 2

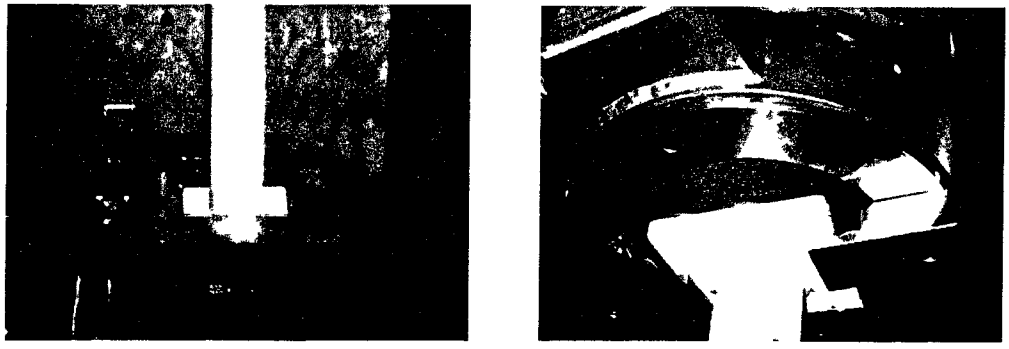

(a) Bottom (b) Top

Figure 6.6. Test Setup for Specimen RF60 - 3

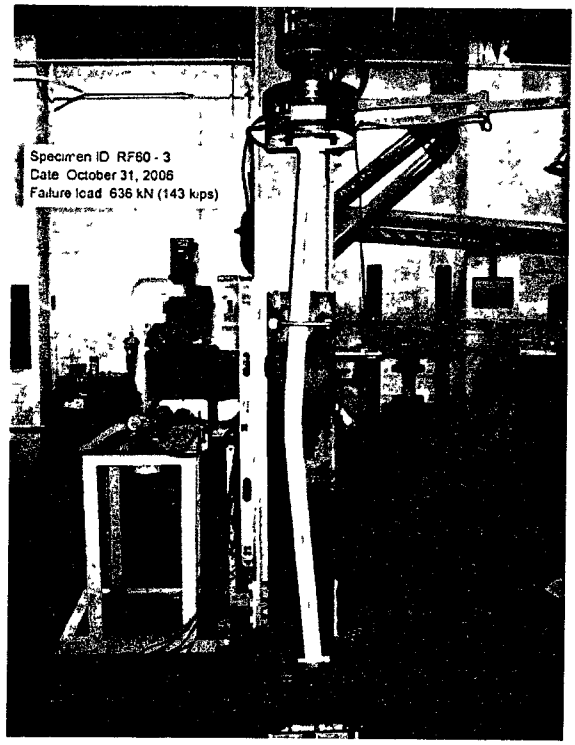

Figure 6.7. Specimen RF60 - 3

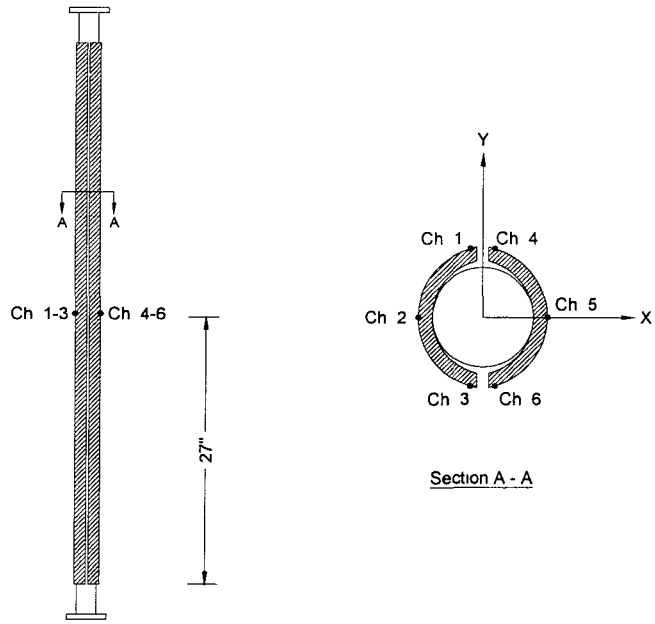

Figure 6.8. Strain Gage Locations for Specimens RF60-B1, RF60-B4, RF60-W1, and RF60-W2

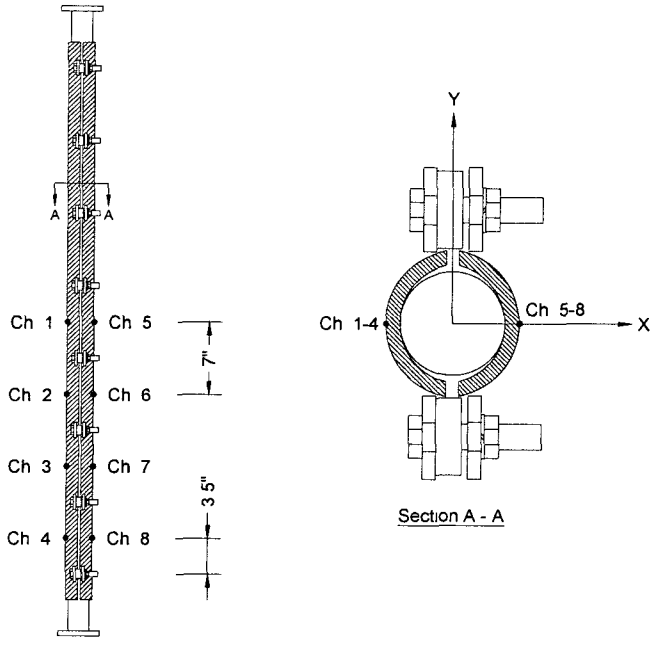

(a) RF60-B2 - 1

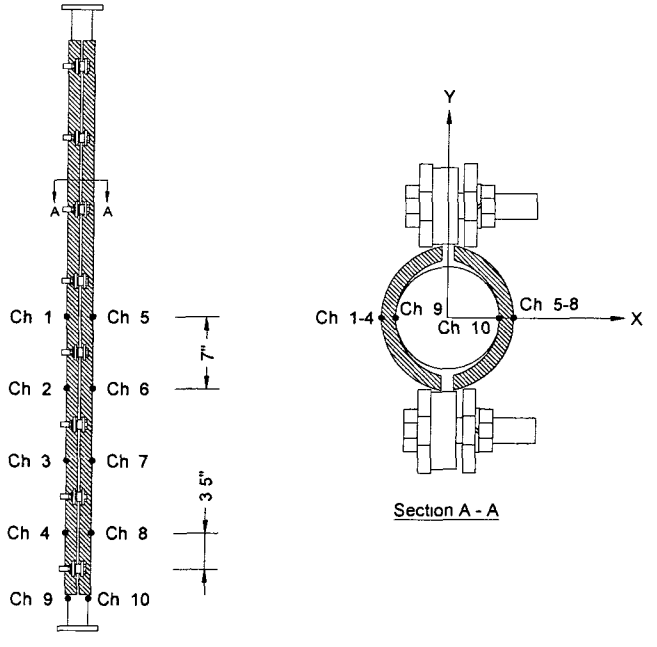

(b) RF60 - B2 - 2

Figure 6.9. Strain Gages Locations of Specimen RF60-B2

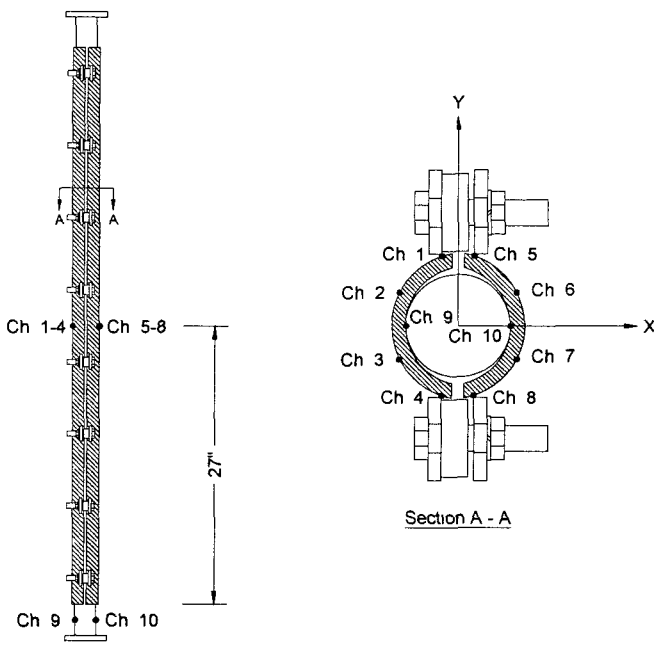

(c) RF60-B2 - 3

Figure 6.9. Strain Gages Locations of Specimen RF60-B2 (concluded)

Table 6.3. Strain Gage Readings for RF60-B1 - 1

Load	Strain (μ)							
(kN)	Ch 1	Ch 2	Ch 3	Ch 4	Ch 5	Ch 6	Ch 7	Ch 8
-71 7	-3 21	-45 8	-182	-34 5	-156	-190	-172	-156
-148	-88 3	-102	-269	-113	-254	-256	-400	-253
-223	-166	-128	-323	-177	-336	-287	-638	-335
-293	-214	-123	-353	-193	-377	-267	-866	-398
-365	-263	-106	-380	-199	-417	-237	-1120	-453
-443	-323	-73 8	-407	-204	-470	-192	-1420	-498
-515	-402	-34 5	-448	-212	-539	-135	-1710	-534
-589	-498	54 6	-487	-199	-616	-18 5	-2040	-547
-662	-625	191	-542	-177	-726	135	-2430	-504
-735	-821	653	-660	-71 4	-1010	444	-2780	-91 5

Table 6.4. Strain Gage Readings for RF60-B1 - 2

Load	Strain (μ)							
(kN)	Ch 1	Ch 2	Ch 3	Ch 4	Ch 5	Ch 6	Ch 7	Ch 8
-73 8	-110	-114	-106	-105	-105	-111	-307	-155
-144	-136	-144	-179	-148	-190	-195	-431	-365
-214	-149	-144	-259	-134	-253	-238	-527	-595
-287	-201	-140	-327	-134	-303	-233	-669	-787
-361	-222	-123	-408	-94 7	-349	-238	-861	-919
-429	-240	-95 5	-481	-49 8	-387	-233	-1060	-1000
-505	-229	-65 8	-575	22 5	-436	-261	-1280	-1100
-574	-207	-28 1	-681	105	-484	-286	-1450	-1180
-647	-205	50 6	-774	185	-551	-285	-1630	-1230
-719	-199	422	-963	401	-823	-207	-2250	-961

Table 6.5. Strain Gage Readings for RF60-B1 - 3

Load	Strain (μ)							
(kN)	Ch 1	Ch 2	Ch 3	Ch 4	Ch 5	Ch 6	Ch 7	Ch 8
-79 0	-174	-89 1	-67 4	-195	-136	-53 0	4 01	-169
-155	-229	-165	-190	-270	-244	-178	-126	-278
-234	-288	-230	-303	-326	-340	-276	-429	-393
-311	-332	-269	-388	-340	-396	-320	-781	-453
-395	-379	-307	-474	-350	-452	-362	-1100	-522
-473	-421	-336	-544	-347	-498	-388	-1310	-591
-548	-430	-331	-575	-326	-512	-379	-1510	-656
-632	-435	-318	-599	-311	-535	-377	-1720	-733
-711	-441	-291	-635	-274	-561	-368	-1890	-760
-788	-466	-24 9	-624	-184	-757	-266	-2330	-636

Table 6.9. Strain Gage Readings for RF60-B4 - 1

Load	Strain (μ)							
(kN)	Ch 1	Ch 2	Ch 3	Ch 4	Ch 5	Ch 6	Ch 7	Ch 8*
-71 1	-110	-24 9	26 5	-129	-1360	14 4	-114	-
-145	-156	-23 3	-14 5	-120	-1400	20 1	-210	-
-217	-179	-25 7	-34 5	-117	-1410	27 3	-352	-
-291	-211	-29 7	-54 6	-125	-1440	25 7	-505	-
-368	-246	-28 1	-69 0	-134	-1460	32 1	-654	-
-436	-270	-6 42	-78 7	-126	-1470	51 4	-765	-
-511	-315	24 1	-105	-112	-1480	78 6	-868	-
-581	-363	73 8	-144	-85 1	-1430	116	-930	-
-655	-434	176	-214	-13 6	-1390	189	-935	-
-730	-561	361	-297	85 1	-918	330	-567	-

* Damaged during loading and no reading was recorded

Table 6.10 Strain Gage Readings for RF60-B4 - 2

Load	Strain (μ)							
(kN)	Ch 1	Ch 2	Ch 3	Ch 4	Ch 5	Ch 6	Ch 7	Ch 8
-71 5	-128	-97 9	-24 1	-140	-102	-14 4	-103	-241
-146	-185	-112	-77 0	-164	-170	-26 5	-211	-498
-212	-211	-94 7	-126	-132	-202	-18 5	-316	-717
-283	-238	-71 4	-170	-102	-230	4 82	-441	-931
-357	-262	-39 3	-213	-65 0	-257	33 7	-570	-1140
-431	-300	-6 42	-264	-33 7	-302	61 0	-704	-1360
-499	-326	43 3	-307	25 7	-335	108	-815	-1570
-571	-376	103	-374	78 7	-392	158	-919	-1800
-642	-435	191	-458	152	-468	235	-983	-2060
-716	-596	579	-673	366	-745	482	-932	-2450

Table 6.11. Strain Gage Readings for RF60-B4 - 3

Load	Strain (μ)							
(kN)	Ch 1	Ch 2	Ch 3	Ch 4	Ch 5	Ch 6	Ch 7	Ch 8
-74 5	-79 5	4 81	7 22	-40 1	-36 1	45 7	-106	-184
-148	-120	3 21	-14 4	-53 8	-61 0	54 6	-276	-388
-220	-148	4 01	-44 1	-55 4	-85 1	57 0	-434	-573
-300	-175	11 2	-69 8	-45 7	-106	65 8	-614	-770
-378	-208	23 3	-97 9	-30 5	-136	85 1	-791	-965
-448	-233	42 5	-120	-10 4	-162	107	-937	-1150
-527	-269	59 4	-148	4 82	-199	129	-1100	-1370
-600	-305	79 5	-172	25 7	-225	165	-1240	-1560
-677	-357	116	-196	46 5	-276	216	-1360	-1800
-748	-476	241	-236	93 9	-440	347	-1420	-2080

Table 6.6. Strain Gage Readings for RF60-B2 - 1

Load	Strain (μ)							
(kN)	Ch 1	Ch 2	Ch 3	Ch 4	Ch 5	Ch 6	Ch 7	Ch 8
45 7	-34 0	-41 0	-52 0	-52 0	-50 0	0 0	-10 0	-37 0
91 4	-19 0	-10 0	-17 0	-34 0	-70 0	-15 0	15 0	38 0
137	-82 0	-69 0	-85 0	-108	-173	-112	-81 0	-37 0
183	-71 0	-50 0	-80 0	-104	-197	-132	-83 0	-36 0
229	-44 0	-30 0	-63 0	-95 0	-207	-123	-70 0	-2 00
274	-33 0	-19 0	-62 0	-96 0	-233	-139	-88 0	-10 0
320	-16 0	-7 00	-61 0	-94 0	-247	-142	-74 0	13 0
366	3 00	4 00	-53 0	-91 0	-248	-150	-72 0	17 0
411	23 0	12 0	-52 0	-96 0	-264	-158	-75 0	-3 00
457	9 00	-3 00	-76 0	-120	-304	-190	-104	-9 00
503	26 0	8 00	-74 0	-126	-310	-200	-104	-12 0
548	36 0	7 00	-85 0	-141	-330	-219	-123	-17 0
594	59 0	20 0	-83 0	-151	-353	-242	-121	-5 00
640	81 0	31 0	-84 0	-162	-383	-250	-129	8 00
686	120	65 0	-71 0	-178	-420	-277	-137	32 0
731	173	114	-41 0	-190	-485	-327	-165	39 0

Table 6.7. Strain Gage Readings for RF60-B2 - 2

Load	Strain (μ)									
(kN)	Ch 1	Ch 2	Ch 3	Ch 4	Ch 5	Ch 6	Ch 7	Ch 8	Ch 9	Ch 10
-6 18	0 0	0 0	0 0	0 0	0 0	0 0	0 0	0 0	0 0	0 0
-79 8	-34 5	-18 5	21 7	64 2	-69 8	-93 9	-104	-84 3	22 5	-455
-159	-17 7	0 802	61 0	120	-98 7	-133	-140	-125	-44 1	-809
-241	-24 9	-8 02	70 6	138	-129	-163	-160	-144	-189	-1050
-320	0 0	17 7	107	176	-139	-181	-171	-155	-314	-1300
-399	13 6	33 7	136	205	-166	-220	-204	-176	-439	-1530
-478	36 1	56 2	168	235	-182	-246	-229	-186	-579	-1760
-557	58 6	80 3	197	261	-189	-266	-250	-193	-726	-1980
-640	77 0	102	224	283	-192	-283	-275	-201	-883	-2180
-798	748	461	370	236	-632	-599	-393	-109	-1820	-1820

Table 6.8. Strain Gage Readings for RF60-B2 - 3

Load	Strain (μ)									
(kN)	Ch 1	Ch 2	Ch 3	Ch 4	Ch 5	Ch 6	Ch 7	Ch 8	Ch 9	Ch 10
-30 7	0 0	0 0	0 0	0 0	0 0	0 0	0 0	0 0	0 0	0 0
-167	-146	-76 2	-23 3	-41 7	-169	-175	-124	-40 9	-204	-386
-247	-148	-59 4	-9 63	-53 0	-180	-202	-153	-41 7	-404	-567
-332	-141	-26 5	22 5	-48 1	-179	-221	-164	-13 6	-639	-743
-414	-149	-9 63	40 1	-57 0	-185	-248	-184	-1 60	-894	-884
-495	-146	15 2	60 2	-68 2	-179	-269	-202	12 8	-1160	-1010
-576	-131	44 1	74 6	-86 7	-161	-281	-221	20 1	-1450	-1120
-662	-113	73 0	88 3	-112	-140	-292	-243	22 5	-1760	-1230
-747	-120	78 6	84 3	-141	-136	-314	-272	17 7	-2070	-1330
-826	-59 4	230	196	-169	-61 8	-362	-331	69 0	-2690	-1300

Table 6.12. Strain Gage Readings for RF60-W1 - 1

Load	Strain (μ)					
(kN)	Ch 1	Ch 2	Ch 3	Ch 4	Ch 5	Ch 6
-74 4	-93 9	-108	-96 3	-84 3	-92 3	-85 1
-146	-207	-222	-197	-180	-215	-192
-219	-335	-339	-297	-286	-342	-295
-296	-477	-469	-396	-405	-474	-396
-370	-612	-583	-484	-524	-604	-490
-437	-733	-677	-556	-633	-722	-570
-508	-860	-768	-630	-752	-854	-654
-591	-1030	-869	-699	-917	-1020	-741
-659	-1200	-955	-736	-1060	-1150	-789
-733	-1540	-1010	-625	-1400	-1300	-699

Table 6.13. Strain Gage Readings for RF60-W1 - 2

Load	Strain (μ)					
(kN)	Ch 1	Ch 2	Ch 3	Ch 4	Ch 5	Ch 6
-82 7	-154	-61 8	2 41	-161	288	-159
-157	-303	-143	-32 1	-311	212	-317
-237	-451	-245	-99 5	-454	117	-480
-313	-587	-360	-184	-580	21 3	-623
-395	-738	-494	-282	-713	-79 8	-770
-473	-879	-628	-380	-831	-177	-903
-554	-997	-795	-535	-910	-303	-1010
-631	-1020	-1030	-819	-862	-493	-1030
-712	-1010	-1280	-1160	-770	-732	-1050
-790	-89 1	-490	-1580	-546	-2040	-3680

Table 6.14. Strain Gage Readings for RF60-W1 - 3

Load	Strain (μ)					
(kN)	Ch 1	Ch 2	Ch 3	Ch 4	Ch 5	Ch 6
-72 3	-32 1	-39 3	-44 8	-93 1	-152	-124
-147	-98 7	-107	-143	-210	-331	-262
-220	-189	-193	-229	-327	-478	-368
-292	-291	-294	-309	-446	-608	-460
-366	-390	-392	-386	-557	-742	-562
-443	-512	-512	-471	-686	-872	-648
-515	-636	-633	-540	-807	-975	-712
-585	-805	-798	-587	-931	-1030	-726
-661	-1120	-1120	-586	-1090	-907	-592
-735	-2660	-1560	393	-2140	-639	545

Table 6.15. Strain Gage Readings for RF60-W2 - 1

Load	Strain (μ)					
(kN)	Ch 1	Ch 2	Ch 3	Ch 4	Ch 5	Ch 6
-68 0	-115	-69 0	-28 1	-120	-107	-53 0
-173	-302	-209	-192	-309	-726	-209
-257	-447	-316	-310	-462	-1070	-237
-334	-594	-425	-417	-608	-1100	-457
-427	-761	-551	-539	-778	-868	-583
-512	-928	-676	-654	-946	-1160	-781
-593	-1100	-789	-758	-1110	-2220	-890
-677	-1270	-893	-850	-1280	-3100	-950
-761	-1490	-990	-892	-1500	-3670	-1010
-847	-2490	-632	-89 9	-2590	-4630	-122

Table 6.16. Strain Gage Readings for RF60-W2 - 2

Load	Strain (μ)					
(kN)	Ch 1	Ch 2	Ch 3	Ch 4	Ch 5	Ch 6
-84 3	-169	-104	-38 5	-223	-74 6	-40 1
-162	-330	-252	-140	-364	-136	-136
-246	-519	-403	-254	-537	-244	-241
-333	-677	-550	-383	-687	-356	-365
-411	-810	-688	-506	-819	-458	-481
-488	-945	-831	-636	-948	-564	-605
-574	19 3	-440	-1700	-1480	1590	-709
-664	-140	-542	-1790	-1640	1260	-817
-744	-352	-631	-1820	-1850	716	-872
-826	-1350	-270	-1020	-2930	-231	20 1

Table 6.17. Strain Gage Readings for RF60-W2 - 3

Load	Strain (μ)					
(kN)	Ch 1	Ch 2	Ch 3	Ch 4	Ch 5	Ch 6
-72 9	-129	-169	-93 1	-105	-76 2	-93 1
-152	-253	-336	-217	-214	174	-205
-227	-367	-485	-348	-322	753	-325
-302	-478	-628	-482	-429	1540	-457
-374	-592	-771	-598	-537	1400	-573
-445	-723	-933	-700	-661	1530	-669
-524	-882	-1140	-806	-811	1770	-774
-598	-994	-1280	-901	-919	1580	-864
-672	-1110	-1410	-1030	-1030	1620	-984
-748	-856	-1430	-1540	-799	-97 1	-1550

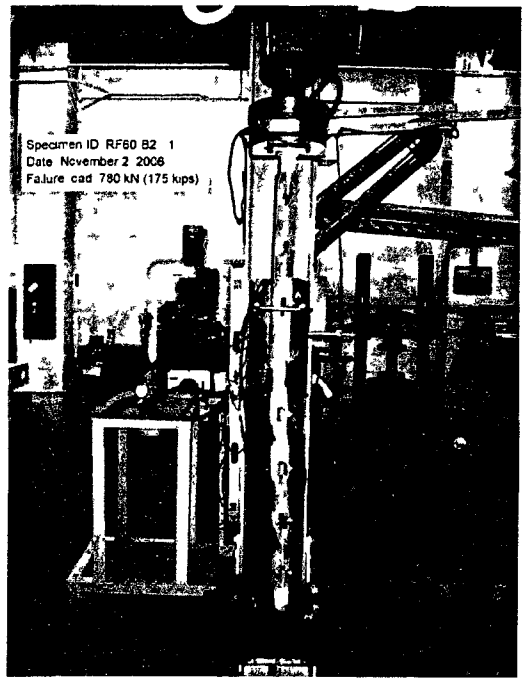

(a) RF60-B2 - 1

(b) RF60-B4 - 1

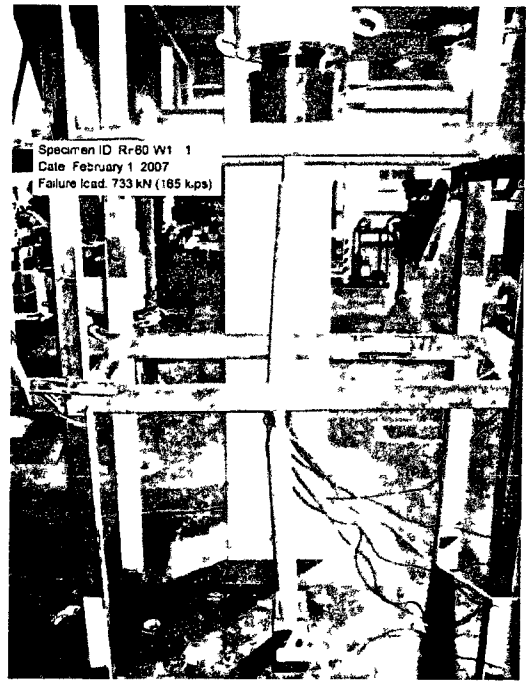

(c) RF60-W1 - 1

Figure 6.10. Photographs of Specimens after Failure (RF60 Series)

6.3.1.3 Test results

The failure loads for 1524 mm long specimens are summarized in Table 6.18. Percentage increase of compressive strength due to strengthening (relative to the average compressive strength of un-strengthened specimen) is calculated and shown in the last column of the same table.

6.3.2 Test Details and Results for 762 mm Long Test Specimens

6.3.2.1 Determination of suitable test setup

Similar with experimental investigation for 1524 mm long test specimens, tests were first conducted on un-strengthened specimens to determine a suitable test setup. Analytical calculation as per Equations [6.6] and [6.8] with effective length factor K of 0.5, Young's modulus E of 200,000 MPa (30,000 ksi), yield strength F_y of 424 MPa (61.5 ksi), and resistance factor ϕ of 1.0, results in 797 kN (179 kip) and 795 kN (178 kip), respectively.

At the bottom end of the specimen, four 50.8 x 50.8 mm (2 x 2 in.), 102 mm (4 in.) long bars were placed on four sides of the bottom plate, thus preventing the bottom plate from slipping. The specimens were tested using a 2670 kN (600 kip) load cell as shown in Figure 6.11. The failure loads for the first two specimens, RF30 - 1 and RF30 - 2, were 672 and 712 kN (151 and 160 kip), respectively. However, it was noticed that the flange of supporting beam located at the bottom of the specimen was bent. Therefore, these results were disregarded and adequate stiffeners were later provided to the beam flange. The failure loads of 27 un-strengthened specimens are shown in Table 6.19.

6.3.2.2 Test details for strengthened specimens

Six strain gages were attached to the split pipes to determine the load carried by the strengthening members. The location of strain gages for each specimen is shown in Figure 6.12. The applied load and strain gage readings are shown in Tables 6.20 to 6.31.

6.3.2.3 Test results

The failure loads of 762 mm long specimens, which are short columns (since 1524 mm long specimens are short columns as discussed in Section 6.3.1.3), and percentage increase of strength due to strengthening are shown in Table 6.32. The strain gages readings were used to

Table 6.18. Summary of Failure Loads of 1524 mm Long Test Specimens (RF60 Series)

Specimen type	Specimen ID	Failure load (kN)	*Load on split pipes (kN)	Average failure load (kN)	Average load on split pipes (kN)	Increase in compressive strength
RF60	RF60 - 1	455***	-	636	-	-
	RF60 - 2	425***				
	RF60 - 3	636				
RF60-B1	RF60-B1 - 1	735	135	747	121	18%
	RF60-B1 - 2	719	129			
	RF60-B1 - 3	788	101			
RF60-B2	RF60-B2 - 1	780	-	801	66	26%
	RF60-B2 - 2	798	85			
	RF60-B2 - 3	826	48			
RF60-B4	RF60-B4 - 1	730	123	731	95	15%
	RF60-B4 - 2	716	100			
	RF60-B4 - 3	748	64			
RF60-W1	RF60-W1 - 1	733	205	752	302	18%
	RF60-W1 - 2	790	350			
	RF60-W1 - 3	735	350			
RF60-W2	RF60-W2 - 1	847	350	807	302	27%
	RF60-W2 - 2	826	350			
	RF60-W2 - 3	748	207			

Note * Minimum value of (i) maximum load based on strain reading and (ii) maximum load based on normal stress

** Unsatisfactory test setup, hence these are not included in the calculation of average failure load

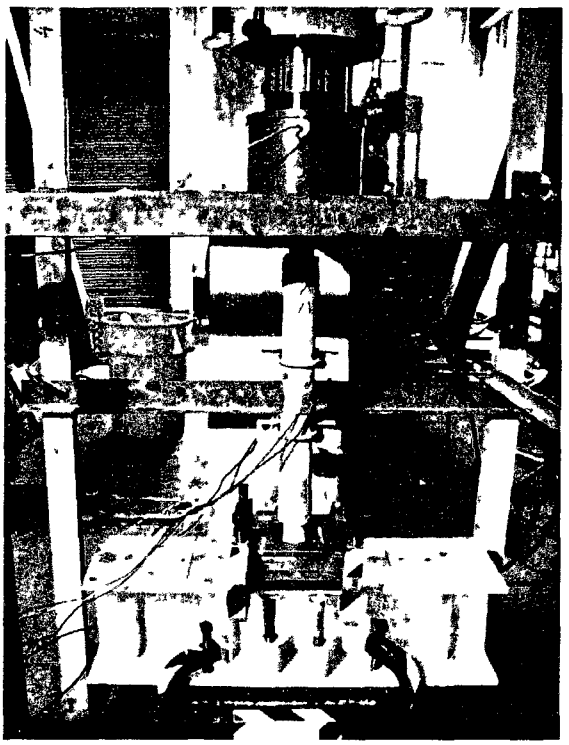

Figure 6.11. Test Setup for 762 mm Long Test Specimens (RF30 Series)

Table 6.19. Failure Loads of 762 mm Long Un-strengthened Test Specimens (RF30 Series)

Specimen ID	Failure load (kN)	Specimen ID	Failure load (kN)	Specimen ID	Failure load (kN)
RF30 - 1	673*	RF30 - 10	898	RF30 - 19	875
RF30 - 2	713*	RF30 - 11	834	RF30 - 20	871
RF30 - 3	838	RF30 - 12	893	RF30 - 21	840
RF30 - 4	885	RF30 - 13	881	RF30 - 22	860
RF30 - 5	824	RF30 - 14	854	RF30 - 23	872
RF30 - 6	854	RF30 - 15	896	RF30 - 24	863
RF30 - 7	839	RF30 - 16	887	RF30 - 25	919
RF30 - 8	851	RF30 - 17	863	RF30 - 26	915
RF30 - 9	874	RF30 - 18	918	RF30 - 27	877
Average failure load = 871 kN					

Note *Unsatisfactory test setup, hence these are not included in the calculation of average failure load

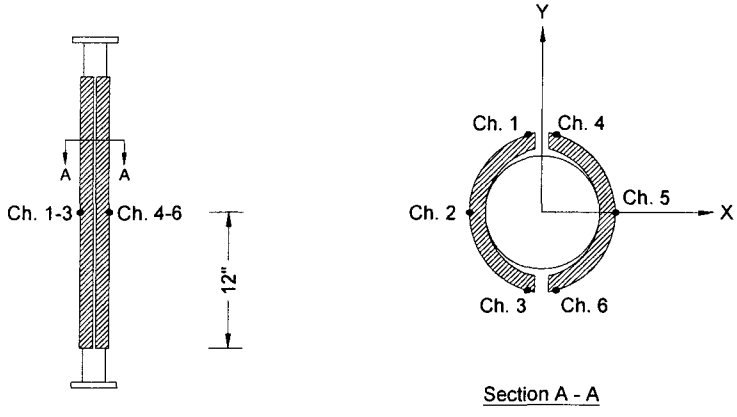

Figure 6.12. Strain Gage Locations for 762 mm Long Test Specimens (RF30 Series)

Table 6.20. Strain Gage Readings for RF30-B1 - 1

Load	Strain (μ)					
(kN)	Ch 1	Ch 2	Ch 3	Ch 4	Ch 5	Ch 6
-79 8	-8 83	-	-114	-34 5	-152	-140
-192	-115	-	-193	-69 8	-244	-125
-286	-142	-	-224	-85 1	-271	-121
-384	-133	-	-238	-96 3	-276	-136
-480	-112	-	-258	-90 7	-274	-163
-573	-85 1	-	-277	-77 0	-260	-193
-668	-43 3	-	-295	-64 2	-246	-240
-766	-9 63	-	-323	-40 1	-236	-281
-858	16 8	-	-328	-39 3	-226	-318
-956	127	-	-242	-173	-85 1	-394

* Damaged during loading and no reading was recorded

Table 6.21. Strain Gage Readings for RF30-B1 - 2

Load	Strain (μ)					
(kN)	Ch 1	Ch 2	Ch 3	Ch 4	Ch 5	Ch 6
-97 6	-83 5	-130	-85 9	-373	-72 2	-174
-183	-97 9	-181	-75 4	-417	-79 5	-212
-277	-89 1	-206	-91 5	-434	-97 9	-265
-365	-88 3	-203	-100	-431	-111	-271
-459	-104	-195	-99 5	-433	-113	-263
-552	-132	-184	-89 1	-448	-116	-242
-642	-188	-158	-68 2	-473	-130	-181
-735	-229	-145	-48 1	-490	-133	-140
-825	-244	-140	-45 7	-497	-134	-133
-918	194	-478	-112	-469	81 1	-682

Table 6.22. Strain Gage Readings for RF30-B1 - 3

Load	Strain (μ)					
(kN)	Ch 1	Ch 2	Ch 3	Ch 4	Ch 5	Ch 6
-70 8	-28 9	32 1	-83 5	-45 7	-104	-104
-173	-162	38 5	-116	-83 5	-200	-67 4
-260	-238	37 7	-81 9	-145	-227	-30 5
-348	-249	27 3	-53 8	-188	-226	-36 9
-434	-240	-8 83	-26 5	-224	-205	-53 8
-522	-213	-107	18 5	-273	-156	-78 7
-607	-177	-185	82 7	-342	-95 5	-114
-695	-160	-233	129	-397	-73 0	-144
-782	-148	-226	107	-376	-92 3	-165
-869	64 2	-396	14 4	-291	217	-307

Table 6.23. Strain Gage Readings for RF30-B2 - 1

Load	Strain (μ)					
(kN)	Ch 1	Ch 2	Ch 3	Ch 4	Ch 5	Ch 6
-88 7	0 000	19 4	-4 85	-18 6	-36 4	-17 0
-171	-1 62	21 8	-3 24	-18 6	-36 4	-14 6
-260	0 808	16 2	-5 66	-13 7	-28 3	-15 4
-345	0 808	13 7	-8 09	-11 3	-23 4	-14 6
-435	-0 807	7 28	-9 70	-6 47	-12 1	-12 1
-523	-4 04	-4 04	-12 9	-1 62	0 807	-8 90
-603	-6 47	-11 3	-15 4	0 807	8 89	-5 67
-696	-7 27	-14 5	-17 0	1 61	13 7	-4 04
-780	-7 27	-12 1	-17 0	3 24	11 3	-7 28
-866	2770	523	-2740	3340	-230	-2550

Table 6.24. Strain Gage Readings for RF30-B2 - 2

Load	Strain (μ)					
(kN)	Ch 1	Ch 2	Ch 3	Ch 4	Ch 5	Ch 6
-663	-6 41	-50 4	-25 6	16 0	-8 00	15 2
-730	-3 21	-60 8	-32 0	23 2	4 00	13 6
-824	-5 61	-75 3	-36 8	27 2	16 8	14 4
-857	-22 4	-46 4	-10 4	0 800	7 21	21 6
-871	-3 21	-11 2	-32 0	7 20	-14 4	-18 4
-865	-12 8	-21 6	-16 0	0 800	-10 4	2 40
-826	141	-24 0	-152	184	-114	-122
-840	563	-106	-592	616	-19 2	-558
-857	926	-99 3	-1050	963	135	-1060
-881	1510	-1550	-31 2	-161	2130	-2490

Table 6.25. Strain Gage Readings for RF30-B2 - 3

Load	Strain (μ)					
(kN)	Ch 1	Ch 2	Ch 3	Ch 4	Ch 5	Ch 6
-115	-105	-77 8	29 9	-105	-1 57	36 3
-181	-95 1	-73 9	27 5	-106	-3 93	35 5
-276	-85 6	-69 1	10 2	-94 3	-9 43	18 2
-371	-61 3	-62 9	-15 7	-72 3	-17 3	-8 69
-464	-51 1	-80 1	-32 2	-58 9	2 35	-19 7
-549	-53 4	-98 2	-30 6	-63 6	21 2	-15 8
-644	-89 6	-125	7 86	-108	49 5	28 4
-740	-116	-140	38 5	-147	64 4	62 4
-831	-121	-144	44 8	-157	73 1	67 1
-921	-1510	1600	-1040	732	-1340	700

Table 6.26. Strain Gage Readings for RF30-W1 - 1

Load	Strain (μ)					
(kN)	Ch 1	Ch 2	Ch 3	Ch 4	Ch 5	Ch 6
-119	-10 4	-140	-184	-65 8	-184	-184
-239	-136	-317	-360	-193	-376	-357
-357	-278	-494	-520	-342	-589	-524
-472	-430	-640	-653	-504	-806	-676
-591	-587	-792	-785	-682	-1030	-823
-710	-754	-949	-902	-861	-1240	-954
-827	-1040	-1820	-1020	-1080	-1300	-945
-944	-1160	-2280	-1170	-1210	-1460	-1090
-1064	-1410	-2870	-1260	-1450	-2280	-1140
-1181	-1810	-2960	-839	-2320	-7620	-1170

Table 6.27. Strain Gage Readings for RF30-W1 - 2

Load	Strain (μ)					
(kN)	Ch 1	Ch 2	Ch 3	Ch 4	Ch 5	Ch 6
-115	69 8	-85 1	-254	64 2	-204	-299
-232	-72 2	-250	-416	-88 3	-400	-472
-345	-222	-432	-579	-235	-573	-628
-460	-390	-636	-748	-388	-740	-780
-580	-593	-880	-920	-555	-880	-900
-692	-795	-1800	-1100	-702	-1000	-1010
-810	-1010	-3150	-1270	-875	-1190	-1140
-926	-1270	-4300	-1370	-1100	-1630	-1240
-1041	-1520	-5290	-1610	-1200	-2010	-1410
-1156	-1940	-7070	-2250	-1130	-1990	-1720

Table 6.28. Strain Gage Readings for RF30-W1 - 3

Load	Strain (μ)					
(kN)	Ch 1	Ch 2	Ch 3	Ch 4	Ch 5	Ch 6
-169	-97 1	-183	-198	-69 8	-117	-177
-287	-257	-389	-363	-204	-274	-333
-403	-426	-581	-506	-358	-453	-482
-515	-575	-742	-628	-510	-640	-632
-635	-765	-876	-722	-722	-880	-770
-747	-937	-1390	-827	-894	-1070	-898
-863	-1100	-1780	-961	-1050	-1230	-1030
-977	-1400	-2150	-1020	-1260	-1320	-1040
-1092	-1630	-2710	-1170	-1400	-1480	-1130
-1208	-2750	-7430	-2260	-1190	-822	-848

Table 6.29. Strain Gage Readings for RF30-W2 - 1

Load	Strain (μ)					
(kN)	Ch 1	Ch 2	Ch 3	Ch 4	Ch 5	Ch 6
-355	-153	-183	-143	-141	-111	-126
-450	-295	-314	-274	-295	-268	-269
-545	-432	-429	-402	-456	-461	-427
-644	-562	-504	-530	-628	-693	-596
-739	-681	-543	-645	-797	-938	-764
-837	-802	-562	-762	-978	-1220	-944
-933	-969	-648	-900	-1140	-1390	-1080
-1028	-1120	-652	-1020	-1320	-1630	-1240
-1125	-1300	-648	-1110	-1550	-1720	-1430
-1222	-1850	77 0	-1090	-2290	-1760	-1850

Table 6.30. Strain Gage Readings for RF30-W2 - 2

Load	Strain (μ)					
(kN)	Ch 1	Ch 2	Ch 3	Ch 4	Ch 5	Ch 6
-122	-280	-61 0	4 82	-286	-232	-30 5
-244	-500	-274	-172	-441	-382	-177
-369	-678	-516	-402	-555	-517	-369
-488	-808	-741	-648	-635	-657	-585
-614	-966	-950	-882	-743	-820	-796
-740	-1160	-1130	-1070	-882	-993	-974
-861	-1400	-1240	-1200	-1060	-1190	-1110
-984	-1650	-1350	-1360	-1200	-1300	-1270
-1105	-1920	-1450	-1550	-1340	-1380	-1440
-1228	-2700	-1490	-2000	-1640	-1080	-1550

Table 6.31. Strain Gage Readings for RF30-W2 - 3

Load	Strain (μ)					
(kN)	Ch 1	Ch 2	Ch 3	Ch 4	Ch 5	Ch 6
-118	-11 2	-144	-249	-28 9	-180	-264
-236	-152	-315	-434	-178	-372	-462
-353	-343	-456	-575	-374	-584	-619
-470	-528	-600	-724	-560	-787	-777
-589	-718	-771	-886	-738	-969	-941
-709	-897	-941	-1060	-909	-1140	-1120
-825	-1100	-1110	-1210	-1090	-1250	-1260
-940	-1400	-1270	-1280	-1340	-1300	-1330
-1059	-1570	-1310	-1450	-1560	-1400	-1540
-1176	-1830	-865	-1650	-1980	-1540	-1950

Table 6.32. Summary of Failure Loads of 762 mm Long Test Specimens (RF30 Series)

Specimen type	Specimen ID	Failure load (kN)	*Load on split pipes (kN)	Average failure load (kN)	Average load on split pipes (kN)	Increase in compressive strength
RF30	RF30 - 1 to RF30 - 27	Refer to Table 6 4	-	871	-	-
RF30-B1	RF30-B1 - 1	956	52 5	914	65 5	4 7%
	RF30-B1 - 2	918	91 2			
	RF30-B1 - 3	869	52 9			
RF30-B2	RF30-B2 - 1	866	350	889	216	2 0%
	RF30-B2 - 2	881	333			
	RF30-B2 - 3	921	201			
RF30-W1	RF30-W1 - 1	1181	350	1182	350	34%
	RF30-W1 - 2	1156	350			
	RF30-W1 - 3	1208	350			
RF30-W2	RF30-W2 - 1	1222	306	1209	307	37%
	RF30-W2 - 2	1228	350			
	RF30-W2 - 3	1176	265			

Note * Minimum value of (i) maximum load based on strain reading and (ii) maximum load based on normal stress

determine percentage of load carried out by strengthening members, which are also shown in the same table.

6.3.3 Conclusions

6.3.3.1 Conclusions on Experimental Results on 1524 mm Long Test Specimens (RF60 Series)

Based on test results shown in Table 6.32, the following conclusions can be drawn:

1. The critical slenderness ratio, from Equation [6.4] and using F_y of 414 MPa, was calculated to be 99. The actual slenderness ratio, KL/r, is 60, thus categorizing 1524 mm specimens as short columns. From Johnson column formula (Equation [6.5]) and F_y of 414 MPa, F_{cr} was found to be 338 MPa. The critical column load is 686 kN, close with the failure loads of strengthened specimens listed in Table 6.18.
2. The percentage increase of compressive strength of solid round strengthened with 1372 mm long split pipes (RF60-B1) was 18%, and those of solid round strengthened with 610 mm long split pipes (RF60-B4) was 15%. Although it will significantly reduce the structure's weight and fabrication costs by using shorter strengthening members, the critical area of buckling (which depends on the initial imperfection of the leg member) is not always in the middle of the leg member (as shown in Figure 6.10(b)), which makes the location of the strengthening members not easy to determine. Therefore it is recommended to use strengthening members along the entire leg member.
3. Comparing RF60-B1 and RF60-W2, it is obvious that end welds increase the strength of leg member. The percentage increase in strength of specimen strengthened with split pipes using U-bolts alone (RF60-B1) was 18%, and that strengthened with split pipes using U-bolts and end welds (RF60-W2) was 27%.
4. The strength increase for specimen strengthened with 1372 mm long split pipes using stitch welds (RF60-W1) was only 18%, the same as that using U-bolts (RF60-B1). Comparing RF60-B2 (strengthening members connected using tabs) with RF60-W2 (strengthening members connected using U-bolts and end welds), both results in approximately 26% increase in strength. It is recommended to connect the strengthening members using U-bolts or tabs since welding is expensive and not easily feasible on higher elevation.

6.3.3.2 Conclusions on Experimental Results on 762 mm Long Test Specimens (RF30 Series)

Based on test results shown in Tables 6.4 and 6.5, the following conclusions can be drawn:

1. The percentage increase of compressive strength of solid round strengthened with split pipes using U-bolts and tabs (RF60-B1 and RF60-B2) was 5% and 2%, respectively. There is only slight benefit of strengthening. From Johnson column formula, F_{cr} was found to be 395 MPa and the critical load is 801 kN. Since the average failure loads of RF60-B1 and RF60-B2 were 916 and 890 kN, respectively, it can be concluded that those specimens failed due to inelastic buckling since they are very close with 900 kN critical load. For short specimens failed by inelastic buckling, there is no advantage of connecting the strengthening members with U-bolts or tabs.
2. Comparing the results of RF60-B1 and RF60-B2 with those of specimens strengthened with split pipes using stitch welds (RF60-W1) and using U-bolts and end welds (RF60-W2), which are 34% and 37%, respectively, it is obvious that connecting the strengthening members using welds provides more favourable results. By using welds, the solid round and the strengthening members resisted the load together as a composite member. Therefore, for short specimens, it is recommended that strengthening members be connected to the main member using welds.

6.4 FINITE ELEMENT ANALYSIS

Since experimental investigation was not always feasible to do due to non-availability of space and/or test equipment, finite element models are required to determine the compressive strength of larger size solid round steel members strengthened with split pipes. Finite element models were built to simulate the experimental investigation discussed in the previous section. The results from finite element analysis would be compared with those of experimental investigation to determine if the finite element models are suitable and can be used to determine compressive strength of any size of solid round steel members strengthened with split pipes.

6.4.1 Finite Element Modelling using ABAQUS

The test specimens discussed in previous section were modelled using ABAQUS version 6.7 [Simulia 2007]. The 1524 mm long solid round test specimens were modelled using 11520 C3D6 (6-node linear triangular prism) as shown in Figure 6.13. Half of this number of elements was used for the 762 mm long test specimens. Each 1372 mm long split pipe was modelled using 4320 C3D8 element, as shown in Figure 6.14, and the number of elements of each 610 mm split pipe is 1920. Both C3D6 and C3D8 are solid (continuum) elements with first-order (linear) interpolation which are used for essentially constant strain elements. Higher order elements are generally for elliptic problems (the governing partial differential equations are elliptic in character, such as elasticity, heat conduction, acoustics, in which smoothness of the solution is assured).

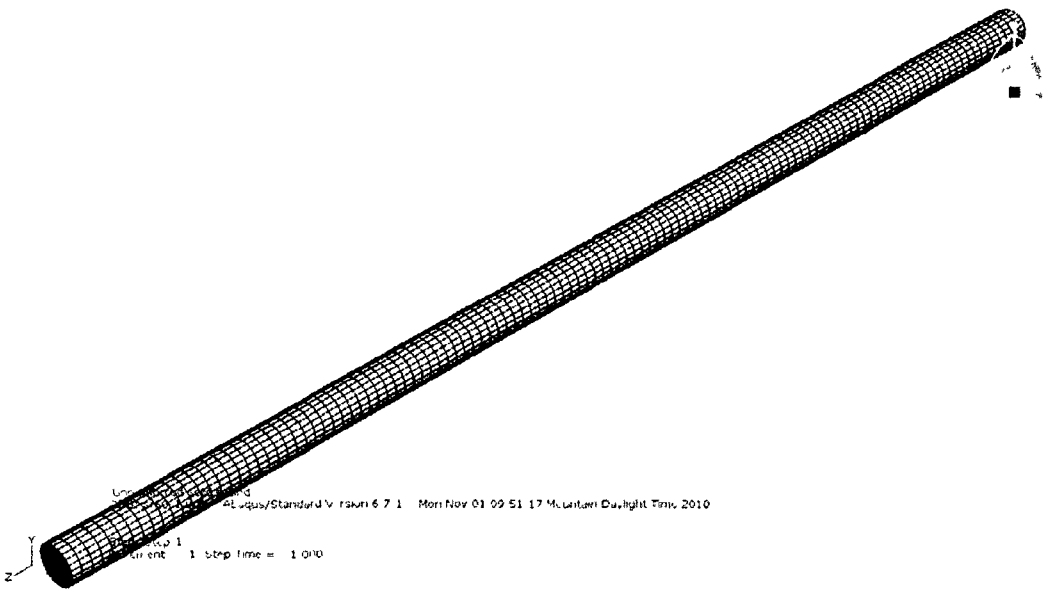

(a) 3-D view

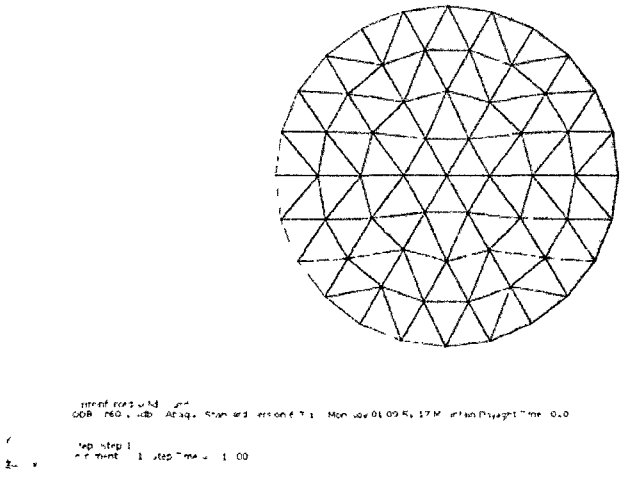

(b) Cross-section view

Figure 6.13. Finite Element Models of 1524 mm Long Un-strengthened Test Specimen

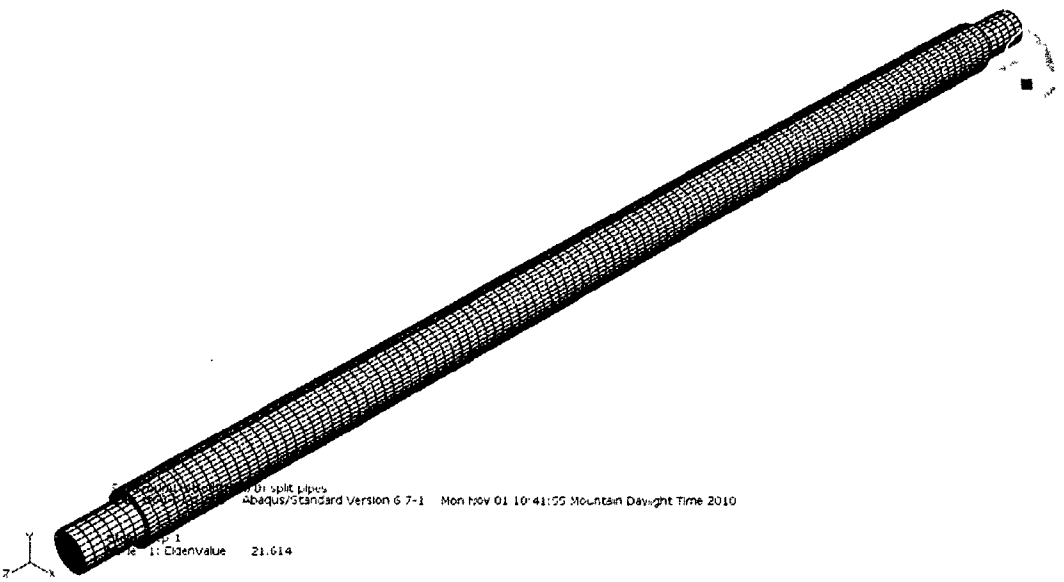

(a) 3-D view

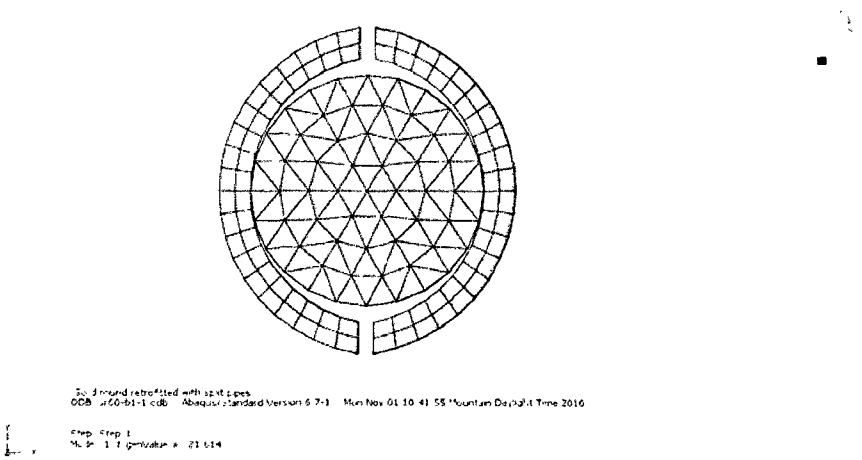

(b) Cross-section view

Figure 6.14. Finite Element Models of 1524 mm Long Strengthened Test Specimen

Surfaces were defined on the contact area between the solid round and split pipes A small sliding interaction was used to simulate the contact pair simulation between those surfaces Small sliding, which assumes that although two bodies may undergo large motions, allows relatively little sliding of one surface along the other [Simulia 2007] With this formulation the contacting surfaces can undergo only relatively small sliding relative to each other, but arbitrary rotation of the bodies is permitted This interaction were chosen since there were intermittent connections between the leg member and the strengthening member to prevent large sliding but still allowing independent rotation of each member A friction coefficient of 0 025 was defined in the sliding interaction A zero friction coefficient means that no shear forces will develop and the contact surfaces are free to slide To take into account imperfection on the surfaces of leg members and strengthening member preventing the load transfer, it was assumed that only very small shear force will develop and a very small number was chosen to model friction between the two surfaces

For boundary conditions, the degrees of freedom 1 to 3 (u_x, u_y, and u_z) at the bottom elements of the model were constrained For the top elements of the model, the degrees of freedom 1 and 2 (u_x and u_y) were constrained

The material properties used are based on the mill test certificates accompanying the test specimens The yield stress and tensile stress of the solid round are 414 MPa and 563 MPa, respectively For the split pipe, the yield stress and tensile stress are 550 MPa and 613 MPa, respectively The Young's modulus of elasticity is 200 GPa and the Poisson's ratio is for 0 3

In practice, strengthening members are usually designed with the assumption that connections have more capacity than those of the members, which means no failure of the connections This no connection failure assumption was also supported by experimental investigation discussed on the previous section For strengthening members, the TIE multi-point connections in *MPC option were defined between connected nodes This type of multi-point constraint makes all degrees of freedom equal between the two nodes, and was used for modelling both the U-bolt and weld connections

6.4.2 Analysis Procedures

6.4.2.1 Eigenvalue buckling prediction [Simulia 2007]

Eigenvalue buckling analysis is generally used to estimate the critical (bifurcation) load of "stiff" structures ABAQUS has the capability of estimating the elastic buckling by eigenvalue

extraction This estimation is typically useful for "stiff" structures, where the pre-buckling response is almost linear The buckling load estimation is obtained as a multiplier of the pattern of perturbation loads, which are added to a set of base state loads The base state of the structure may have resulted from any type of response history, including non-linear effects It represents the initial state to which the perturbation loads are added The response to the perturbation loads must be elastic up to the estimated buckling load values for the eigenvalue to be realistic

In simple cases, linear eigenvalue analysis may be sufficient for design evaluation But if there is concern about material non-linearity, geometric non-linearity prior to buckling, or unstable post-buckling response, a load-deflection analysis (e g , modified static Riks method) must be performed to investigate the problem further

6.4.2.2 Modified Riks algorithm [Simulia 2007]

It is necessary to obtain non-linear static equilibrium solutions for unstable problems, where the load-displacement response can exhibit a behaviour similar to the behaviour sketched in Figure 6 15(a), i e , during periods of response, the load and/or the displacement may decrease as the solution evolves The modified Riks method is an algorithm that allows effective solution of such cases It is assumed that the loading is proportional (Figure 6 15(b)), i e , all load magnitudes vary with a single scalar parameter It is also assumed that the response is reasonably smooth, i e , sudden bifurcations do not occur

The essence of the method is that the solution is viewed as the discovery of a single equilibrium path in a space defined by the nodal variables and the loading parameter Development of the solution requires that the path is traversed as far as required The basic algorithm remains the Newton method Therefore, there will be a finite radius of convergence at any time Further, many of the materials (and possibly loadings) of interest will have path-dependent response For these reasons, it is essential to limit the increment size

In the modified Riks algorithm, the increment size is limited by moving a given distance (determined by the standard, convergence rate-dependent, automatic increment algorithm for static case) along the tangent line to the current solution point and then searching for equilibrium in the plane that passes through the point thus obtained and that is orthogonal to the same tangent line Here the geometry referred to is the space of displacements, rotations, and the load parameter mentioned above

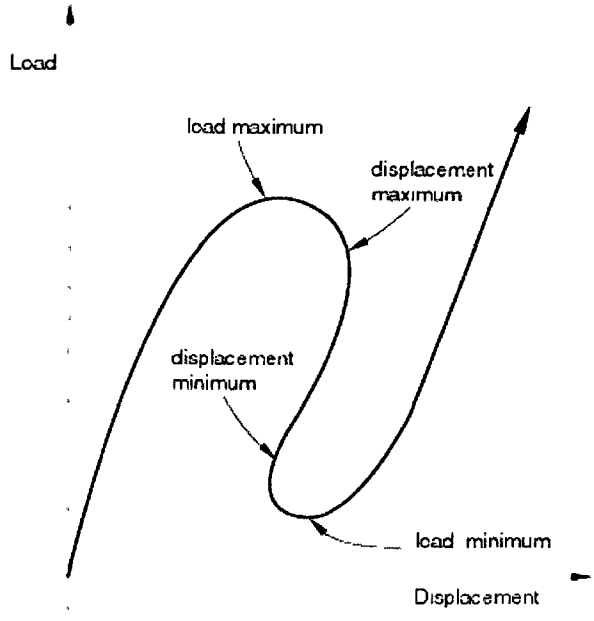

(a) Typical Unstable Static Response

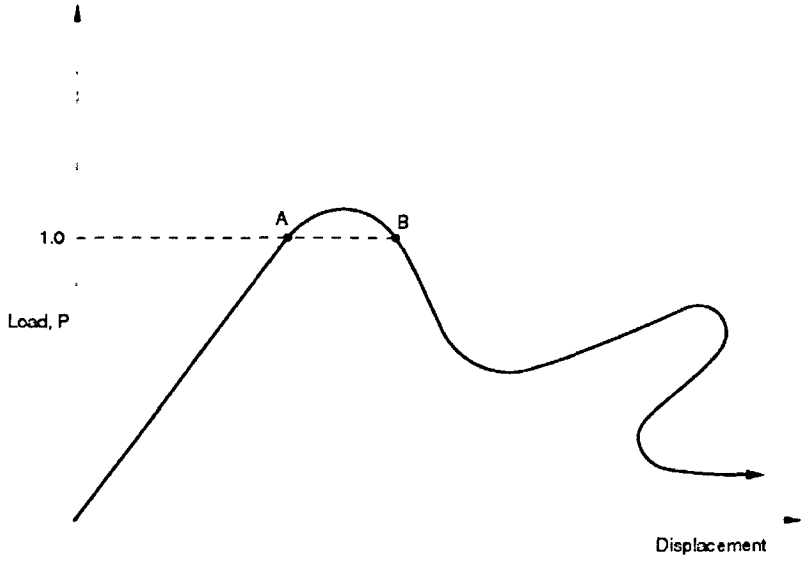

(b) Proportional Loading with Unstable Response

Figure 6.15. Load-Displacement Curves of Unstable Response [Simulia 2007]

ABAQUS defines P^N (N = 1, 2, ... are the degrees of freedom of the model) as the loading pattern, and λ as the load magnitude parameter. At any time, the actual load state is λP^N, and u^N be the displacements at that time. The solution space is scaled to make the dimensions approximately the same magnitude on each axis. In ABAQUS this is done by measuring the maximum absolute value of all displacement variables in the initial (linear) iteration.

The Riks method uses the load magnitude as an additional unknown, it solves simultaneously for loads and displacements. Another quantity, i.e., "arc length", is used to measure the progress of the solution along the static equilibrium path in load-displacement space. This approach provides solutions regardless of whether the response is stable or unstable. This method, which is available in ABAQUS, is generally used to predict unstable, geometrically non-linear collapse of a structure. This method can also include non-linear materials and boundary conditions and often follows an eigenvalue buckling analysis to provide complete information about a structure's collapse. It can be used to solve post-buckling problems, both with stable and unstable post-buckling behaviour.

However, the exact post-buckling response cannot be analyzed directly due to the discontinuous response at the point of buckling. To analyze a post-buckling problem, it must be turned into a problem with continuous response instead of bifurcation. This effect can be accomplished by introducing an initial imperfection into a "perfect" geometry so that there is some response in the buckling mode before the critical load is reached. The imperfections are usually introduced by perturbations in the geometry, although perturbations in loads or boundary conditions can also be used to introduce initial imperfections.

Unless the precise shape of an imperfection is known, an imperfection consisting of multiple superimposed buckling modes must be introduced. In this way, the Riks method can be used to perform post-buckling analyses of structures that show linear behaviour prior to (bifurcation) buckling. Imperfections based on linear buckling modes can also be useful for the analysis of structures that behave inelastically prior to reaching peak load.

6.4.3 Analysis Steps

For each model, there were two analyses, one step in each analysis. The first analysis performed an eigenvalue buckling analysis on the member. This facilitated the introduction of geometric imperfection, i.e., initial out-of-straightness, to the member. The fundamental buckling modes of the un-strengthened and strengthened specimens are shown in Figure 6.16.

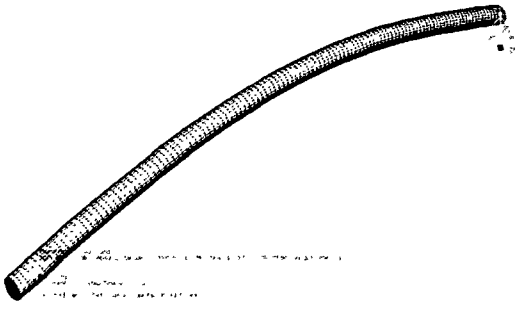

(a) Un-strengthened model – 1524 mm

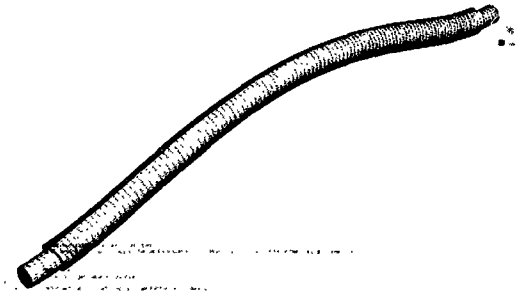

(b) Strengthened model – 1524 mm

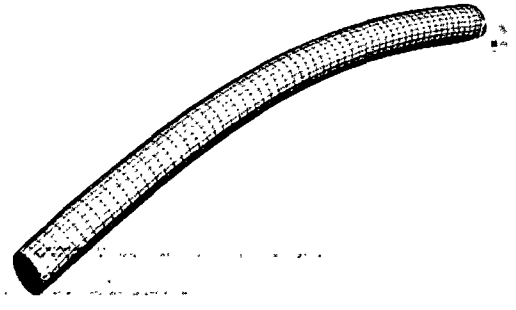

(c) Un-strengthened model – 762 mm

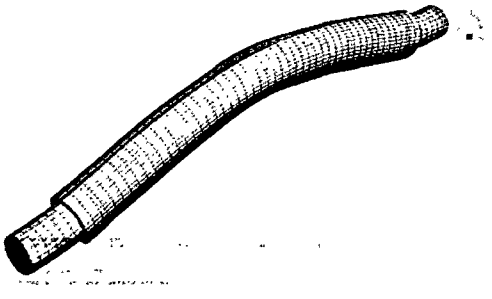

(d) Strengthened model – 762 mm

Figure 6.16. Fundamental Buckling Modes of Finite Element Models of Test Specimens

In the second analysis, an imperfection in the geometry was added to the straight member using results of the first analysis. For main leg members, L/400 was used as initial out-of-straightness as per recommendation given by Timoshenko and Gere [1961]. Using modified static Riks method, a geometrically non-linear load-displacement analysis of the models containing the imperfection was performed.

The result of this second analysis was the load magnitude parameter λ, which results in the actual load λP^N if multiplied by the applied load during analysis. Example of ABAQUS input files for 1524 mm long finite element models, RF60-B2 and RF60-W1, are shown in Appendix F.

The Von Mises stress contour diagram and deflected shape of 1524 mm long test specimens (RF60 and RF60-B4) and 762 mm long test specimens (RF30 and RF30-W1), are shown in Figures 6.17 and 6.18, respectively.

6.4.4 Analysis Results

The results of finite element analysis of 1524 mm and 762 mm long test specimens are shown in Tables 6.33 and 6.34, respectively. For the purpose of comparison, the results from experimental investigation are also displayed on the same Tables. From Table 6.33, it can be concluded that the failure loads obtained from finite element analysis are comparable to those obtained from experimental investigation, with difference ranging from 0.5% to 4.9%. The maximum difference in strength increase percentage between finite element results and experimental results are 9%. From Table 6.34, it is also shown that the failure loads obtained from finite element analysis are comparable with those obtained from experimental investigation. Thus, the finite element models can be used to simulate the behaviour of solid round steel test specimens, either un-strengthened or strengthened with split pipes, to obtain their compressive failure loads.

6.5 CONCLUSIONS

From experimental investigation and finite element simulation described in Sections 6.2 to 6.4, the following conclusions can be drawn:

1. Based on the experimental investigation and finite element analysis, the percentage increase of compressive strength of solid round strengthened with 1372 mm long split pipes (RF60-B1) was 18% and 19%, respectively. In comparison, the percentage increase of compressive strength of solid round strengthened with 610 mm long split pipes (RF60-B4) was 15% and 12%, based on experimental investigation and finite element analysis, respectively. To be on

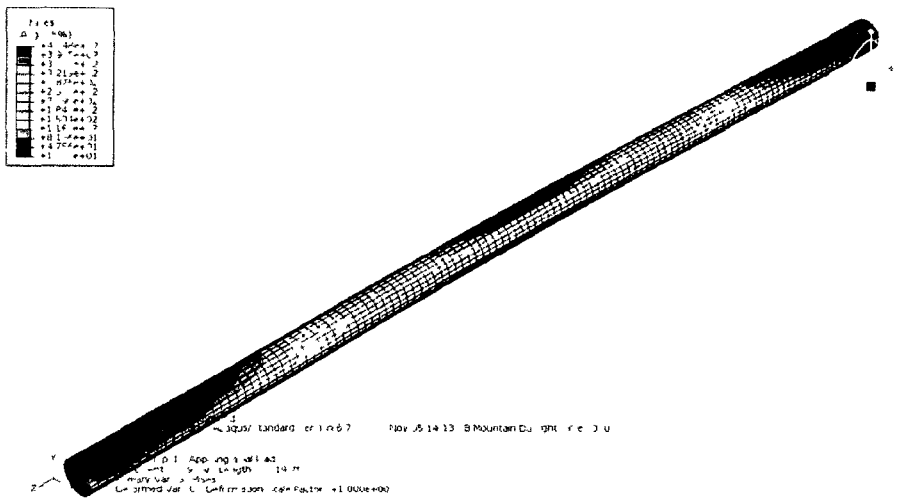

(a) 1524 mm long un-strengthened model of test specimen (RF60)

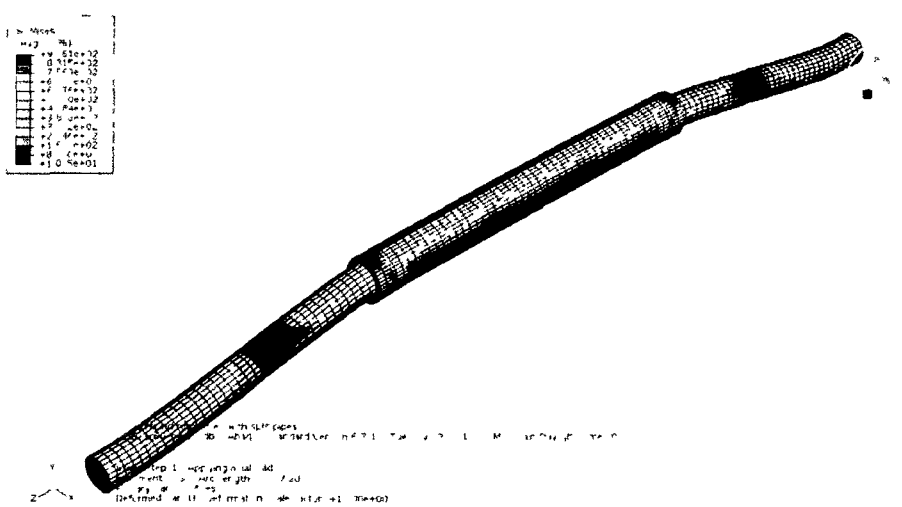

(b) 1524 mm long model of test specimen strengthened with 610 mm long split pipes (RF60-B4)

Figure 6.17. Von Mises Stress Contour Diagram and Deflected Shape of Test Specimens RF60 and RF60-B4

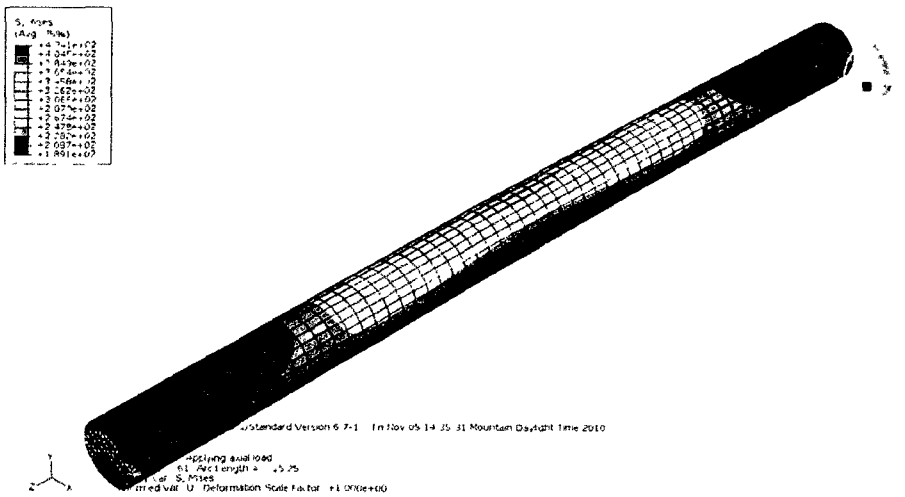

(a) 752 mm long un-strengthened model of test specimen (RF30)

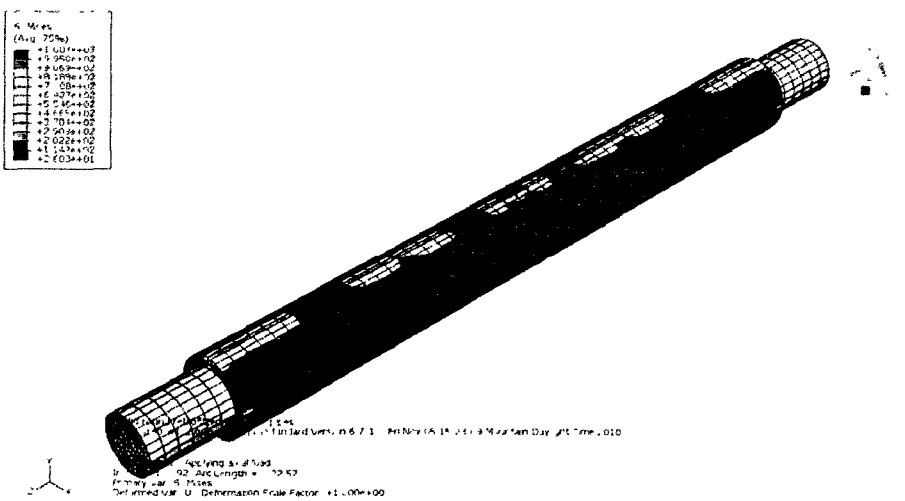

(b) 762 mm long model strengthened with split pipes connected with stitch weld (RF30-W1)

Figure 6.18. Von Mises Stress Contour Diagram and Deflected Shape of Test Specimens RF30 and RF30-W1

Table 6.33. Comparison of Failure Loads for 1524 mm Long Test Specimens Obtained from Finite Element Analysis and Experimental Investigation

Specimen type	Average failure load (kN)		Increase in compressive strength		Difference in failure loads
	Finite element analysis	Experimental investigation	Finite element analysis	Experimental investigation	
RF60	615	636	-	-	3 4%
RF60-B1	751	747	22%	18%	0 5%
RF60-B2	772	801	26%	26%	3 8%
RF60-B4	724	731	18%	15%	1 0%
RF60-W1	791	752	29%	18%	4 9%
RF60-W2	826	807	34%	27%	2 3%

Table 6.34. Comparison of Failure Loads for 762 mm Long Test Specimens Obtained from Finite Element Analysis and Experimental Investigation

Specimen type	Average failure load (kN)		Increase in compressive strength		Difference in failure loads
	Finite element analysis	Experimental investigation	Finite element analysis	Experimental investigation	
RF30	887	791	-	-	8 5%
RF30-B1	934	833	5 3%	4 7%	9 8%
RF30-B2	942	844	6 7%	2 0%	5 4%
RF30-W1	1140	1182	44%	34%	3 7%
RF30-W2	1320	1150	45%	37%	5 1%

the conservative side, it is recommended to use strengthening members along the entire leg member.

2. Results from both experimental investigation and finite element analysis show that end welds increase the strength of strengthened leg member, for both 1524 mm and 762 mm long test specimens. Therefore, whenever possible to do, end welds are recommended to be used in addition to U-bolts to connect the strengthening members to the main member.
3. For 1524 mm long test specimens, connecting the strengthening members using stitch weld results in comparable results with failure loads of specimens connected with U-bolts only. However, for stocky 762 mm long test specimens with stitch weld connection, the additional strength is increased significantly. Therefore, for solid rounds with compressive failure load almost reaching the load obtained from direct stress, stitch welds are preferable to U-bolts or tabs connection. There is only slight increase of strength for 762 mm long solid round test specimens with U-bolts and tabs connections, as confirmed by experimental investigation and finite element analysis.
4. The finite element models discussed in Section 6.4 can be used by tower design engineers to simulate the failure loads of solid round steel members, either un-strengthened or strengthened with split pipes. As per requirements of CSA S37-01 [CSA 2001] and CSA S16-09, nominal yield strength has to be used instead of the value obtained from mill test certificates. In addition, to be on conservative side, it is recommended that imperfection of L/250, which is the permissible variation in straightness for bars as per the CISC Handbook of Steel Construction [CISC 2010], be used instead of L/400.

REFERENCES

AISC. 2005. Steel Construction Manual. 13th ed. American Institute of Steel Construction, Chicago, IL.

Bleich, F. 1952. Buckling strength of metal structures. McGraw-Hill, New York, NY.

CISC. 2010. Handbook of Steel Construction. 10th ed. Canadian Institute of Steel Construction, Markham, ON.

Craig, R.R., Jr. 1996. Mechanics of materials. Wiley, New York, NY.

CSA. 2001. Antennas, towers, and antenna-supporting structures. S37-01. Canadian Standards Association, Toronto, ON.

Dinnik, D.N. 1932. Design of columns of varying cross section. Translated by M. Maletz. Transactions of American Society of Mechanical Engineers, **54**: 165-171.

Kumalasari, C., Ding, Y., Madugula, M.K.S., and Ghrib, F. 2006. Compressive strength of solid round steel members strengthened with rods or angles. Canadian Journal of Civil Engineering, Special Issue on Recent Advances in Steel Structures Research, **33**(4): 451-457.

Kumalasari, C., Madugula, M.K.S., and Ghrib, F. 2005. Strengthening of lattice communication towers with rods and angles. *In* Proceedings of Annual General Conference of the Canadian Society for Civil Engineering, Toronto, ON, 2-4 June 2005. Canadian Society of Civil Engineering, Montréal, QC, pp. GC-255.

Madugula, M.K.S., Kennedy, J.B., and Kumalasari, C. 2007. Retrofitting of masts of guyed lattice communication towers. *In* Proceedings of International Conference on Civil Engineering in the New Millennium: Opportunities and Challenges (CENeM-2007), 11-14 January 2007. Bengal Engineering and Science University, Shibpur, India, pp. 1203-1208.

Simulia. 2007. ABAQUS Version 6.7-1. Program documentation. Dassault Systèmes Simulia Corp., Providence, RI.

Timoshenko, S.P., and Gere, J.M. 1961. Theory of elastic stability. 2nd ed. McGraw-Hill, New York, NY.

Young, W.C., and Budynas, R.G. 2002. Roark's formulas for stress and strain. 7th ed. McGraw-Hill, New York, NY.

Ziemian, R.D. 2010. Guide to stability design criteria for metal structures. 6th ed. John Wiley & Sons, Hoboken, NJ.

CHAPTER 7
CONTRIBUTIONS AND RECOMMENDATIONS

7.1 RESEARCH CONTRIBUTIONS

This research contributes applicable knowledge in the field of communication tower industry. The author had authored/co-authored the following refereed publications related to the research as follows:

1. Dynamic load amplification factors of guy wires in a communication tower due to sudden rupture of one guy wire [Dostatni et al. 2010].
2. Retrofitting of masts of guyed lattice communication tower [Madugula et al. 2007].
3. Prying action in bolted steel circular flange connections [Kumalasari et al. 2006*a*].
4. Compressive strength of solid round steel members strengthened with rods or angles [Kumalasari et al. 2006*b*].
5. Strengthening of lattice communication towers with rods and angles [Kumalasari et al. 2005*a*].
6. Tensile strength of bolted ring-type connections of solid round leg members of guyed communication towers [Kumalasari et al. 2005*b*].

Throughout the duration of the research, the following research reports had been submitted to Electronics Research Inc., Chandler, Indiana, USA:

1. Results of additional compressive strength tests on solid round steel members reinforced with split pipes [Madugula and Kumalasari 2007].
2. Compressive strength of solid round steel members reinforced with split pipes [Madugula and Kumalasari 2006*a*].
3. Experimental investigation of load amplification factors due to sudden guy rupture and guy slippage [Madugula and Kumalasari 2006*b*].
4. Experimental investigation of dynamic amplification factors due to sudden guy rupture [Madugula and Kumalasari 2005].
5. Yield and failure loads of bolted flange connections subjected to axial tension [Madugula and Kumalasari 2004].
6. Compressive strength of solid round steel members reinforced with rods/angles [Madugula et al. 2004a].
7. Tensile strength of bolted ring-type connections of solid round leg members [Madugula et al. 2004*b*].
8. Prying action in bolted steel circular flange connections [Madugula et al. 2004*c*].
9. Design of bolted connections subjected to flexural tension [Madugula et al. 2004*d*].

10. Strength of solid round steel leg members reinforced with split pipe [Madugula et al. 2004e].

7.2 RECOMMENDATIONS FOR FUTURE RESEARCH

For future research, the following recommendations are made:

1. Further research on the effect of sudden guy rupture on guyed towers, by conducting experimental investigation on small-scale guyed tower test specimens with wind loading and masses as tower appurtenances. A study on the effect of temperature variations is also suggested.
2. Further study on the effect of sudden guy slippage, by conducting experimental investigation on small-scale and step-by-step stacking of tower sections to simulate actual erection of guyed towers, with and without wind loading.
3. Study the effect of eccentricity on bolted ring-type test specimens, by conducting experimental investigation on whole tower section to find the contribution of horizontals and diagonals on the capacity of the connection. In addition, the study of the effect of bolt length and length of the leg member on such connection is also suggested
4. Study the prying action on bolted triangular splice connections subjected to tensile load, and on bolted circular splice connection subjected to bending moment (which is encountered on monopole splices).
5. Further research and parametric study on strengthening of existing tower legs and diagonals are suggested, e.g., determination of compressive loads of hollow structural section tower legs strengthened with concrete and steel rebar. In addition, research on strengthening of monopoles is also suggested.

REFERENCES

Dostatni, C., Kennedy, J.B., Madugula, M.K.S., and Ghrib, F. 2010. Dynamic load amplification factors of guy wires in a communication tower due to sudden rupture of one guy wire. *In* Proceedings of 2nd International Structures Specialty Conference of the Canadian Society for Civil Engineering, Winnipeg, MB, 9-12 June 2010. Canadian Society of Civil Engineering, Montréal, QC, pp. ST-035.

Kumalasari, C., Ding, Y., and Madugula, M.K.S. 2006*a*. Prying action in bolted steel circular flange connections. Canadian Journal of Civil Engineering, Special Issue on Recent Advances in Steel Structures Research, **33**(4): 497-500.

Kumalasari, C., Ding, Y., Madugula, M.K.S., and Ghrib, F. 2006*b*. Compressive strength of solid round steel members strengthened with rods or angles. Canadian Journal of Civil Engineering, Special Issue on Recent Advances in Steel Structures Research, **33**(4): 451-457.

Kumalasari, C., Madugula, M.K.S., and Ghrib, F. 2005*a*. Strengthening of lattice communication towers with rods and angles. *In* Proceedings of Annual General Conference of the Canadian Society for Civil Engineering, Toronto, ON, 2-4 June 2005. Canadian Society of Civil Engineering, Montréal, QC, pp. GC-255.

Kumalasari, C., Shen, L., Madugula, M.K.S, and Ghrib, F. 2005*b*. Tensile strength of bolted ring-type connections of solid round leg members of guyed communication towers. Canadian Journal of Civil Engineering, **32**(3): 595-600.

Madugula, M.K.S., and Kumalasari, C. 2004. Yield and failure loads of bolted flange connections subjected to axial tension. University of Windsor, Windsor, ON. Report presented to Electronics Research Inc., Chandler, IN.

Madugula, M.K.S., and Kumalasari, C. 2005. Experimental investigation of dynamic amplification factors due to sudden guy rupture. University of Windsor, Windsor, ON. Report presented to Electronics Research Inc., Chandler, IN.

Madugula, M.K.S., and Kumalasari, C. 2006*a*. Compressive strength of solid round steel members reinforced with split pipes. University of Windsor, Windsor, ON. Report presented to Electronics Research Inc., Chandler, IN.

Madugula, M.K.S., and Kumalasari, C. 2006*b*. Experimental investigation of load amplification factors due to sudden guy rupture and guy slippage. University of Windsor, Windsor, ON. Report presented to Electronics Research Inc., Chandler, IN.

Madugula, M.K.S., and Kumalasari, C. 2007. Results of additional compressive strength tests on solid round steel members reinforced with split pipes. University of Windsor, Windsor, ON. Report presented to Electronics Research Inc., Chandler, IN.

Madugula, M.K.S., Ghrib, F., and Kumalasari, C. 2004*a*. Compressive strength of solid round steel members reinforced with rods/angles. University of Windsor, Windsor, ON. Report presented to Electronics Research Inc., Chandler, IN.

Madugula, M.K.S., Ghrib, F., Kumalasari, C., and Shen, L. 2004*b*. Tensile strength of bolted ring-type connections of solid round leg members. University of Windsor, Windsor, ON. Report presented to Electronics Research Inc., Chandler, IN.

Madugula, M.K.S., Kennedy, J.B., and Kumalasari, C. 2007. Retrofitting of masts of guyed lattice communication towers. *In* Proceedings of International Conference on Civil Engineering in the New Millennium: Opportunities and Challenges (CENeM-2007), 11-14 January 2007. Bengal Engineering and Science University, Shibpur, India, pp. 1203-1208.

Madugula, M.K.S., Kumalasari, C., and Ding, Y. 2004*c*. Prying action in bolted steel circular flange connections. University of Windsor, Windsor, ON. Report presented to Electronics Research Inc., Chandler, IN.

Madugula, M.K.S., Kumalasari, C., and Sarker, B. 2004*d*. Design of bolted connections subjected to flexural tension. University of Windsor, Windsor, ON. Report presented to Electronics Research Inc., Chandler, IN.

Madugula, M.K.S., Kumalasari, C., and Tickle, V. 2004*e*. Strength of solid round steel leg members reinforced with split pipe. University of Windsor, Windsor, ON. Report presented to Electronics Research Inc., Chandler, IN.

APPENDIX A
CALCULATION OF MAXIMUM STRESS IN LOAD CELL RING

Ring dimensions (refer to Figure A1):

Outside diameter, OD = 37.6 mm
Inside diameter, ID = 24.9 mm
Wall thickness, t = 6.35 mm = 0.25 in.
Thickness, b = 6.3 mm = 0.248 in.
Average radius:

$$R = 0.5 \times \frac{37.6 + 24.9}{2}$$

$$= 15.6\ \text{mm} = 0.615\ \text{in.}$$

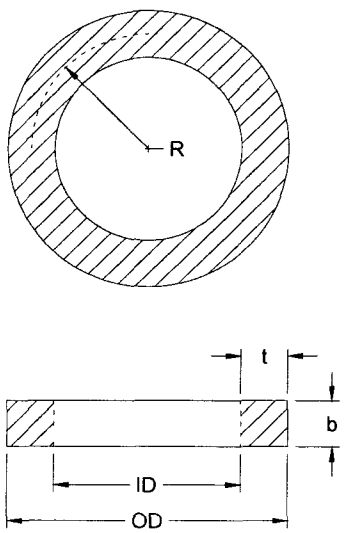

Figure A1. Ring Dimensions

Aluminum properties:
Young's modulus, E = 70 GPa = 10.2 x 10^6 psi
Yield strength = 95 MPa = 13.8 ksi

Calculation based on Table 9.2 (page 314) of Roark's Formulas for Stress and Strain [Young and Budynas 2002] (refer to Figure A2):

W = applied load = 445 N (100 lb)
h = distance from centroidal axis to neutral axis measured toward centre of curvature = 0

$$\alpha = \frac{h}{R} \rightarrow \text{for thick ring}$$

$$= \frac{0}{15.6} = 0$$

$$k_2 = 1 - \alpha = 1 - 0 = 1$$

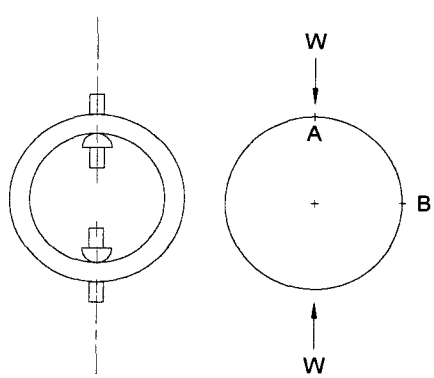

Figure A2. Load Applied to Ring

Maximum positive moment (at point A):

$M_A = 0.3183\ W\ R\ k_2$

$= 0.3183\ (-100)\ (0.615)\ (1) = -19.6$ lb-in (governs)

Maximum negative moment (at point B):

$M_B = -\ (0.5 - 0.3183\ k_2)\ W\ R$

$= -\ (0.5 - 0.3183\ (1))\ (-100)\ (0.615) = 11.2$ lb-in

Maximum stress:

$$\sigma = \frac{M_A \times y}{I} = \frac{M_A \times \frac{t}{2}}{\frac{1}{12} \times b \times t^3} = \frac{19.6 \times 0.125}{\frac{1}{12} \times 0.248 \times 0.25^3}$$

$= 7\,587$ psi $\leq 13\,800$ psi $\rightarrow$ OK

Corresponding strain: $\varepsilon = \frac{\sigma}{E} = \frac{7\,587}{10.2 \times 10^6} = 744 \times 10^{-6}$

APPENDIX B

CALIBRATION OF LOAD CELLS

Table B1. Load Cells Calibration

Load	Strain readings of load cell (μ)								
N (lb)	# 1	# 2	# 3	# 4	# 5	# 6	# 7	# 8	# 9
0 (0)	1100	1760	1070	1220	1470	3140	-148	1300	-834
4 45 (1 00)	1110	1770	1090	1230	1480	3150	-137	1310	-820
48 9 (11 0)	1230	1900	1210	1350	1610	3270	-19 8	1450	-690
93 4 (21 0)	1360	2030	1340	1470	1740	3400	97 4	1580	-560
138 (31 0)	1490	2160	1470	1600	1870	3520	215	1710	-429
182 (41 0)	1610	2300	1590	1710	2000	3650	332	1840	-299
227 (51 0)	1740	2430	1720	1820	2130	3770	450	1980	-168

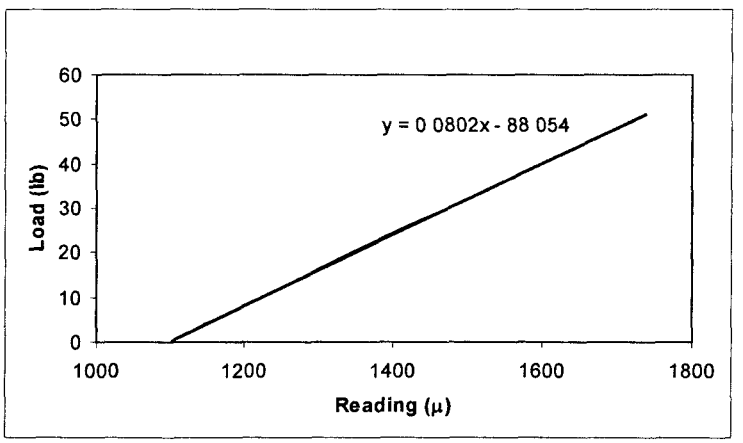

Figure B1. Load-strain Curve for Load Cell # 1

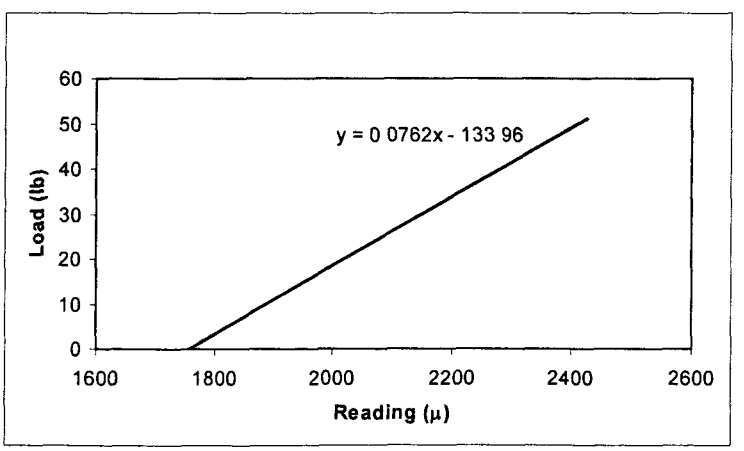

Figure B2. Load-strain Curve for Load Cell # 2

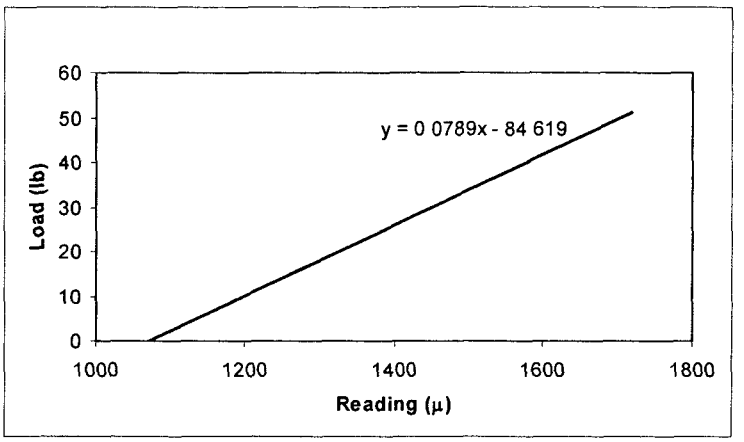

Figure B3. Load-strain Curve for Load Cell # 3

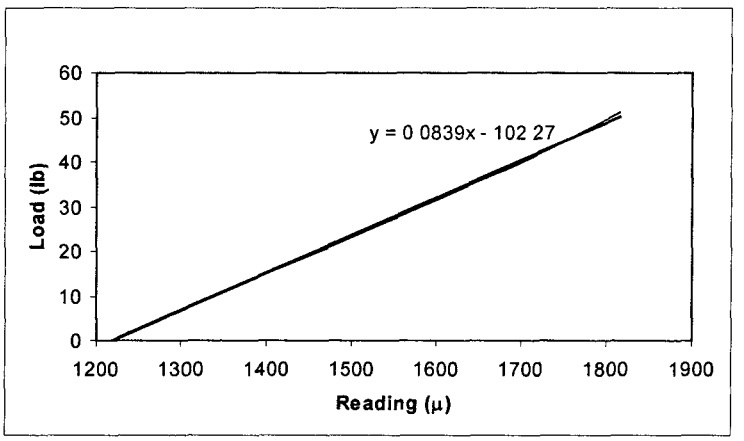

Figure B4. Load-strain Curve for Load Cell # 4

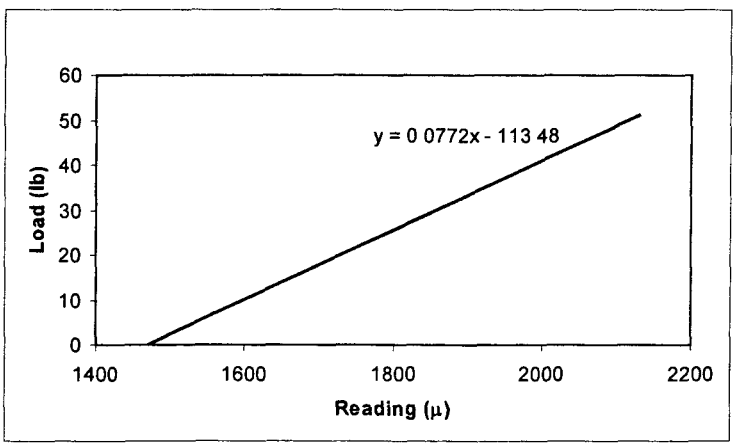

Figure B5. Load-strain Curve for Load Cell # 5

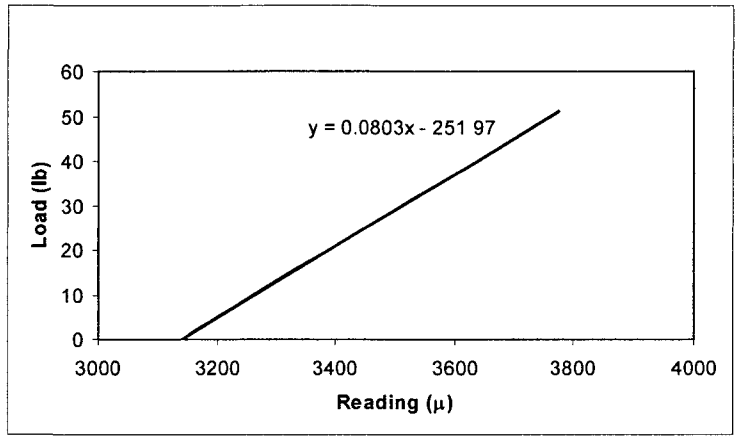

Figure B6. Load-strain Curve for Load Cell # 6

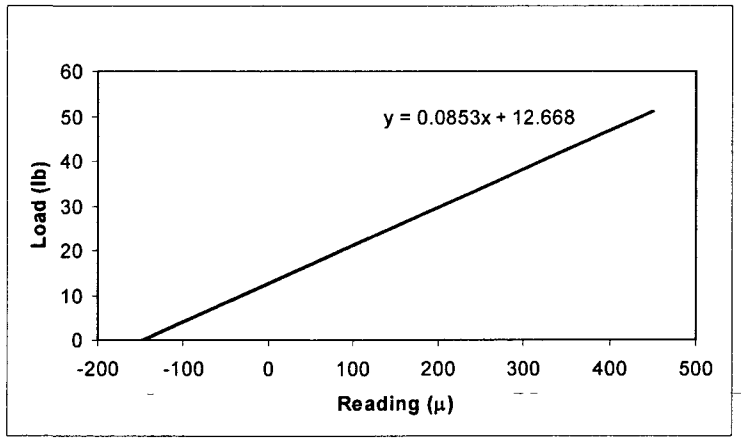

Figure B7. Load-strain Curve for Load Cell # 7

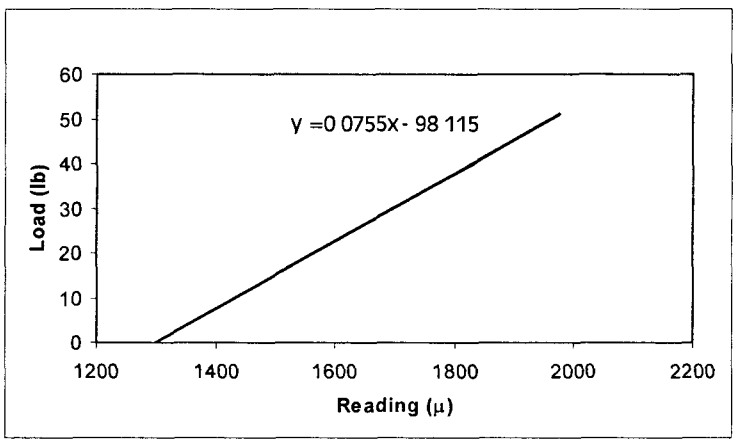

Figure B8. Load-strain Curve for Load Cell # 8

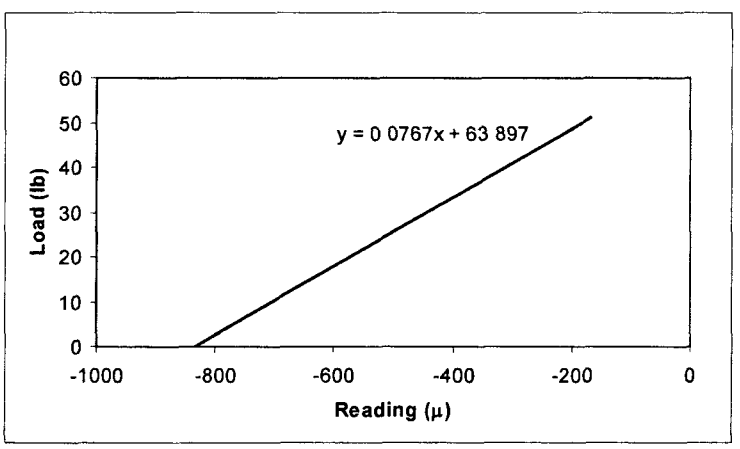

Figure B9. Load-strain Curve for Load Cell # 9

APPENDIX C

ABAQUS INPUT FILE FOR DYNAMIC ANALYSIS OF GUY WIRE RUPTURE

```
*HEADING
 Guy rupture model - 3 level
 Unit  N, m, s
 Rupture on G1 - 1
 G3 at level 5
 G2 at level 2
 G1 at level 1
 Tower 25
 Initial tension 100 lb
*NODE
 10, 0, 0, 0
 20, 0, 0, 0 3
 30, 0, 0, 0 6
 40, 0, 0, 1 5
 50, 0, 0, 2 2
*NODE, NSET = cable-end
 101, -1 2, 0, 0
 102, -1 2, 0, 0
 103, -1 2, 0, 0
 104, 0 6, 1 0392, 0
 105, 0 6, 1 0392, 0
 106, 0 6, 1 0392, 0
 107, 0 6, -1 0392, 0
 108, 0 6, -1 0392, 0
 109, 0 6, -1 0392, 0
*NODE
 1101, 0, 0, 0 3
 1102, 0, 0, 0 6
 1103, 0, 0, 1 5
 1104, 0, 0, 0 3
 1105, 0, 0, 0 6
 1106, 0, 0, 1 5
 1107, 0, 0, 0 3
 1108, 0, 0, 0 6
 1109, 0, 0, 1 5
*NGEN, NSET = mast
 10, 20, 2
 20, 30, 2
 30, 40, 2
 40, 50, 2
*NGEN, NSET = guy
 101, 1101, 100
 102, 1102, 100
 103, 1103, 100
 104, 1104, 100
 105, 1105, 100
 106, 1106, 100
 107, 1107, 100
 108, 1108, 100
 109, 1109, 100
*ELEMENT, TYPE = B31
 10, 10, 12
*ELGEN, ELSET = mast
 10, 20, 2, 2
*ELEMENT, TYPE = B31, ELSET = guy1-dir1
 101, 101, 301
```

```
 901, 901, 20
*ELEMENT, TYPE = B31, ELSET = guy2-dir1
 102, 102, 302
 902, 902, 30
*ELEMENT, TYPE = B31, ELSET = guy3-dir1
 103, 103, 303
 903, 903, 40
*ELGEN, ELSET = guy1
 101, 3, 3, 3, 4, 200, 200
*ELGEN, ELSET = guy2
 102, 3, 3, 3, 4, 200, 200
*ELGEN, ELSET = guy3
 103, 3, 3, 3, 4, 200, 200
*ELSET, ELSET = guy1-dir1, GENERATE
 101, 901, 200
*ELSET, ELSET = guy2-dir1, GENERATE
 102, 902, 200
*ELSET, ELSET = guy3-dir1, GENERATE
 103, 903, 200
*ELSET, ELSET = guy1-dir2, GENERATE
 104, 904, 200
*ELSET, ELSET = guy2-dir2, GENERATE
 105, 905, 200
*ELSET, ELSET = guy3-dir2, GENERATE
 106, 906, 200
*ELSET, ELSET = guy1-dir3  GENERATE
 107, 907, 200
*ELSET, ELSET = guy2-dir3, GENERATE
 108, 908, 200
*ELSET, ELSET = guy3-dir3, GENERATE
 109, 909, 200
*ELEMENT, TYPE = B31
 904, 904, 20
 905, 905, 30
 906, 906, 40
 907, 907, 20
 908, 908, 30
 909, 909, 40
*ELSET, ELSET = cbl-rel, GENERATE
 901, 909
*ELSET, ELSET = guy1, GENERATE
 901, 907, 3
*ELSET, ELSET = guy2, GENERATE
 902, 908, 3
*ELSET, ELSET = guy3, GENERATE
 903, 909, 3
*RELEASE
 cbl-rel, S2, M1-M2
*PRE-TENSION SECTION, ELEMENT = 101, NODE = 201
*PRE-TENSION SECTION, ELEMENT = 102, NODE = 202
*PRE-TENSION SECTION, ELEMENT = 103, NODE = 203
*PRE-TENSION SECTION, ELEMENT = 104, NODE = 204
*PRE-TENSION SECTION, ELEMENT = 105, NODE = 205
*PRE-TENSION SECTION, ELEMENT = 106, NODE = 206
*PRE-TENSION SECTION, ELEMENT = 107, NODE = 207
*PRE-TENSION SECTION, ELEMENT = 108, NODE = 208
*PRE-TENSION SECTION, ELEMENT = 109, NODE = 209
*NSET, NSET = pret, GENERATE
 201, 209
*NSET, NSET = guy1-dir1
 201
*NSET, NSET = guy2-dir1
```

```
 202
*NSET, NSET = guy3-dir1
 203
*NSET, NSET = guy1-dir2
 204
*NSET, NSET = guy2-dir2
 205
*NSET, NSET = guy3-dir2
 206
*NSET, NSET = guy1-dir3
 207
*NSET, NSET = guy2-dir3
 208
*NSET, NSET = guy3-dir3
 209
*ELSET, ELSET = guy
 guy1, guy2, guy3
*NSET, NSET = coor, GENERATE
 901, 909
*BEAM GENERAL SECTION, ELSET = mast, DENSITY = 7850
 0 000161, 0 00000000708, 0, 0 00000000708, 0 0000000142
 0, -1, 0
 200000000000, 77000000000
*BEAM GENERAL SECTION, ELSET = guy1, DENSITY = 7850
 1 9793260902246E-06, 3 11763188566724E-13, 0, 3 11763188566724E-13, 3 11763188566724E-13

 165360000000, 63663600000
*BEAM GENERAL SECTION, ELSET = guy2, DENSITY = 7850
 1 9793260902246E-06, 3 11763188566724E-13, 0, 3 11763188566724E-13, 3 11763188566724E-13

 165360000000, 63663600000
*BEAM GENERAL SECTION, ELSET = guy3, DENSITY = 7850
 1 9793260902246E-06, 3 11763188566724E-13, 0, 3 11763188566724E-13, 3 11763188566724E-13

 165360000000, 63663600000
*BOUNDARY
 10, 1, 3
 10, 6, 6
 cable-end, ENCASTRE
*NSET, NSET = n-all
 guy, mast
*ELSET, ELSET = e-all
 guy, mast
**********
*STEP, NLGEOM
 (1) Pretension-1
*STATIC
*CLOAD
 pret, 1, 44 48
*OUTPUT, FIELD, FREQUENCY = 1
*NODE OUTPUT, NSET = n-all
 U
*ELEMENT OUTPUT, ELSET = e-all
 SF
*ENDSTEP
**********
*STEP, NLGEOM
 (2) Gravity
*STATIC
*DLOAD
 mast, GRAV, 9 81, 0, 0, -1
 guy, GRAV, 9 81, 0, 0, -1
```

```
*OUTPUT, FIELD, FREQUENCY = 1
*NODE OUTPUT, NSET = n-all
 U
*ELEMENT OUTPUT, ELSET = e-all
 SF
*ENDSTEP
**********
*STEP, NLGEOM
 (3) Pretension-2
*STATIC
*CLOAD, OP = NEW
 guy1-dir1, 1, 444 8
 guy2-dir1, 1, 444 8
 guy3-dir1, 1, 444 8
 guy1-dir2, 1, 444 8
 guy2-dir2, 1, 444 8
 guy3-dir2, 1, 444 8
 guy1-dir3, 1, 444 8
 guy2-dir3, 1, 444 8
 guy3-dir3, 1, 444 8
*OUTPUT, FIELD, FREQUENCY = 1
*NODE OUTPUT, NSET = n-all
 U
*ELEMENT OUTPUT, ELSET = e-all
 SF
*ENDSTEP
**********
*STEP, NLGEOM
 (4) Fix
*STATIC
 0 001, 1, 0 00001, 1
*BOUNDARY, OP = NEW
 10, 1, 3
 10, 6, 6
 cable-end, 1, 3
*BOUNDARY, OP = NEW, FIXED
 pret, 1, 1
*NODE PRINT
COORD
*EL PRINT, ELSET = guy1-dir1
 SF
*OUTPUT, FIELD, FREQUENCY = 1
*NODE OUTPUT, NSET = n-all
 U
COORD
*ELEMENT OUTPUT, ELSET = e-all
 SF
*ENDSTEP
**********
*AMPLITUDE, NAME = remove
 0, 0, 0 01, 1
**********
*STEP, NLGEOM
 (5) Guy rupture - 1
*STATIC
 0 001, 0 01
*MODEL CHANGE, REMOVE
 guy1-dir1
*CLOAD, AMPLITUDE = remove
 20, 1, -431 563747253965
 20, 3, -107 962126808968
*OUTPUT, FIELD, FREQUENCY = 1
```

```
*NODE OUTPUT, NSET = n-all
 U
*ELEMENT OUTPUT, ELSET = e-all
 SF
*ENDSTEP
**********************
*STEP, NLGEOM, INC = 250
 (6) Guy rupture - 2
*DYNAMIC, HAFTOL = 20000
 0 01, 10, 0 000001, 1
*CLOAD
 20, 1, 0
 20, 3, 0
*OUTPUT, HISTORY, FREQUENCY = 1
*NODE OUTPUT, NSET = n-all
 U
 A
*ELEMENT OUTPUT, ELSET = e-all
 SF
*OUTPUT, FIELD, FREQUENCY = 1
*NODE OUTPUT, NSET = n-all
 U
 A
*ELEMENT OUTPUT, ELSET = e-all
 SF
*ENDSTEP
```

APPENDIX D

ABAQUS INPUT FILES TO DETERMINE THE LOAD AMPLIFICATION FACTORS USING EUROCODE METHOD

D1. ABAQUS Input Files with One Guy Wire Removed

```
*HEADING
 Guy rupture model - 3 level
 Unit N, m, s
 Rupture on G1
 Tower 25
 G3 at level 5
 G2 at level 2
 G1 at level 1
 Initial tension 50 lb
*NODE
 10, 0, 0, 0
 20, 0, 0, 0 3
 30, 0, 0, 0 6
 40, 0, 0, 1 5
 50, 0, 0, 2 2
*NODE, NSET = cable-end
 101, -1 2, 0, 0
 102, -1 2, 0, 0
 103, -1 2, 0, 0
 104, 0 6, 1 0392, 0
 105, 0 6, 1 0392, 0
 106, 0 6, 1 0392, 0
 107, 0 6, -1 0392, 0
 108, 0 6, -1 0392, 0
 109, 0 6, -1 0392, 0
*NODE
 1101, 0, 0, 0 3
 1102, 0, 0, 0 6
 1103, 0, 0, 1 5
 1104, 0, 0, 0 3
 1105, 0, 0, 0 6
 1106, 0, 0, 1 5
 1107, 0, 0, 0 3
 1108, 0, 0, 0 6
 1109, 0, 0, 1 5
*NGEN, NSET = mast
 10, 20, 2
 20, 30, 2
 30, 40, 2
 40, 50, 2
*NGEN, NSET = guy
 101, 1101, 100
 102, 1102, 100
 103, 1103, 100
 104, 1104, 100
 105, 1105, 100
 106, 1106, 100
 107, 1107, 100
 108, 1108, 100
 109, 1109, 100
*ELEMENT, TYPE = B31
 10, 10, 12
*ELGEN, ELSET = mast
```

```
 10, 20, 2, 2
*ELEMENT, TYPE = B31, ELSET = guy1-dir1
 101, 101, 301
 901, 901, 20
*ELEMENT, TYPE = B31, ELSET = guy2-dir1
 102, 102, 302
 902, 902, 30
*ELEMENT, TYPE = B31, ELSET = guy3-dir1
 103, 103, 303
 903, 903, 40
*ELGEN, ELSET = guy1
 101, 3, 3, 3, 4, 200, 200
*ELGEN, ELSET = guy2
 102, 3, 3, 3, 4, 200, 200
*ELGEN, ELSET = guy3
 103, 3, 3, 3, 4, 200, 200
*ELSET, ELSET = guy1-dir1, GENERATE
 101, 901, 200
*ELSET, ELSET = guy2-dir1, GENERATE
 102, 902, 200
*ELSET, ELSET = guy3-dir1, GENERATE
 103, 903, 200
*ELEMENT, TYPE = B31
 904, 904, 20
 905, 905, 30
 906, 906, 40
 907, 907, 20
 908, 908, 30
 909, 909, 40
*ELSET, ELSET = cbl-rel, GENERATE
 901, 909
*ELSET, ELSET = guy1, GENERATE
 901, 907, 3
*ELSET, ELSET = guy2, GENERATE
 902, 908, 3
*ELSET, ELSET = guy3, GENERATE
 903, 909, 3
*RELEASE
 cbl-rel, S2, M1-M2
*PRE-TENSION SECTION, ELEMENT = 101, NODE = 201
*PRE-TENSION SECTION, ELEMENT = 102, NODE = 202
*PRE-TENSION SECTION, ELEMENT = 103, NODE = 203
*PRE-TENSION SECTION, ELEMENT = 104, NODE = 204
*PRE-TENSION SECTION, ELEMENT = 105, NODE = 205
*PRE-TENSION SECTION, ELEMENT = 106, NODE = 206
*PRE-TENSION SECTION, ELEMENT = 107, NODE = 207
*PRE-TENSION SECTION, ELEMENT = 108, NODE = 208
*PRE-TENSION SECTION, ELEMENT = 109, NODE = 209
*NSET, NSET = pret, GENERATE
 201, 209
*NSET, NSET = guy1, GENERATE
 201, 207, 3
*NSET, NSET = guy2, GENERATE
 202, 208, 3
*NSET, NSET = guy3, GENERATE
 203, 209, 3
*ELSET, ELSET = guy
 guy1, guy2, guy3
*NSET, NSET = coor, GENERATE
 901, 909
*BEAM GENERAL SECTION, ELSET = mast, DENSITY = 7850
 0 000161, 0 00000000708, 0, 0 00000000708, 0 0000000142
```

```
 1, 0, 0
 200000000000, 77000000000
*BEAM GENERAL SECTION, ELSET = guy1, DENSITY = 7850
 1 9793260902246E-06, 3 11763188566724E-13, 0, 3 11763188566724E-13, 3 11763188566724E-13

 165360000000, 63663600000
*BEAM GENERAL SECTION, ELSET = guy2, DENSITY = 7850
 1 9793260902246E-06, 3 11763188566724E-13, 0, 3 11763188566724E-13, 3 11763188566724E-13

 165360000000, 63663600000
*BEAM GENERAL SECTION, ELSET = guy3, DENSITY = 7850
 1 9793260902246E-06, 3 11763188566724E-13, 0, 3 11763188566724E-13, 3 11763188566724E-13

 165360000000, 63663600000
*BOUNDARY
 10, 1, 3
 10, 6, 6
 cable-end, ENCASTRE
*NSET, NSET = n-all
 guy, mast
*ELSET, ELSET = e-all
 guy, mast
**********
*STEP, NLGEOM
 (1) Pretension-1
*STATIC
*CLOAD
 pret, 1, 22 24
*OUTPUT, FIELD, FREQUENCY = 1
*NODE OUTPUT, NSET = n-all
 U
*ELEMENT OUTPUT, ELSET = e-all
 SF
*ENDSTEP
**********
*STEP, NLGEOM
 (2) Gravity
*STATIC
*DLOAD
 mast, GRAV, 9 81, 0, 0, -1
 guy, GRAV, 9 81, 0, 0, -1
*OUTPUT, FIELD, FREQUENCY = 1
*NODE OUTPUT, NSET = n-all
 U
*ELEMENT OUTPUT, ELSET = e-all
 SF
*ENDSTEP
**********
*STEP, NLGEOM
 (3) Pretension-2
*STATIC
*CLOAD, OP = NEW
 guy1, 1, 222 4
 guy2, 1, 222 4
 guy3, 1, 222 4
*OUTPUT, FIELD, FREQUENCY = 1
*NODE OUTPUT, NSET = n-all
 U
*ELEMENT OUTPUT, ELSET = e-all
 SF
*ENDSTEP
**********
```

```
*STEP, NLGEOM
 (4) Fix
*STATIC
*BOUNDARY, OP = NEW
 10, 1, 3
 10, 6, 6
 cable-end, 1, 3
*BOUNDARY, OP = NEW, FIXED
 pret, 1, 1
*NODE PRINT
COORD
*EL PRINT, ELSET = guy1
 SF
*OUTPUT, FIELD, FREQUENCY = 1
*NODE OUTPUT, NSET = n-all
 U
COORD
*ELEMENT OUTPUT, ELSET = e-all
 SF
*ENDSTEP
**********************
*STEP, NLGEOM
 (5) Guy rupture - 1
*STATIC
 0.1, 1, , 0.1
*MODEL CHANGE, REMOVE
 guy1
***
***
*OUTPUT, FIELD, FREQUENCY = 1
*NODE OUTPUT, NSET = n-all
 U
*ELEMENT OUTPUT, ELSET = e-all
 SF
*ENDSTEP
**********************
*STEP, NLGEOM
 (6) Guy rupture - 2
*STATIC
 0.01, 1, 0.00001, 0.05
*CLOAD
 20, 1, 500
*OUTPUT, HISTORY, FREQUENCY = 1
*NODE OUTPUT, NSET = n-all
 U
COORD
*ELEMENT OUTPUT, ELSET = e-all
 SF
*OUTPUT, FIELD, FREQUENCY = 1
*NODE OUTPUT, NSET = n-all
 U
COORD
*ELEMENT OUTPUT, ELSET = e-all
 SF
*ENDSTEP
```

D2. ABAQUS Input Files with Three Guy Wires Removed

```
*HEADING
 Guy rupture model - 3 level
 Unit  N, m, s
 Rupture on G1
 Tower 25
 G3 at level 5
 G2 at level 2
 G1 at level 1
 Initial tension 50 lb
*NODE
 10, 0, 0, 0
 20, 0, 0, 0 3
 30, 0, 0, 0 6
 40, 0, 0, 1 5
 50, 0, 0, 2 2
*NODE, NSET = cable-end
 101, -1 2, 0, 0
 102, -1 2, 0, 0
 103, -1 2, 0, 0
 104, 0 6, 1 0392, 0
 105, 0 6, 1 0392, 0
 106, 0 6, 1 0392, 0
 107, 0 6, -1 0392, 0
 108, 0 6, -1 0392, 0
 109, 0 6, -1 0392, 0
*NODE
 1101, 0, 0, 0 3
 1102, 0, 0, 0 6
 1103, 0, 0, 1 5
 1104, 0, 0, 0 3
 1105, 0, 0, 0 6
 1106, 0, 0, 1 5
 1107, 0, 0, 0 3
 1108, 0, 0, 0 6
 1109, 0, 0, 1 5
*NGEN, NSET = mast
 10, 20, 2
 20, 30, 2
 30, 40, 2
 40, 50, 2
*NGEN, NSET = guy
 101, 1101, 100
 102, 1102, 100
 103, 1103, 100
 104, 1104, 100
 105, 1105, 100
 106, 1106, 100
 107, 1107, 100
 108, 1108, 100
 109, 1109, 100
*ELEMENT, TYPE = B31
 10, 10, 12
*ELGEN, ELSET = mast
 10, 20, 2, 2
*ELEMENT, TYPE = B31, ELSET = guy1-dir1
 101, 101, 301
 901, 901, 20
*ELEMENT, TYPE = B31, ELSET = guy2-dir1
 102, 102, 302
 902, 902, 30
*ELEMENT, TYPE = B31, ELSET = guy3-dir1
```

```
 103, 103, 303
 903, 903, 40
*ELGEN, ELSET = guy1
 101, 3, 3, 3, 4, 200, 200
*ELGEN, ELSET = guy2
 102, 3, 3, 3, 4, 200, 200
*ELGEN, ELSET = guy3
 103, 3, 3, 3, 4, 200, 200
*ELSET, ELSET = guy1-dir1, GENERATE
 101, 901, 200
*ELSET, ELSET = guy2-dir1, GENERATE
 102, 902, 200
*ELSET, ELSET = guy3-dir1, GENERATE
 103, 903, 200
*ELEMENT, TYPE = B31
 904, 904, 20
 905, 905, 30
 906, 906, 40
 907, 907, 20
 908, 908, 30
 909, 909, 40
*ELSET, ELSET = cbl-rel, GENERATE
 901, 909
*ELSET, ELSET = guy1, GENERATE
 901, 907, 3
*ELSET, ELSET = guy2, GENERATE
 902, 908, 3
*ELSET, ELSET = guy3, GENERATE
 903, 909, 3
*RELEASE
 cbl-rel, S2, M1-M2
*PRE-TENSION SECTION, ELEMENT = 101, NODE = 201
*PRE-TENSION SECTION, ELEMENT = 102, NODE = 202
*PRE-TENSION SECTION, ELEMENT = 103, NODE = 203
*PRE-TENSION SECTION, ELEMENT = 104, NODE = 204
*PRE-TENSION SECTION, ELEMENT = 105, NODE = 205
*PRE-TENSION SECTION, ELEMENT = 106, NODE = 206
*PRE-TENSION SECTION, ELEMENT = 107, NODE = 207
*PRE-TENSION SECTION, ELEMENT = 108, NODE = 208
*PRE-TENSION SECTION, ELEMENT = 109, NODE = 209
*NSET, NSET = pret, GENERATE
 201, 209
*NSET, NSET = guy1, GENERATE
 201, 207, 3
*NSET, NSET = guy2, GENERATE
 202, 208, 3
*NSET, NSET = guy3, GENERATE
 203, 209, 3
*ELSET, ELSET = guy
 guy1, guy2, guy3
*NSET, NSET = coor, GENERATE
 901, 909
*BEAM GENERAL SECTION, ELSET = mast, DENSITY = 7850
 0.000161, 0.00000000708, 0, 0.00000000708, 0.0000000142
 1, 0, 0
 200000000000, 77000000000
*BEAM GENERAL SECTION, ELSET = guy1, DENSITY = 7850
 1.9793260902246E-06, 3.11763188566724E-13, 0, 3.11763188566724E-13, 3.11763188566724E-13

 165360000000, 63663600000
*BEAM GENERAL SECTION, ELSET = guy2, DENSITY = 7850
 1.9793260902246E-06, 3.11763188566724E-13, 0, 3.11763188566724E-13, 3.11763188566724E-13
```

```
 165360000000, 63663600000
*BEAM GENERAL SECTION, ELSET = guy3, DENSITY = 7850
 1 9793260902246E-06, 3 11763188566724E-13, 0, 3 11763188566724E-13, 3 11763188566724E-13

 165360000000, 63663600000
*BOUNDARY
 10, 1, 3
 10, 6, 6
 cable-end, ENCASTRE
*NSET, NSET = n-all
 guy, mast
*ELSET, ELSET = e-all
 guy, mast
**********
*STEP, NLGEOM
 (1) Pretension-1
*STATIC
*CLOAD
 pret, 1, 22 24
*OUTPUT, FIELD, FREQUENCY = 1
*NODE OUTPUT, NSET = n-all
 U
*ELEMENT OUTPUT, ELSET = e-all
 SF
*ENDSTEP
**********
*STEP, NLGEOM
 (2) Gravity
*STATIC
*DLOAD
 mast, GRAV, 9 81, 0, 0, -1
 guy, GRAV, 9 81, 0, 0, -1
*OUTPUT, FIELD, FREQUENCY = 1
*NODE OUTPUT, NSET = n-all
 U
*ELEMENT OUTPUT, ELSET = e-all
 SF
*ENDSTEP
**********
*STEP, NLGEOM
 (3) Pretension-2
*STATIC
*CLOAD, OP = NEW
 guy1, 1, 222 4
 guy2, 1, 222 4
 guy3, 1, 222 4
*OUTPUT, FIELD, FREQUENCY = 1
*NODE OUTPUT, NSET = n-all
 U
*ELEMENT OUTPUT, ELSET = e-all
 SF
*ENDSTEP
**********
*STEP, NLGEOM
 (4) Fix
*STATIC
*BOUNDARY, OP = NEW
 10, 1, 3
 10, 6, 6
 cable-end, 1, 3
*BOUNDARY, OP = NEW, FIXED
```

```
 pret, 1, 1
*NODE PRINT
COORD
*EL PRINT, ELSET = guy1-dir1
 SF
*OUTPUT, FIELD, FREQUENCY = 1
*NODE OUTPUT, NSET = n-all
 U
COORD
*ELEMENT OUTPUT, ELSET = e-all
 SF
*ENDSTEP
**********
*STEP, NLGEOM
 (5) Guy rupture - 1
*STATIC
 0.1, 1, , 0.1
*MODEL CHANGE, REMOVE
 guy1-dir1
*CLOAD
 20, 1, -125
*OUTPUT, FIELD, FREQUENCY = 1
*NODE OUTPUT, NSET = n-all
 U
*ELEMENT OUTPUT, ELSET = e-all
 SF
*ENDSTEP
**********
*STEP, NLGEOM
 (6) Guy rupture - 2
*STATIC
 0.01, 1, 0.00001, 0.05
*CLOAD
 20, 1, 250
*OUTPUT, HISTORY, FREQUENCY = 1
*NODE OUTPUT, NSET = n-all
 U
COORD
*ELEMENT OUTPUT, ELSET = e-all
 SF
*OUTPUT, FIELD, FREQUENCY = 1
*NODE OUTPUT, NSET = n-all
 U
COORD
*ELEMENT OUTPUT, ELSET = e-all
 SF
*ENDSTEP
```

APPENDIX E

ABAQUS INPUT FILE FOR DYNAMIC ANALYSIS OF GUY WIRE SLIPPAGE

```
*HEADING
 Guy rupture model - 3 level
 Unit  N, m, s
 Rupture on G3 - 7
 G3 at level 7
 G2 at level 6
 G1 at level 5
 Tower 1
 Initial tension 50 lb
*NODE
 10, 0, 0, 0
 20, 0, 0, 1 5
 30, 0, 0, 1 8
 40, 0, 0, 2 1
 50, 0, 0, 2 2
*NODE, NSET = cable-end
 101, -1 2, 0, 0
 102, -1 2, 0, 0
 103, -1 2, 0, 0
 104, 0 6, 1 0392, 0
 105, 0 6, 1 0392, 0
 106, 0 6, 1 0392, 0
 107, 0 6, -1 0392, 0
 108, 0 6, -1 0392, 0
 109, 0 6, -1 0392, 0
*NODE
 1101, 0, 0, 1 5
 1102, 0, 0, 1 8
 1103, 0, 0, 2 1
 1104, 0, 0, 1 5
 1105, 0, 0, 1 8
 1106, 0, 0, 2 1
 1107, 0, 0, 1 5
 1108, 0, 0, 1 8
 1109, 0, 0, 2 1
*NGEN, NSET = mast
 10, 20, 2
 20, 30, 2
 30, 40, 2
 40, 50, 2
*NGEN, NSET = guy
 101, 1101, 100
 102, 1102, 100
 103, 1103, 100
 104, 1104, 100
 105, 1105, 100
 106, 1106, 100
 107, 1107, 100
 108, 1108, 100
 109, 1109, 100
*ELEMENT, TYPE = B31
 10, 10, 12
*ELGEN, ELSET = mast
 10, 20, 2, 2
*ELEMENT, TYPE = B31, ELSET = guy1-dir1
 101, 101, 301
```

```
 901, 901, 20
*ELEMENT, TYPE = B31, ELSET = guy2-dir1
 102, 102, 302
 902, 902, 30
*ELEMENT, TYPE = B31, ELSET = guy3-dir1
 103, 103, 303
 903, 903, 40
*ELGEN, ELSET = guy1
 101, 3, 3, 3, 4, 200, 200
*ELGEN, ELSET = guy2
 102, 3, 3, 3, 4, 200, 200
*ELGEN, ELSET = guy3
 103, 3, 3, 3, 4, 200, 200
*ELSET, ELSET = guy1-dir1, GENERATE
 101, 901, 200
*ELSET, ELSET = guy2-dir1, GENERATE
 102, 902, 200
*ELSET, ELSET = guy3-dir1, GENERATE
 103, 903, 200
*ELSET, ELSET = guy1-dir2, GENERATE
 104, 904, 200
*ELSET, ELSET = guy2-dir2, GENERATE
 105, 905, 200
*ELSET, ELSET = guy3-dir2, GENERATE
 106, 906, 200
*ELSET, ELSET = guy1-dir3, GENERATE
 107, 907, 200
*ELSET, ELSET = guy2-dir3, GENERATE
 108, 908, 200
*ELSET, ELSET = guy3-dir3, GENERATE
 109, 909, 200
*ELEMENT, TYPE = B31
 904, 904, 20
 905, 905, 30
 906, 906, 40
 907, 907, 20
 908, 908, 30
 909, 909, 40
*ELSET, ELSET = cbl-rel, GENERATE
 901, 909
*ELSET, ELSET = guy1, GENERATE
 901, 907, 3
*ELSET, ELSET = guy2, GENERATE
 902, 908, 3
*ELSET, ELSET = guy3, GENERATE
 903, 909, 3
*RELEASE
 cbl-rel, S2, M1-M2
*PRE-TENSION SECTION, ELEMENT = 101, NODE = 201
*PRE-TENSION SECTION, ELEMENT = 102, NODE = 202
*PRE-TENSION SECTION, ELEMENT = 103, NODE = 203
*PRE-TENSION SECTION, ELEMENT = 104, NODE = 204
*PRE-TENSION SECTION, ELEMENT = 105, NODE = 205
*PRE-TENSION SECTION, ELEMENT = 106, NODE = 206
*PRE-TENSION SECTION, ELEMENT = 107, NODE = 207
*PRE-TENSION SECTION, ELEMENT = 108, NODE = 208
*PRE-TENSION SECTION, ELEMENT = 109, NODE = 209
*NSET, NSET = pret, GENERATE
 201, 209
*NSET, NSET = guy1-dir1
 201
*NSET, NSET = guy2-dir1
```

```
 202
*NSET, NSET = guy3-dir1
 203
*NSET, NSET = guy1-dir2
 204
*NSET, NSET = guy2-dir2
 205
*NSET, NSET = guy3-dir2
 206
*NSET, NSET = guy1-dir3
 207
*NSET, NSET = guy2-dir3
 208
*NSET, NSET = guy3-dir3
 209
*ELSET, ELSET = guy
 guy1, guy2, guy3
*NSET, NSET = coor, GENERATE
 901, 909
*BEAM GENERAL SECTION, ELSET = mast, DENSITY = 7850
 0 000161, 0 00000000708, 0, 0 00000000708, 0 0000000142
 0, -1, 0
 200000000000, 77000000000
*BEAM GENERAL SECTION, ELSET = guy1, DENSITY = 7850
 1 9793260902246E-06, 3 11763188566724E-13, 0, 3 11763188566724E-13, 3 11763188566724E-13

 165360000000, 63663600000
*BEAM GENERAL SECTION, ELSET = guy2, DENSITY = 7850
 1 9793260902246E-06, 3 11763188566724E-13, 0, 3 11763188566724E-13, 3 11763188566724E-13

 165360000000, 63663600000
*BEAM GENERAL SECTION, ELSET = guy3, DENSITY = 7850
 1 9793260902246E-06, 3 11763188566724E-13, 0, 3 11763188566724E-13, 3 11763188566724E-13

 165360000000, 63663600000
*BOUNDARY
 10, 1, 3
 10, 6, 6
 cable-end, ENCASTRE
*NSET, NSET = n-all
 guy, mast
*ELSET, ELSET = e-all
 guy, mast
**********
*STEP, NLGEOM
 (1) Pretension-1
*STATIC
*CLOAD
 pret, 1, 22 24
*OUTPUT, FIELD, FREQUENCY = 1
*NODE OUTPUT, NSET = n-all
 U
*ELEMENT OUTPUT, ELSET = e-all
 SF
*ENDSTEP
**********
*STEP, NLGEOM
 (2) Gravity
*STATIC
*DLOAD
 mast, GRAV, 9 81, 0, 0, -1
 guy, GRAV, 9 81, 0, 0, -1
```

```
*OUTPUT, FIELD, FREQUENCY = 1
*NODE OUTPUT, NSET = n-all
 U
*ELEMENT OUTPUT, ELSET = e-all
 SF
*ENDSTEP
**********
*STEP, NLGEOM
 (3) Pretension-2
*STATIC
*CLOAD, OP = NEW
 guy1-dir1, 1, 222 4
 guy2-dir1, 1, 222 4
 guy3-dir1, 1, 222 4
 guy1-dir2, 1, 222 4
 guy2-dir2, 1, 222 4
 guy3-dir2, 1, 222 4
 guy1-dir3, 1, 222 4
 guy2-dir3, 1, 222 4
 guy3-dir3, 1, 222 4
*OUTPUT, FIELD, FREQUENCY = 1
*NODE OUTPUT, NSET = n-all
 U
*ELEMENT OUTPUT, ELSET = e-all
 SF
*ENDSTEP
**********
*STEP, NLGEOM
 (4) Fix
*STATIC
 0 001, 1, 0 00001, 1
*BOUNDARY, OP = NEW
 10, 1, 3
 10, 6, 6
 cable-end, 1, 3
*BOUNDARY, OP = NEW, FIXED
 pret, 1, 1
*NODE PRINT
COORD
*EL PRINT, ELSET = e-all
 SF
*OUTPUT, FIELD, FREQUENCY = 1
*NODE OUTPUT, NSET = n-all
 U
COORD
*ELEMENT OUTPUT, ELSET = e-all
 SF
*ENDSTEP
**********
*STEP, NLGEOM, INC = 250
 (5) Guy slippage
*DYNAMIC, HAFTOL = 20000
 0 01, 10, 0 000001, 1
*MODEL CHANGE, REMOVE
 103
*OUTPUT, HISTORY, FREQUENCY = 1
*NODE OUTPUT, NSET = n-all
 U
 A
*ELEMENT OUTPUT, ELSET = e-all
 SF
*OUTPUT, FIELD, FREQUENCY = 1
```

```
*NODE OUTPUT, NSET = n-all
 U
 A
*ELEMENT OUTPUT, ELSET = e-all
 SF
*ENDSTEP
```

APPENDIX F

ABAQUS INPUT FILE FOR SOLID ROUND MEMBER STRENGTHENED WITH SPLIT PIPES

F1. Input Files for 1524 Mm Long Test Specimens Strengthened with Split Pipes Connected with (8) U-Bolts and End Welding (RF60-B2)

```
*HEADING
 Solid round retrofitted with split pipes
 Number of split pipe = 2
 Unit = N-mm
 SR length = 60 in.
 SP length = 54 in.
 SR diameter = 2 in.
 SP OD = 2.875 in.
 SP thickness = 0.276 in.
 Alpha = 78.75 deg
 No of bolts = 8
 Weld length = 0 in.
 Type = b2
Friction = 0.025
*PARAMETER
 L = 1524
 Modescale = L / 400
***
**DEFINING SOLID ROUND SECTION
***
***
*NODE, NSET = centre
 1, 0, 0, 0
*NODE, NSET = sr-in1-bot
 101, -6.35, 0, 0
 137, 6.35, 0, 0
*NODE, NSET = sr-in2-bot
 201, -12.7, 0, 0
 237, 12.7, 0, 0
*NODE, NSET = sr-in3-bot
 301, -19.05, 0, 0
 337, 19.05, 0, 0
*NODE, NSET = sr-out-bot
 401, -25.4, 0, 0
 437, 25.4, 0, 0
*NGEN, LINE = C, NSET = sr-in1-bot
 101, 137, 12, 1, 0, 0, 0, 0, 0, -1
*NGEN, LINE = C, NSET = sr-in2-bot
 201, 237, 6, 1, 0, 0, 0, 0, 0, -1
*NGEN, LINE = C, NSET = sr-in3-bot
 301, 337, 4, 1, 0, 0, 0, 0, 0, -1
*NGEN, LINE = C, NSET = sr-out-bot
 401, 437, 3, 1, 0, 0, 0, 0, 0, -1
*NCOPY, SHIFT, OLD SET = sr-in1-bot, NEW SET = sr-in1-bot, CHANGE NUMBER = 36

 0, 0, 0, 0, 0, 1, 180
*NCOPY, SHIFT, OLD SET = sr-in2-bot, NEW SET = sr-in2-bot, CHANGE NUMBER = 36

 0, 0, 0, 0, 0, 1, 180
*NCOPY, SHIFT, OLD SET = sr-in3-bot, NEW SET = sr-in3-bot, CHANGE NUMBER = 36
```

```
 0, 0, 0, 0, 0, 1, 180
*NCOPY, SHIFT, OLD SET = sr-out-bot, NEW SET = sr-out-bot, CHANGE NUMBER = 36

 0, 0, 0, 0, 0, 1, 180
*NSET, NSET = sr-bot
 centre, sr-in1-bot, sr-in2-bot, sr-in3-bot, sr-out-bot
*NCOPY, SHIFT, OLD SET = sr-bot, NEW SET = sr-top, CHANGE NUMBER = 240000
 0, 0, 1524

*NFILL, NSET = solid round
 sr-bot, sr-top, 120, 2000
*ELEMENT, TYPE = C3D6, ELSET = sr-centre
 101, 1, 113, 101, 2001, 2113, 2101
 102, 1, 125, 113, 2001, 2125, 2113
 103, 1, 137, 125, 2001, 2137, 2125
 104, 1, 149, 137, 2001, 2149, 2137
 105, 1, 161, 149, 2001, 2161, 2149
 106, 1, 101, 161, 2001, 2101, 2161
*ELEMENT, TYPE = C3D6, ELSET = sr-inside
 201, 101, 207, 201, 2101, 2207, 2201
 202, 101, 113, 207, 2101, 2113, 2207
 203, 113, 213, 207, 2113, 2213, 2207
 204, 113, 219, 213, 2113, 2219, 2213
 205, 113, 125, 219, 2113, 2125, 2219
 206, 125, 225, 219, 2125, 2225, 2219
 207, 125, 231, 225, 2125, 2231, 2225
 208, 137, 231, 125, 2137, 2231, 2125
 209, 137, 237, 231, 2137, 2237, 2231
 210, 137, 243, 237, 2137, 2243, 2237
 211, 137, 149, 243, 2137, 2149, 2243
 212, 149, 249, 243, 2149, 2249, 2243
 213, 149, 255, 249, 2149, 2255, 2249
 214, 149, 161, 255, 2149, 2161, 2255
 215, 161, 261, 255, 2161, 2261, 2255
 216, 161, 267, 261, 2161, 2267, 2261
 217, 101, 267, 161, 2101, 2267, 2161
 218, 101, 201, 267, 2101, 2201, 2267
 301, 201, 305, 301, 2201, 2305, 2301
 302, 201, 207, 305, 2201, 2207, 2305
 303, 207, 309, 305, 2207, 2309, 2305
 304, 207, 213, 309, 2207, 2213, 2309
 305, 213, 313, 309, 2213, 2313, 2309
 306, 213, 317, 313, 2213, 2317, 2313
 307, 213, 219, 317, 2213, 2219, 2317
 308, 219, 321, 317, 2219, 2321, 2317
 309, 321, 219, 225, 2321, 2219, 2225
 310, 225, 325, 321, 2225, 2325, 2321
 311, 225, 329, 325, 2225, 2329, 2325
 312, 225, 231, 329, 2225, 2231, 2329
 313, 231, 333, 329, 2231, 2333, 2329
 314, 237, 333, 231, 2237, 2333, 2231
 315, 237, 337, 333, 2237, 2337, 2333
 316, 237, 341, 337, 2237, 2341, 2337
 317, 237, 243, 341, 2237, 2243, 2341
 318, 243, 345, 341, 2243, 2345, 2341
 319, 243, 249, 345, 2243, 2249, 2345
 320, 249, 349, 345, 2249, 2349, 2345
 321, 249, 353, 349, 2249, 2353, 2349
 322, 249, 255, 353, 2249, 2255, 2353
 323, 255, 357, 353, 2255, 2357, 2353
 324, 357, 255, 261, 2357, 2255, 2261
```

```
 325, 261, 361, 357, 2261, 2361, 2357
 326, 261, 365, 361, 2261, 2365, 2361
 327, 261, 267, 365, 2261, 2267, 2365
 328, 267, 369, 365, 2267, 2369, 2365
 329, 201, 369, 267, 2201, 2369, 2267
 330, 201, 301, 369, 2201, 2301, 2369
*ELEMENT, TYPE = C3D6, ELSET = sr-surface
 401, 301, 404, 401, 2301, 2404, 2401
 402, 301, 305, 404, 2301, 2305, 2404
 403, 305, 407, 404, 2305, 2407, 2404
 404, 305, 309, 407, 2305, 2309, 2407
 405, 309, 410, 407, 2309, 2410, 2407
 406, 309, 313, 410, 2309, 2313, 2410
 407, 313, 413, 410, 2313, 2413, 2410
 408, 313, 416, 413, 2313, 2416, 2413
 409, 313, 317, 416, 2313, 2317, 2416
 410, 317, 419, 416, 2317, 2419, 2416
 411, 317, 321, 419, 2317, 2321, 2419
 412, 321, 422, 419, 2321, 2422, 2419
 413, 321, 325, 422, 2321, 2325, 2422
 414, 325, 425, 422, 2325, 2425, 2422
 415, 325, 428, 425, 2325, 2428, 2425
 416, 325, 329, 428, 2325, 2329, 2428
 417, 329, 431, 428, 2329, 2431, 2428
 418, 329, 333, 431, 2329, 2333, 2431
 419, 333, 434, 431, 2333, 2434, 2431
 420, 337, 434, 333, 2337, 2434, 2333
 421, 337, 437, 434, 2337, 2437, 2434
 422, 337, 440, 437, 2337, 2440, 2437
 423, 337, 341, 440, 2337, 2341, 2440
 424, 341, 443, 440, 2341, 2443, 2440
 425, 341, 345, 443, 2341, 2345, 2443
 426, 345, 446, 443, 2345, 2446, 2443
 427, 345, 349, 446, 2345, 2349, 2446
 428, 349, 449, 446, 2349, 2449, 2446
 429, 349, 452, 449, 2349, 2452, 2449
 430, 349, 353, 452, 2349, 2353, 2452
 431, 353, 455, 452, 2353, 2455, 2452
 432, 353, 357, 455, 2353, 2357, 2455
 433, 357, 458, 455, 2357, 2458, 2455
 434, 357, 361, 458, 2357, 2361, 2458
 435, 361, 461, 458, 2361, 2461, 2458
 436, 361, 464, 461, 2361, 2464, 2461
 437, 361, 365, 464, 2361, 2365, 2464
 438, 365, 467, 464, 2365, 2467, 2464
 439, 365, 369, 467, 2365, 2369, 2467
 440, 369, 470, 467, 2369, 2470, 2467
 441, 301, 470, 369, 2301, 2470, 2369
 442, 301, 401, 470, 2301, 2401, 2470
*ELGEN, ELSET = sr-centre
 101, 120, 2000, 2000
 102, 120, 2000, 2000
 103, 120, 2000, 2000
 104, 120, 2000, 2000
 105, 120, 2000, 2000
 106, 120, 2000, 2000
*ELGEN, ELSET = sr-inside
 201, 120, 2000, 2000
 202, 120, 2000, 2000
 203, 120, 2000, 2000
 204, 120, 2000, 2000
 205, 120, 2000, 2000
```

206, 120, 2000, 2000
207, 120, 2000, 2000
208, 120, 2000, 2000
209, 120, 2000, 2000
210, 120, 2000, 2000
211, 120, 2000, 2000
212, 120, 2000, 2000
213, 120, 2000, 2000
214, 120, 2000, 2000
215, 120, 2000, 2000
216, 120, 2000, 2000
217, 120, 2000, 2000
218, 120, 2000, 2000
301, 120, 2000, 2000
302, 120, 2000, 2000
303, 120, 2000, 2000
304, 120, 2000, 2000
305, 120, 2000, 2000
306, 120, 2000, 2000
307, 120, 2000, 2000
308, 120, 2000, 2000
309, 120, 2000, 2000
310, 120, 2000, 2000
311, 120, 2000, 2000
312, 120, 2000, 2000
313, 120, 2000, 2000
314, 120, 2000, 2000
315, 120, 2000, 2000
316, 120, 2000, 2000
317, 120, 2000, 2000
318, 120, 2000, 2000
319, 120, 2000, 2000
320, 120, 2000, 2000
321, 120, 2000, 2000
322, 120, 2000, 2000
323, 120, 2000, 2000
324, 120, 2000, 2000
325, 120, 2000, 2000
326, 120, 2000, 2000
327, 120, 2000, 2000
328, 120, 2000, 2000
329, 120, 2000, 2000
330, 120, 2000, 2000
*ELGEN, ELSET = sr-surface
401, 120, 2000, 2000
402, 120, 2000, 2000
403, 120, 2000, 2000
404, 120, 2000, 2000
405, 120, 2000, 2000
406, 120, 2000, 2000
407, 120, 2000, 2000
408, 120, 2000, 2000
409, 120, 2000, 2000
410, 120, 2000, 2000
411, 120, 2000, 2000
412, 120, 2000, 2000
413, 120, 2000, 2000
414, 120, 2000, 2000
415, 120, 2000, 2000
416, 120, 2000, 2000
417, 120, 2000, 2000
418, 120, 2000, 2000

419, 120, 2000, 2000
420, 120, 2000, 2000
421, 120, 2000, 2000
422, 120, 2000, 2000
423, 120, 2000, 2000
424, 120, 2000, 2000
425, 120, 2000, 2000
426, 120, 2000, 2000
427, 120, 2000, 2000
428, 120, 2000, 2000
429, 120, 2000, 2000
430, 120, 2000, 2000
431, 120, 2000, 2000
432, 120, 2000, 2000
433, 120, 2000, 2000
434, 120, 2000, 2000
435, 120, 2000, 2000
436, 120, 2000, 2000
437, 120, 2000, 2000
438, 120, 2000, 2000
439, 120, 2000, 2000
440, 120, 2000, 2000
441, 120, 2000, 2000
442, 120, 2000, 2000
*ELSET, ELSET = sr-top
238101
238102
238103
238104
238105
238106
238201
238202
238203
238204
238205
238206
238207
238208
238209
238210
238211
238212
238213
238214
238215
238216
238217
238218
238301
238302
238303
238304
238305
238306
238307
238308
238309
238310
238311
238312
238313

238314
238315
238316
238317
238318
238319
238320
238321
238322
238323
238324
238325
238326
238327
238328
238329
238330
238401
238402
238403
238404
238405
238406
238407
238408
238409
238410
238411
238412
238413
238414
238415
238416
238417
238418
238419
238420
238421
238422
238423
238424
238425
238426
238427
238428
238429
238430
238431
238432
238433
238434
238435
238436
238437
238438
238439
238440
238441
238442
*ELSET, ELSET = solid round
sr-centre, sr-inside, sr-surface
***

```
*EQUATION
 2
 240401, 3, 1, 240404, 3, -1
*EQUATION
 2
 240404, 3, 1, 240407, 3, -1
*EQUATION
 2
 240407, 3, 1, 240410, 3, -1
*EQUATION
 2
 240410, 3, 1, 240413, 3, -1
*EQUATION
 2
 240413, 3, 1, 240416, 3, -1
*EQUATION
 2
 240416, 3, 1, 240419, 3, -1
*EQUATION
 2
 240419, 3, 1, 240422, 3, -1
*EQUATION
 2
 240422, 3, 1, 240425, 3, -1
*EQUATION
 2
 240425, 3, 1, 240428, 3, -1
*EQUATION
 2
 240428, 3, 1, 240431, 3, -1
*EQUATION
 2
 240431, 3, 1, 240434, 3, -1
*EQUATION
 2
 240434, 3, 1, 240437, 3, -1
*EQUATION
 2
 240437, 3, 1, 240440, 3, -1
*EQUATION
 2
 240440, 3, 1, 240443, 3, -1
*EQUATION
 2
 240443, 3, 1, 240446, 3, -1
*EQUATION
 2
 240446, 3, 1, 240449, 3, -1
*EQUATION
 2
 240449, 3, 1, 240452, 3, -1
*EQUATION
 2
 240452, 3, 1, 240455, 3, -1
*EQUATION
 2
 240455, 3, 1, 240458, 3, -1
*EQUATION
 2
 240458, 3, 1, 240461, 3, -1
*EQUATION
 2
```

```
 240461, 3, 1, 240464, 3, -1
*EQUATION
 2
 240464, 3, 1, 240467, 3, -1
*EQUATION
 2
 240467, 3, 1, 240470, 3, -1
*EQUATION
 2
 240470, 3, 1, 240301, 3, -1
*EQUATION
 2
 240301, 3, 1, 240305, 3, -1
*EQUATION
 2
 240305, 3, 1, 240309, 3, -1
*EQUATION
 2
 240309, 3, 1, 240313, 3, -1
*EQUATION
 2
 240313, 3, 1, 240317, 3, -1
*EQUATION
 2
 240317, 3, 1, 240321, 3, -1
*EQUATION
 2
 240321, 3, 1, 240325, 3, -1
*EQUATION
 2
 240325, 3, 1, 240329, 3, -1
*EQUATION
 2
 240329, 3, 1, 240333, 3, -1
*EQUATION
 2
 240333, 3, 1, 240337, 3, -1
*EQUATION
 2
 240337, 3, 1, 240341, 3, -1
*EQUATION
 2
 240341, 3, 1, 240345, 3, -1
*EQUATION
 2
 240345, 3, 1, 240349, 3, -1
*EQUATION
 2
 240349, 3, 1, 240353, 3, -1
*EQUATION
 2
 240353, 3, 1, 240357, 3, -1
*EQUATION
 2
 240357, 3, 1, 240361, 3, -1
*EQUATION
 2
 240361, 3, 1, 240365, 3, -1
*EQUATION
 2
 240365, 3, 1, 240369, 3, -1
*EQUATION
```

```
 2
 240369, 3, 1, 240201, 3, -1
*EQUATION
 2
 240201, 3, 1, 240207, 3, -1
*EQUATION
 2
 240207, 3, 1, 240213, 3, -1
*EQUATION
 2
 240213, 3, 1, 240219, 3, -1
*EQUATION
 2
 240219, 3, 1, 240225, 3, -1
*EQUATION
 2
 240225, 3, 1, 240231, 3, -1
*EQUATION
 2
 240231, 3, 1, 240237, 3, -1
*EQUATION
 2
 240237, 3, 1, 240243, 3, -1
*EQUATION
 2
 240243, 3, 1, 240249, 3, -1
*EQUATION
 2
 240249, 3, 1, 240255, 3, -1
*EQUATION
 2
 240255, 3, 1, 240261, 3, -1
*EQUATION
 2
 240261, 3, 1, 240267, 3, -1
*EQUATION
 2
 240267, 3, 1, 240101, 3, -1
*EQUATION
 2
 240101, 3, 1, 240113, 3, -1
*EQUATION
 2
 240113, 3, 1, 240125, 3, -1
*EQUATION
 2
 240125, 3, 1, 240137, 3, -1
*EQUATION
 2
 240137, 3, 1, 240149, 3, -1
*EQUATION
 2
 240149, 3, 1, 240161, 3, -1
***
*BOUNDARY
 sr-bot, 1, 3
 sr-top, 1, 2
***
**DEFINING SPLIT PIPE 1 SECTION
***
**Number of section per quarter = 10
**Number of section of split pipe thickness = 2
```

```
***
*NODE
 300001, 4 1021, 0, 76 2
*NODE, NSET = sp-in-bot
 300002, -1 65347418915202, 28 9352254209841, 76 2
 300022, -1 65347418915202, -28 9352254209841, 76 2
*NGEN, LINE = C, NSET = sp-in-bot
 300002, 300022, 1, 300001, 4 1021, 0, 76 2, 0, 0, 77 2
*NODE, NSET = sp-out-bot
 300084, -1 65347418915202, 35 9456254209841, 76 2
 300104, -1 65347418915202, -35 9456254209841, 76 2
*NGEN, LINE = C, NSET = sp-out-bot
 300084, 300104, 1, 300001, 4 1021, 0, 76 2, 0, 0, 77 2
*NFILL, NSET = sp-bot
 sp-in-bot, sp-out-bot, 2, 41
*NCOPY, SHIFT, OLD SET = sp-bot, NEW SET = sp-bot-t, CHANGE NUMBER = 600
 0, 0, 38 1

*NCOPY, SHIFT, OLD SET = sp-bot-t, NEW SET = bolt-1b, CHANGE NUMBER = 200
 0, 0, 6 35

*NCOPY, SHIFT, OLD SET = bolt-1b, NEW SET = bolt-1t, CHANGE NUMBER = 600
 0, 0, 38 1

*NCOPY, SHIFT, OLD SET = bolt-1t, NEW SET = bolt-2b, CHANGE NUMBER = 2200
 0, 0, 139 7

*NCOPY, SHIFT, OLD SET = bolt-2b, NEW SET = bolt-2t, CHANGE NUMBER = 600
 0, 0, 38 1

*NCOPY, SHIFT, OLD SET = bolt-2t, NEW SET = bolt-3b, CHANGE NUMBER = 2200
 0, 0, 139 7

*NCOPY, SHIFT, OLD SET = bolt-3b, NEW SET = bolt-3t, CHANGE NUMBER = 600
 0, 0, 38 1

*NCOPY, SHIFT, OLD SET = bolt-3t, NEW SET = bolt-4b, CHANGE NUMBER = 2200
 0, 0, 139 7

*NCOPY, SHIFT, OLD SET = bolt-4b, NEW SET = bolt-4t, CHANGE NUMBER = 600
 0, 0, 38 1

*NCOPY, SHIFT, OLD SET = bolt-4t, NEW SET = bolt-5b, CHANGE NUMBER = 2200
 0, 0, 139 7

*NCOPY, SHIFT, OLD SET = bolt-5b, NEW SET = bolt-5t, CHANGE NUMBER = 600
 0, 0, 38 1

*NCOPY, SHIFT, OLD SET = bolt-5t, NEW SET = bolt-6b, CHANGE NUMBER = 2200
 0, 0, 139 7

*NCOPY, SHIFT, OLD SET = bolt-6b, NEW SET = bolt-6t, CHANGE NUMBER = 600
 0, 0, 38 1

*NCOPY, SHIFT, OLD SET = bolt-6t, NEW SET = bolt-7b, CHANGE NUMBER = 2200
 0, 0, 139 7

*NCOPY, SHIFT, OLD SET = bolt-7b, NEW SET = bolt-7t, CHANGE NUMBER = 600
 0, 0, 38 1

*NCOPY, SHIFT, OLD SET = bolt-7t, NEW SET = bolt-8b, CHANGE NUMBER = 2200
 0, 0, 139 7
```

```
*NCOPY, SHIFT, OLD SET = bolt-8b, NEW SET = bolt-8t, CHANGE NUMBER = 600
 0, 0, 38.1

*NCOPY, SHIFT, OLD SET = bolt-8t, NEW SET = sp-top-b, CHANGE NUMBER = 200
 0, 0, 6.35

*NCOPY, SHIFT, OLD SET = sp-top-b, NEW SET = sp-top, CHANGE NUMBER = 600
 0, 0, 38.1

*NFILL, NSET = split-pipe-1
 sp-bot, sp-bot-t, 3, 200
 sp-bot-t, bolt-1b, 1, 200
 bolt-1b, bolt-1t, 3, 200
 bolt-1t, bolt-2b, 11, 200
 bolt-2b, bolt-2t, 3, 200
 bolt-2t, bolt-3b, 11, 200
 bolt-3b, bolt-3t, 3, 200
 bolt-3t, bolt-4b, 11, 200
 bolt-4b, bolt-4t, 3, 200
 bolt-4t, bolt-5b, 11, 200
 bolt-5b, bolt-5t, 3, 200
 bolt-5t, bolt-6b, 11, 200
 bolt-6b, bolt-6t, 3, 200
 bolt-6t, bolt-7b, 11, 200
 bolt-7b, bolt-7t, 3, 200
 bolt-7t, bolt-8b, 11, 200
 bolt-8b, bolt-8t, 3, 200
 bolt-8t, sp-top-b, 1, 200
 sp-top-b, sp-top, 3, 200
*ELEMENT, TYPE = C3D8
 300002, 300002, 300043, 300044, 300003, 300202, 300243, 300244, 300203
 300042, 300043, 300084, 300085, 300044, 300243, 300284, 300285, 300244
*ELGEN, ELSET = sp-surface-in-1
 300002, 20, 1, 1, 109, 200, 200
*ELGEN, ELSET = sp-surface-out-1
 300042, 20, 1, 1, 109, 200, 200
*ELSET, ELSET = split-pipe-1
 sp-surface-in-1, sp-surface-out-1
*ELSET, ELSET = bolt - 1, GENERATE
 300842, 300861
 303642, 303661
 306442, 306461
 309242, 309261
 312042, 312061
 314842, 314861
 317642, 317661
 320442, 320461
*ELSET, ELSET = bolt - 1, GENERATE
 301042, 301061
 303842, 303861
 306642, 306661
 309442, 309461
 312242, 312261
 315042, 315061
 317842, 317861
 320642, 320661
*ELSET, ELSET = bolt - 1, GENERATE
 301242, 301261
 304042, 304061
 306842, 306861
 309642, 309661
```

```
 312442, 312461
 315242, 315261
 318042, 318061
 320842, 320861
***
**DEFINING SPLIT PIPE 2 SECTION
***
**Number of section per quarter = 10
**Number of section of split pipe thickness = 2
***
*NODE
 400001, -4.1021, 0, 76.2
*NODE, NSET = sp2-in-bot
 400002, 1.65347418915202, 28.9352254209841, 76.2
 400022, 1.65347418915202, -28.9352254209841, 76.2
*NGEN, LINE = C, NSET = sp2-in-bot
 400002, 400022, 1, 400001, -4.1021, 0, 76.2, 0, 0, -1
*NODE, NSET = sp2-out-bot
 400084, 1.65347418915202, 35.9456254209841, 76.2
 400104, 1.65347418915202, -35.9456254209841, 76.2
*NGEN, LINE = C, NSET = sp2-out-bot
 400084, 400104, 1, 400001, -4.1021, 0, 76.2, 0, 0, -1
*NFILL, NSET = sp2-bot
 sp2-in-bot, sp2-out-bot, 2, 41
*NCOPY, SHIFT, OLD SET = sp2-bot, NEW SET = sp2-bot-t, CHANGE NUMBER = 600
 0, 0, 38.1

*NCOPY, SHIFT, OLD SET = sp2-bot-t, NEW SET = bolt2-1b, CHANGE NUMBER = 200
 0, 0, 6.35

*NCOPY, SHIFT, OLD SET = bolt2-1b, NEW SET = bolt2-1t, CHANGE NUMBER = 600
 0, 0, 38.1

*NCOPY, SHIFT, OLD SET = bolt2-1t, NEW SET = bolt2-2b, CHANGE NUMBER = 2200
 0, 0, 139.7

*NCOPY, SHIFT, OLD SET = bolt2-2b, NEW SET = bolt2-2t, CHANGE NUMBER = 600
 0, 0, 38.1

*NCOPY, SHIFT, OLD SET = bolt2-2t, NEW SET = bolt2-3b, CHANGE NUMBER = 2200
 0, 0, 139.7

*NCOPY, SHIFT, OLD SET = bolt2-3b, NEW SET = bolt2-3t, CHANGE NUMBER = 600
 0, 0, 38.1

*NCOPY, SHIFT, OLD SET = bolt2-3t, NEW SET = bolt2-4b, CHANGE NUMBER = 2200
 0, 0, 139.7

*NCOPY, SHIFT, OLD SET = bolt2-4b, NEW SET = bolt2-4t, CHANGE NUMBER = 600
 0, 0, 38.1

*NCOPY, SHIFT, OLD SET = bolt2-4t, NEW SET = bolt2-5b, CHANGE NUMBER = 2200
 0, 0, 139.7

*NCOPY, SHIFT, OLD SET = bolt2-5b, NEW SET = bolt2-5t, CHANGE NUMBER = 600
 0, 0, 38.1

*NCOPY, SHIFT, OLD SET = bolt2-5t, NEW SET = bolt2-6b, CHANGE NUMBER = 2200
 0, 0, 139.7

*NCOPY, SHIFT, OLD SET = bolt2-6b, NEW SET = bolt2-6t, CHANGE NUMBER = 600
 0, 0, 38.1
```

```
*NCOPY, SHIFT, OLD SET = bolt2-6t, NEW SET = bolt2-7b, CHANGE NUMBER = 2200
 0, 0, 139 7

*NCOPY  SHIFT, OLD SET = bolt2-7b, NEW SET = bolt2-7t, CHANGE NUMBER = 600
 0, 0, 38 1

*NCOPY, SHIFT, OLD SET = bolt2-7t, NEW SET = bolt2-8b, CHANGE NUMBER = 2200
 0, 0, 139 7

*NCOPY, SHIFT, OLD SET = bolt2-8b, NEW SET = bolt2-8t, CHANGE NUMBER = 600
 0, 0, 38 1

*NCOPY, SHIFT, OLD SET = bolt2-8t, NEW SET = sp2-top-b, CHANGE NUMBER = 200
 0, 0, 6 35

*NCOPY, SHIFT, OLD SET = sp2-top-b, NEW SET = sp2-top, CHANGE NUMBER = 600
 0, 0, 38 1

*NFILL, NSET = split-pipe-2
 sp2-bot, sp2-bot-t, 3, 200
 sp2-bot-t, bolt2-1b, 1, 200
 bolt2-1b, bolt2-1t, 3, 200
 bolt2-1t, bolt2-2b, 11, 200
 bolt2-2b, bolt2-2t, 3, 200
 bolt2-2t, bolt2-3b, 11, 200
 bolt2-3b, bolt2-3t, 3, 200
 bolt2-3t, bolt2-4b, 11, 200
 bolt2-4b, bolt2-4t, 3, 200
 bolt2-4t, bolt2-5b, 11, 200
 bolt2-5b, bolt2-5t, 3, 200
 bolt2-5t, bolt2-6b, 11, 200
 bolt2-6b, bolt2-6t, 3, 200
 bolt2-6t, bolt2-7b, 11, 200
 bolt2-7b, bolt2-7t, 3, 200
 bolt2-7t, bolt2-8b, 11, 200
 bolt2-8b, bolt2-8t, 3, 200
 bolt2-8t, sp2-top-b, 1, 200
 sp2-top-b, sp2-top, 3, 200
*ELEMENT, TYPE = C3D8
 400002, 400002, 400003, 400044, 400043, 400202, 400203, 400244, 400243
 400042, 400043, 400044, 400085, 400084, 400243, 400244, 400285, 400284
*ELGEN, ELSET = sp-surface-in-2
 400002, 20, 1, 1, 109, 200, 200
*ELGEN, ELSET = sp-surface-out-2
 400042, 20, 1, 1, 109, 200, 200
*ELSET, ELSET = split-pipe-2
 sp-surface-in-2, sp-surface-out-2
*ELSET, ELSET = bolt - 2, GENERATE
 400842, 400861
 403642, 403661
 406442, 406461
 409242, 409261
 412042, 412061
 414842, 414861
 417642, 417661
 420442, 420461
*ELSET, ELSET = bolt - 2, GENERATE
 401042, 401061
 403842, 403861
 406642, 406661
 409442, 409461
```

```
 412242, 412261
 415042, 415061
 417842, 417861
 420642, 420661
*ELSET, ELSET = bolt - 2, GENERATE
 401242, 401261
 404042, 404061
 406842, 406861
 409642, 409661
 412442, 412461
 415242, 415261
 418042, 418061
 420842, 420861
***
*SURFACE, NAME = sr-surface
 sr-surface
*SURFACE, NAME = sp-surface-in-1
 sp-surface-in-1
*SURFACE, NAME = sp-surface-in-2
 sp-surface-in-2
***
*CONTACT PAIR, INTERACTION = slide, SMALL SLIDING
 sp-surface-in-1, sr-surface
*CONTACT PAIR, INTERACTION = slide, SMALL SLIDING
 sp-surface-in-2, sr-surface
***
*SURFACE INTERACTION, NAME = slide
*FRICTION
 0 025
***
*MPC
 TIE, bolt-1b, bolt2-1b
 TIE, bolt-1t, bolt2-1t
 TIE, bolt-2b, bolt2-2b
 TIE, bolt-2t, bolt2-2t
 TIE, bolt-3b, bolt2-3b
 TIE, bolt-3t, bolt2-3t
 TIE, bolt-4b, bolt2-4b
 TIE, bolt-4t, bolt2-4t
 TIE, bolt-5b, bolt2-5b
 TIE, bolt-5t, bolt2-5t
 TIE, bolt-6b, bolt2-6b
 TIE, bolt-6t, bolt2-6t
 TIE, bolt-7b, bolt2-7b
 TIE, bolt-7t, bolt2-7t
 TIE, bolt-8b, bolt2-8b
 TIE, bolt-8t, bolt2-8t
*CONSTRAINT CONTROLS, NO CHECKS
***
*SOLID SECTION, ELSET = solid round, MATERIAL = solid round
*ELSET, ELSET = split-pipe
 split-pipe-1, split-pipe-2
*SOLID SECTION, ELSET = split-pipe, MATERIAL = split-pipe
*MATERIAL, NAME = solid round
*ELASTIC
 200000, 0 3
*PLASTIC
 414, 0
 563, 0 225
*MATERIAL, NAME = split-pipe
*ELASTIC
 200000, 0 3
```

```
*PLASTIC
 550, 0
 613, 0 27
***
*ELSET, ELSET = e-all
 split-pipe, solid round
*NSET, NSET = n-all
 split-pipe-2, split-pipe-1, solid round
***
***
*STEP
*BUCKLE
 1
*DLOAD
 sr-top, P2, 49 3381310347496
*NODEFILE, MODE = 1
 U
*END STEP
***
***
**Second analysis = Static Riks analysis (on separate input files)
***
***
*IMPERFECTION, FILE = sr60-b2-1, STEP = 1
 1, <Modescale>
***
*STEP, NLGEOM
 Applying axial load
*STATIC, RIKS
 0 1, , , 0 25
*DLOAD
 sr-top, P2, 49 3381310347496
*END STEP
```

F2. Input Files for 1524 mm Long Test Specimens Strengthened with Split Pipes Connected with Stitch Weld (RF60-W1)

```
*HEADING
 Solid round retrofitted with split pipes
 Number of split pipe = 2
 Unit = N-mm
 SR length = 60 in
 SP length = 54 in
 SR diameter = 2 in
 SP OD = 2 875 in
 SP thickness = 0 276 in
 Alpha = 78 75 deg
 No of bolts = 0
 Weld length = 2 in
 Type = w1
 Friction = 0 025
*PARAMETER
 L = 1524
 Modescale = L / 400
***
**DEFINING SOLID ROUND SECTION
***
***
*NODE, NSET = centre
 1, 0, 0, 0
*NODE, NSET = sr-in1-bot
 101, -6 35, 0, 0
 137, 6 35, 0, 0
*NODE, NSET = sr-in2-bot
 201, -12 7, 0, 0
 237, 12 7, 0, 0
*NODE, NSET = sr-in3-bot
 301, -19 05, 0, 0
 337, 19 05, 0, 0
*NODE, NSET = sr-out-bot
 401, -25 4, 0, 0
 437, 25 4, 0, 0
*NGEN, LINE = C, NSET = sr-in1-bot
 101, 137, 12, 1, 0, 0, 0, 0, 0, -1
*NGEN, LINE = C, NSET = sr-in2-bot
 201, 237, 6, 1, 0, 0, 0, 0, 0, -1
*NGEN, LINE = C, NSET = sr-in3-bot
 301, 337, 4, 1, 0, 0, 0, 0, 0, -1
*NGEN, LINE = C, NSET = sr-out-bot
 401, 437, 3, 1, 0, 0, 0, 0, 0, -1
*NCOPY, SHIFT, OLD SET = sr-in1-bot, NEW SET = sr-in1-bot, CHANGE NUMBER = 36

 0, 0, 0, 0, 0, 1, 180
*NCOPY, SHIFT, OLD SET = sr-in2-bot, NEW SET = sr-in2-bot, CHANGE NUMBER = 36

 0, 0, 0, 0, 0, 1, 180
*NCOPY, SHIFT, OLD SET = sr-in3-bot, NEW SET = sr-in3-bot, CHANGE NUMBER = 36

 0, 0, 0, 0, 0, 1, 180
*NCOPY, SHIFT, OLD SET = sr-out-bot, NEW SET = sr-out-bot, CHANGE NUMBER = 36

 0, 0, 0, 0, 0, 1, 180
*NSET, NSET = sr-bot
 centre, sr-in1-bot, sr-in2-bot, sr-in3-bot, sr-out-bot
*NCOPY, SHIFT, OLD SET = sr-bot, NEW SET = sr-top, CHANGE NUMBER = 240000
```

```
 0, 0, 1524

*NFILL, NSET = solid round
 sr-bot, sr-top, 120, 2000
*NSET, NSET = sr-edge1-b
 419
*NSET, NSET = sr-edge2-b
 455
*NCOPY, SHIFT, OLD SET = sr-edge1-b, NEW SET = sr-weld-edge1-1b, CHANGE NUMBER = 12000
 0, 0, 76 2

*NCOPY, SHIFT, OLD SET = sr-weld-edge1-1b, NEW SET = sr-weld-edge1-1t, CHANGE NUMBER = 8000
 0, 0, 50.8

*NCOPY, SHIFT, OLD SET = sr-weld-edge1-1t, NEW SET = sr-weld-edge1-2b, CHANGE NUMBER =
16000
 0, 0, 101 6

*NCOPY, SHIFT, OLD SET = sr-weld-edge1-2b, NEW SET = sr-weld-edge1-2t, CHANGE NUMBER = 8000
 0, 0, 50.8

*NCOPY, SHIFT, OLD SET = sr-weld-edge1-2t, NEW SET = sr-weld-edge1-3b, CHANGE NUMBER =
16000
 0, 0, 101.6

*NCOPY, SHIFT, OLD SET = sr-weld-edge1-3b, NEW SET = sr-weld-edge1-3t, CHANGE NUMBER = 8000
 0, 0, 50 8

*NCOPY, SHIFT, OLD SET = sr-weld-edge1-3t, NEW SET = sr-weld-edge1-4b, CHANGE NUMBER =
16000
 0, 0, 101.6

*NCOPY, SHIFT, OLD SET = sr-weld-edge1-4b, NEW SET = sr-weld-edge1-4t, CHANGE NUMBER = 8000
 0, 0, 50 8

*NCOPY, SHIFT, OLD SET = sr-weld-edge1-4t, NEW SET = sr-weld-edge1-5b, CHANGE NUMBER =
16000
 0, 0, 101.6

*NCOPY, SHIFT, OLD SET = sr-weld-edge1-5b, NEW SET = sr-weld-edge1-5t, CHANGE NUMBER = 8000
 0, 0, 50 8

*NCOPY, SHIFT, OLD SET = sr-weld-edge1-5t, NEW SET = sr-weld-edge1-6b, CHANGE NUMBER = 8000
 0, 0, 50.8

*NCOPY, SHIFT, OLD SET = sr-weld-edge1-6b, NEW SET = sr-weld-edge1-6t, CHANGE NUMBER = 8000
 0, 0, 50.8

*NCOPY, SHIFT, OLD SET = sr-weld-edge1-6t, NEW SET = sr-weld-edge1-7b, CHANGE NUMBER =
16000
 0, 0, 101.6

*NCOPY, SHIFT, OLD SET = sr-weld-edge1-7b, NEW SET = sr-weld-edge1-7t, CHANGE NUMBER = 8000
 0, 0, 50 8

*NCOPY, SHIFT, OLD SET = sr-weld-edge1-7t, NEW SET = sr-weld-edge1-8b, CHANGE NUMBER =
16000
 0, 0, 101.6

*NCOPY, SHIFT, OLD SET = sr-weld-edge1-8b, NEW SET = sr-weld-edge1-8t, CHANGE NUMBER = 8000
 0, 0, 50 8
```

*NCOPY, SHIFT, OLD SET = sr-weld-edge1-8t, NEW SET = sr-weld-edge1-9b, CHANGE NUMBER = 16000
0, 0, 101.6

*NCOPY, SHIFT, OLD SET = sr-weld-edge1-9b, NEW SET = sr-weld-edge1-9t, CHANGE NUMBER = 8000
0, 0, 50.8

*NCOPY, SHIFT, OLD SET = sr-weld-edge1-9t, NEW SET = sr-weld-edge1-10b, CHANGE NUMBER = 16000
0, 0, 101.6

*NCOPY, SHIFT, OLD SET = sr-weld-edge1-10b, NEW SET = sr-weld-edge1-10t, CHANGE NUMBER = 8000
0, 0, 50.8

*NCOPY, SHIFT, OLD SET = sr-weld-edge1-10t, NEW SET = sr-edge1-t, CHANGE NUMBER = 12000
0, 0, 76.2

*NCOPY, SHIFT, OLD SET = sr-edge2-b, NEW SET = sr-weld-edge2-1b, CHANGE NUMBER = 12000
0, 0, 76.2

*NCOPY, SHIFT, OLD SET = sr-weld-edge2-1b, NEW SET = sr-weld-edge2-1t, CHANGE NUMBER = 8000
0, 0, 50.8

*NCOPY, SHIFT, OLD SET = sr-weld-edge2-1t, NEW SET = sr-weld-edge2-2b, CHANGE NUMBER = 16000
0, 0, 101.6

*NCOPY, SHIFT, OLD SET = sr-weld-edge2-2b, NEW SET = sr-weld-edge2-2t, CHANGE NUMBER = 8000
0, 0, 50.8

*NCOPY, SHIFT, OLD SET = sr-weld-edge2-2t, NEW SET = sr-weld-edge2-3b, CHANGE NUMBER = 16000
0, 0, 101.6

*NCOPY, SHIFT, OLD SET = sr-weld-edge2-3b, NEW SET = sr-weld-edge2-3t, CHANGE NUMBER = 8000
0, 0, 50.8

*NCOPY, SHIFT, OLD SET = sr-weld-edge2-3t, NEW SET = sr-weld-edge2-4b, CHANGE NUMBER = 16000
0, 0, 101.6

*NCOPY, SHIFT, OLD SET = sr-weld-edge2-4b, NEW SET = sr-weld-edge2-4t, CHANGE NUMBER = 8000
0, 0, 50.8

*NCOPY, SHIFT, OLD SET = sr-weld-edge2-4t, NEW SET = sr-weld-edge2-5b, CHANGE NUMBER = 16000
0, 0, 101.6

*NCOPY, SHIFT, OLD SET = sr-weld-edge2-5b, NEW SET = sr-weld-edge2-5t, CHANGE NUMBER = 8000
0, 0, 50.8

*NCOPY, SHIFT, OLD SET = sr-weld-edge2-5t, NEW SET = sr-weld-edge2-6b, CHANGE NUMBER = 8000
0, 0, 50.8

*NCOPY, SHIFT, OLD SET = sr-weld-edge2-6b, NEW SET = sr-weld-edge2-6t, CHANGE NUMBER = 8000
0, 0, 50.8

*NCOPY, SHIFT, OLD SET = sr-weld-edge2-6t, NEW SET = sr-weld-edge2-7b, CHANGE NUMBER = 16000
0, 0, 101.6

```
*NCOPY, SHIFT, OLD SET = sr-weld-edge2-7b, NEW SET = sr-weld-edge2-7t, CHANGE NUMBER = 8000
 0, 0, 50 8

*NCOPY, SHIFT, OLD SET = sr-weld-edge2-7t, NEW SET = sr-weld-edge2-8b, CHANGE NUMBER =
16000
 0, 0, 101 6

*NCOPY, SHIFT, OLD SET = sr-weld-edge2-8b, NEW SET = sr-weld-edge2-8t, CHANGE NUMBER = 8000
 0, 0, 50 8

*NCOPY, SHIFT, OLD SET = sr-weld-edge2-8t, NEW SET = sr-weld-edge2-9b, CHANGE NUMBER =
16000
 0, 0, 101 6

*NCOPY, SHIFT, OLD SET = sr-weld-edge2-9b, NEW SET = sr-weld-edge2-9t, CHANGE NUMBER = 8000
 0, 0, 50 8

*NCOPY, SHIFT, OLD SET = sr-weld-edge2-9t, NEW SET = sr-weld-edge2-10b, CHANGE NUMBER =
16000
 0, 0, 101 6

*NCOPY, SHIFT, OLD SET = sr-weld-edge2-10b, NEW SET = sr-weld-edge2-10t, CHANGE NUMBER =
8000
 0, 0, 50 8

*NCOPY, SHIFT, OLD SET = sr-weld-edge2-10t, NEW SET = sr-edge2-t, CHANGE NUMBER = 12000
 0, 0, 76 2

*NFILL, NSET = sr-weld-1
 sr-weld-edge1-1b, sr-weld-edge1-1t, 4, 2000
 sr-weld-edge1-2b, sr-weld-edge1-2t, 4, 2000
 sr-weld-edge1-3b, sr-weld-edge1-3t, 4, 2000
 sr-weld-edge1-4b, sr-weld-edge1-4t, 4, 2000
 sr-weld-edge1-5b, sr-weld-edge1-5t, 4, 2000
 sr-weld-edge1-6b, sr-weld-edge1-6t, 4, 2000
 sr-weld-edge1-7b, sr-weld-edge1-7t, 4, 2000
 sr-weld-edge1-8b, sr-weld-edge1-8t, 4, 2000
 sr-weld-edge1-9b, sr-weld-edge1-9t, 4, 2000
 sr-weld-edge1-10b, sr-weld-edge1-10t, 4, 2000
*NFILL, NSET = sr-weld-2
 sr-weld-edge2-1b, sr-weld-edge2-1t, 4, 2000
 sr-weld-edge2-2b, sr-weld-edge2-2t, 4, 2000
 sr-weld-edge2-3b, sr-weld-edge2-3t, 4, 2000
 sr-weld-edge2-4b, sr-weld-edge2-4t, 4, 2000
 sr-weld-edge2-5b, sr-weld-edge2-5t, 4, 2000
 sr-weld-edge2-6b, sr-weld-edge2-6t, 4, 2000
 sr-weld-edge2-7b, sr-weld-edge2-7t, 4, 2000
 sr-weld-edge2-8b, sr-weld-edge2-8t, 4, 2000
 sr-weld-edge2-9b, sr-weld-edge2-9t, 4, 2000
 sr-weld-edge2-10b, sr-weld-edge2-10t, 4, 2000
*NSET, NSET = sr2-edge1-b
 422
*NSET, NSET = sr2-edge2-b
 458
*NCOPY, SHIFT, OLD SET = sr2-edge1-b, NEW SET = sr2-weld-edge1-1b, CHANGE NUMBER = 12000
 0, 0, 76 2

*NCOPY, SHIFT, OLD SET = sr2-weld-edge1-1b, NEW SET = sr2-weld-edge1-1t, CHANGE NUMBER =
8000
 0, 0, 50 8
```

*NCOPY, SHIFT, OLD SET = sr2-weld-edge1-1t, NEW SET = sr2-weld-edge1-2b, CHANGE NUMBER = 16000
0, 0, 101 6

*NCOPY, SHIFT, OLD SET = sr2-weld-edge1-2b, NEW SET = sr2-weld-edge1-2t, CHANGE NUMBER = 8000
0, 0, 50 8

*NCOPY, SHIFT, OLD SET = sr2-weld-edge1-2t, NEW SET = sr2-weld-edge1-3b, CHANGE NUMBER = 16000
0, 0, 101 6

*NCOPY, SHIFT, OLD SET = sr2-weld-edge1-3b, NEW SET = sr2-weld-edge1-3t, CHANGE NUMBER = 8000
0, 0, 50 8

*NCOPY, SHIFT, OLD SET = sr2-weld-edge1-3t, NEW SET = sr2-weld-edge1-4b, CHANGE NUMBER = 16000
0, 0, 101 6

*NCOPY, SHIFT, OLD SET = sr2-weld-edge1-4b, NEW SET = sr2-weld-edge1-4t, CHANGE NUMBER = 8000
0, 0, 50 8

*NCOPY, SHIFT, OLD SET = sr2-weld-edge1-4t, NEW SET = sr2-weld-edge1-5b, CHANGE NUMBER = 16000
0, 0, 101 6

*NCOPY, SHIFT, OLD SET = sr2-weld-edge1-5b, NEW SET = sr2-weld-edge1-5t, CHANGE NUMBER = 8000
0, 0, 50 8

*NCOPY, SHIFT, OLD SET = sr2-weld-edge1-5t, NEW SET = sr2-weld-edge1-6b, CHANGE NUMBER = 8000
0, 0, 50 8

*NCOPY, SHIFT, OLD SET = sr2-weld-edge1-6b, NEW SET = sr2-weld-edge1-6t, CHANGE NUMBER = 8000
0, 0, 50 8

*NCOPY, SHIFT, OLD SET = sr2-weld-edge1-6t, NEW SET = sr2-weld-edge1-7b, CHANGE NUMBER = 16000
0, 0, 101 6

*NCOPY, SHIFT, OLD SET = sr2-weld-edge1-7b, NEW SET = sr2-weld-edge1-7t, CHANGE NUMBER = 8000
0, 0, 50 8

*NCOPY, SHIFT, OLD SET = sr2-weld-edge1-7t, NEW SET = sr2-weld-edge1-8b, CHANGE NUMBER = 16000
0, 0, 101 6

*NCOPY, SHIFT, OLD SET = sr2-weld-edge1-8b, NEW SET = sr2-weld-edge1-8t, CHANGE NUMBER = 8000
0, 0, 50 8

*NCOPY, SHIFT, OLD SET = sr2-weld-edge1-8t, NEW SET = sr2-weld-edge1-9b, CHANGE NUMBER = 16000
0, 0, 101 6

*NCOPY, SHIFT, OLD SET = sr2-weld-edge1-9b, NEW SET = sr2-weld-edge1-9t, CHANGE NUMBER = 8000

0, 0, 50 8

*NCOPY, SHIFT, OLD SET = sr2-weld-edge1-9t, NEW SET = sr2-weld-edge1-10b, CHANGE NUMBER = 16000
0, 0, 101 6

*NCOPY, SHIFT, OLD SET = sr2-weld-edge1-10b, NEW SET = sr2-weld-edge1-10t, CHANGE NUMBER = 8000
0, 0, 50 8

*NCOPY, SHIFT, OLD SET = sr2-weld-edge1-10t, NEW SET = sr2-edge1-t, CHANGE NUMBER = 12000
0, 0, 76 2

*NCOPY, SHIFT, OLD SET = sr2-edge2-b, NEW SET = sr2-weld-edge2-1b, CHANGE NUMBER = 12000
0, 0, 76 2

*NCOPY, SHIFT, OLD SET = sr2-weld-edge2-1b, NEW SET = sr2-weld-edge2-1t, CHANGE NUMBER = 8000
0, 0, 50 8

*NCOPY, SHIFT, OLD SET = sr2-weld-edge2-1t, NEW SET = sr2-weld-edge2-2b, CHANGE NUMBER = 16000
0, 0, 101 6

*NCOPY, SHIFT, OLD SET = sr2-weld-edge2-2b, NEW SET = sr2-weld-edge2-2t, CHANGE NUMBER = 8000
0, 0, 50 8

*NCOPY, SHIFT, OLD SET = sr2-weld-edge2-2t, NEW SET = sr2-weld-edge2-3b, CHANGE NUMBER = 16000
0, 0, 101 6

*NCOPY, SHIFT, OLD SET = sr2-weld-edge2-3b, NEW SET = sr2-weld-edge2-3t, CHANGE NUMBER = 8000
0, 0, 50 8

*NCOPY, SHIFT, OLD SET = sr2-weld-edge2-3t, NEW SET = sr2-weld-edge2-4b, CHANGE NUMBER = 16000
0, 0, 101 6

*NCOPY, SHIFT, OLD SET = sr2-weld-edge2-4b, NEW SET = sr2-weld-edge2-4t, CHANGE NUMBER = 8000
0, 0, 50 8

*NCOPY, SHIFT, OLD SET = sr2-weld-edge2-4t, NEW SET = sr2-weld-edge2-5b, CHANGE NUMBER = 16000
0, 0, 101 6

*NCOPY, SHIFT, OLD SET = sr2-weld-edge2-5b, NEW SET = sr2-weld-edge2-5t, CHANGE NUMBER = 8000
0, 0, 50 8

*NCOPY, SHIFT, OLD SET = sr2-weld-edge2-5t, NEW SET = sr2-weld-edge2-6b, CHANGE NUMBER = 8000
0, 0, 50 8

*NCOPY, SHIFT, OLD SET = sr2-weld-edge2-6b, NEW SET = sr2-weld-edge2-6t, CHANGE NUMBER = 8000
0, 0, 50 8

*NCOPY, SHIFT, OLD SET = sr2-weld-edge2-6t, NEW SET = sr2-weld-edge2-7b, CHANGE NUMBER = 16000

```
 0  0, 101 6

*NCOPY, SHIFT, OLD SET = sr2-weld-edge2-7b, NEW SET = sr2-weld-edge2-7t, CHANGE NUMBER =
8000
 0, 0, 50 8

*NCOPY, SHIFT, OLD SET = sr2-weld-edge2-7t, NEW SET = sr2-weld-edge2-8b, CHANGE NUMBER =
16000
 0, 0, 101 6

*NCOPY, SHIFT, OLD SET = sr2-weld-edge2-8b, NEW SET = sr2-weld-edge2-8t, CHANGE NUMBER =
8000
 0, 0, 50 8

*NCOPY, SHIFT, OLD SET = sr2-weld-edge2-8t, NEW SET = sr2-weld-edge2-9b, CHANGE NUMBER =
16000
 0, 0, 101 6

*NCOPY, SHIFT, OLD SET = sr2-weld-edge2-9b, NEW SET = sr2-weld-edge2-9t, CHANGE NUMBER =
8000
 0, 0, 50 8

*NCOPY, SHIFT, OLD SET = sr2-weld-edge2-9t, NEW SET = sr2-weld-edge2-10b, CHANGE NUMBER =
16000
 0, 0, 101 6

*NCOPY, SHIFT, OLD SET = sr2-weld-edge2-10b, NEW SET = sr2-weld-edge2-10t, CHANGE NUMBER =
8000
 0, 0, 50 8

*NCOPY, SHIFT, OLD SET = sr2-weld-edge2-10t, NEW SET = sr2-edge2-t, CHANGE NUMBER = 12000
 0, 0, 76 2

*NFILL, NSET = sr2-weld-1
 sr2-weld-edge1-1b, sr2-weld-edge1-1t, 4, 2000
 sr2-weld-edge1-2b, sr2-weld-edge1-2t, 4, 2000
 sr2-weld-edge1-3b, sr2-weld-edge1-3t, 4, 2000
 sr2-weld-edge1-4b, sr2-weld-edge1-4t, 4, 2000
 sr2-weld-edge1-5b, sr2-weld-edge1-5t, 4, 2000
 sr2-weld-edge1-6b, sr2-weld-edge1-6t, 4, 2000
 sr2-weld-edge1-7b, sr2-weld-edge1-7t, 4, 2000
 sr2-weld-edge1-8b, sr2-weld-edge1-8t, 4, 2000
 sr2-weld-edge1-9b, sr2-weld-edge1-9t, 4, 2000
 sr2-weld-edge1-10b, sr2-weld-edge1-10t, 4, 2000
*NFILL, NSET = sr2-weld-2
 sr2-weld-edge2-1b, sr2-weld-edge2-1t, 4, 2000
 sr2-weld-edge2-2b, sr2-weld-edge2-2t, 4, 2000
 sr2-weld-edge2-3b, sr2-weld-edge2-3t, 4, 2000
 sr2-weld-edge2-4b, sr2-weld-edge2-4t, 4, 2000
 sr2-weld-edge2-5b, sr2-weld-edge2-5t, 4, 2000
 sr2-weld-edge2-6b, sr2-weld-edge2-6t, 4, 2000
 sr2-weld-edge2-7b, sr2-weld-edge2-7t, 4, 2000
 sr2-weld-edge2-8b, sr2-weld-edge2-8t, 4, 2000
 sr2-weld-edge2-9b, sr2-weld-edge2-9t, 4, 2000
 sr2-weld-edge2-10b, sr2-weld-edge2-10t, 4, 2000
*ELEMENT, TYPE = C3D6, ELSET = sr-centre
 101, 1, 113, 101, 2001, 2113, 2101
 102, 1, 125, 113, 2001, 2125, 2113
 103, 1, 137, 125, 2001, 2137, 2125
 104, 1, 149, 137, 2001, 2149, 2137
 105, 1, 161, 149, 2001, 2161, 2149
 106, 1, 101, 161, 2001, 2101, 2161
```

```
*ELEMENT, TYPE = C3D6, ELSET = sr-inside
 201, 101, 207, 201, 2101, 2207, 2201
 202, 101, 113, 207, 2101, 2113, 2207
 203, 113, 213, 207, 2113, 2213, 2207
 204, 113, 219, 213, 2113, 2219, 2213
 205, 113, 125, 219, 2113, 2125, 2219
 206, 125, 225, 219, 2125, 2225, 2219
 207, 125, 231, 225, 2125, 2231, 2225
 208, 137, 231, 125, 2137, 2231, 2125
 209, 137, 237, 231, 2137, 2237, 2231
 210, 137, 243, 237, 2137, 2243, 2237
 211, 137, 149, 243, 2137, 2149, 2243
 212, 149, 249, 243, 2149, 2249, 2243
 213, 149, 255, 249, 2149, 2255, 2249
 214, 149, 161, 255, 2149, 2161, 2255
 215, 161, 261, 255, 2161, 2261, 2255
 216, 161, 267, 261, 2161, 2267, 2261
 217, 101, 267, 161, 2101, 2267, 2161
 218, 101, 201, 267, 2101, 2201, 2267
 301, 201, 305, 301, 2201, 2305, 2301
 302, 201, 207, 305, 2201, 2207, 2305
 303, 207, 309, 305, 2207, 2309, 2305
 304, 207, 213, 309, 2207, 2213, 2309
 305, 213, 313, 309, 2213, 2313, 2309
 306, 213, 317, 313, 2213, 2317, 2313
 307, 213, 219, 317, 2213, 2219, 2317
 308, 219, 321, 317, 2219, 2321, 2317
 309, 321, 219, 225, 2321, 2219, 2225
 310, 225, 325, 321, 2225, 2325, 2321
 311, 225, 329, 325, 2225, 2329, 2325
 312, 225, 231, 329, 2225, 2231, 2329
 313, 231, 333, 329, 2231, 2333, 2329
 314, 237, 333, 231, 2237, 2333, 2231
 315, 237, 337, 333, 2237, 2337, 2333
 316, 237, 341, 337, 2237, 2341, 2337
 317, 237, 243, 341, 2237, 2243, 2341
 318, 243, 345, 341, 2243, 2345, 2341
 319, 243, 249, 345, 2243, 2249, 2345
 320, 249, 349, 345, 2249, 2349, 2345
 321, 249, 353, 349, 2249, 2353, 2349
 322, 249, 255, 353, 2249, 2255, 2353
 323, 255, 357, 353, 2255, 2357, 2353
 324, 357, 255, 261, 2357, 2255, 2261
 325, 261, 361, 357, 2261, 2361, 2357
 326, 261, 365, 361, 2261, 2365, 2361
 327, 261, 267, 365, 2261, 2267, 2365
 328, 267, 369, 365, 2267, 2369, 2365
 329, 201, 369, 267, 2201, 2369, 2267
 330, 201, 301, 369, 2201, 2301, 2369
*ELEMENT, TYPE = C3D6, ELSET = sr-surface
 401, 301, 404, 401, 2301, 2404, 2401
 402, 301, 305, 404, 2301, 2305, 2404
 403, 305, 407, 404, 2305, 2407, 2404
 404, 305, 309, 407, 2305, 2309, 2407
 405, 309, 410, 407, 2309, 2410, 2407
 406, 309, 313, 410, 2309, 2313, 2410
 407, 313, 413, 410, 2313, 2413, 2410
 408, 313, 416, 413, 2313, 2416, 2413
 409, 313, 317, 416, 2313, 2317, 2416
 410, 317, 419, 416, 2317, 2419, 2416
 411, 317, 321, 419, 2317, 2321, 2419
 412, 321, 422, 419, 2321, 2422, 2419
```

413, 321, 325, 422, 2321, 2325, 2422
414, 325, 425, 422, 2325, 2425, 2422
415, 325, 428, 425, 2325, 2428, 2425
416, 325, 329, 428, 2325, 2329, 2428
417, 329, 431, 428, 2329, 2431, 2428
418, 329, 333, 431, 2329, 2333, 2431
419, 333, 434, 431, 2333, 2434, 2431
420, 337, 434, 333, 2337, 2434, 2333
421, 337, 437, 434, 2337, 2437, 2434
422, 337, 440, 437, 2337, 2440, 2437
423, 337, 341, 440, 2337, 2341, 2440
424, 341, 443, 440, 2341, 2443, 2440
425, 341, 345, 443, 2341, 2345, 2443
426, 345, 446, 443, 2345, 2446, 2443
427, 345, 349, 446, 2345, 2349, 2446
428, 349, 449, 446, 2349, 2449, 2446
429, 349, 452, 449, 2349, 2452, 2449
430, 349, 353, 452, 2349, 2353, 2452
431, 353, 455, 452, 2353, 2455, 2452
432, 353, 357, 455, 2353, 2357, 2455
433, 357, 458, 455, 2357, 2458, 2455
434, 357, 361, 458, 2357, 2361, 2458
435, 361, 461, 458, 2361, 2461, 2458
436, 361, 464, 461, 2361, 2464, 2461
437, 361, 365, 464, 2361, 2365, 2464
438, 365, 467, 464, 2365, 2467, 2464
439, 365, 369, 467, 2365, 2369, 2467
440, 369, 470, 467, 2369, 2470, 2467
441, 301, 470, 369, 2301, 2470, 2369
442, 301, 401, 470, 2301, 2401, 2470
*ELGEN, ELSET = sr-centre
101, 120, 2000, 2000
102, 120, 2000, 2000
103, 120, 2000, 2000
104, 120, 2000, 2000
105, 120, 2000, 2000
106, 120, 2000, 2000
*ELGEN, ELSET = sr-inside
201, 120, 2000, 2000
202, 120, 2000, 2000
203, 120, 2000, 2000
204, 120, 2000, 2000
205, 120, 2000, 2000
206, 120, 2000, 2000
207, 120, 2000, 2000
208, 120, 2000, 2000
209, 120, 2000, 2000
210, 120, 2000, 2000
211, 120, 2000, 2000
212, 120, 2000, 2000
213, 120, 2000, 2000
214, 120, 2000, 2000
215, 120, 2000, 2000
216, 120, 2000, 2000
217, 120, 2000, 2000
218, 120, 2000, 2000
301, 120, 2000, 2000
302, 120, 2000, 2000
303, 120, 2000, 2000
304, 120, 2000, 2000
305, 120, 2000, 2000
306, 120, 2000, 2000

307, 120, 2000, 2000
308, 120, 2000, 2000
309, 120, 2000, 2000
310, 120, 2000, 2000
311, 120, 2000, 2000
312, 120, 2000, 2000
313, 120, 2000, 2000
314, 120, 2000, 2000
315, 120, 2000, 2000
316, 120, 2000, 2000
317, 120, 2000, 2000
318, 120, 2000, 2000
319, 120, 2000, 2000
320, 120, 2000, 2000
321, 120, 2000, 2000
322, 120, 2000, 2000
323, 120, 2000, 2000
324, 120, 2000, 2000
325, 120, 2000, 2000
326, 120, 2000, 2000
327, 120, 2000, 2000
328, 120, 2000, 2000
329, 120, 2000, 2000
330, 120, 2000, 2000
*ELGEN, ELSET = sr-surface
401, 120, 2000, 2000
402, 120, 2000, 2000
403, 120, 2000, 2000
404, 120, 2000, 2000
405, 120, 2000, 2000
406, 120, 2000, 2000
407, 120, 2000, 2000
408, 120, 2000, 2000
409, 120, 2000, 2000
410, 120, 2000, 2000
411, 120, 2000, 2000
412, 120, 2000, 2000
413, 120, 2000, 2000
414, 120, 2000, 2000
415, 120, 2000, 2000
416, 120, 2000, 2000
417, 120, 2000, 2000
418, 120, 2000, 2000
419, 120, 2000, 2000
420, 120, 2000, 2000
421, 120, 2000, 2000
422, 120, 2000, 2000
423, 120, 2000, 2000
424, 120, 2000, 2000
425, 120, 2000, 2000
426, 120, 2000, 2000
427, 120, 2000, 2000
428, 120, 2000, 2000
429, 120, 2000, 2000
430, 120, 2000, 2000
431, 120, 2000, 2000
432, 120, 2000, 2000
433, 120, 2000, 2000
434, 120, 2000, 2000
435, 120, 2000, 2000
436, 120, 2000, 2000
437, 120, 2000, 2000

```
 438, 120, 2000, 2000
 439, 120, 2000, 2000
 440, 120, 2000, 2000
 441, 120, 2000, 2000
 442, 120, 2000, 2000
*ELSET, ELSET = sr-top
 238101
 238102
 238103
 238104
 238105
 238106
 238201
 238202
 238203
 238204
 238205
 238206
 238207
 238208
 238209
 238210
 238211
 238212
 238213
 238214
 238215
 238216
 238217
 238218
 238301
 238302
 238303
 238304
 238305
 238306
 238307
 238308
 238309
 238310
 238311
 238312
 238313
 238314
 238315
 238316
 238317
 238318
 238319
 238320
 238321
 238322
 238323
 238324
 238325
 238326
 238327
 238328
 238329
 238330
 238401
 238402
```

```
 238403
 238404
 238405
 238406
 238407
 238408
 238409
 238410
 238411
 238412
 238413
 238414
 238415
 238416
 238417
 238418
 238419
 238420
 238421
 238422
 238423
 238424
 238425
 238426
 238427
 238428
 238429
 238430
 238431
 238432
 238433
 238434
 238435
 238436
 238437
 238438
 238439
 238440
 238441
 238442
*ELSET, ELSET = solid round
 sr-centre, sr-inside, sr-surface
***
*EQUATION
 2
 240401, 3, 1, 240404, 3, -1
*EQUATION
 2
 240404, 3, 1, 240407, 3, -1
*EQUATION
 2
 240407, 3, 1, 240410, 3, -1
*EQUATION
 2
 240410, 3, 1, 240413, 3, -1
*EQUATION
 2
 240413, 3, 1, 240416, 3, -1
*EQUATION
 2
 240416, 3, 1, 240419, 3, -1
*EQUATION
```

```
 2
 240419, 3, 1, 240422, 3, -1
*EQUATION
 2
 240422, 3, 1, 240425, 3, -1
*EQUATION
 2
 240425, 3, 1, 240428, 3, -1
*EQUATION
 2
 240428, 3, 1, 240431, 3, -1
*EQUATION
 2
 240431, 3, 1, 240434, 3, -1
*EQUATION
 2
 240434, 3, 1, 240437, 3, -1
*EQUATION
 2
 240437, 3, 1, 240440, 3, -1
*EQUATION
 2
 240440, 3, 1, 240443, 3, -1
*EQUATION
 2
 240443, 3, 1, 240446, 3, -1
*EQUATION
 2
 240446, 3, 1, 240449, 3, -1
*EQUATION
 2
 240449, 3, 1, 240452, 3, -1
*EQUATION
 2
 240452, 3, 1, 240455, 3, -1
*EQUATION
 2
 240455, 3, 1, 240458, 3, -1
*EQUATION
 2
 240458, 3, 1, 240461, 3, -1
*EQUATION
 2
 240461, 3, 1, 240464, 3, -1
*EQUATION
 2
 240464, 3, 1, 240467, 3, -1
*EQUATION
 2
 240467, 3, 1, 240470, 3, -1
*EQUATION
 2
 240470, 3, 1, 240301, 3, -1
*EQUATION
 2
 240301, 3, 1, 240305, 3, -1
*EQUATION
 2
 240305, 3, 1, 240309, 3, -1
*EQUATION
 2
 240309, 3, 1, 240313, 3, -1
```

```
*EQUATION
 2
 240313, 3, 1, 240317, 3, -1
*EQUATION
 2
 240317, 3, 1, 240321, 3, -1
*EQUATION
 2
 240321, 3, 1, 240325, 3, -1
*EQUATION
 2
 240325, 3, 1, 240329, 3, -1
*EQUATION
 2
 240329, 3, 1, 240333, 3, -1
*EQUATION
 2
 240333, 3, 1, 240337, 3, -1
*EQUATION
 2
 240337, 3, 1, 240341, 3, -1
*EQUATION
 2
 240341, 3, 1, 240345, 3, -1
*EQUATION
 2
 240345, 3, 1, 240349, 3, -1
*EQUATION
 2
 240349, 3, 1, 240353, 3, -1
*EQUATION
 2
 240353, 3, 1, 240357, 3, -1
*EQUATION
 2
 240357, 3, 1, 240361, 3, -1
*EQUATION
 2
 240361, 3, 1, 240365, 3, -1
*EQUATION
 2
 240365, 3, 1, 240369, 3, -1
*EQUATION
 2
 240369, 3, 1, 240201, 3, -1
*EQUATION
 2
 240201, 3, 1, 240207, 3, -1
*EQUATION
 2
 240207, 3, 1, 240213, 3, -1
*EQUATION
 2
 240213, 3, 1, 240219, 3, -1
*EQUATION
 2
 240219, 3, 1, 240225, 3, -1
*EQUATION
 2
 240225, 3, 1, 240231, 3, -1
*EQUATION
 2
```

```
 240231, 3, 1, 240237, 3, -1
*EQUATION
 2
 240237, 3, 1, 240243, 3, -1
*EQUATION
 2
 240243, 3, 1, 240249, 3, -1
*EQUATION
 2
 240249, 3, 1, 240255, 3, -1
*EQUATION
 2
 240255, 3, 1, 240261, 3, -1
*EQUATION
 2
 240261, 3, 1, 240267, 3, -1
*EQUATION
 2
 240267, 3, 1, 240101, 3, -1
*EQUATION
 2
 240101, 3, 1, 240113, 3, -1
*EQUATION
 2
 240113, 3, 1, 240125, 3, -1
*EQUATION
 2
 240125, 3, 1, 240137, 3, -1
*EQUATION
 2
 240137, 3, 1, 240149, 3, -1
*EQUATION
 2
 240149, 3, 1, 240161, 3, -1
***
*BOUNDARY
 sr-bot, 1, 3
 sr-top, 1, 2
***
**DEFINING SPLIT PIPE 1 SECTION
***
**Number of section per quarter = 10
**Number of section of split pipe thickness = 2
***
*NODE
 300001, 4 1021, 0, 76 2
*NODE, NSET = sp-in-bot
 300002, -1 65347418915202, 28 9352254209841, 76 2
 300022, -1 65347418915202, -28 9352254209841, 76 2
*NGEN, LINE = C, NSET = sp-in-bot
 300002, 300022, 1, 300001, 4 1021, 0, 76 2, 0, 0, 77 2
*NODE, NSET = sp-out-bot
 300084, -1 65347418915202, 35 9456254209841, 76 2
 300104, -1 65347418915202, -35 9456254209841, 76 2
*NGEN, LINE = C, NSET = sp-out-bot
 300084, 300104, 1, 300001, 4 1021, 0, 76 2, 0, 0, 77 2
*NFILL, NSET = sp-bot
 sp-in-bot, sp-out-bot, 2, 41
*NSET, NSET = edge1-1b
 300002, 300043, 300084
*NSET, NSET = edge2-1b
 300022, 300063, 300104
```

```
*NCOPY, SHIFT, OLD SET = sp-bot, NEW SET = sp-weld-1t, CHANGE NUMBER = 800
 0, 0, 50 8

*NCOPY, SHIFT, OLD SET = sp-weld-1t, NEW SET = sp-weld-2b, CHANGE NUMBER = 1600
 0, 0, 101 6

*NCOPY, SHIFT, OLD SET = sp-weld-2b, NEW SET = sp-weld-2t, CHANGE NUMBER = 800
 0, 0, 50 8

*NCOPY, SHIFT, OLD SET = sp-weld-2t, NEW SET = sp-weld-3b, CHANGE NUMBER = 1600
 0, 0, 101 6

*NCOPY, SHIFT, OLD SET = sp-weld-3b, NEW SET = sp-weld-3t, CHANGE NUMBER = 800
 0, 0, 50 8

*NCOPY, SHIFT, OLD SET = sp-weld-3t, NEW SET = sp-weld-4b, CHANGE NUMBER = 1600
 0, 0, 101 6

*NCOPY, SHIFT, OLD SET = sp-weld-4b, NEW SET = sp-weld-4t, CHANGE NUMBER = 800
 0, 0, 50 8

*NCOPY, SHIFT, OLD SET = sp-weld-4t, NEW SET = sp-weld-5b, CHANGE NUMBER = 1600
 0, 0, 101 6

*NCOPY, SHIFT, OLD SET = sp-weld-5b, NEW SET = sp-weld-5t, CHANGE NUMBER = 800
 0, 0, 50 8

*NCOPY, SHIFT, OLD SET = sp-weld-5t, NEW SET = sp-weld-6b, CHANGE NUMBER = 800
 0, 0, 50 8

*NCOPY, SHIFT, OLD SET = sp-weld-6b, NEW SET = sp-weld-6t, CHANGE NUMBER = 800
 0, 0, 50 8

*NCOPY, SHIFT, OLD SET = sp-weld-6t, NEW SET = sp-weld-7b, CHANGE NUMBER = 1600
 0, 0, 101 6

*NCOPY, SHIFT, OLD SET = sp-weld-7b, NEW SET = sp-weld-7t, CHANGE NUMBER = 800
 0, 0, 50 8

*NCOPY, SHIFT, OLD SET = sp-weld-7t, NEW SET = sp-weld-8b, CHANGE NUMBER = 1600
 0, 0, 101 6

*NCOPY, SHIFT, OLD SET = sp-weld-8b, NEW SET = sp-weld-8t, CHANGE NUMBER = 800
 0, 0, 50 8

*NCOPY, SHIFT, OLD SET = sp-weld-8t, NEW SET = sp-weld-9b, CHANGE NUMBER = 1600
 0, 0, 101 6

*NCOPY, SHIFT, OLD SET = sp-weld-9b, NEW SET = sp-weld-9t, CHANGE NUMBER = 800
 0, 0, 50 8

*NCOPY, SHIFT, OLD SET = sp-weld-9t, NEW SET = sp-weld-10b, CHANGE NUMBER = 1600
 0, 0, 101 6

*NCOPY, SHIFT, OLD SET = sp-weld-10b, NEW SET = sp-weld-10t, CHANGE NUMBER = 800
 0, 0, 50 8

*NFILL, NSET = split-pipe-1
 sp-bot, sp-weld-1t, 4, 200
 sp-weld-1t, sp-weld-2b, 8, 200
 sp-weld-2b, sp-weld-2t, 4, 200
 sp-weld-2t, sp-weld-3b, 8, 200
```

```
sp-weld-3b, sp-weld-3t, 4, 200
sp-weld-3t, sp-weld-4b, 8, 200
sp-weld-4b, sp-weld-4t, 4, 200
sp-weld-4t, sp-weld-5b, 8, 200
sp-weld-5b, sp-weld-5t, 4, 200
sp-weld-5t, sp-weld-6b, 4, 200
sp-weld-6b, sp-weld-6t, 4, 200
sp-weld-6t, sp-weld-7b, 8, 200
sp-weld-7b, sp-weld-7t, 4, 200
sp-weld-7t, sp-weld-8b, 8, 200
sp-weld-8b, sp-weld-8t, 4, 200
sp-weld-8t, sp-weld-9b, 8, 200
sp-weld-9b, sp-weld-9t, 4, 200
sp-weld-9t, sp-weld-10b, 8, 200
sp-weld-10b, sp-weld-10t, 4, 200
*NSET, NSET = weld-edge1-1b
300084
*NSET, NSET = weld-edge1-1t
300884
*NSET, NSET = weld-edge1-2b
302484
*NSET, NSET = weld-edge1-2t
303284
*NSET, NSET = weld-edge1-3b
304884
*NSET, NSET = weld-edge1-3t
305684
*NSET, NSET = weld-edge1-4b
307284
*NSET, NSET = weld-edge1-4t
308084
*NSET, NSET = weld-edge1-5b
309684
*NSET, NSET = weld-edge1-5t
310484
*NSET, NSET = weld-edge1-6b
311284
*NSET, NSET = weld-edge1-6t
312084
*NSET, NSET = weld-edge1-7b
313684
*NSET, NSET = weld-edge1-7t
314484
*NSET, NSET = weld-edge1-8b
316084
*NSET, NSET = weld-edge1-8t
316884
*NSET, NSET = weld-edge1-9b
318484
*NSET, NSET = weld-edge1-9t
319284
*NSET, NSET = weld-edge1-10b
320884
*NSET, NSET = weld-edge1-10t
321684
*NFILL, NSET = sp-weld-1
weld-edge1-1b, weld-edge1-1t, 4, 200
weld-edge1-2b, weld-edge1-2t, 4, 200
weld-edge1-3b, weld-edge1-3t, 4, 200
weld-edge1-4b, weld-edge1-4t, 4, 200
weld-edge1-5b, weld-edge1-5t, 4, 200
weld-edge1-6b, weld-edge1-6t, 4, 200
```

```
 weld-edge1-7b, weld-edge1-7t, 4, 200
 weld-edge1-8b, weld-edge1-8t, 4, 200
 weld-edge1-9b, weld-edge1-9t, 4, 200
 weld-edge1-10b, weld-edge1-10t, 4, 200
*NSET, NSET = weld-edge2-1b
 300104
*NSET, NSET = weld-edge2-1t
 300904
*NSET, NSET = weld-edge2-2b
 302504
*NSET, NSET = weld-edge2-2t
 303304
*NSET, NSET = weld-edge2-3b
 304904
*NSET, NSET = weld-edge2-3t
 305704
*NSET, NSET = weld-edge2-4b
 307304
*NSET, NSET = weld-edge2-4t
 308104
*NSET, NSET = weld-edge2-5b
 309704
*NSET, NSET = weld-edge2-5t
 310504
*NSET, NSET = weld-edge2-6b
 311304
*NSET, NSET = weld-edge2-6t
 312104
*NSET, NSET = weld-edge2-7b
 313704
*NSET, NSET = weld-edge2-7t
 314504
*NSET, NSET = weld-edge2-8b
 316104
*NSET, NSET = weld-edge2-8t
 316904
*NSET, NSET = weld-edge2-9b
 318504
*NSET, NSET = weld-edge2-9t
 319304
*NSET, NSET = weld-edge2-10b
 320904
*NSET, NSET = weld-edge2-10t
 321704
*NFILL, NSET = sp-weld-2
 weld-edge2-1b, weld-edge2-1t, 4, 200
 weld-edge2-2b, weld-edge2-2t, 4, 200
 weld-edge2-3b, weld-edge2-3t, 4, 200
 weld-edge2-4b, weld-edge2-4t, 4, 200
 weld-edge2-5b, weld-edge2-5t, 4, 200
 weld-edge2-6b, weld-edge2-6t, 4, 200
 weld-edge2-7b, weld-edge2-7t, 4, 200
 weld-edge2-8b, weld-edge2-8t, 4, 200
 weld-edge2-9b, weld-edge2-9t, 4, 200
 weld-edge2-10b, weld-edge2-10t, 4, 200
*ELEMENT, TYPE = C3D8
 300002, 300002, 300043, 300044, 300003, 300202, 300243, 300244, 300203
 300042, 300043, 300084, 300085, 300044, 300243, 300284, 300285, 300244
*ELGEN, ELSET = sp-surface-in-1
 300002, 20, 1, 1, 108, 200, 200
*ELGEN, ELSET = sp-surface-out-1
 300042, 20, 1, 1, 108, 200, 200
```

```
*ELSET, ELSET = split-pipe-1
 sp-surface-in-1, sp-surface-out-1
***
**DEFINING SPLIT PIPE 2 SECTION
***
**Number of section per quarter = 10
**Number of section of split pipe thickness = 2
***
*NODE
 400001, -4 1021, 0, 76 2
*NODE, NSET = sp2-in-bot
 400002, 1 65347418915202, 28 9352254209841, 76 2
 400022, 1 65347418915202, -28 9352254209841, 76 2
*NGEN, LINE = C, NSET = sp2-in-bot
 400002, 400022, 1, 400001, -4 1021, 0, 76 2, 0, 0, -1
*NODE, NSET = sp2-out-bot
 400084, 1 65347418915202, 35 9456254209841, 76 2
 400104, 1 65347418915202, -35 9456254209841, 76 2
*NGEN, LINE = C, NSET = sp2-out-bot
 400084, 400104, 1, 400001, -4 1021, 0, 76 2, 0, 0, -1
*NFILL, NSET = sp2-bot
 sp2-in-bot, sp2-out-bot, 2, 41
*NSET, NSET = sp2-edge1-1b
 400002, 400043, 400084
*NSET, NSET = sp2-edge2-1b
 400022, 400063, 400104
*NCOPY, SHIFT, OLD SET = sp2-bot, NEW SET = sp2-weld-1t, CHANGE NUMBER = 800
 0, 0, 50 8

*NCOPY, SHIFT, OLD SET = sp2-weld-1t, NEW SET = sp2-weld-2b, CHANGE NUMBER = 1600
 0, 0, 101 6

*NCOPY, SHIFT, OLD SET = sp2-weld-2b, NEW SET = sp2-weld-2t, CHANGE NUMBER = 800
 0, 0, 50 8

*NCOPY, SHIFT, OLD SET = sp2-weld-2t, NEW SET = sp2-weld-3b, CHANGE NUMBER = 1600
 0, 0, 101 6

*NCOPY, SHIFT, OLD SET = sp2-weld-3b, NEW SET = sp2-weld-3t, CHANGE NUMBER = 800
 0, 0, 50 8

*NCOPY, SHIFT, OLD SET = sp2-weld-3t, NEW SET = sp2-weld-4b, CHANGE NUMBER = 1600
 0, 0, 101 6

*NCOPY, SHIFT, OLD SET = sp2-weld-4b, NEW SET = sp2-weld-4t, CHANGE NUMBER = 800
 0, 0, 50 8

*NCOPY, SHIFT, OLD SET = sp2-weld-4t, NEW SET = sp2-weld-5b, CHANGE NUMBER = 1600
 0, 0, 101 6

*NCOPY, SHIFT, OLD SET = sp2-weld-5b, NEW SET = sp2-weld-5t, CHANGE NUMBER = 800
 0, 0, 50 8

*NCOPY, SHIFT, OLD SET = sp2-weld-5t, NEW SET = sp2-weld-6b, CHANGE NUMBER = 800
 0, 0, 50 8

*NCOPY, SHIFT, OLD SET = sp2-weld-6b, NEW SET = sp2-weld-6t, CHANGE NUMBER = 800
 0, 0, 50 8

*NCOPY, SHIFT, OLD SET = sp2-weld-6t, NEW SET = sp2-weld-7b, CHANGE NUMBER = 1600
 0, 0, 101 6
```

```
*NCOPY, SHIFT, OLD SET = sp2-weld-7b, NEW SET = sp2-weld-7t, CHANGE NUMBER = 800
 0, 0, 50 8

*NCOPY, SHIFT, OLD SET = sp2-weld-7t, NEW SET = sp2-weld-8b, CHANGE NUMBER = 1600
 0, 0, 101 6

*NCOPY, SHIFT, OLD SET = sp2-weld-8b, NEW SET = sp2-weld-8t, CHANGE NUMBER = 800
 0, 0, 50 8

*NCOPY, SHIFT, OLD SET = sp2-weld-8t, NEW SET = sp2-weld-9b, CHANGE NUMBER = 1600
 0, 0, 101 6

*NCOPY, SHIFT, OLD SET = sp2-weld-9b, NEW SET = sp2-weld-9t, CHANGE NUMBER = 800
 0, 0, 50 8

*NCOPY, SHIFT, OLD SET = sp2-weld-9t, NEW SET = sp2-weld-10b, CHANGE NUMBER = 1600
 0, 0, 101 6

*NCOPY, SHIFT, OLD SET = sp2-weld-10b, NEW SET = sp2-weld-10t, CHANGE NUMBER = 800
 0, 0, 50 8

*NFILL, NSET = split-pipe-2
 sp2-bot, sp2-weld-1t, 4, 200
 sp2-weld-1t, sp2-weld-2b, 8, 200
 sp2-weld-2b, sp2-weld-2t, 4, 200
 sp2-weld-2t, sp2-weld-3b, 8, 200
 sp2-weld-3b, sp2-weld-3t, 4, 200
 sp2-weld-3t, sp2-weld-4b, 8, 200
 sp2-weld-4b, sp2-weld-4t, 4, 200
 sp2-weld-4t, sp2-weld-5b, 8, 200
 sp2-weld-5b, sp2-weld-5t, 4, 200
 sp2-weld-5t, sp2-weld-6b, 4, 200
 sp2-weld-6b, sp2-weld-6t, 4, 200
 sp2-weld-6t, sp2-weld-7b, 8, 200
 sp2-weld-7b, sp2-weld-7t, 4, 200
 sp2-weld-7t, sp2-weld-8b, 8, 200
 sp2-weld-8b, sp2-weld-8t, 4, 200
 sp2-weld-8t, sp2-weld-9b, 8, 200
 sp2-weld-9b, sp2-weld-9t, 4, 200
 sp2-weld-9t, sp2-weld-10b, 8, 200
 sp2-weld-10b, sp2-weld-10t, 4, 200
*NSET, NSET = weld2-edge1-1b
 400084
*NSET, NSET = weld2-edge1-1t
 400884
*NSET, NSET = weld2-edge1-2b
 402484
*NSET, NSET = weld2-edge1-2t
 403284
*NSET, NSET = weld2-edge1-3b
 404884
*NSET, NSET = weld2-edge1-3t
 405684
*NSET, NSET = weld2-edge1-4b
 407284
*NSET, NSET = weld2-edge1-4t
 408084
*NSET, NSET = weld2-edge1-5b
 409684
*NSET, NSET = weld2-edge1-5t
 410484
*NSET, NSET = weld2-edge1-6b
```

411284
*NSET, NSET = weld2-edge1-6t
412084
*NSET, NSET = weld2-edge1-7b
413684
*NSET, NSET = weld2-edge1-7t
414484
*NSET, NSET = weld2-edge1-8b
416084
*NSET, NSET = weld2-edge1-8t
416884
*NSET, NSET = weld2-edge1-9b
418484
*NSET, NSET = weld2-edge1-9t
419284
*NSET, NSET = weld2-edge1-10b
420884
*NSET, NSET = weld2-edge1-10t
421684
*NFILL, NSET = sp2-weld-1
weld2-edge1-1b, weld2-edge1-1t, 4, 200
weld2-edge1-2b, weld2-edge1-2t, 4, 200
weld2-edge1-3b, weld2-edge1-3t, 4, 200
weld2-edge1-4b, weld2-edge1-4t, 4, 200
weld2-edge1-5b, weld2-edge1-5t, 4, 200
weld2-edge1-6b, weld2-edge1-6t, 4, 200
weld2-edge1-7b, weld2-edge1-7t, 4, 200
weld2-edge1-8b, weld2-edge1-8t, 4, 200
weld2-edge1-9b, weld2-edge1-9t, 4, 200
weld2-edge1-10b, weld2-edge1-10t, 4, 200
*NSET, NSET = weld2-edge2-1b
400104
*NSET, NSET = weld2-edge2-1t
400904
*NSET, NSET = weld2-edge2-2b
402504
*NSET, NSET = weld2-edge2-2t
403304
*NSET, NSET = weld2-edge2-3b
404904
*NSET, NSET = weld2-edge2-3t
405704
*NSET, NSET = weld2-edge2-4b
407304
*NSET, NSET = weld2-edge2-4t
408104
*NSET, NSET = weld2-edge2-5b
409704
*NSET, NSET = weld2-edge2-5t
410504
*NSET, NSET = weld2-edge2-6b
411304
*NSET, NSET = weld2-edge2-6t
412104
*NSET, NSET = weld2-edge2-7b
413704
*NSET, NSET = weld2-edge2-7t
414504
*NSET, NSET = weld2-edge2-8b
416104
*NSET, NSET = weld2-edge2-8t
416904

```
*NSET, NSET = weld2-edge2-9b
 418504
*NSET, NSET = weld2-edge2-9t
 419304
*NSET, NSET = weld2-edge2-10b
 420904
*NSET, NSET = weld2-edge2-10t
 421704
*NFILL, NSET = sp2-weld-2
 weld2-edge2-1b, weld2-edge2-1t, 4, 200
 weld2-edge2-2b, weld2-edge2-2t, 4, 200
 weld2-edge2-3b, weld2-edge2-3t, 4, 200
 weld2-edge2-4b, weld2-edge2-4t, 4, 200
 weld2-edge2-5b, weld2-edge2-5t, 4, 200
 weld2-edge2-6b, weld2-edge2-6t, 4, 200
 weld2-edge2-7b, weld2-edge2-7t, 4, 200
 weld2-edge2-8b, weld2-edge2-8t, 4, 200
 weld2-edge2-9b, weld2-edge2-9t, 4, 200
 weld2-edge2-10b, weld2-edge2-10t, 4, 200
*ELEMENT, TYPE = C3D8
 400002, 400002, 400003, 400044, 400043, 400202, 400203, 400244, 400243
 400042, 400043, 400044, 400085, 400084, 400243, 400244, 400285, 400284
*ELGEN, ELSET = sp-surface-in-2
 400002, 20, 1, 1, 108, 200, 200
*ELGEN, ELSET = sp-surface-out-2
 400042, 20, 1, 1, 108, 200, 200
*ELSET, ELSET = split-pipe-2
 sp-surface-in-2, sp-surface-out-2
***
*SURFACE, NAME = solid round
 solid round
*SURFACE, NAME = sp-surface-in-1
 sp-surface-in-1
*SURFACE, NAME = sp-surface-in-2
 sp-surface-in-2
***
*CONTACT PAIR, INTERACTION = slide, SMALL SLIDING
 sp-surface-in-1, solid round
*CONTACT PAIR, INTERACTION = slide, SMALL SLIDING
 sp-surface-in-2, solid round
***
*SURFACE INTERACTION, NAME = slide
*FRICTION
 0 025
***
*MPC
 TIE, sr-weld-edge1-1b, weld-edge1-1b
 TIE, sr-weld-edge1-1t, weld-edge1-1t
 TIE, sr-weld-edge1-2b, weld-edge1-2b
 TIE, sr-weld-edge1-2t, weld-edge1-2t
 TIE, sr-weld-edge1-3b, weld-edge1-3b
 TIE, sr-weld-edge1-3t, weld-edge1-3t
 TIE, sr-weld-edge1-4b, weld-edge1-4b
 TIE, sr-weld-edge1-4t, weld-edge1-4t
 TIE, sr-weld-edge1-5b, weld-edge1-5b
 TIE, sr-weld-edge1-5t, weld-edge1-5t
 TIE, sr-weld-edge1-6b, weld-edge1-6b
 TIE, sr-weld-edge1-6t, weld-edge1-6t
 TIE, sr-weld-edge1-7b, weld-edge1-7b
 TIE, sr-weld-edge1-7t, weld-edge1-7t
 TIE, sr-weld-edge1-8b, weld-edge1-8b
 TIE, sr-weld-edge1-8t, weld-edge1-8t
```

TIE, sr-weld-edge1-9b, weld-edge1-9b
TIE, sr-weld-edge1-9t, weld-edge1-9t
TIE, sr-weld-edge1-10b, weld-edge1-10b
TIE, sr-weld-edge1-10t, weld-edge1-10t
*MPC
TIE, sr2-weld-edge1-1b, weld2-edge1-1b
TIE, sr2-weld-edge1-1t, weld2-edge1-1t
TIE, sr2-weld-edge1-2b, weld2-edge1-2b
TIE, sr2-weld-edge1-2t, weld2-edge1-2t
TIE, sr2-weld-edge1-3b, weld2-edge1-3b
TIE, sr2-weld-edge1-3t, weld2-edge1-3t
TIE, sr2-weld-edge1-4b, weld2-edge1-4b
TIE, sr2-weld-edge1-4t, weld2-edge1-4t
TIE, sr2-weld-edge1-5b, weld2-edge1-5b
TIE, sr2-weld-edge1-5t, weld2-edge1-5t
TIE, sr2-weld-edge1-6b, weld2-edge1-6b
TIE, sr2-weld-edge1-6t, weld2-edge1-6t
TIE, sr2-weld-edge1-7b, weld2-edge1-7b
TIE, sr2-weld-edge1-7t, weld2-edge1-7t
TIE, sr2-weld-edge1-8b, weld2-edge1-8b
TIE, sr2-weld-edge1-8t, weld2-edge1-8t
TIE, sr2-weld-edge1-9b, weld2-edge1-9b
TIE, sr2-weld-edge1-9t, weld2-edge1-9t
TIE, sr2-weld-edge1-10b, weld2-edge1-10b
TIE, sr2-weld-edge1-10t, weld2-edge1-10t
*MPC
TIE, sr-weld-edge2-1b, weld-edge2-1b
TIE, sr-weld-edge2-1t, weld-edge2-1t
TIE, sr-weld-edge2-2b, weld-edge2-2b
TIE, sr-weld-edge2-2t, weld-edge2-2t
TIE, sr-weld-edge2-3b, weld-edge2-3b
TIE, sr-weld-edge2-3t, weld-edge2-3t
TIE, sr-weld-edge2-4b, weld-edge2-4b
TIE, sr-weld-edge2-4t, weld-edge2-4t
TIE, sr-weld-edge2-5b, weld-edge2-5b
TIE, sr-weld-edge2-5t, weld-edge2-5t
TIE, sr-weld-edge2-6b, weld-edge2-6b
TIE, sr-weld-edge2-6t, weld-edge2-6t
TIE, sr-weld-edge2-7b, weld-edge2-7b
TIE, sr-weld-edge2-7t, weld-edge2-7t
TIE, sr-weld-edge2-8b, weld-edge2-8b
TIE, sr-weld-edge2-8t, weld-edge2-8t
TIE, sr-weld-edge2-9b, weld-edge2-9b
TIE, sr-weld-edge2-9t, weld-edge2-9t
TIE, sr-weld-edge2-10b, weld-edge2-10b
TIE, sr-weld-edge2-10t, weld-edge2-10t
*MPC
TIE, sr2-weld-edge2-1b, weld2-edge2-1b
TIE, sr2-weld-edge2-1t, weld2-edge2-1t
TIE, sr2-weld-edge2-2b, weld2-edge2-2b
TIE, sr2-weld-edge2-2t, weld2-edge2-2t
TIE, sr2-weld-edge2-3b, weld2-edge2-3b
TIE, sr2-weld-edge2-3t, weld2-edge2-3t
TIE, sr2-weld-edge2-4b, weld2-edge2-4b
TIE, sr2-weld-edge2-4t, weld2-edge2-4t
TIE, sr2-weld-edge2-5b, weld2-edge2-5b
TIE, sr2-weld-edge2-5t, weld2-edge2-5t
TIE, sr2-weld-edge2-6b, weld2-edge2-6b
TIE, sr2-weld-edge2-6t, weld2-edge2-6t
TIE, sr2-weld-edge2-7b, weld2-edge2-7b
TIE, sr2-weld-edge2-7t, weld2-edge2-7t
TIE, sr2-weld-edge2-8b, weld2-edge2-8b

```
 TIE, sr2-weld-edge2-8t, weld2-edge2-8t
 TIE, sr2-weld-edge2-9b, weld2-edge2-9b
 TIE, sr2-weld-edge2-9t, weld2-edge2-9t
 TIE, sr2-weld-edge2-10b, weld2-edge2-10b
 TIE, sr2-weld-edge2-10t, weld2-edge2-10t
*CONSTRAINT CONTROLS, NO CHECKS
***
*SOLID SECTION, ELSET = solid round, MATERIAL = solid round
*ELSET, ELSET = split-pipe
 split-pipe-1, split-pipe-2
*SOLID SECTION, ELSET = split-pipe, MATERIAL = split-pipe
*MATERIAL, NAME = solid round
*ELASTIC
 200000, 0.3
*PLASTIC
 414, 0
 563, 0.225
*MATERIAL, NAME = split-pipe
*ELASTIC
 200000, 0.3
*PLASTIC
 550, 0
 613, 0.27
***
*ELSET, ELSET = e-all
 split-pipe, solid round
*NSET, NSET = n-all
 split-pipe-2, split-pipe-1, solid round
***
***
*STEP
*BUCKLE
 1
*DLOAD
 sr-top, P2, 49.3381310347496
*NODEFILE, MODE = 1
 U
*END STEP
***
***
*Second analysis = Static Riks analysis (on separate input files)
***
***
*IMPERFECTION, FILE = sr60-w1-1, STEP = 1
 1, <Modescale>
***
*STEP, NLGEOM
 Applying axial load
*STATIC, RIKS
 0.1, , , 0.25
*DLOAD
 sr-top, P2, 49.3381310347496
*END STEP
```

APPENDIX G

PERMISSION FROM COPYRIGHT HOLDER

NRC RESEARCH PRESS LICENSE
TERMS AND CONDITIONS

Jul 07, 2010

This is a License Agreement between Cindy Dostatni ("You") and NRC Research Press ("NRC Research Press") provided by Copyright Clearance Center ("CCC"). The license consists of your order details, the terms and conditions provided by NRC Research Press, and the payment terms and conditions.

All payments must be made in full to CCC. For payment instructions, please see information listed at the bottom of this form.

License Number	2463990528830
License date	Jul 07, 2010
Licensed content publisher	NRC Research Press
Licensed content publication	Canadian Journal of Civil Engineering
Licensed content title	Tensile strength of bolted ring-type splices of solid round leg members of guyed communication towers
Licensed content author	Cindy Kumalasari, Lihong Shen, Murty K.S Madugula, et al
Licensed content date	Jun 1, 2005
Volume number	32
Issue number	3
Type of Use	Thesis/Dissertation
Requestor type	Author (original work)
Format	Print
Portion	Full article
Order reference number	
Title of your thesis / dissertation	Analysis, Design, and Reinforcement of Communication Towers
Expected completion date	Sep 2010
Estimated size(pages)	200
Total	0.00 CAD
Terms and Conditions	

General Terms & Conditions

Permission is granted upon the requester's compliance with the following terms and conditions:

1. A credit line will be prominently placed in your product(s) and include: for books the author, book title, editor, copyright holder, year of publication; for journals the author, title of article, title of journal, volume number, issue number, and the inclusive pages. The credit line must include the following wording: "© 2008 NRC Canada or its

licensors. Reproduced with permission," except when an author of an original article published in 2009 or later is reproducing his/her own work.

2. The requester warrants that the material shall not be used in any manner that may be derogatory to the title, content, or authors of the material or to National Research Council Canada, including but not limited to an association with conduct that is fraudulent or otherwise illegal.
3. Permission is granted for the term (for Books/CDs-Shelf Life; for Internet/Intranet-In perpetuity; for all other forms of print-the life of the title) and purpose specified in your request. Once term has expired, permission to renew must be made in writing.
4. Permission granted is nonexclusive, and is valid throughout the world in English and the languages specified in your original request. A new permission must be requested for revisions of the publication under current consideration.
5. National Research Council Canada cannot supply the requester with the original artwork or a "clean copy."
6. If the National Research Council Canada material is to be translated, the following lines must be included: The authors, editors, and National Research Council Canada are not responsible for errors or omissions in translations.

v1.3

Gratis licenses (referencing $0 in the Total field) are free. Please retain this printable license for your reference. No payment is required.

If you would like to pay for this license now, please remit this license along with your payment made payable to "COPYRIGHT CLEARANCE CENTER" otherwise you will be invoiced within 48 hours of the license date. Payment should be in the form of a check or money order referencing your account number and this invoice number RLNK10811954.
Once you receive your invoice for this order, you may pay your invoice by credit card. Please follow instructions provided at that time.

Make Payment To:
Copyright Clearance Center
Dept 001
P.O. Box 843006
Boston, MA 02284-3006

If you find copyrighted material related to this license will not be used and wish to cancel, please contact us referencing this license number 2463990528830 and noting the reason for cancellation.

Questions? customercare@copyright.com or +1-877-622-5543 (toll free in the US) or +1-978-646-2777.

NRC RESEARCH PRESS LICENSE TERMS AND CONDITIONS

Jul 07, 2010

This is a License Agreement between Cindy Dostatni ("You") and NRC Research Press ("NRC Research Press") provided by Copyright Clearance Center ("CCC"). The license consists of your order details, the terms and conditions provided by NRC Research Press, and the payment terms and conditions.

All payments must be made in full to CCC. For payment instructions, please see information listed at the bottom of this form.

License Number	2463990242875
License date	Jul 07, 2010
Licensed content publisher	NRC Research Press
Licensed content publication	Canadian Journal of Civil Engineering
Licensed content title	Prying action in bolted steel circular flange connections
Licensed content author	Cindy Kumalasari, Yongcong Ding, and Murty K.S Madugula
Licensed content date	Apr 1, 2006
Volume number	33
Issue number	4
Type of Use	Thesis/Dissertation
Requestor type	Author (original work)
Format	Print
Portion	Full article
Order reference number	
Title of your thesis / dissertation	Analysis, Design, and Reinforcement of Communication Towers
Expected completion date	Sep 2010
Estimated size(pages)	200
Total	0.00 CAD
Terms and Conditions	

General Terms & Conditions

Permission is granted upon the requester's compliance with the following terms and conditions:

1. A credit line will be prominently placed in your product(s) and include: for books the author, book title, editor, copyright holder, year of publication; for journals the author, title of article, title of journal, volume number, issue number, and the inclusive pages. The credit line must include the following wording: "© 2008 NRC Canada or its licensors. Reproduced with permission," except when an author of an original article

published in 2009 or later is reproducing his/her own work.

2. The requester warrants that the material shall not be used in any manner that may be derogatory to the title, content, or authors of the material or to National Research Council Canada, including but not limited to an association with conduct that is fraudulent or otherwise illegal.
3. Permission is granted for the term (for Books/CDs-Shelf Life; for Internet/Intranet-In perpetuity; for all other forms of print-the life of the title) and purpose specified in your request. Once term has expired, permission to renew must be made in writing.
4. Permission granted is nonexclusive, and is valid throughout the world in English and the languages specified in your original request. A new permission must be requested for revisions of the publication under current consideration.
5. National Research Council Canada cannot supply the requester with the original artwork or a "clean copy."
6. If the National Research Council Canada material is to be translated, the following lines must be included: The authors, editors, and National Research Council Canada are not responsible for errors or omissions in translations.

v1.3

Gratis licenses (referencing $0 in the Total field) are free. Please retain this printable license for your reference. No payment is required.

If you would like to pay for this license now, please remit this license along with your payment made payable to "COPYRIGHT CLEARANCE CENTER" otherwise you will be invoiced within 48 hours of the license date. Payment should be in the form of a check or money order referencing your account number and this invoice number RLNK10811952.
Once you receive your invoice for this order, you may pay your invoice by credit card. Please follow instructions provided at that time.

Make Payment To:
Copyright Clearance Center
Dept 001
P.O. Box 843006
Boston, MA 02284-3006

If you find copyrighted material related to this license will not be used and wish to cancel, please contact us referencing this license number 2463990242875 and noting the reason for cancellation.

Questions? customercare@copyright.com or +1-877-622-5543 (toll free in the US) or +1-978-646-2777.

VITA AUCTORIS

The author was born in 1980 on Surabaya, Indonesia. She received an S.T. (B.Sc. equivalent) degree in Structural Engineering from Petra Christian University, Surabaya, Indonesia, in 2002. She had worked for one year (2002-2003) as a Civil Engineer at CH Contractor and Engineering, Surabaya, Indonesia. She came to Canada in 2003 and obtained an M.A.Sc. degree in Civil Engineering from the University of Windsor in 2004.

She currently holds a position as the Director of Engineering for Westower Communications Ltd., Mid-West region, at the main office located in Thorsby, Alberta. Prior to this position, she was working it the same company as a Design Engineer from 2007 to 2009. In 2009, she changed her surname from Kumalasari to Dostatni.

She is currently registered as a Ph.D. candidate in the Civil and Environmental Engineering Department of the University of Windsor and expects to graduate in Winter 2011.